UNIVERSIDADE FEDERAL DO CEARÁ
CENTRO DE CIÊNCIAS
DEPARTAMENTO DE FÍSICA
PROGRAMA DE PÓS-GRADUAÇÃO EM FÍSICA
DOUTORADO EM FÍSICA

ADAILTON AZEVÊDO ARAÚJO FILHO

THERMAL ASPECTS OF FIELD THEORIES

Fortaleza - CE
2022

ADAILTON AZEVÊDO ARAÚJO FILHO

THERMAL ASPECTS OF FIELD THEORIES

Tese apresentada ao programa de pós-graduação em Física da Universidade Federal do Ceará como parte dos requisitos para obtenção do título de Doutor em Física. Área de Concentração: Teoria de Campos.
Orientador: Raimundo Nogueira da Costa Filho.
Co-orientador: Albert Yu. Petrov.

Fortaleza - CE
2022

Dados Internacionais de Catalogação na Publicação
Universidade Federal do Ceará
Biblioteca Universitária
Gerada automaticamente pelo módulo Catalog, mediante os dados fornecidos pelo(a) autor(a)

A687t Araújo Filho, Adailton Azevêdo.
Thermal aspects of field theories / Adailton Azevêdo Araújo Filho. – 2022.
191 f. : il. color.

Tese (doutorado) – Universidade Federal do Ceará, Centro de Ciências, Programa de Pós-Graduação em Física , Fortaleza, 2022.
Orientação: Prof. Dr. Raimundo Nogueira da Costa Filho.
Coorientação: Prof. Dr. Albert Petrov.

1. Statistical mechanics. 2. Relativistic quantum mechanics. 3. Lorentz violation. 4. Quantum gases. 5. Bosons and fermions. I. Título.

CDD 530

ADAILTON AZEVÊDO ARAÚJO FILHO

THERMAL ASPECTS OF FIELD THEORIES

Tese apresentada ao programa de pós-graduação em Física da Universidade Federal do Ceará como parte dos requisitos para obtenção do título de Doutor em Física.

Aprovada em 18 de Julho de 2022.

BANCA EXAMINADORA

Prof. Dr. Raimundo Nogueira da Costa Filho (Orientador)
Universidade Federal do Ceará – UFC

Prof. Dr. Albert Yu. Petrov (Co-orientador)
Universidade Federal da Paraíba – UFPB

Prof. Dr. Job Saraiva Furtado Neto
Universidade Federal do Cariri – UFCA

Prof. Dr. Saulo Davi Soares e Reis
Universidade Federal do Ceará – UFC

Prof. Dr. Makarius Oliveira Tahim
Universidade Estadual do Ceará – UECE

To the Brazilian citizens

ACKNOWLEDGMENTS

Many people have passed through my way leaving my journey softer in a such way that I could integrally focus on doing my research without any significant disturbing issues. Thereby, having peace and time to think turned out to be an advantage in my carrier which, naturally, some resealable ideas brought out. What I became, during this ten years – graduation, master and Ph.D, could not be possible without many people who surrounded me. Many challenges appeared within this walk as one can naturally expect. Nevertheless, we wish we could that it would be harder because, if it would, it would not entail that we overcame the easier things; it would mean that we became better and stronger. Since it is an end of a cycle, I hope that I can point out all people who made difference during this period. Then, the huge list is presented as follows:

I would like to thank God for His indefinitely mercy and compassion given to me.

I would like to thank the funding agencies which partially supported my work during my Ph.D: Conselho Nacional de Desenvolvimento Científico e Tecnológico (CNPq) - 142412/2018-0, and CAPES-PRINT (PRINT - PROGRAMA INSTITUCIONAL DE INTERNACIONALIZAÇÃO) - 88887.508184/2020-00.

I would like to thank my parents, i.e., Euzimar and Adailton, for all the support and opportunities they gave to my existence, looking over me when I needed most. Without any doubt, it is a gift to have you in my daily life – I really appreciate you both and I hope naively that you will be with me forever.

I would like to thank R. N. Costa Filho for the fruitful suggestions given to me and for the supervision of my Ph.D.

I would like to thank my Co-supervisors Albert Petrov and Paulo Porfirio for their indefinitely forbearance in guiding me through the confection of many scientific projects; moreover, for their huge availability to discuss about physical results while we were producing some papers.

I would like to thank my main collaborators, i.e., Alfieres Reis, Rubens Oliveira and Subir Ghosh for the remarkable ideas shared to each other and for the assistance given to me during this whole process.

I would like to express my gratitude for D. M. Dantas for the help with computer calculations – from the installation until the obtainment of the results. I am really in indebted to you; without this knowledge, certainly my thesis would not be possible in this present version.

I would like to share my gratitude to Belisa Aguiar, who gave me much unspeakable funny moment, peace and love, especially, in the end of this cycle. Many unforgettable recipes pairing with exceptional champagnes turned out to be our identity when “I say a little prayer” was played through the night. And, thank you for letting me contemplate our

existence during the Andre Rieu concert in Madrid – it was unbelievable!

I would like to thank Lívia Mesquita to have brought me to back the flame of life; for all sweet, fruitful, magical, indescribable, and unspeakable moments that we could share to ourselves when the night turned out to be a morning; for all suggestions given to the confection/writing of my manuscripts. Thank you for being the exact trigger in the exact moment – *courage is the fear walking*.

I would like to point out the pleasure of contemplating the human existence even though the world started to play its drums in a chaotic manner– being in a safe closed peaceful bubble collecting beautiful stuffed animals. The appreciation of unforgettable receipts while there existed a soft jazz playing through the rain had fulfill our souls. Daydreams in some ordinary days turned out to be unspeakable specially when some bottles of wine no longer belonged to the restaurant in an opera evening. Many discussions in order to get a better comprehension of the critique of pure reason with or without fair sentences belonging to the previous argumentation, were brought certainly about. All of this was mixed like a shake; yes, a milkshake.

Me gustaría expresar mi gratitud por mi familia hecha en València: Nicolás, Nerea, Ilde, Dean, Jose, Silvia, Serji, Adrià, Paul, Victor, Paulo, y Azmat. En especial, me gustaría destacar mi agradecimiento a Ana Martínez por todos los dulces, inmejorables, inefables, indescriptibles y soberanos momentos vividos juntos. Gracias por poder haber disfrutado un día de tu existencia mientras bebíamos caba, así como por el privilegio de ser tu primer alumno de español y por tu infinita paciencia al repetir a menudo frases, sonidos y dichos populares.

I would like to thank Dean(hi guys! Muy bien tío!) for his infinitely kindness and generosity; also for the walking during the evenings in Valencia talking about much aspects of the society and gastronomy. After the first meeting 08/10/2020 in your sweet home, my whole life have changed in a positive way– I knew many people who left my stay in Valencia easier. I'm definitely indebted to you my oldest brother.

I would like to thank Adriana for hanging out with me through the city purely contemplating the pleasure of being. Also, for the wisdom words and for the new tastes that I knew from her.

I would like to thank V. N. Freire for having proportioned my first contact with science in condensed matter physics from my first scholarship, and for having taught me how the academic stuffs work; and I would like to thank R. V. Maluf for having opened up the doors of postgraduate world and for his indefinitely much forbearance in having me in his office removing the barriers of my ignorance during the pleasing 2 minutes; also for the opportunity to do many calculations together with him on the blackboard on Thursday and Friday evenings.

I would like to thank Gonzalo. J. Olmo for the kind hospitality, for the all background that I learned from his group, and for the opportunity to collaborate with him when I was at Facultad de Física - Universitat de València.

"So, because you are lukewarm, and neither hot nor cold, I will spit you out of my mouth."

– Revelation 3:16

One day I thought it would never be possible. Nevertheless, here it is.

RESUMO

Esta tese se concentra em examinar as propriedades termodinâmicas de várias teorias de campos, envolvendo física de alta energia e matéria condensada. Em particular, fazemos a utilização da teoria dos ensembles para realizar nossas análises. Inicialmente, fornecemos as propriedades termodinâmicas baseadas no formalismo de ensemble canônico para o anel quântico de Aharonov-Bohm considerando ambos os cenários: os casos relativístico e não relativístico. Em seguida, construímos um modelo para estudar gases quânticos. Neste contexto, examinamos bósons, férmions e partículas sem spin dentro do ensemble grande-canônico levando em consideração duas abordagens diferentes: partículas *interagentes* e *não interagentes*. Para corroborar nossos resultados, nós os aplicamos ao condensado de Bose-Einstein e aos dímeros de hélio. A mesma abordagem é aplicada considerando a violação de Lorentz. Além disso, neste contexto, também propomos duas aplicações para apoiar nossos cálculos teóricos: camadas de *fosforeno* e *precessão de spin* de gases quânticos. Em seguida, as propriedades termodinâmicas são investigadas também para uma variedade de modelos/teorias (sobre diferentes relações de dispersão de energia) quando a simetria de Lorentz não é mais mantida dentro do formalismo de ensemble canônico. Para esses casos, três cenários térmicos distintos do universo são considerados: a radiação cósmica de fundo em micro-ondas, a época eletrofraca e o período inflacionário.

Palavras-chave: mecânica estatística; mecânica quântica relativística; violação de Lorentz; gases quânticos; bósons; férmions.

ABSTRACT

This thesis focus on examining the thermodynamic properties of various prominent field theories concerning high-energy and condensed matter physics. We make the usage of the theory of ensembles to perform our analysis. At the beginning, we supply the thermodynamic properties based on the formalism of canonical ensemble to the Aharonov-Bohm quantum ring considering both scenarios: the relativistic and the non-relativistic cases. Next, we construct a model in order to study quantum gases. In this context, we examine bosons, fermions and spinless particles within the grand-canonical ensemble taking into account two different approaches: *interacting* and *noninteracting* particles. To corroborate our results, we apply them to the Bose-Einstein condensate and to the helium dimmers. The same approach is applied considering rather Lorentz violation. Moreover, in this context, we also propose two applications to support our theoretical calculations: *phosphorene* layers and *spin precession* of quantum gases. Next, the thermodynamic properties are investigated as well to a variety of models/theories (regarding different energy dispersion relations) when the Lorentz symmetry is no longer maintained within the canonical ensemble formalism. To these cases, three distinct thermal scenarios of the universe are considered: the cosmic microwave background, the electroweak epoch, and the inflationary period.

Keywords: statistical mechanics; relativistic quantum mechanics; Lorentz violation; quantum gases; bosons; fermions.

List of Figures

2.1 Numerical solutions for the thermodynamic properties of the Aharanov-Bohm ring for the relativistic case: (a) The Helmholtz free energy; (b) the mean energy; (c) the entropy and (d) the heat capacity. In this case, we consider $\tau = K_B T$. 27

2.2 Numerical solutions for the thermodynamic properties of the Aharanov-Bohm ring for the non-relativistic case: (a) the Helmholtz free energy; (b) the mean energy; (c) the entropy and (d) the heat capacity. 28

3.1 The Helmholtz free energy, entropy per particle, the internal energy and heat capacity per particle, respectively 34

3.2 The different behaviors for the entropy, mean energy and heat capacity, respactively 48

3.3 Path behavior through a torus knot for different winding numbers 49

3.4 Energy behavior in the low-temperature regime for different values of winding number α for the torus knot. 50

3.5 Heat capacity in the low-temperature regime for different values of winding number α for the torus knot. 51

4.1 A representation of a torus knot (2,3). The wire represents the path followed by the particles on its surface 53

4.2 Helmholtz free energy ($\mathcal{F}$) and entropy ($\mathcal{S}$) versus temperature (T) 56

4.3 Internal energy ($\mathcal{U}$) and Heat capacity ($\mathcal{C}$) versus temperature (T) 57

4.4 Magnetization ($\mathcal{M}$) and Susceptibility ($\succ$) versus temperature (T) 57

4.5 These plots exhibit the Helmholtz free energy for different configurations of temperature and magnetic field. It also displays the behavior of Helmholtz energy as a function of the wind numbers (p, q). Note that Free energy increases when magnetic field increases and also when both p and q increases. 58

4.6 These plots exhibit the entropy for different configurations of temperature and magnetic field. We also see its behavior as a function of the wind numbers (p, q). The behavior of the entropy is similar to the free energy, i.e. it increases with the parameters p and q. 59

4.7 These plots exhibit the contour plot for the mean energy for different configurations of temperature and magnetic field. In those plots we can see the behavior of the Energy as a function of the wind numbers (p, q). 60
4.8 The contour plots for the Heat Capacity for different configurations of temperature and magnetic field. In these ones, we can see the behavior of the Heat Capacity as a function of the wind numbers (p, q). 61
4.9 These contour plots show the magnetization for different configurations of temperature and magnetic field. In these ones, we can see the behavior of the magnetization as a function of the wind numbers (p, q). 62
4.10 The contour plots show how the susceptibility varies for different configurations of temperature and magnetic field. In these plots, we see the behavior of the Susceptibility as a function of the wind numbers (p, q). 63
4.11 Entropy and internal energy 67
4.12 Heat capacity 67
4.13 Magnetization and Susceptibility 68

5.1 This figure shows a comparison between mean particle number for different background configurations. These plots are normalized by the standard result, which means that the value 1 is the behavior regardless Lorentz violation. In order to clarify the notation, we should notice that $\delta\mathcal{N}_i$ means the deviation from the standard result using the values 10^{-3}, 10^{-5} and 10^{-7} for the controlling coefficient respectively. 82
5.2 This figure shows the general behavior of spin-degenerate case for fermions, where the same notation as in Fig. 5.1 is used. As one can see, the deviation from the standard results become relevant for high energy regime, which means small β. Here, it is worth to remember that temperature is given in eV. 83
5.3 These plots exhibit the general behavior to spin-nondegenerate case for fermions. 93
5.4 This figure shows a comparison between particle number to different background configurations for bosons. Here, the normalization is also applied. . . 93

6.1 The figure shows the behavior of the black body radiation as a function of the frequency ν for different values of θ within Podolsky electrodynamics considering $h = 1$. 97
6.2 The figure shows the correction to the *Stefan–Boltzmann* law represented by parameter $\tilde{\alpha}$ as a function of θ considering $k_B = 1$ and the temperature in the early inflationary universe i.e., $\beta = 10^{-13}$ GeV^{-1}. 98
6.3 The figure exhibits the solutions to Helmholtz free energy $F(\theta)$ at high temperature regime considering $k_B = 1$. 99

6.4 These three graphics exhibit the behavior of the entropy $S(\theta)$ considering the temperature in the primitive inflationary universe where $k_B = 1$. 100
6.5 The plots exhibit solutions to the heat capacity $C_V(\theta)$ considering $k_B = 1$ and the temperature at the beginning inflationary universe. 101
6.6 The figure shows the behavior of the black body radiation in the generalized Podolsky electrodynamics with Lorentz violation for fixed values of $\theta = 10$ and $D_{00} = 1$. 102
6.7 The graphics show the correction to the *Stefan–Boltzmann* law $\bar{\alpha}(\eta)$, entropy $\bar{S}(\eta)$, Helmholtz free energy $\bar{F}(\eta)$ and heat capacity $\bar{C}_V(\eta)$ regarding $k_B = 1$. 103

7.1 The plots exhibit how the spectral radiance $\chi(\nu)$ changes as a function of frequency ν for different scenarios with $h = 1$. 109
7.2 The figure shows the correction to the so-called *Stefan–Boltzmann* law represented by parameter $\tilde{\alpha}(\xi)$, the entropy $S(\xi)$, the Helmholtz free energy $F(\xi)$ and the heat capacity $C_V(\xi)$, considering $\kappa_B = 1$ in the high temperature regime of the universe, namely, $\beta = 10^{-13}$ GeV^{-1}. 110
7.3 This figure shows the behavior of the spectral radiance $\bar{\chi}(\nu)$ for different values of η_2 and ν. We consider fixed values of B_0, C_0 and θ, i.e., $\eta_1 = B_0 = C_0 = 1$ and $\theta = 10$, in the context of the temperature in the inflationary era of the universe, i.e., $\beta = 10^{-13}$ GeV^{-1}. 113
7.4 The figure displays the correction to the so-called *Stefan–Boltzmann* law represented by parameter $\bar{\alpha}(\eta_2)$, the entropy $\bar{S}(\eta_2)$, the Helmholtz free energy $\bar{F}(\eta_2)$ and the heat capacity $\bar{C}_V(\eta_2)$ considering $\kappa_B = 1$ in the inflationary epoch of the universe, i.e., $\beta = 10^{-13}$ GeV^{-1}. 115

8.1 The plots exhibit the spectral radiance $\chi(\nu)$ changing for different values of frequency ν and the Lorentz-breaking parameter σ (its unit is GeV^{-1}). The top left (dotted) is the configuration to the cosmic microwave background, i.e., $\beta = 10^{13}$ GeV^{-1}; the top right (dot-dashed) is ascribed to the electroweak configuration, i.e., $\beta = 10^{-3}$ GeV^{-1}; the bottom plot shows the black body radiation to the inflationary period of the Universe, i.e., $\beta = 10^{-13}$ GeV^{-1}. 121
8.2 The figure shows the correction to the *Stefan–Boltzmann* law ascribed to parameter $\tilde{\alpha}$ as a function of σ (its unit is GeV^{-1}) for the temperatures of cosmic microwave background (top left), electroweak scenario (top right) and the early inflationary universe (bottom). 122
8.3 This figure shows the behavior of the equation of states when the high temperature limit, namely $\frac{\beta}{\sigma} \ll 1$, is taken into account. 125

8.4 This figure shows the behavior of the equation of states when the low temperature limit, namely $\frac{\beta}{\sigma} \gg 1$, is taken into account. 125
8.5 The figure shows the modification of the Helmholtz free energy $F(\sigma)$ due to the parameter σ (its unit is GeV^{-1}) considering the temperatures of cosmic microwave background (top left), electroweak scenario (top right) and the early inflationary universe (bottom). 126
8.6 The plots show the modification to the entropy $S(\sigma)$ as a function of σ (its unit is GeV^{-1}) considering the temperatures of cosmic microwave background (top left), electroweak scenario (top right), and the early inflationary universe (bottom). 127
8.7 The plots show the modification to the heat capacity $C_V(\sigma)$ as a function of σ (its unit is GeV^{-1}) considering the temperatures of cosmic microwave background (top left), electroweak scenario (top right), and the early inflationary universe (bottom). 128
8.8 The plots show how the spectral radiance $\bar{\chi}(\nu)$ changes as a function of frequency ν and l(whose dimension is $m \cdot kg^{-1/2} \cdot s^{-1}$) for three different cases. The top left (dotted) is configuration to the cosmic microwave background, i.e., $\beta = 10^{13}$ GeV^{-1}; the top right (dot-dashed) is ascribed to the electroweak configuration, i.e., $\beta = 10^{-3}$ GeV^{-1}; the bottom plot shows the black body radiation to the inflationary period of the Universe, i.e., $\beta = 10^{-13}$ GeV^{-1}. 129
8.9 The figure shows the correction to the *Stefan–Boltzmann* law represented by parameter $\bar{\alpha}$ as a function of l(whose dimension is $m \cdot kg^{-1/2} \cdot s^{-1}$) considering the temperatures of cosmic microwave background (top left), electroweak scenario (top right), and the early inflationary universe (bottom). 130
8.10 The figure shows the modification of the Helmholtz free energy $\bar{F}$ as a function of l(whose dimension is $m \cdot kg^{-1/2} \cdot s^{-1}$) considering the temperatures of cosmic microwave background (top left), electroweak scenario (top right), and the early inflationary universe (bottom). 131
8.11 The figure shows the modification of the entropy $\bar{S}$ as a function of l(whose dimension is $m \cdot kg^{-1/2} \cdot s^{-1}$) considering the temperatures of cosmic microwave background (top left), electroweak scenario (top right) and the early inflationary universe (bottom). 132
8.12 The figure shows the modification of the heat capacity $\bar{C}_V$ as a function of l(whose dimension is $m \cdot kg^{-1/2} \cdot s^{-1}$) considering the temperatures of cosmic microwave background (top left), electroweak scenario (top right) and the early inflationary universe (bottom). 133

8.13 The figure shows the equation of states for different values of p, T, and l(whose dimension is $m \cdot kg^{-1/2} \cdot s^{-1}$). 134

9.1 The accessible states of the system to the inflationary period. 136
9.2 The accessible states of the system to the electroweak period. 137
9.3 The accessible states of the system to the cosmic microwave background. . . 137
9.4 The spectral radiance to inflationary (top left), electroweak (top right) and cosmic microwave back ground (the bottom) periods of the universe for different values of l_P. 140
9.5 The spectral radiance to inflationary (top left), electroweak (top right) and cosmic microwave back ground (the bottom) periods of the universe for different values of η. 141
9.6 The Helmholtz free energy for different values of l_P. 142
9.7 The Helmholtz free energy for different values of η. 143
9.8 Entropy for different values of l_P. 144
9.9 Entropy for different values of η. 145

List of Tables

3.1 The parameters a, b and c for two distinct configurations. 33

5.1 This table summarizes four particular cases of δ_r, namely, scalar, vector, pseudovector and tensor operators for the fermion sector. Their respective definitions are shown as well. 80

5.2 This table summarizes two particular cases of δ_r, i.e., vector and tensor operators for the boson sector. The respective definitions are exhibited as well. . 83

5.3 The scalar operator concerning the fermion sector. 91

5.4 The vector operator concerning the fermion sector. 91

5.5 The pseudovector operator for fermions. 91

5.6 The tensor operator for fermions. 92

5.7 The vector operator in the boson sector. 92

5.8 The tensor operator for the boson sector. 92

Summary

1 INTRODUCTION **1**

1.1 **Motivations** 18

2 THERMODYNAMIC PROPERTIES OF AN AHARONOV BOHM QUANTUM RING **21**

2.1 **An AB ring modeled by (1+1)-dimensional Dirac equation** 21

2.2 **Thermodynamic properties of the AB ring** 23

2.2.1 The relativistic case 23

2.2.2 The non-relativistic case 25

2.2.3 Results and discussions 25

3 HOW DOES GEOMETRY AFFECT QUANTUM GASES? **29**

3.1 **Spectral energy for different geometries** 29

3.2 **Noninteracting gases: spinless particles** 31

3.2.1 Thermodynamic approach 31

3.2.2 Numerical analysis 32

3.3 **Noninteracting gases: Bosons and fermions** 34

3.3.1 Thermodynamic approach 35

3.3.2 Numerical analysis 37

3.4 **Ideal quantum gas on a torus knot** 38

3.5 **Further applications: noninteracting gases** 39

3.5.1 Bose-Einstein condensate 39

3.5.2 Helium atoms - ^{3}He and ^{4}He 39

3.6 **Interacting gases: an analytical approach** 40

3.6.1 The model 40

3.6.2 Thermodynamic state quantities 42

3.6.3 Analytical results for three-dimensional boxes 44

3.6.4 Analytical results for angular constraints 46

3.6.5 Analytical results for the torus 47

4 FERMIONS ON A TORUS KNOT **52**

4.1 **Statistical mechanics of N particles in a torus knot subjected to a magnetic field** . . . 52
4.1.1 Thin torus: the limit $a \to 0$ . . . 59
4.2 **Fermions on a Torus Knot** . . . 63
4.3 **Interacting Fermions on a Torus Knot** . . . 68

5 THERMAL ASPECTS OF INTERACTING QUANTUM GASES IN LORENTZ-VIOLATING SCENARIOS 69
5.1 **SME Fermion Sector** . . . 69
5.2 **Lorentz-Violating Scalar Fields** . . . 71
5.3 **Thermodynamic model** . . . 72
5.4 **Thermodynamic state quantities** . . . 75
5.5 **Interacting fermions** . . . 80
5.6 **Interacting bosons** . . . 82
5.7 **Results and discussions** . . . 84
5.8 **Applications** . . . 86
5.8.1 Phosphorene . . . 87
5.8.2 Spin precession . . . 88
5.9 **Are they still extensive state quantities?** . . . 89
5.10 **Numerical analyses** . . . 90

6 THERMODYNAMIC PROPERTIES IN HIGHER-DERIVATIVE ELECTRODYNAMICS 94
6.1 **Podolsky electrodynamics** . . . 94
6.1.1 The model . . . 94
6.1.2 Thermodynamic properties . . . 95
6.2 **Podolsky with Lorentz violation** . . . 99
6.2.1 The model . . . 99
6.2.2 Thermodynamic properties . . . 101
6.3 **Results and discussions** . . . 104

7 LORENTZ-VIOLATING SCENARIOS IN A THERMAL RESERVOIR 106
7.1 **Graviton with Lorentz violation** . . . 106
7.2 **Generalized model with Podolsky and Lee-Wick terms** . . . 111
7.3 **Results and discussions** . . . 114

8 HIGHER-DERIVATIVE LORENTZ-BREAKING DISPERSION RELATIONS: A THERMAL DESCRIPTION 117
8.1 **Thermodynamical aspects of CPT-even higher-derivative LV theory** . . . 117

8.2 **Thermodynamical aspects of CPT-odd higher-derivative LV theory** 125

9 BOUNCING UNIVERSE IN A HEAT BATH **135**
9.1 **Modified dispersion relations and their thermodynamical impacts** 135

10 CONCLUSION AND PERSPECTIVES **147**
BIBLIOGRAPHY 153
APPENDIX – LIST OF PUBLICATIONS 188

1. INTRODUCTION

Statistical mechanics is a formalism which has the purpose of describing physical aspects of matter, correlating the macroscopic properties with its microscopical constituents. In principle, there is no limitation of applying this formalism to different states of matter which, therefore, suffices to describe fairly enough so many natural phenomena in an accurate way. Indeed, having a significant prosperity in many fields, the statistical mechanics has been employed to liquid, [1, 2, 3, 4] solid [5, 6, 7], and gaseous states [8, 9, 10, 11, 12], matter composed of several components [13, 14, 15, 16], matter under extreme conditions of density and temperature [17, 18], biological systems [19, 20, 21, 22, 23, 24, 25, 16], and so forth. More so, within the scenario of statistical mechanics, we may properly examine both equilibrium and non-equilibrium states as well. Actually, these explorations allow us to comprehend the way of such physical systems behave when the variable time is taken into account.

In opposition to the present state of its progress concerning the prosperity of its applications, the genesis of statistical mechanics was rather quite unpretentious. Besides some archaic references, e.g., Gassendi (1592-1655) [26], and Hooke (1635-1703) [27], the genuine work of this feat was brought about significantly by Bernoulli (1700-1782) [28], Herapath (1790-1868) [29], and Joule (1818-1889) [30]. They tried to address a foundation set for the kinetic theory of gases in their own personal manners. In essence, the foundations of these works were aimed at developing a method where the thermodynamic state quantities of a given gas would arise from the motion of its constituents, the molecules – being directly estimated by regarding the dynamical influence of the molecular bombing through the walls of the reservoir. In this way, Bernoulli and Herapath showed that the pressure p of an arbitrary gas, for a constant temperature, is inversely proportional to the volume V of the reservoir (it does not essentially depend on the shape of the container) – the Boyle's law. In other words, it entails that, for a given temperature, the average speed of the particles does not depend on pressure and volume. Moreover, Bernoulli also made some attempts to establish the first-order corrections to such approach. He suggested the concept of a finite size to molecules, and proposed that the volume V should be written instead in terms of $V - a'$, where a' is the individual volume carried by each particle.

In a pioneer manner, with a similar method to describe particles/molecules, it was Joule who first showed that pressure p was proportional to the square of the particle speed v.

Introducing the so-called "quasistatistical" consideration, Krönig (1822-1279) [31] went beyond assuming that, for any arbitrary time t, the molecules were flying against each other in six independent directions. He also presumed that the molecular speed v should be maintained the same for all constituents of matter having their kinetic energy proportional to the absolute temperature T of the respective gas.

In 1857, Clausius (1822-1888) [32] derived the concept of an **ideal gas** – law under which all assumptions are much less involving than Krönig's. Discarding the leading preliminaries ascribed to Krönig, he showed that $p = \frac{n}{3}mv^2$ [1] was still valid. In 1859, Clausius also introduced the notion of the *mean free path* and, therefore, turned out to be the first scientist to inspect a notable concept which would be named afterwards as the transport phenomena [33]. Moreover, within his studies, a remarkable consideration gave rise to: the hypothesis which states the number of collisions among particles, the so-called "Stosszahlansatz"[2]. Fundamentally, such assumption played an important role in the brilliant work made by Boltzmann (1844-1906) [36]. According to Maxwell (1831-1879) [37], in his famous article called "Molecules" [38] written for the *Encyclopedia Britannica*, referred Clausius as being the "principal founder of the kinetic theory of gases," while, on the other hand, Gibbs, as "father of statistical mechanics."

As a matter of fact, Maxwell got seduced by the brand new ideas coming from Clausius. In 1860, he showed up for the first time to the scientific community with his work entitled *Illustrations of the dynamical theory of gases* [39, 40], that went beyond his antecedents by performing his famous law: *the distribution of molecular speeds*. Stimulated by the *Gaussian law of distribution of random errors*, Maxwell was fundamentally propped up by fundamental aspects of probability. Moreover, a derivation totally based on the requisite that *the equilibrium distribution of molecular speeds, once acquired, should remain invariant under molecular collisions* [41] brought out in 1867. As a straightforward consequence, this guided him to set up the Maxwell's transport equation – this led to the same consequences whether one takes into account a theory based on the more fundamental concepts: Boltzmann's ideas. After he obtained a position at the Cavendish laboratory at Cambridge, his contributions concerning that subject fade considerably.

On the other hand, during the period 1868–1871, Boltzmann generalized the so-called Maxwell's distribution law considering rather polyatomic gases. From such approach, emerged the well-known Boltzmann factor $e^{-\beta E}$ – in which E represents the energy of a given molecule.

[1] Here, n denotes the number of particles, m the respective mass.

[2] "In the kinetic theory of gases in physics, the molecular chaos hypothesis (also called Stosszahlansatz in the writings of Paul Ehrenfest[34, 35]) is the assumption that the velocities of colliding particles are uncorrelated, and independent of position. This means the probability that a pair of particles with given velocities will collide can be calculated by considering each particle separately and ignoring any correlation between the probability for finding one particle with velocity v and probability for finding another velocity v' in a small region ."– https://en.wikipedia.org/wiki/Molecular_chaoscite_note-1

These accomplishments also conduced the **equipartition theorem**[3]. More so, Boltzmann afterwards proved , as the distribution proposed by Maxwell, one different generalized distribution – currently, we call it as **Maxwell–Boltzmann distribution**, is stationary in relation to molecular collisions.

The eminent **H-theorem**[4] came up in 1872 providing a molecular approach to the inherent tendency of physical systems: the equilibrium state. This allowed the connection between the microscopic – which genuinely characterizes the statistical mechanics, and the phenomenological world – which naturally depicts thermodynamics much more clearly than ever before. Furthermore, it is worth mentioning that it also established a straightforward method aimed at calculating the entropy, of a given physical system, from a simply microscopic viewpoint. Mathematically, Boltzmann proved that there exists a unique distribution which keeps invariant under molecular collisions: *Maxwell–Boltzmann distribution.* Any other one, turned out to go over such distribution. Also, in 1876, he proposed his notable transport equation; thereby, in possession with this feat, Chapman (1888-1970) [42, 43] and Enskog [44] (1884-1947) verified a highly potent apparatus to study the macroscopic aspects of systems in non-equilibrium states.

Nevertheless, things turned out to be hard for Boltzmann. He suffered much criticism due to his scientific propositions mainly by Loschmidt (1821–1895) [45] and Zermelo (1871-1953) [46]. While Loschmidt wondered to know the impact of this theorem, Zermelo was focused on fitting these effects with the quasiperiodic behavior of closed systems. Although much efforts in order to defend himself, Boltzmann could not persuade his adversaries to the completeness of his point of view. In parallel, the "energeticists" – mainly led by Mach (1838-1916) [47] and Ostwald (1853-1932) [48], did criticize the molecular basis of the kinetic theory. On the other hand, Kelvin (1824-1907) did point out the *nineteenth-century clouds hovering over the dynamical theory of light and heat* [49].

This entire situation made Boltzmann had an intense melancholy in a such way that he felt desperate culminating in a persecution complex. In his work entitled *Vorlesungen über Gastheorie* [50], he wrote such introduction: *I am convinced that the attacks (on the kinetic theory) rest on misunderstandings and that the role of the kinetic theory is not yet played*

[3]In classical statistical mechanics, the equipartition theorem is a general formulation that relates the temperature of a system to its average energy. It is also known as equipartition law, equipartition energy or simply equipartition. The central idea of such theorem is that, in thermal equilibrium, energy is shared equally between its various forms, e.g., the average kinetic energy in the translational motion of a molecule must equal the average kinetic energy of its rotational motion.

[4]Introduced by Ludwig Boltzmann in 1872, the H-theorem describes the tendency to decrease the quantity $H(t) = \int_0^\infty f(t,E)\left[\ln\left(\frac{f(t,E)}{\sqrt{E}}\right)\right] \mathrm{d}E$ in a quasi-ideal gas of molecules. Since this quantity H was supposed to represent the entropy, theorem H was an early demonstration of the power of statistical mechanics, as it claimed to derive the second law of thermodynamics—a statement about fundamentally irreversible processes—from reversible microscopic mechanics. Theorem H is a natural consequence of the Boltzmann-derived kinetic equation that came to be known as the Boltzmann equation.

out. In my opinion it would be a blow to science if contemporary opposition were to cause kinetic theory to sink into the oblivion which was the fate suffered by the wave theory of light through the authority of Newton. I am aware of the weakness of one individual against the prevailing currents of opinion. In order to insure that not too much will have to be rediscovered when people return to the study of kinetic theory I will present the most difficult and misunderstood parts of the subject in as clear a manner as I can. [51]

In statistical mechanics, an **ensemble** is an idealization approach which consists in a large number of virtual copies of a system, considered all at once, each of which represents a possible state that the real system might be in. The notional size of ensembles in thermodynamics, statistical mechanics and quantum statistical mechanics can be very large, including every possible microscopic state the system could be in, consistent with its observed macroscopic properties. For many important physical cases, it is possible to calculate **averages** directly over the whole of the thermodynamic ensemble, to obtain explicit formulas for many of the thermodynamic quantities of interest, often in terms of the appropriate **partition function**.

The concept of an equilibrium or stationary ensemble is crucial to many applications of statistical ensembles. Although a mechanical system certainly evolves over time, the ensemble does not necessarily have to evolve. In fact, the ensemble will not evolve if it contains all past and future phases of the system. Such a statistical ensemble, one that does not change over time, is called stationary and can be said to be in statistical equilibrium.

The study of thermodynamics is concerned with systems that appear to human perception to be "static", and which can be described simply by a set of macroscopically observable variables. These systems can be described by statistical ensembles that depend on a few observable parameters, and which are in statistical equilibrium. Gibbs noted that different macroscopic constraints lead to different types of ensembles, with particular statistical characteristics. In essence, three important thermodynamic ensembles were defined by Gibbs.

First, the **microcanonical ensemble** is a statistical ensemble where the total energy of the system and the number of particles in the system are each fixed to particular values; each of the members of the ensemble are required to have the same total energy and particle number. The system must remain totally isolated (unable to exchange energy or particles with its environment) in order to stay in statistical equilibrium [52].

Second, the **canonical ensemble** is a statistical ensemble where the energy is not known exactly but the number of particles is fixed. In place of the energy, the temperature is specified. The canonical ensemble is appropriate for describing a closed system which is in, or has been in, weak thermal contact with a heat bath. In order to be in statistical equilibrium, the system must remain totally closed (unable to exchange particles with its environment) and may come into weak thermal contact with other systems that are described by ensembles with the same temperature [53].

Third, the **grand canonical ensemble** is a statistical ensemble where neither the energy nor particle number are fixed. In their place, the temperature and chemical potential are specified. The grand canonical ensemble is appropriate for describing an open system: one which is in, or has been in, weak contact with a reservoir (thermal contact, chemical contact, radiative contact, electrical contact, etc.). The ensemble remains in statistical equilibrium if the system comes into weak contact with other systems that are described by ensembles with the same temperature and chemical potential.

Within the ensemble theory, the dynamics of a certain system are governed by the generalized coordinates q_i and momenta p_i. This pair of configuration represents a point $G(q_i, p_i)$ in the phase space. The evolution of the system with respect to a given time t "scratches" a trajectory within the phase space – which in general does not represent/correspond a trajectory in the configuration space. In a fundamental manner, the respective equations of motion represent the "path" of the trajectory and may be limited by the nature of the possible physical constraints. For the sake of creating an suitable formalism, one may regard a given system provided by an indefinitely huge number of "identical copies" – independents from each other; in other words, it would be an ensemble of equivalent systems under matching physical constraints – we must have infinitely many $G(q_i, p_i)$-points in the phase space. Explicitly, the conceptualization of these "pillars" was first proposed by Maxwell [54] who occasionally utilized the vocable "statistico-mechanical" to design the investigation of ensembles in the context of gaseous systems.

One of the most prominent parameter within the ensemble theory is the density function, $\rho(q_i, p_i; t)$, of the $G(q_i, p_i)$-points in the phase space. In essence, if there exists a stationary distribution – $\partial\rho/\partial t = 0$, the system lies in the equilibrium state. Boltzmann and Maxwell restricted their respective investigations to ensembles whose the function ρ had the dependency exclusively on the energy E of the system. This also incorporated the particular case involving ergodic systems. As a result, the average over the ensemble, $\langle f \rangle$, for a given physical quantity f (considering at any given time t) should be the same as the long-time average, $\bar{f}$, belonging to any arbitrary portion of the ensemble. Thereby, after performing the measurement of a physical system, it is the quantity $\bar{f}$ that we expect to acquire. In this way, we naturally presume to obtain the connection between theory with experiment by obtaining the quantity $\langle f \rangle$. With this, we get the advantage to walk through an alternative path using the microscopic theory of matter rather than the empirical old fashioned method of thermodynamics.

A substantial progress in such a direction was also accomplished by Gibbs (1839-1903). He made the theory of ensembles be more treatable for the scientific community with his *Elementary Principles of Statistical Mechanics* [55, 56]. Taking the advantage of using purely the mechanical peculiarity of the microscopic constituents, Gibbs empowered one to calculate

a complete set of thermodynamic state quantities of a given system under consideration by developing some methods. These ones turned out to be more generic than any treatment made before. Essentially, his proposition lied in requirement of having a system which obeyed Hamilton's, and Lagrange's equations of motion. In this sense, as an analogy, Gibbs's work can be thought to have a notable contribution to thermodynamics as well as Maxwell's work had the contribution to the electrodynamics.

In the same concomitant decade, these achievements concurred with one of the most brilliant insights into physics – the great revolution that entailed by the seminal work brought about by Planck (1858-1947) in 1900 [57]. Initially, the Planck's quantum theory worked out with the essential mysteries of the **black body radiation**[5] in a successful manner. Thereby, he could unify some concepts coming the well established subjects in the literature – thermodynamics, mechanics, and electrodynamics.

The succeeding works were provided by Einstein (1879-1955) [58] – considering the photoelectric effect and Compton (1892-1962) [59, 60] – investigating the scattering of x-rays and, therefore, discovering the occurrence of the quantum of radiation. Employing analogously the same notion that Maxwell used to acquired his law of distribution of molecular speeds considering a gas made by standard molecules, Planck derived his radiation formula by addressing the black-body radiation as a photon gas instead. As a result, one simple question naturally arises: is there exist a considerable difference in the distribution analysis of particles between a photon gas and the "conventional" gas of molecules?

Satisfactorily, the answer to this issue was given when Bose also obtained the same results proposed by Planck on his own. In his unforgettable manuscript in 1924 [61], Bose considered the black-body radiation within the context of a gas of photons. Nevertheless, despite of proposing a method governed by allocated photons, he focused his attention rather on the number of accessible states of the system, which accounts for "the portion of particular number" of photons. Moreover, it seemed to be Einstein who had translated for the first time the manuscript of Bose from Germany to English; in this translation, Einstein pointed out that: *"Bose's derivation of Planck's formula is in my opinion an important step forward. The method employed here would also yield the quantum theory of an ideal gas, which I propose to demonstrate elsewhere."* [52].

Implicitly, within the Bose formalism, there existed one important aspect: the set of numbers of particles (photons) are in a different energy state of the system, instead of being particularized in a specific one. Essentially, it means that these particles under consideration are indistinguishable. Furthermore, Einstein commented that the Bose's ideas should also be applied to the material particles. With this in mind, he used the application of Bose's approach in two of his works to study the ideal gas – nowadays, we now call such study as

[5]This subject will be one of the central theme of this thesis – in following chapters, we shall propose some corrections to the black body radiation for different scenarios in field theories.

the Bose–Einstein statistics [62, 63].

Einstein pointed out that the crucial difference between the new statistics and the classical *Maxwell–Boltzmann* one came out so naturally regarding the indistinguishability of the molecules. In the same manuscripts, a new phenomena gave rise to: the *Bose–Einstein condensation*. Such phenomena, afterwards, would be adopted by London [64, 65] as the basis for a microscopic comprehension at low temperatures of the intriguing aspects of liquid ^{4}He.

Taking into account the announcement of Pauli's (1900-1958) exclusion principle in 1925 [66], Fermi (1901-1954) in the subsequent year, proved that no more than one particle could occupy the same energy state ($n_i = 0, 1$), and that corresponding physical system should be in agreement with a brand new type of distribution, the Fermi–Dirac statistics. It worth mentioning that the Bose's method also leads to such statistic regarding certain limits.

After that, many applications were proposed by the scientific community. For instance, the Fermi–Dirac distribution was used by Fowler (1911-1995) [67] to investigate white dwarf stars within the viewpoint of equilibrium states; and Pauli [68] to explain some intriguing aspects concerning paramagnetism of alkali metals – in both of them, we have to deal with a "highly degenerate" gas of fermions (electrons) that agrees with Fermi–Dirac statistics.

In parallel, Sommerfeld (1868-1951) produced one of his principal works in 1928 [69] that did not merely regard the electron theory of metals, but instead it also provided a fresh start in the correct direction. Following the ideas from the classical theories proposed by Riecke (1845-1915) [70], Drude (1863-1906) [71], and Lorentz (1904–1905) [72, 73], Sommerfeld could practically explain all the most important properties of metals that came from the conduction of electrons; more so, he also got results which had better agreement with experiments. About the same epoch, Fermi [74] and Thomas (1903-1992) [75, 76] analyzed the electron behavior within the context of heavier atoms and acquired theoretically a resealable approximation for some binding energies. Such studies led to the progress of the so-called Thomas–Fermi model of the atoms, which was afterwards generalized in a such way that it could also be used for molecules, solids, as well as nuclei.

The entire construction of statistical mechanics was revised by the concept of indistinguishability of particles. The statistical features of the system was now expanded by another statistical facet that emerged from the probabilistic characteristic of the **wave mechanical description**. Naturally, this particularity was associated with the necessity of formulating a new approach of the ensemble theory. Initially, it was accomplished by Landau (1908-1968) [77] and von-Neumann (1903-1957) [78] who used the so-called **density matrix** – it is the quantum version analogy of the density function of the classical phase space. In a generalized way, taking into account both statistical and quantum mechanical viewpoint, Dirac (1902-1984) [79, 80, 81, 82, 83] made a theory putting all these concepts together. Taken

the advantage of utilizing the classical ensemble theory, these authors regarded merely the microcanonical and the canonical ensembles. Afterwards, Pauli introduced the concept of the grand canonical ensembles within the context of quantum statistics [84].

The important question as to which particles would obey **Bose–Einstein statistics** and which Fermi–Dirac remained theoretically unsettled until Belinfante (1913-1991) [85, 86, 87] and Pauli [88, 89] discovered the vital connection between spin and statistics. It turns out that those particles whose spin is an integral multiple of $\hbar$ obey Bose–Einstein statistics while those whose spin is a half-odd integral multiple of $\hbar$ obey Fermi–Dirac statistics [52].

In this sense, in recent years, the study of quantum rings (QRs) [90, 91, 92, 93, 94] has received much attention due to its variety of technological applications in single-photon emitters, nanoflash memories [95, 96], photonic detectors [97, 98, 99, 100] and qubits for spintronic quantum computing [95]. Moreover, quantum rings (QRs) is a fruitful subject for studying topological influence in condensed matter physics [95]. They are remarkable nanostructures with a non-simply connected topology which gives rise an intriguing energy structure [101] which differs from most others low-dimensional systems such as quantum dots, quantum wires and quantum wells. Besides QRs are divided into two categories: the one-dimensional (1D) (rings of constant radius) [102, 103, 104, 105, 106, 107, 108, 109, 110] and the two-dimensional rings (2D) (rings of variable radius) [111, 112, 113, 114, 115, 116, 117].

In particular, a special case of 1D QRs has obtained notoriety in the literature, the so-called Aharonov-Bohm (AB) rings [118, 119, 120, 121]. Currently, there are several number of works that analyze the dynamics of AB rings in both theoretical and experimental approaches. For instance, AB rings are studied in connection with the Aharonov-Casher (AC) effect [118, 119, 120, 121, 122], Lorentz symmetry violation [120], mesoscopic decoherence [123], electromagnetic resonator [124] and Rashba spin-orbit interaction [121, 125, 126].

The investigation of thermal aspects of materials has gained considerable attention in recent years especially in the context of condensed-matter physics and the development of new materials [127, 128, 129, 130]. Given the existence of some well-known approximations, the electrons of a metal can be assumed to be a gas, as they are effectively free particles [131, 132, 133, 134, 135, 136]. Such electron systems are worth exploring due to their relevance in fundamental [137, 138] and applied [139, 140] physical contexts. In parallel, a longstanding issue in quantum mesoscopic systems is how to perform an exact sum over the states of either *interacting* or *noninteracting* particles. Depending on the situation, the boundary effects cannot be neglected; instead, they should be taken into account in order to acquire a better agreement with the experimental results. Moreover, the properties of some systems are assumed to be shape dependent [141, 142, 143] and sensitive to their topology [144, 145, 146, 147, 148].

From a theoretical viewpoint, a related problem of statistical mechanics is to perform the sum over all accessible quantum states to obtain the physical quantities [52, 149]. Normally, the spectrum of particle states, which are confined in a volume, will be elucidated by the study of boundary effects. Nevertheless, if the particle wavelength is too short in comparison with the characteristic scale of the system under consideration, boundary effects can be overlooked. In previous years, such an assumption was supported by Rayleigh and Jeans in their radiation theory of electromagnetism [150]. Furthermore, such an involvement also emerged in a purely mathematical context and was rigorously solved afterwards by Weyl [151].

The knowledge of thermodynamic properties of many body systems plays an essential role in condensed matter physics, especially in case of developing new materials [152, 153, 154, 155, 156, 157, 158]. Electrons in metals, under widely varying circumstances, behave as free particles and can be treated as electron gas under certain approximations [132, 159, 160, 131, 161, 162, 163, 164, 165]. In this regard, surface effects such as shape dependence [166, 167, 168] and non-trivial topology [169, 170, 171, 172] can lead to novel and unexpected features. A generic computational problem is to derive the partition function that requires a sum over all accessible quantum states [173, 174, 175]. For higher temperatures the particle effective wavelength turns out to be too short in comparison to the characteristic dimension of the system and, therefore, the boundary effect can be overlooked. Previously, such idea was exploited by Rayleigh and Jeans in radiation theory of electromagnetism [176, 177, 178] and this was corroborated in a purely mathematical framework by Weyl [179].

Quantum mechanics of particle on a torus knot was analysed [180]. Further topological aspects such as Berry phase and Hannay angle features in this model were investigated in [181, 182]. A more elaborate investigation of knotted path effects on quantum dynamics was recently proposed in the literature where curvature and torsion effects were taken into account [183]. The generic problem was considered earlier in [184, 185, 186, 187, 188].

On the other hand, modern searches for **Lorentz violation** are scientific studies that look for deviations from Lorentz invariance or symmetry, a set of fundamental frameworks that underpin modern science and fundamental physics in particular. These studies try to determine whether violations or exceptions might exist for well-known physical laws such as special relativity and CPT symmetry, as predicted by some variations of quantum gravity, string theory, and some alternatives to general relativity.

Lorentz violations concern the fundamental predictions of special relativity, such as the principle of relativity, the constancy of the speed of light in all inertial frames of reference, and time dilation, as well as the predictions of the standard model of particle physics. To assess and predict possible violations, test theories of special relativity and effective field theories (EFT) such as the **Standard-Model Extension** (SME) have been invented. These models

introduce Lorentz and CPT violations through spontaneous symmetry breaking caused by hypothetical background fields, resulting in some sort of preferred frame effects. This could lead, for instance, to modifications of the dispersion relation, causing differences between the maximal attainable speed of matter and the speed of light. It is exactly about this feature that the second part of this thesis is devoted to.

Knot theory is a well known branch in pure mathematics [189, 190]. On the other hand, the quantum mechanics on particles on torus knot can be motivated by the carbon nanorings (made from carbon nanotubes [191]) that are intimately associated to the edges of nanotubes, nanochains, graphene, and nanocones [192, 193]. Such nanorings (or nanotori) have a variety of notable features, being mostly investigated within the ab initio calculations [194], especially in multiresonant properties [195], magneto-optical activity [196], paramagnetism [197], and ferromagnetism [198, 199]. Moreover, these present nanostructures may also be employed in optical communications [200], isolators, traps for ions and atoms [201], and lubricants [202].

The well-known Lorentz symmetry is an equivalence of observation as a result of Special Relativity. This entails that the physical laws keep the same for all observers as long as the condition of inertial frames is ensured. Being the association of both rotational and boost symmetries, the Lorentz invariance is a fundamental feature when one regards the General Relativity and the Standard Model of particle physics. On the other hand, if one considers a violation of such condition, one will generally produce either directional or velocity dependences modifying, therefore, the dynamics of particles and waves [203, 204, 205, 206, 207, 208, 209].

Generically, any symmetry breaking process brings about unusual consequences, which can exhibit some fingerprints of new physical phenomena. Specially when the Lorentz symmetry is broken it leads to various particularities [210, 211, 212] being possibly feasible in quantum gravity [213]. Moreover, models involving closed-string theories [214, 215, 216, 217, 218], loop quantum gravity [219, 220], noncommutative spacetimes [221, 222], spacetime foam models [223, 224], (chiral) field theories defined on spacetimes with nontrivial topologies [225, 226, 227, 228], Hořava-Lifshitz gravity [229] and cosmology [230, 231] are also based on the assumption that Lorentz invariance is no longer maintained. In this sense, in order to entirely characterize the effects due to Lorentz symmetry violation, one requires the obtainment of a reasonable theory that gives a dynamical characteristic to the system.

Thereby, there exists a widespread theoretical framework to support such approach, the Standard Model Extension (SME) [232, 233, 234, 235, 236]. In a general manner, it describes violations of CPT and Lorentz symmetries concerning both General Relativity and the Standard Model at attainable energies [233, 232, 236, 237, 238]. The Lorentz-violating operators are rather tensor terms coupled with physical fields that acquire a nonzero vacuum

expectation value [239]. This latter feature gives rise to a violation of Lorentz symmetry when particle frames are taken into account and a preservation of its invariance when observer frames are assumed though [240]. In this manner, this theoretical background gave the viability for many works involving the fermion sector [241, 242, 243, 244, 245, 246, 247] and electromagnetic CPT-odd [248, 249, 250, 251, 252, 253, 254, 255, 256] as well as CPT-even coefficients [257, 258, 259, 260].

In addition, the connection established from Lorentz violation and theories including higher-dimensional operators has gained much attention through the last years. Within such approach, we can have operators with higher mass dimensions concerning higher-derivative terms for instance. The nonminimal version of SME has the advantage to hold indefinite numbers of such contributions [261, 262, 263, 264, 265] in contrast with its minimal version. In this context, there are many works whose theoretical properties were studied involving nonrenormalizable operators [266, 267, 268, 269, 270, 271, 272, 273, 274].

Although there are some works in the literature looking towards to investigate the thermodynamic aspects of distinct systems with Lorentz violation [275, 276, 277, 278, 279, 280, 281, 282, 283], up to date, there is a lack of studies considering relativistic interacting quantum gases governed by higher-dimensional operators. In such a way, we pioneer present a model in order to provide such derivation. Here, we focus on the following quantities of interest: particle number, entropy, mean energy and pressure. For doing so, we utilize the so-called grand canonical partition function and the grand canonical potential. With them, all the following evaluations could be carried out in high temperature regime.

In theoretical physics, there exists a memorable problem which is putting on an equal footing the so-called Standard Model [284], provided by a consistent experimental data in predicting the behavior of fundamental particle physics, and the widespread General Relativity [285], which has the purpose of regarding gravity as a geometric theory. Since all these approaches are intensively well tested, if there exists a conciliation for both, one will expect a unique and fundamental theory of quantum gravity [213]. Moreover, this structure could bring about the feasibility of investigating some new phenomena not yet individually described by them. Nevertheless, up to now, there is neither experimental nor observational indications of any fingerprints of such a unified theory perhaps due to the fact that its effects are highlighted when the energy range around the Planck mass, i.e., $m_{\mathrm{P}} \sim 10^{19}$ GeV, is taken into account.

Nowadays, since it is impossible to have the access of such scale, a reasonable way of working on it has been developed considering the viewpoint that quantum gravity phenomena can be recognized by the proliferation of their effects at attainable energies. In this sense, one of the most remarkable possibilities regards the violation of Lorentz symmetry. Supporting such theory, there are many different mechanisms that bring out Lorentz-violating effects

such as in string theory [286], Horava-Lifshitz gravity [287], noncommutative field theories [288] and loop quantum gravity [289].

Having been proposed about thirty years ago by Kostelecký *et al.*, the Standard Model Extension (SME) [232, 233, 234, 235, 236] is an extended version for the usual Standard Model theory. It possesses Lorentz-violating terms, which are rather tensor terms acquiring a nonzero vacuum expectation value, coupled with physical fields preserving their coordinate invariance and a violation of Lorentz symmetry when particle frames are considered [240]. Likewise, such theoretical background has been the precursor for an expressive number of works involving the fermionic sector [241, 242, 243, 244, 245], the electromagnetic CPT-odd and Lorentz-odd term [290, 291, 292, 293, 294, 295] as well as the CPT-even and Lorentz odd gauge sector [257, 258, 259, 260].

Over the last years, the connection between Lorentz violation and theories including higher derivative operators has received much attention [266, 267, 268, 269, 270, 271, 272, 273, 274]. As a matter of fact, it may have operators of higher mass dimensions incorporating for instance higher-derivative terms. Being in contrast to the minimal version of the Lorentz violating extensions, its nonminimal approach has the advantage of possessing an indefinite number of such contributions [269]. In this sense, the latter version of the SME was first proposed considering both the photon [261] and the fermionic sectors [263].

In this direction, the first illustration of a higher-derivative electrodynamics was proposed by Podolsky [296] having a noticeable feature which is the generation of a massive mode without losing the gauge symmetry. In that paper, it was initially studied the gauge-invariant dimension-6 term, $\theta^2\partial_\alpha F^{\alpha\beta}\partial_\lambda F^{\lambda}{}_{\beta}$, with a coupling constant θ, which afterwards would be known as the Podolsky parameter, with the mass dimension being -1. Clearly, such theory displays two distinct dispersion relations, i.e., the usual massless mode and the massive mode which possesses the advantage of avoiding divergences ascribed to the pointlike self-energy. Nevertheless, considering the quantum level, the latter mode gives rise to the appearance of ghosts [297].

Additionally, in the late 1960s, there exists another noteworthy extension of Maxwell theory with higher derivatives being described by the dimension-6 term $F_{\mu\nu}\partial_\alpha\partial^\alpha F^{\mu\nu}$, the Lee-Wick electrodynamics [298, 299]. Notably, this theory leads to a finite self-energy for a pointlike charge in $(1+3)$ spacetime dimensions and to the appearance of a bilinear contribution to the Maxwell Lagrangian. This is analogous to the Podolsky term showing an opposite sign though. Such "incorrect" sign outputs energy instabilities at the classical level, whereas it brings out a negative norm states in the Hilbert space at the quantum level. Moreover, it was also Lee and Wick who first proposed a mechanism seeking the preservation of unitarity by removing all states with negative norm from the Hilbert space. In the last decade, this theory came back to obtain notability with the proposal of the Lee-

Wick Standard Model [300, 301, 302], based on non-Abelian gauge structure free of quadratic divergences. Such model was widespread having many contributions for both theoretical and phenomenological approaches [303, 304]. Furthermore, it is worth mentioning that, in this general context, investigations of Lorentz violation extensions are discussed [305] including applications to the interaction of pointlike and spatially extended sources [306, 307].

On the other hand, the focus on an extension of the SME, which takes into account gravity, arouses from the fact that the Lorentz violation can be expected to be a key element for a quantum theory of gravitation. As a matter of fact, it is important to note that Lorentz-violating effects might be expressive in regions where the curvature or torsion are accentuated, as in the vicinity of black holes for instance [308]. Besides, these implications can represent a notable role in cosmological scenarios being illustrated by either dark energy [309] or dark matter [310]. Moreover, there are others whose anisotropy factors can be added in the Friedman-Robertson-Walker solutions [311]. In addition, the main motivation of constructing a theory consistent with gravity, i.e., being in agreement with Bianchi identities and so forth, is having a consistent formalism seeking to maintain the local observer Lorentz covariance, despite the presence of local particle Lorentz violation [237]. In this way, it is worth pointing out that there are investigations regarding Lorentz violation in the linearized gravity [312] and others [313, 314].

The concept the mass is a key issue in theoretical physics, particularly within the context of particle physics. For instance, the Higgs mechanism [315, 316] is the most known approach to generate mass for the particles from a genuine gauge-invariant theory. After all, the interactions between the constituents of matter are usually expressed in terms of gauge theories, which are supposed to be massless. With a different viewpoint, the presence of a massive vector field, commonly ascribed to the Proca's model, possesses many consequences well encountered in the literature [317, 318]. As a result, since the electromagnetic interactions are described in terms of the symmetry group, namely $U(1)$, the Quantum Electrodynamics should be reexamined whether massive modes were taken into account [319].

On the other hand, if one deals with the Podolsky electrodynamics [296, 320, 321], one will obtain remarkable features. Among them, we can point out that such theory brings about a massive mode without losing the gauge symmetry. Moreover, it was also Podolsky who first attempted to describe the interpretation of this massive mode, i.e.; it was depicted as a neutrino. In this case, the propagator has two poles, one corresponding to the massless mode and the other one associated with the massive mode. Thereby, considering the classical approach, the latter has a feature of removing singularities associated with the pointlike self-energy. Nevertheless, if one regards quantum properties, one will obtain the appearance of ghosts [297]. The appropriate gauge condition to provide Podolsky electrodynamics is no longer the common Lorenz gauge but rather a modified one [322], being consistent with the

existence of five degrees of freedom. Two of them are related to the massless photon mode while the other three ones are related to the massive longitudinal mode [271]. Besides, it is worth mentioning that, in the presence of the Podolsky term, there exist other remarks involving quantum field theory in the context of renormalization [323], path integral quantization and fine-temperature approach [324, 325, 326], multipole expansions [327], black holes [328], cosmology [329] and others [330, 270, 331, 332, 333, 274].

About twenty years up to now, the Lorentz-violating contributions of mass dimensions 3 and 4 have been taken into account within both theoretical and phenomenological scenarios in the photon and lepton sectors [334]. Recently, theories with higher-dimension operators have received much attention after a generalized approach proposed by Mewes and Kostelecký in Ref. [335]. In the CPT-even photon sector, the leading-order contributions in an expansion in terms of additional derivatives are dimension-6 ones. Hence, these are also the most prominent ones that could play a role in nature if higher-derivative Lorentz violation (LV) existed [271].

Although the Lorentz invariance is a well-established symmetry of the nature, its possible violation is assumed within many contexts [336, 337, 338]. During the last years, the Lorentz symmetry breaking and its possible implications are intensively studied in different scenarios, see f.e. [339, 340, 341, 342, 343]. As it is known, the Lorentz-breaking parameters are experimentally presumed to be very tiny [344]. Nevertheless, this does not imply that they contribute to the physical processes in a negligible manner. Moreover, the presence of Lorentz-violating (LV) higher-derivative additive terms can imply in arising of large quantum corrections [345, 346].

All this clearly motivates us to investigate the higher-derivative LV terms. The first known example of such term was originally introduced by Myers and Pospelov many years ago [347]. The key feature of this term is that it involves higher (third) derivatives, being proportional to a Lorentz-breaking constant vector and to a small constant parameter (treated as an inverse of some large mass scale). Furthermore, various issues related to them were studied, including its perturbative generation and dispersion relations (for a review on such terms see f.e. [348]. An exhaustive list of such terms with dimensions up to 6 can be found in [265]). It was argued in Ref. [349] that a theory involving such a term can be treated consistently as a series in the above-mentioned inverse mass scale.

One of the important issues related to higher-derivative LV theories is certainly their thermodynamical aspects. Studies on the thermodynamics of LV extensions of various field theory models could provide additional information about initial stages of expansion of the Universe, whose size at these stages was compatible with characteristic scales of Lorentz symmetry breaking [344]. The methodology for studying the thermodynamical aspects in LV theories has firstly been presented in [350]. Since then, various applications of this

procedure have been developed [351, 352, 353, 354, 355, 356, 357, 358, 359, 360].

The idea that the widely-spread gravitational theory may be outlined by entropy, was formulated for the first time by Jacobson [361] and afterwards received further developments [362, 363, 364, 365, 366, 367, 368, 369, 370, 371]. Additionally, in order to overcome the longstanding issue of the cosmological singularity present within the Big Bounce model, a notable approach was used considering the semiclassical limit [372, 373, 374, 375].

For instance, in Ref. [362], the authors assumed, as the starting point, a certain dispersion relation rather than a particular Lagrangian. With this, a remarkable aspect emerged: the avoidance of divergences in cosmological scenarios when the high energy limit was taken into account. In other words, they obtained a bouncing solution, i.e., with the absence of singularity, ascribed to the modification of the Friedmann equations. This procedure is absolutely reasonable since, being in agreement with previous studies, starting only from such modified dispersion relations can be considered though as an alternative way to investigate for instance cosmological scenarios [376, 354, 377].

Moreover, one significant aspect which is worth investigating in the context of Lorentz symmetry violation is actually the respective thermal aspects of the corresponding theory. With such study, we can obtain a better comprehension of how massless and massive modes behave when different range of temperatures are taken into account. This might possibly give us additional information to confront the theoretical background with the experimental results in order to help searching for any trace of the Lorentz symmetry violation. Furthermore, the investigation based on the thermodynamic properties and the Lorentz-violating (LV) effects could supply further knowledge concerning primordial stages of expansion of the universe, whose size is consistent with characteristic scales of Lorentz symmetry breaking [344].

In chapter 2, we investigate the thermodynamic properties of an Aharonov-Bohm (AB) quantum ring in a heat bath for both the relativistic and non-relativistic cases. For accomplishing this, we use the partition function obtained by the Euler-Maclaurin formula. In particular, we determined the energy spectrum as well as the behavior of the main thermodynamic functions of the canonical ensemble, namely, the Helmholtz free energy, the mean energy, the entropy, and the heat capacity. We noticed that in the low-energy regime the relativistic thermodynamic functions are reduced to the non-relativistic, and the Dulong-Petit law was verified as well.

Additionally, in chapter 3, we study the thermodynamic functions of quantum gases confined to spaces of various shapes, namely, a sphere, a cylinder, an ellipsoid, and a torus. We start with the simplest situation, namely, a spinless gas treated within the canonical ensemble framework. As a next step, we consider *noninteracting* gases (fermions and bosons) with the usage of the grand canonical ensemble description. For this case, the calculations

are performed numerically. We also observe that our results may possibly be applied to *Bose-Einstein condensate* and to *helium dimer*. Moreover, the bosonic sector, independently of the geometry, acquires entropy and internal energy greater than for the fermionic case. Another notable aspect is present as well: the thermal properties turn out to be sensitive to the topological parameter (winding number) of the toroidal case. Finally, we also devise a model allowing us to perform analytically the calculations in the case of *interacting* quantum gases, and, afterwards, we apply it to three different cases: a cubical box, a ring and a torus.

After, in chapter 4, we investigate the topological effects of a novel thermodynamic system following a closed path through the surface of a non-trivial torus knot. Initially, we consider the grand canonical ensemble as the starting point to derive our calculations, which are carried out considering both *non-interacting* and *interacting* fermions. To the latter case, all the results are accomplished *analytically*. More so, we also study the behavior of the Helmholtz free energy, the mean energy, the magnetization and the susceptibility for such particle modes. Finally, to corroborate our results, we examine how the Fermi energy level is modified when such a system configuration is taken into account.

Further, in chapter 5, we study the interaction of quantum gases in Lorentz-violating scenarios considering both boson and fermion sectors. In the latter case, we investigate the consequences of a system governed by scalar, vector, pseudovector and tensor operators. Besides, we examine the implications of $\left(\hat{k}_a\right)^{\kappa}$ and $\left(\hat{k}_c\right)^{\kappa\xi}$ operators for the boson case and the upper bounds are estimated. To do so, we regard the grand canonical ensemble seeking the so-called partition function, which suffices to provide analytically the calculations of interest, i.e., the mean particle number, the entropy, the mean total energy and the pressure. Furthermore, in low temperature regime, such quantities converge until reaching a similar behavior being in contrast with what is shown in high temperature regime, which brings out the differentiation of their effects. In addition, the particle number, the entropy and the energy exhibit an extensive characteristic even in the presence of Lorentz violation. Also, for the pseudovector and the tensor operators, we notice a remarkable feature due to the breaking process of spin degeneracy: the system turns out to have greater energy and particle number for the spin-down particles in comparison with the spin-up ones. Finaly, we propose two feasible applications to corroborate our results: *phosphorene* and *spin precession.*

Subsequently, in chapter 7, we analyse the thermodynamic properties of the graviton and the generalized model involving anisotropic Podolsky and Lee-Wick terms with Lorentz violation. We build up the so-called partition function from the accessible states of the system seeking the following thermodynamic functions: spectral radiance, mean energy, Helmholtz free energy, entropy and heat capacity. Besides, we verify that, when the temperature rises, the spectral radiance $\chi(\nu)$ tends to attenuate for fixed values of ξ. Notably, when parameter η_2 increases, the spectral radiance $\bar{\chi}(\eta_2, \nu)$ weakens until reaching a flat characteristic.

Finally, for both theories, we perform the calculation of the modified black body radiation and the correction to the *Stefan–Boltzmann* law in the inflationary era of the universe.

Next, in this chapter 6, we study the thermodynamic properties of a photon gas in a heat bath within the context of higher-derivative electrodynamics. Specifically, we analyze Podolsky's theory and its extension involving the Lorentz symmetry violation recently proposed in the literature. First, we use the concept of the number of available states of the system in order to construct the partition function. Next, we calculate the main thermodynamic functions: Helmholtz free energy, mean energy, entropy, and heat capacity. In particular, we verify that there exist significant changes in heat capacity and mean energy due to Lorentz violation. Additionally, the modification of the black body radiation and the correction to the *Stefan–Boltzmann* law in the context of the primordial inflationary universe are provided for both theories as well.

Adjacently, chapter 8 is devoted to study the thermal aspects of a photon gas within the context of Planck-scale-modified dispersion relations. We study the spectrum of radiation and the correction to the *Stefan–Boltzmann* law in different cases when the Lorentz symmetry is no longer preserved. Explicitly, we examine two models within the context of CPT-even and CPT-odd sectors respectively. To do so, three distinct scenarios of the Universe are considered: the Cosmic Microwave Background (CMB), the electroweak epoch, and the inflationary era. Moreover, the equations of state in these cases turn out to display a dependence on Lorentz-breaking parameters. Finally, we also provide for both theories the analyses of the Helmholtz free energy, the mean energy, the entropy and the heat capacity.

Finally, chapter 9, we develop a thermal description for photon modes within the context of bouncing universe. Within this study, we start with a Lorentz-breaking dispersion relation which accounts for modified Friedmann equations with a bounce solution. We calculate the spectral radiance, the entropy, the Helmholtz free energy, the heat capacity, and the mean energy. Nevertheless, the latter two ones turn out to contribute only in a trivial manner. Furthermore, one intriguing aspect gives rise to: for some configurations of η, l_P, and T, the thermodynamical behavior of the system seems to indicate instability. However, despite of showing this particularity, the solutions of the thermodynamic functions in general turn out to agree with the literature, e.g., the second law of thermodynamics is maintained. More so, all the results are derived *analytically* and three different regimes of temperature of the universe are also considered, i.e., the inflationary era, the electroweak epoch and the cosmic microwave background.

1.1 Motivations

The study of physical properties of materials, focusing on their thermal properties, is of great interest in the condensed matter physics, especially in solid state. Indeed, it is justified by practical needs and the fundamental science knowledge [378]. It is worth mentioning that in Refs. [378, 379, 380, 381, 382] were investigated the thermal properties of graphene, graphite, carbon nanotubes and nanostructured carbon materials. Nevertheless, the energy spectra of relativistic and non-relativistic cases as well as the thermodynamic properties for a Dirac fermion confined in a AB quantum ring are lack up to date. The answer to this question is address in chapter 2.

In order to investigate how geometry modifies the thermodynamic properties of quantum gases, chapter 3 aims at studying how the thermodynamic functions of quantum gases behave within different geometries, i.e., spherical, cylindrical, ellipsoidal and toroidal ones. Additionally, we employ a toy model to accomplish such calculations for both *noninteracting* and *interacting* particles. Therefore, our results might serve as a basis for practical applications, and might help to nuance an emerging phenomena concerning further promising studies in condensed-matter physics and statistical mechanics.

In the literature, there is a lack of investigation of the thermal properties of fermions on a torus knot. In this sense, in chapter 4, we examine the topological effects of a novel thermodynamic system comprising of a gas of fermions, that follows a closed path with non-trivial knot structure on the surface of a torus. For convenience, one might visualize the particles moving within a carbon nanotube wound around the torus in the form of a knot. We calculate the Helmholtz free energy, mean energy, magnetization and susceptibility of the system. In our investigation, we exploit the formalism of [383, 384] to derive the thermodynamic quantities, using results from [182], for both *interacting* and *non-interacting* fermion particles.

Although there are some works in the literature looking towards to investigate the thermodynamic aspects of distinct systems with Lorentz violation [275, 276, 277, 278, 279, 280, 281, 282, 283], up to date, there is a lack of studies considering relativistic interacting quantum gases governed by higher-dimensional operators. In such a way, we present a model in order to provide such derivation. Here, we focus on the following quantities of interest: particle number, entropy, mean energy and pressure. For doing so, we utilize the so-called grand canonical partition function and the grand canonical potential. With them, all the following evaluations could be carried out in high temperature regime.

In order to overcome such a gap in the literature, in chapter 5, we consider both fermion and boson sectors to proceed our calculations. Additionally, not being restricted to the case involving Lorentz symmetry breaking, the present model, which regards the treatment of

the energy of an arbitrary quantum state, can lead to further analyses for different scenarios. It is worth mentioning that it is only possible to accomplish this as long as the operators, which modify the kinematics, be written in terms of momenta only.

Up to now, there are many works based on the analysis of the thermodynamic functions in the gravitational scenario mainly regarding the Cosmic Microwave Background (CMB) [385, 386, 387, 388, 389]. However, there are very few studies of such thermodynamic properties ascribed to the linearized theory of gravity within the context of Lorentz violation. In this sense, our starting point is taking into account a similar analysis encountered in Refs. [385, 386, 387, 388, 389], but proposing rather the inflationary epoch of the universe, i.e., $\beta = 1/\kappa_B T = 10^{-13}$ GeV^{-1} , within the context of Lorentz violation to utilize the modification from the black body radiation spectra as well as from the *Stefan-Boltzmann* law as an alternative to investigate cosmological scenarios. Besides, for the sake of giving a complement to this analysis, we provide the calculation of Helmholtz free energy, mean energy, entropy and heat capacity.

In addition, there is a lack in the literature ascribed to the investigation of the thermodynamic properties for the generalized anisotropic Podolsky electrodynamics with Lee-Wick terms. In this viewpoint, it is noteworthy to accomplish such analysis in order to verify how the modified massless mode behaves to perhaps reveal new phenomena which might be applied to either condensed matter or statistical thermal physics. All of these themes are addressed in chapter 7.

About twenty years up to now, the Lorentz-violating contributions of mass dimensions 3 and 4 have been taken into account within both theoretical and phenomenological scenarios in the photon and lepton sectors [334]. Recently, theories with higher-dimension operators have received much attention after a generalized approach proposed by Mewes and Kostelecký in Ref. [335]. In the CPT-even photon sector, the leading-order contributions in an expansion in terms of additional derivatives are dimension-6 ones. Hence, these are also the most prominent ones that could play a role in nature if higher-derivative Lorentz violation (LV) existed [271]. In such a way, there is a lack in the literature concerning the study of its respective thermodynamic properties. In this context, it is important to conduct further investigations. Therefore, the physical implications of the thermodynamic properties of such theories should be taken into account in order to possibly address some fingerprints of a new physics that might be mapped into future applications in either condensed matter physics or statistical mechanics. Thereby, we present, in chapter 6, a theoretical background in order to might serve as a basis for further experimental studies seeking any trace of Lorentz violation.

One of the important issues related to higher-derivative LV theories is certainly their thermodynamical aspects. Studies on the thermodynamics of LV extensions of various field

theory models could provide additional information about initial stages of expansion of the Universe, whose size was compatible with characteristic scales of Lorentz symmetry breaking [344]. The methodology for studying the thermodynamical aspects in LV theories has firstly been presented in [350]. Since then, various applications of this procedure have been developed [351, 352, 353, 354, 355, 356, 357, 358]. However, the higher-derivative cases have not been much explored up to now in this context.

In this sense, in chapter 8, we follow the procedure proposed by Amelino-Camelia [377] where the starting point in the study is the LV dispersion relations rather than the Lagrangian formalism of the corresponding field models. Nevertheless, we note that in many cases it is possible to indicate at least some simplified models yielding such dispersion relations. We note that the dispersion relations that we consider in the present manuscript might possibly be used to describe some quantum gravity effects (see discussions in [377]), or, at least, they can probably arise in some LV extensions of QED. We consider two examples, CPT-even and CPT-odd ones. In principle, our results involving thermal radiation may be confronted with experimental data as soon as they are available. In this sense, our study might help in the investigation of any trace of the Lorentz violation within cosmological scenarios concerning thermal radiation as the starting point.

Moreover, one significant aspect which is worth investigating in the context of Lorentz symmetry violation is actually the respective thermal aspects of the corresponding theory. With such study, we can obtain a better comprehension of how massless and massive modes behave when different range of temperatures are taken into account. This might possibly give us additional information to confront the theoretical background with the experimental results in order to help searching for any trace of the Lorentz symmetry violation. Furthermore, the investigation based on the thermodynamic properties and the Lorentz-violating (LV) effects could supply further knowledge concerning primordial stages of expansion of the universe, whose size is consistent with characteristic scales of Lorentz symmetry breaking [344]. Initially, the procedure to carry out the thermodynamic aspects involving Lorentz violation regarding statistical mechanics was proposed in Ref. [350]. After that, several works using such method have been developed within different scenarios [351, 352, 353, 383, 390, 354, 357, 358, 391]. Nevertheless, in the context of Ref. [350], the examination of the thermodynamic properties concerning bouncing universe cases has not yet been explored up to date. Therefore, in chapter 9, we study the thermal behavior of a photon gas in a bouncing universe, for a certain form of dispersion relation.

2. THERMODYNAMIC PROPERTIES OF AN AHARON BOHM QUANTUM RING

2.1 An AB ring modeled by (1+1)-dimensional Dirac equation

In this section, we obtain the relativistic and non-relativistic energy spectra of an AB ring modeled by the Dirac equation in polar coordinates whose signature of the metric tensor is $(+--)$. Introducing initially the Dirac equation in the $(3+1)$-dimensional Minkowski spacetime written in an orthogonal system (in natural units $\hbar = c = 1$) [392]

$$\left\{ i\gamma^{\mu} D_{\mu} + \frac{i}{2} \sum_{k=1}^{3} \gamma^{k} \left[D_{k} \ln\left(\frac{h_1 h_2 h_3}{h_k} \right) \right] - m \right\} \psi(t, \mathbf{r}) = 0, \quad (\mu = 0, 1, 2, 3), \tag{2.1}$$

where γ^{μ} are gamma matrices, $D_{\mu} = \frac{1}{h_{\mu}} \partial_{\mu}$ are the derivative, h_k are scale factors of the corresponding to coordinate system, m is the rest mass and $\psi(t, \mathbf{r})$ is the Dirac spinor. In polar coordinates (t, ρ, θ), the scale factors are $h_0 = 1$, $h_1 = 1$, $h_2 = \rho = a$ and $h_3 = 1$, where $a =$ const is the radius of the ring for modeling a 1D circular ring [101, 102, 103, 104, 105, 106]. In this sense, Eq. (2.1) turns out to be

$$i \frac{\partial \psi(t, \theta)}{\partial t} = (\alpha^2 p_{\theta} + \gamma^0 m) \psi(t, \theta), \tag{2.2}$$

where $p_{\theta} = -\frac{i}{a} \frac{\partial}{\partial \theta}$, and θ is the azimuthal angel which lies in $0 \leq \theta \leq 2\pi$.

Considering that the AB ring admits stationary states whose two-component Dirac spinor are given by $\psi(t, \theta) = e^{-iEt} f(\theta)$, and that the electromagnetic minimal coupling, Eq. (2.2) becomes

$$E f(\theta) = H_{ring} f(\theta) = \left[\alpha^2 \left(p_{\theta} - q A_{\theta} \right) + \gamma^0 m \right] f(\theta) \tag{2.3}$$

where E is the relativistic total energy of fermion with electric charge q.

Since we are working in a $(1+1)$-dimensional Minkowski spacetime, it is convenient to define the Dirac matrices α^2 and β in terms of the Pauli matrices, i.e., $\alpha^2 = -\alpha_2 = -\sigma_2$

and $\gamma^0 = \sigma_3$. Writing $f(\theta) = (R^+(\theta), R^-(\theta))^T$, we transform Eq. (2.3) as follows

$$\begin{pmatrix} m & \frac{1}{a}\frac{d}{d\theta} - iqA_\theta \\ -\frac{1}{a}\frac{d}{d\theta} + iqA_\theta & -m \end{pmatrix} \begin{pmatrix} R^+(\theta) \\ R^-(\theta) \end{pmatrix} = E \begin{pmatrix} R^+(\theta) \\ R^-(\theta) \end{pmatrix}. \tag{2.4}$$

To configure an AB ring we must use the vector potential of the AB effect for a fermion restricted to move in a circle of radius a. Explicitly, this vector potential is written as $\mathbf{A} = \frac{\Phi}{2\pi a}\hat{e}_\theta$, where $\Phi = \pi b^2 B$ is the magnetic flux of the solenoid of radius b and B is the constant magnetic field inside the solenoid [393]. We transform Eq. (2.4) in a system of two first-order coupled differential equations given by

$$(E - m)R^+(\theta) = \frac{1}{a}\left(\frac{d}{d\theta} - \frac{\Phi}{\Phi_0}\right) R^-(\theta), \tag{2.5}$$

$$(E + m)R^-(\theta) = \frac{1}{a}\left(-\frac{d}{d\theta} + \frac{\Phi}{\Phi_0}\right) R^+(\theta), \tag{2.6}$$

where $\Phi_0 \equiv \frac{2\pi}{q}$ is the magnetic quantum flux. Now, Substituting (6) into (5), we obtain a linear differential equation with constant coefficients

$$\left[\frac{d^2}{d\theta^2} - 2i\frac{\Phi}{\Phi_0}\frac{d}{d\theta} + a^2(E^2 - m^2) - \frac{\Phi^2}{\Phi_0^2}\right] R^+(\theta) = 0 \tag{2.7}$$

with normalized solutions are given by $R^+(\theta) = \frac{1}{\sqrt{2\pi}} e^{i\lambda\theta}$. Consequently, the coefficient λ is

$$\lambda_\pm = \frac{\Phi}{\Phi_0} \pm a\sqrt{E^2 - m^2}. \tag{2.8}$$

However, since $R^+(\theta)$ satisfies the periodicity condition $R^+(\theta + 2\pi) = R^+(\theta)$, it requires that $\lambda_\pm$ is an integer number. In this sense, we obtain the following relativistic energy spectrum and the spinor for the Dirac fermion confined in an AB ring [394]:

$$\begin{aligned} E_{n,s} &= \pm\sqrt{m^2 + \frac{1}{a^2}\left(n - s\frac{\Phi}{\Phi_0}\right)^2}, \quad (n = 0, \pm1, \pm2, \ldots) \\ \psi(t,\theta) &= \frac{e^{i(\lambda\theta - Et)}}{\sqrt{2\pi}} \begin{pmatrix} 1 \\ -i\nu\lambda + \nu\frac{\Phi}{\Phi_0} \end{pmatrix}, \end{aligned} \tag{2.9}$$

where $\nu = \frac{1}{a(E+m)}$ and $s = \pm1$. This parameter comes from the following relation: $\Phi_0 \to s\Phi_0$, where $\Phi_0 = \frac{2\pi}{e} > 0$, and $s = +1$ is regarded to be a positive charged fermion, $s = -1$ to a negative charged fermion and $e > 0$ is the elementary electric charge.

Now, using the prescription $E = \epsilon + m$ in (2.9), where $\epsilon << m$, we obtain the following

non-relativistic energy spectrum of a Dirac fermion confined in an AB ring [395, 396, 394, 397, 398, 399]

$$\epsilon_{n,s} = \frac{1}{2ma^2}\left(n - s\frac{\Phi}{\Phi_0}\right)^2, \quad (n = 0, \pm 1, \pm 2, \ldots). \tag{2.10}$$

We see that the relativistic and non-relativistic energy spectra are non-degenerated. However, in the limit $\Phi \to 0$, the energy spectra have a twofold degeneracy, i.e., each energy level is doubly degenerate (except for $n = 0$). Moreover, positive n represents a fermion traveling in the same direction of the current of the solenoid and negative n describes a fermion traveling in the opposite direction.

2.2 Thermodynamic properties of the AB ring

In this section, we calculate the thermodynamic properties of the AB ring in contact with a thermal reservoir at finite temperature for the relativistic and non-relativistic cases. These properties are given by following thermodynamic quantities, namely, the Helmholtz free energy, the mean energy, the entropy and the heat capacity. For the sake of simplicity we assume that only fermions with positive energy ($E > 0$) [400, 401], negatively charged ($s = -1$) are regarded to constitute the thermodynamic ensemble [402].

2.2.1 The relativistic case

For calculating the thermodynamic properties, let us begin defining initially the fundamental object in statistical mechanics, the so-called partition function Z. Given the non-degenerate energy spectrum, we can define it by a sum over all possible states of the system

$$Z_1 = \sum_{n=0}^{\infty} e^{-\beta E_n}, \tag{2.11}$$

where $\beta = \frac{1}{k_B T}$, and k_B the Boltzmann constant and T is the thermodynamic equilibrium temperature. After we obtain Z_1, all thermodynamic properties of the AB ring can be addressed. The main thermodynamic functions of our interest are the Helmholtz free energy F, the mean energy U, the entropy S and the heat capacity C_V which are defined as follows

$$F = -\frac{1}{\beta}\ln Z_N, \quad U = -\frac{\partial}{\partial\beta}\ln Z_N, \quad S = k_B\beta^2\frac{\partial F}{\partial\beta}, \quad C_V = -k_B\beta^2\frac{\partial U}{\partial\beta}, \tag{2.12}$$

where Z_N is the total partition function for an set of non-interacting indistinguishable N-fermions.

In particular, let us consider the partition function regarding the relativistic case. Using the expressions (2.9) and (2.11), one obtains that for a one-fermion confined in the AB ring

the partition function is

$$Z_1 = \sum_{n=0}^{\infty} e^{-\beta\sqrt{An^2+Bn+C}}, \tag{2.13}$$

where $A = \frac{1}{a^2}$, $B = \frac{1}{a^2}\frac{\Phi}{\Phi_0}$ and $C = 1 + \left(\frac{\Phi}{a\Phi_0}\right)^2$.

Since Eq. (8.22) cannot be evaluated in a closed form, we assume that AB ring is submitted to strong enough magnetic field ($\Phi \gg \Phi_0$) and the above equation turns out to be $f(n) \simeq e^{-\beta\sqrt{Bn+C}}$, which is a monotonically decreasing function and the associated integral

$$\int_0^{\infty} e^{-\beta\sqrt{Bx+C}}dx = \frac{2}{B\beta^2}(1+\beta\sqrt{C})e^{-\beta\sqrt{C}} \tag{2.14}$$

is convergent and may be evaluated. With the sake of calculating it, now, let us invoke the so-called Euler-MacLaurin sum formula [403]

$$Z_1 = \sum_{n=0}^{\infty} f(n) \simeq \frac{1}{2}f(0) + \int_0^{\infty} f(x)dx - \sum_{p=1}^{\infty}\frac{1}{(2p)!}B_{2p}f^{(2p-1)}(0), \tag{2.15}$$

which may be rewritten simply as

$$Z_1 = \sum_{n=0}^{\infty} f(n) \simeq \frac{1}{2}f(0) + \int_0^{\infty} f(x)dx - \frac{1}{12}f'(0) + \frac{1}{720}f'''(0) - \ldots +, \tag{2.16}$$

where B_{2p} are the Bernoulli numbers. Explicitly, above equation takes the form

$$Z_1 \simeq e^{-\beta\sqrt{C}}\left[\frac{2}{B\beta^2}(1+\beta\sqrt{C}) + \frac{1}{2} + \left(\frac{B}{24\sqrt{C}} - \frac{B^3}{720\sqrt{C^5}}\right)\beta + \frac{1}{90}\left(\frac{A}{2C} - \frac{B^2}{8C^2}\right)\beta^2 - \mathcal{O}(\beta^3)\right]. \tag{2.17}$$

where $\mathcal{O}(\beta^3)$ are terms involving higher order terms of β which will be neglected henceforth. Notice that when one considers the high temperatures regime ($\beta \ll 1$), Eq. (2.17) becomes

$$Z_1 \simeq \frac{2}{B\beta^2}(1+\beta\sqrt{C}), \tag{2.18}$$

which straightforwardly yields

$$Z_N \simeq \left[\frac{2}{B\beta^2}(1+\beta\sqrt{C})\right]^N. \tag{2.19}$$

Therefore, using the partition function (2.19), the Helmholtz free energy, the mean energy, the entropy and the heat capacity for the relativistic case are written as follows

$$F \simeq -\frac{N}{\beta}\ln\left[\frac{2}{B\beta^2}(1+\beta\sqrt{C})\right], \quad U \simeq N\frac{(2+\beta\sqrt{C})}{(\beta+\beta^2\sqrt{C})}, \tag{2.20}$$

$$S \simeq Nk_B \left\{ \ln\left[\frac{2}{B\beta^2}(1+\beta\sqrt{C})\right] + \frac{(2+\beta\sqrt{C})}{(1+\beta\sqrt{C})} \right\}, \; C_V \simeq Nk_B \left[\frac{2+4\beta\sqrt{C}+\beta^2 C}{(1+\beta\sqrt{C})^2}\right]. \quad (2.21)$$

2.2.2 The non-relativistic case

Now, let us take into account the non-relativistic case where most of phenomena in condensed matter physics take place. Substituting our previous result of the energy spectrum (2.10) in the partition function (2.11) and considering the condition where $\Phi \gg \Phi_0$, we obtain

$$Z_1 \simeq \sum_{n=0}^{\infty} e^{-\beta(\bar{B}n+\bar{C})} \quad (2.22)$$

where $\bar{B} = \frac{\Phi}{ma^2\Phi_0}$ and $\bar{C} = \left(\frac{\Phi}{\sqrt{2}ma\Phi_0}\right)^2$. In an explicit form, above expression is given by

$$Z_1 \simeq \frac{e^{-\beta\bar{C}}}{1-e^{-\beta\bar{B}}} \quad (2.23)$$

and the total partition function for a set of non-interacting indistinguishable N-fermions is

$$Z_N \simeq \left[\frac{e^{-\beta\bar{C}}}{1-e^{-\beta\bar{B}}}\right]^N. \quad (2.24)$$

Therefore, taking into account (2.24) and the previous definition in (2.12) the required thermodynamic functions, namely, the Helmholtz free energy, the mean energy, the entropy and the heat capacity for the non-relativistic case are written as

$$\bar{F} \simeq -\frac{N}{\beta} \ln\left(\frac{e^{-\beta\bar{C}}}{1-e^{-\beta\bar{C}}}\right), \quad \bar{S} \simeq Nk_B \left[\beta\left(\bar{C}+\frac{\bar{B}}{e^{\beta\bar{B}}-1}\right) + \ln\left(\frac{e^{\beta(\bar{B}-\bar{C})}}{e^{\beta\bar{B}}-1}\right)\right], \quad (2.25)$$

$$\bar{U} \simeq N\left(\frac{\bar{B}}{e^{\beta\bar{B}}-1}+\bar{C}\right), \quad \bar{C}_V \simeq Nk_B\beta^2\left[\frac{\bar{B}^2 e^{\beta\bar{B}}}{(1-e^{\beta\bar{B}})^2}\right]. \quad (2.26)$$

In what follows, all discussions and remarks concerned to both the relativistic and the non-relativistic cases are presented in the next section. The construction and the analysis of graphics are provided as well to elucidate the behavior of the thermodynamic functions calculated previously. Finally, we make our final remarks in the conclusion.

2.2.3 Results and discussions

In the sequel, we used the Euler-Maclaurin formula regarding a strong magnetic field to evaluate the partition function numerically. In all calculations we assume $k_B = a = m = 1$.

In figs. 2.1 and 2.2 we plot all profiles of the thermal quantities as a function of temperature T for different values 109 of the magnetic flux Φ, namely, $\Phi = 50\Phi_0$, $100\Phi_0$, $150\Phi_0$, $200\Phi_0$. Considering the relativistic case, we see from fig. 2.1 that the Helmholtz function $F(T)/N$ has a little increase when T starts to increase. Nevertheless, it decreases for high values of T and has higher values when the magnetic flux grows. The mean energy $U(T)/N$ exhibits a nearly linear behavior with very close profiles. As the magnetic flux decreases the curve of the mean energy grows faster. The entropy $S(T)/N$ is slowly increasing for large T and decreases for large magnetic fluxes Φ's. The heat capacity $CV(T)/N$ tends to an asymptotic behavior fixed in the value 2 when T increases. For the non-relativistic case, we see from fig. 2.2 that the Helmholtz function $\bar{F}(T)/N$ decreases with a nearly linear behavior when T increases and has higher values when the magnetic flux Φ increases. The mean energy $\bar{U}(T)/N$ increases with an entirely linear behavior when T increases which is similar when one compares at with the relativistic case. The entropy $\bar{S}(T)/N$ as in the relativistic case, is slowly increasing. The heat capacity $\bar{C}_V(T)/N$ differently to the relativistic case, has an asymptotic behavior in the value 1.

From the analysis of the profiles of the curves for the main thermodynamic functions, we can extract information about the thermal behavior of our system. We observe that the Helmholtz free energy, in both the relativistic and non-relativistic cases, presents a critical point for low temperature, that is, close to $T = 0$. Moreover, once the temperature of the system increases, the amount of free energy available to perform the ensemble work decreases rapidly. On the other hand, we noted that when this ensemble tends to the thermal equilibrium in the reservoir, the mean energy of the system increases continuously. Besides, the thermal variation of the AB ring tends to increase until reaching the thermal equilibrium in both cases, and once the equilibrium is reached, the heat capacity remains constant. We also observed that the thermodynamic quantities studied have a higher intensity in the relativistic case, that is, all the amounts assume higher values for low temperatures, as predicted in the literature. These results are because in the relativistic case we have a more energetic quantum system than in the non-relativistic case. Finally, we note that the well-known Dulong-Petit law is satisfied, namely, for the relativistic case $C_V(T \to 0)/N \simeq 2k_B$ and for the non-relativistic case, $\bar{C}_V(T \to 0)/N \simeq k_B$. Thus, the heat capacity in the relativistic case is twice that of the non-relativistic case.

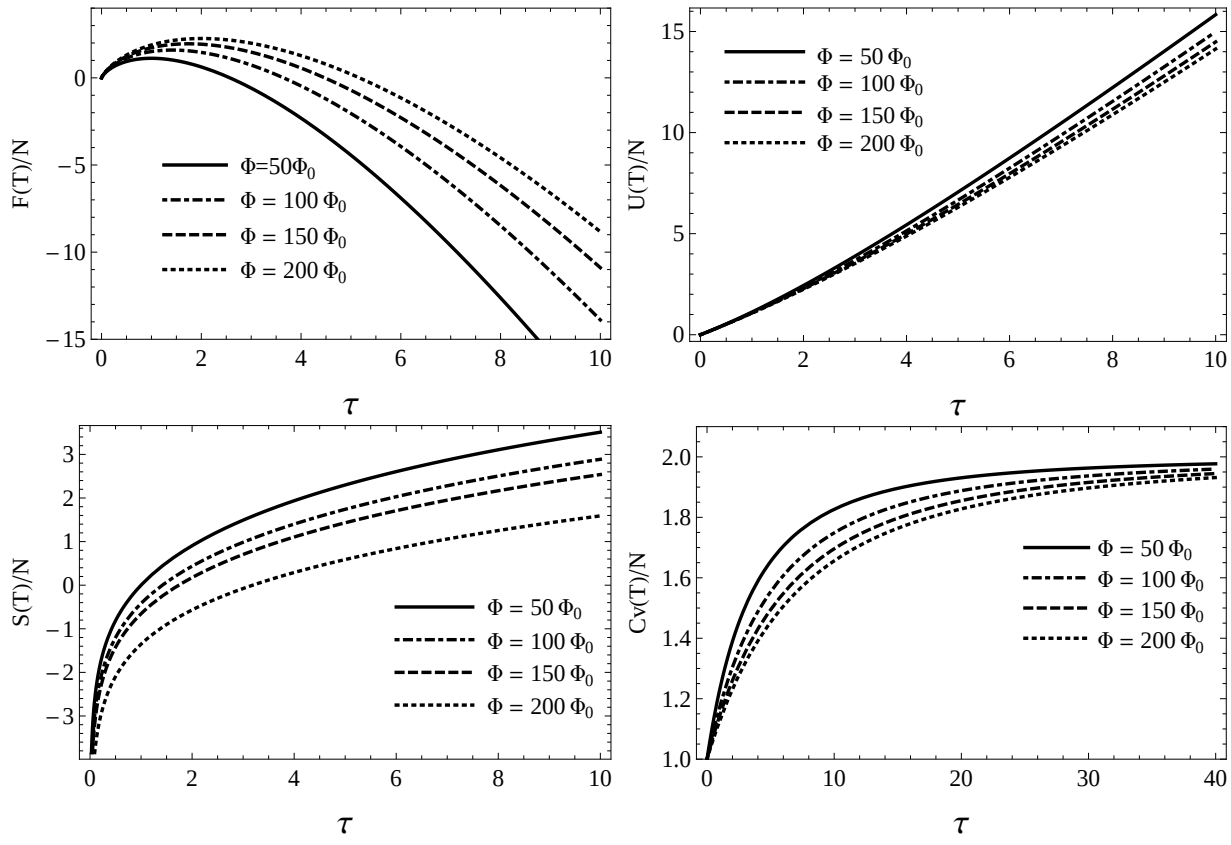

Fig. 2.1: Numerical solutions for the thermodynamic properties of the Aharanov-Bohm ring for the relativistic case: (a) The Helmholtz free energy; (b) the mean energy; (c) the entropy and (d) the heat capacity. In this case, we consider $\tau = K_B T$.

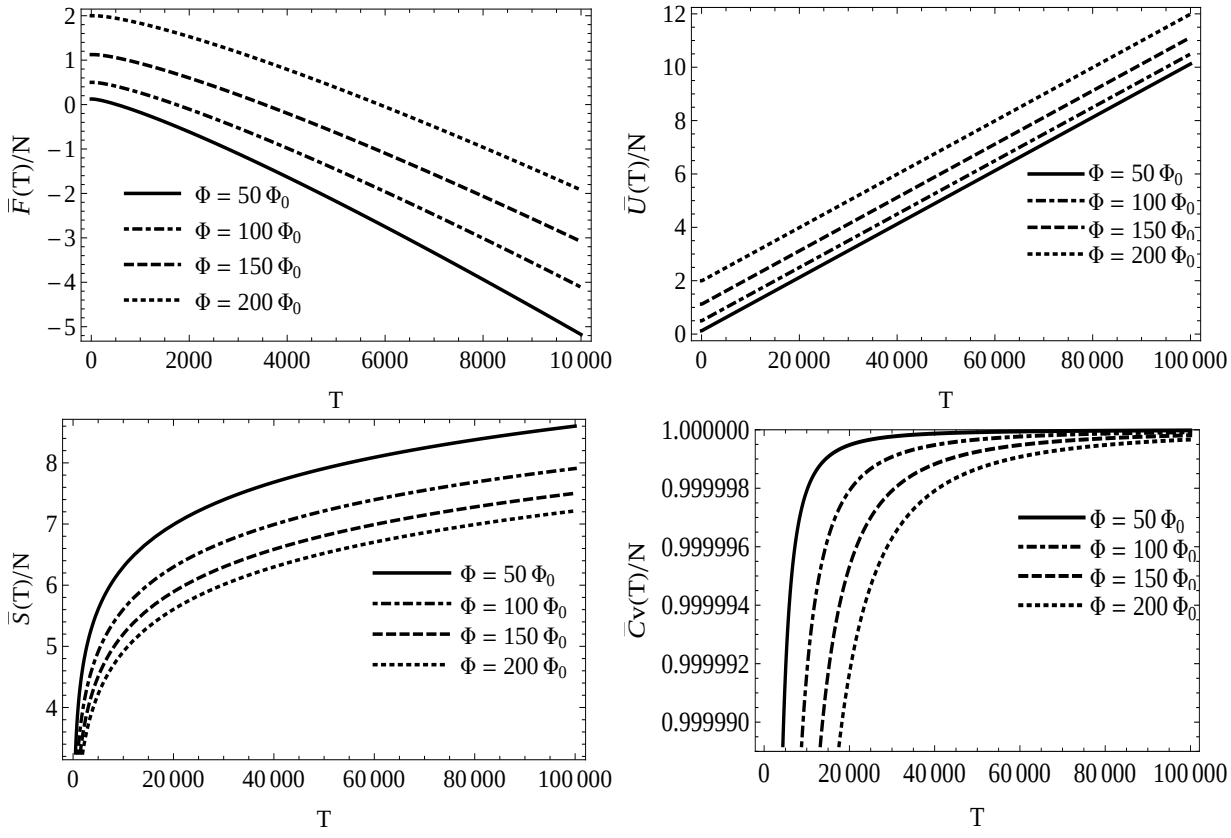

Fig. 2.2: Numerical solutions for the thermodynamic properties of the Aharanov-Bohm ring for the non-relativistic case: (a) the Helmholtz free energy; (b) the mean energy; (c) the entropy and (d) the heat capacity.

3. HOW DOES GEOMETRY AFFECT QUANTUM GASES?

3.1 Spectral energy for different geometries

Initially, we study the thermodynamic properties of confined gases consisting of spinless particles. Moreover, fermions and bosons with a nonzero spin are also taken into account in our investigation. To do so, we must solve the Schrödinger equation for particular symmetries with appropriate boundary conditions. With this, the spectral energy can be derived after some algebraic manipulations. In particular, we choose four different geometries, namely, spherical, cylindrical, ellipsoidal and toroidal ones. The potentials for each configuration are given below:

$$\mathcal{V}_{\text{Sphere}}(r) = \begin{cases} 0, \text{ if } r < a \\ \infty, \text{ if } r > a \end{cases}, \tag{3.1a}$$

$$\mathcal{V}_{\text{Cylinder}}(\rho, z) = \begin{cases} 0, \text{ if } \rho < b \text{ and } 0 < z < 2c \\ \infty, \text{otherwise} \end{cases}, \tag{3.1b}$$

$$\mathcal{V}_{\text{Ellipsoid}}(x, y, z) = \begin{cases} 0, \text{ if } x, y, z \text{ satisfy } \frac{x^2+y^2}{b^2} + \frac{z^2}{c^2} < 1 \\ \infty, \text{ if } x, y, z \text{ satisfy } \frac{x^2+y^2}{b^2} + \frac{z^2}{c^2} \geq 1 \end{cases}, \tag{3.1c}$$

and

$$\mathcal{V}_{\text{Torus}}(x, y, z) = \begin{cases} 0, \text{ if } (\sqrt{x^2+y^2} - R)^2 + z^2 < x^2 + y^2 + z^2 \\ \infty, \text{otherwise} \end{cases}. \tag{3.2}$$

where a, b and c are geometric parameters defining the size of the potential, and R is the distance from the center of the toroidal tube to the center of the coordinate system[1]. In order to make a comparison between our thermodynamic results in the next sections, we must choose the parameters a, b, and c such that all configurations provide the same volume. Since we have already set up our potentials, we can solve the time-independent Schrödinger

[1] Although this potential illustrates the content inside this given region, all calculations concerning the torus knot will be derived considering only its surface.

equation

$$-\frac{\hbar^2}{2\mathrm{M}}\nabla^2\psi + V(r)\,\psi = E\psi, \tag{3.3}$$

for each geometry whose solutions can be obtained using the well-known method of separation of variables [404, 405, 406, 150]. Particularly, the wavefunction for the spherical case can be written as

$$\psi_{l,n,m}(r,\theta,\phi) = \begin{cases} A_{l,n} j_l(k_{l,n}r) Y_l^m(\theta,\phi), & \text{if } r \leq a \\ 0, & \text{if } r \geq a \end{cases}, \tag{3.4}$$

where $j_l(k_{l,n}r)$ is a spherical Bessel function, $Y_l^m(\theta,\phi)$ is a spherical harmonic and $A_{l,n}$ is a normalization factor; thereby, the Fourier transform of $\psi_{l,n,m}(r,\theta,\phi)$ is

$$\tilde{\psi}_{l,n,m}(k) = \frac{1}{\sqrt{(2\pi\hbar)^3}} A_{l,n} \int e^{i\mathbf{k}\cdot\mathbf{r}} j_l(k_{l,n}r) Y_l^m(\theta,\phi) r^2 \mathrm{d}r\mathrm{d}\Omega \tag{3.5}$$

and using the orthogonality properties of the Bessel functions [407, 408, 409], we can infer the momentum distribution $\tilde{n}(k)$

$$\tilde{n}(k) = s\sum_{l,n} |\tilde{\psi}_{l,n}(k)|^2 = \frac{3sV}{4\pi^2(\pi\hbar)^3} \sum_{l,n} (2l+1) j_l^2(ka) \frac{(k_{l,n}a/\pi)^2}{[(k_{l,n}a/\pi)^2 - (ka/\pi)^2]^2}, \tag{3.6}$$

where s is the spin degeneracy, $k_{l,n}a$ is the n-th root of $j_l(ka) = 0$, V is the volume, and k the momentum distribution – it is considered to be continuous in the infinite volume limit. In Ref. [410], some approximations in order to perform analytical and numerical analyses of *noninteracting* particles at zero temperature were made. The shape dependence was investigated as well to see how such geometries would influence the momentum distribution $\tilde{n}(k)$. Our approach, on the other hand, intends to examine the impact of all mentioned shapes on the thermodynamic properties and implies different results in comparison to the literature [142, 143]. To perform the following calculations, we consider spherical, cylindrical, ellipsoidal and toroidal configurations. Solving the Schrödinger equation for the spherical potential [404], we have

$$E_{n,l}^{\mathrm{Sphere}} = (2l+1)\frac{\hbar^2}{2\mathrm{M}a^2} j_{nl}^2 \tag{3.7a}$$

where j_{nl} is the n-th zero of the l-th spherical Bessel function. Clearly, each level has a $(2l+1)$ degeneracy. For ellipsoidal [405], cylindrical [404] and toroidal [411] shapes, we

obtain

$$E_{m,n,l}^{\text{Ellipsoid}} = \frac{\hbar^2}{2\mathrm{M}}\left[\frac{J_{n,l}^2}{b^2} + \frac{2J_{n,l}}{bc}\left(m+\frac{1}{2}\right)\right], \tag{3.7b}$$

$$E_{m,n,l}^{\text{Cylinder}} = \frac{\hbar^2}{2\mathrm{M}}\left[\frac{J_{n,l}^2}{b^2} + \left(\frac{\pi m}{2c}\right)^2\right], \tag{3.7c}$$

and

$$E_n^{\text{Torus}} = \frac{n^2}{2\mathrm{M}\mathfrak{a}^2 p^2}\frac{\cosh^2\eta}{\alpha^2+\sinh^2\eta-1}, \tag{3.7d}$$

where $J_{n,l}$ is the n-th root of the l-th Bessel function, $\eta = \cosh^{-1} R/d$ is a parameter which fixes the toroidal surface, α is the winding number, $\mathfrak{a} = \sqrt{R^2-d^2}$, p describes the number of loops in the toroidal direction and $n = 0, 1, \ldots$. Using these spectra energies, an analysis of the thermal properties can be properly carried out in the next sections.

3.2 Noninteracting gases: spinless particles

In this section, we present the thermodynamic approach based on the canonical ensemble.

3.2.1 Thermodynamic approach

Whenever we are dealing with a spinless gas, the theory of the canonical ensemble is sufficient for a full thermodynamical description. Thereby, the partition function is given by

$$\mathcal{Z} = \sum_{\{\Omega\}} \exp\left(-\beta E_\Omega\right), \tag{3.8}$$

where Ω is related to accessible quantum states. Since we are dealing with *noninteracting* particles, the partition function (3.8) can be factorized which gives rise to the result below

$$\mathcal{Z} = \mathcal{Z}_1^N = \left\{\sum_{\{\Omega\}} \exp\left(-\beta E_\Omega\right)\right\}^N, \tag{3.9}$$

where we have defined the single partition function as

$$\mathcal{Z}_1 = \sum_{\Omega} \exp\left(-\beta E_\Omega\right). \tag{3.10}$$

It is known that the thermodynamical description of the system can also be done via Helmholtz free energy

$$f = -\frac{1}{\beta} \lim_{N\to\infty} \frac{1}{N} \ln \mathcal{Z}, \tag{3.11}$$

where rather for convenience we write the Helmholtz free energy per particle. With this, we can derive the following thermodynamic state functions[2], i.e., entropy, heat capacity, and mean energy

$$s = -\frac{\partial f}{\partial T}, \tag{3.12a}$$

$$c = T\frac{\partial s}{\partial T}, \tag{3.12b}$$

and

$$u = -\frac{\partial}{\partial \beta} \ln \mathcal{Z}. \tag{3.12c}$$

The sum in Eq. (3.10) cannot be expressed in a closed form. This does not allow us to proceed analytically. To overcome this issue, we perform a numerical analysis plotting the respective functions in terms of the temperature in order to understand their behaviors. Our main interest lies in the study of the low-temperature regime.

3.2.2 Numerical analysis

To provide the numerical results below, we sum over fifty thousand terms in Eq. (4.3). With this, we can guarantee the accuracy of such procedure keeping the maximum of details. For the plots below, the values for the parameters a, b and c[3] that control the size of the potential are displayed in Tab. 3.1. For now on, we will refer the first set of parameters as configuration 1 (thick lines in the plots) and to the second set as configuration 2 (dashed lines in the plots). Note that configuration 2 has a larger volume than configuration 1. However, the parameters are chosen such that the wells considered (sphere, cylinder and ellipsoid) have the same volume in each configuration. The graphics for the configurations described here are displayed in Fig. 3.1

Let us start analyzing the Helmholtz free energy. In Fig. 3.1, we see that configuration 1 provides larger values of the Helmholtz free energy than configuration 2. Besides, we also see that the values of the energy are larger for the sphere in comparison to the ellipsoid; and the latter are again larger in comparison with the cylinder for both configurations. In what follows, we will employ the short-hand notation *Sphere* > *Ellipsoid* > *Cylinder*. The behavior for the entropy, on the other hand, seems to be different. We notice that

[2]All of them are written in a "per particle form" for convenience.

[3]The unit used for these parameters is the nanometer.

		a	b	c
Config. 1	Sphere	1.0	-	-
	Cylinder	-	1.0	0.66
	Ellipsoid	-	1.22	0.66
Config. 2	Sphere	1.5	-	-
	Cylinder	-	1.22	1.5
	Ellipsoid	-	1.67	1.2

Tab. 3.1: The parameters a, b and c for two distinct configurations.

configuration 2 provides an entropy larger than configuration 1 and, when we look at the geometry itself, we observe the pattern *Cylinder* > *Ellipsoid* > *Sphere*. In this comparison, the *Ellipsoidal* geometry always takes a position in the middle. This fact is rather natural since this geometry is actually a "transition" between a cylinder and a sphere.

Also in Fig. 3.1, we find the plots for the internal energy and for the heat capacity. Configuration 1 exhibits energies larger than those of configuration 2 and we see that the internal energy increases according to *Sphere* > *Ellipsoid* > *Cylinder* for both configurations. The heat capacities for all configurations approach the value $3/2$ as the temperature increases. Configuration 2, that has a larger volume, reaches the asymptotic value faster than configuration 1.

Differently from what we saw for the other thermodynamic quantities, it is not possible to establish a common behavior among *Ellipsoid*, *Cylinder* and *Sphere* geometries because of different temperature ranges and well sizes the heat capacity varies drastically. For instance, in the second row of Fig. 3.1, configuration 2 in the range $0 < T < 5$ K, we see that the heat capacity follows the rule *Ellipsoid* > *Cylinder* > *Sphere*. However, in the same range of temperature, configuration 1 displays two different behaviors, that is for $0 < T < 2.5$ K we have *Cylinder* > *Ellipsoid* > *Sphere* and for 2.5 K $< T < 5$ K we have *Ellipsoid* > *Cylinder* > *Sphere*. For a fixed value of the volume, there exists a temperature where the heat capacity will follow the rule *Sphere* > *Ellipsoid* > *Cylinder* until it reaches the value $3/2$. This temperature increases as the volume decreases. For configuration 1 the temperatures where we have this behaviour is around 29 K and for configuration 2, that has a larger volume, it happens at 9 K.

It is interesting to see that for the cylindrical geometry a mound appears around 0.5 K and tends to disappear when the volume of the cylinder increases. This effect is clearly caused by the finite size of the geometry since the expected behavior would be to go to zero almost linearly. However, both the sphere and the ellipsoid do not exhibit such an effect. We could conclude about the absence of such effect that the surfaces of the former cases that accentuate those geometries are smooth and the cylinder, on the other hand, is smooth just by parts. As we will see in Sec. 3.6 and in Ref. [143], it is possible to identify the

contribution that comes from the geometry itself by considering an analytical model.

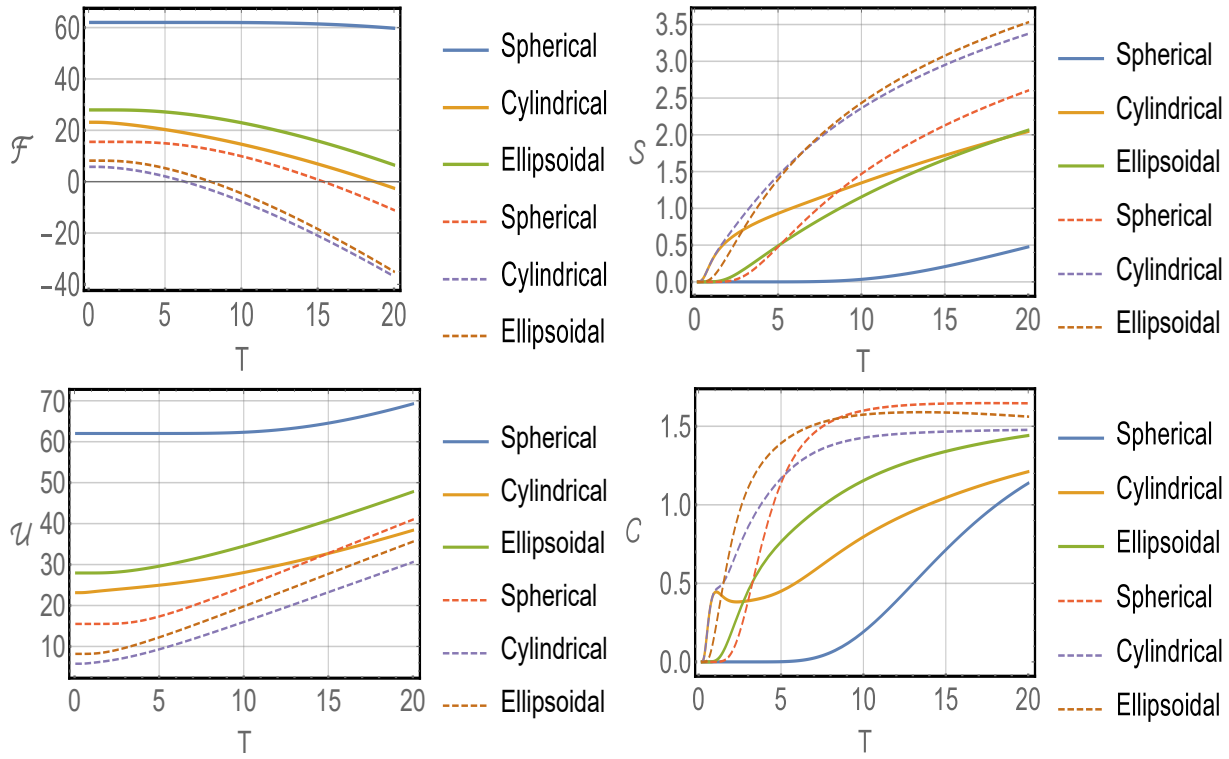

Fig. 3.1: The Helmholtz free energy, entropy per particle, the internal energy and heat capacity per particle, respectively

3.3 Noninteracting gases: Bosons and fermions

Although interactions of atoms and molecules are treated in many experimental approaches, and several features may only be recognized and understood by taking the interactions into account [412, 413, 414, 415], some fascinating characteristics are well described by assuming *noninteracting* systems [416, 290, 291, 292, 293, 294, 295, 417, 418, 419, 420, 421, 422].

Studies of *noninteracting* particles (bosons and fermions) have many applications, especially in chemistry [420, 421] and condensed-matter physics [416, 290, 291, 292, 293, 294, 295, 417, 418, 419, 422, 423]; for instance, in the case of *bulk*, which is usually assumed to calculate the energy spectrum and use the *Fermi-Dirac* distribution to examine how its statistics behaves, it is sufficient to describe the system of a *noninteracting* electron gas. Such an assumption is totally reasonable since if the *Fermi energy* is large enough, the kinetic energy of electrons, close to the Fermi level, will be much greater than the potential energy of the *electron-electron* interaction.

On the other hand, one of the pioneer studies which addressed the analysis of the *Bose-Einstein condensate* in a theoretical viewpoint was presented in [424]. The authors utilize a gas of *noninteracting* bosons to perform their calculations. As we shall see, we proceed in a similar way taking into account different geometries though. Furthermore, we discuss applying them in different scenarios in condensed-matter physics.

3.3.1 Thermodynamic approach

We apply the grand canonical ensemble theory to *noninteracting* particles with different spins (fermions and bosons); we will treat both cases separately. The grand canonical partition function for the present problem reads

$$\Xi = \sum_{N=0}^{\infty} \exp\left(\beta\mu N\right) \mathcal{Z}\left[N_\Omega\right], \tag{3.13}$$

where $\mathcal{Z}\left[N_\Omega\right]$ is the usual canonical partition function which now depends on the occupation number N_Ω, and on the μ, which is the chemical potential. Since we are dealing with fermions and bosons, it is well-known that the occupation number must be restricted in the following manner: $N_\Omega = \{0,1\}$ for fermions and $N_\Omega = \{0,\ldots\infty\}$ for bosons. Also, for an arbitrary quantum state, the energy depends on the occupation number as

$$E\left\{N_\Omega\right\} = \sum_{\{\Omega\}} N_\Omega E_\Omega$$

where we have

$$\sum_{\{\Omega\}} N_\Omega = N.$$

In this way, the partition function becomes

$$\mathcal{Z}\left[N_\Omega\right] = \sum_{\{N_\Omega\}} \exp\left[-\beta \sum_{\{\Omega\}} N_\Omega E_\Omega\right], \tag{3.14}$$

which leads to

$$\Xi = \sum_{N=0}^{\infty} \exp\left(\beta\mu N\right) \sum_{\{N_\Omega\}} \exp\left[-\beta \sum_{\{\Omega\}} N_\Omega E_\Omega\right], \tag{3.15}$$

or can be rewritten as

$$\Xi = \prod_{\{\Omega\}} \left\{ \sum_{\{N_\Omega\}} \exp\left[-\beta N_\Omega \left(E_\Omega - \mu\right)\right] \right\}. \tag{3.16}$$

After performing the sum over the possible occupation numbers, we get

$$\Xi = \prod_{\{\Omega\}} \{1 + \chi \exp\left[-\beta\left(E_\Omega - \mu\right)\right]\}^{\chi}, \tag{3.17}$$

where we have now introduced the convenient notation $\chi = +1$ for fermions and $\chi = -1$ for bosons. The connection with thermodynamics is made by using the grand thermodynamical potential given by

$$\Phi = -\frac{1}{\beta} \ln \Xi. \tag{3.18}$$

Replacing Ξ in the above equation, we get

$$\Phi = -\frac{\chi}{\beta} \sum_{\{\Omega\}} \ln\left\{1 + \chi \exp\left[-\beta\left(E_\Omega - \mu\right)\right]\right\}. \tag{3.19}$$

The entropy of the system can be cast into the following compact form, namely

$$S = -\frac{\partial \Phi}{\partial T} = -k_B \sum_{\{\Omega\}} \mathcal{N}_\Omega \ln \mathcal{N}_\Omega + \chi\left(1 - \chi \mathcal{N}_\Omega\right) \ln\left(1 - \chi \mathcal{N}_\Omega\right)$$

where

$$\mathcal{N}_\Omega = \frac{1}{\exp\left[\beta\left(E_\Omega - \mu\right)\right] + \chi}.$$

Moreover, we can also use the grand potential to calculate other thermodynamic properties, such as, the mean particle number, energy, heat capacity, and pressure using the following expressions:

$$\mathcal{N} = -\frac{\partial \Phi}{\partial \mu}, \tag{3.20a}$$

$$\mathcal{U} = -T^2 \frac{\partial}{\partial T}\left(\frac{\Phi}{T}\right), \tag{3.20b}$$

$$C = T \frac{\partial S}{\partial T}, \tag{3.20c}$$

$$\mathcal{P} = -\frac{\partial \Phi}{\partial V} = -\frac{\Phi}{V}. \tag{3.20d}$$

In possession of these terms, calculating the thermodynamic quantities should be a straightforward task, since we only would need to perform the sum presented in Eq. (3.19). Unfortunately, this sum cannot be obtained in a closed form for the spectral energy that we chose. Instead of this, a numerical analysis, similar to what we have done in Sec. 3.2.2, can be provided to overcome this difficulty; thereby, we can obtain the behavior of all quantities considering mainly low temperature regimes (keeping the volume constant). In what follows, we devote our attention to study such properties in a numerical manner.

3.3.2 Numerical analysis

Here, as in Section 3.2.2, we consider two particular cases whose parameters are the same presented in Tab. 3.1. For numerical purpose we choose for the chemical potential the value $\mu = 0.5$ eV. Next, we also use thick and dashed lines to represent fermions and bosons in the plots presented in Fig. 3.2. In first row of Fig. 3.2, we present the entropy for the two different cases. The first one, in Fig. 3.2(a), represents configuration 1 and Fig. 3.2(b) configuration 2, where we compare fermions (thick lines) and bosons (dashed lines) for sphere, cylinder and ellipsoid geometries. We can see from the plots that bosons, independently of the previous set of geometry we chose, acquire an entropy larger than that of fermions. We can also realize that the pattern *Ellipsoid* > *Cylinder* > *Sphere* always occurs for fermions and bosons when we consider the entropy. In both cases the pattern described above repeats and shows that the entropy is a monotonically increasing function for the volume and temperature.

For the internal energy, displayed in the second row Fig. 3.2, we see the entire behavior being repeated, that is, the internal energy follows the rule *Ellipsoid* > *Cylinder* > *Sphere* and the energy for bosons are greater than for fermions when we compare their values for the same geometry. It is also important to notice that the internal energy is a monotonically increasing function for both volume and temperature.

Another important property analyzed here is the heat capacity, showed in the third row of Fig. 3.2. We know from the literature [52, 149] that the heat capacity for an electron gas at low temperature ($T \ll T_{Fermi}$) is proportional to the temperature. On the other hand, for the boson gas, the heat capacity is proportional to $T^{3/2}$ (both behaviors are obtained in the classical limit). However, as we can deduce from the graphics, in both cases presented in Fig. 3.2, fermions do not follow this rule. We see deviations form a straight line, where one can infer that this effect is caused by the finite volume. We must remember that our systems are under confinement in very small containers[4] and, in addition, a large number of energy levels were considered in the numerical analysis. As a direct consequence, the entire behavior at low temperature when compared to the usual electron gas will be drastically different. On the other hand, bosons behave exactly like a function proportional to $T^{3/2}$. It suggests that fermions are more sensitive to the geometry and size of the system than bosons. Besides the discussion above, we can also see that in general the heat capacity follows the pattern *Ellipsoid* > *Cylinder* > *Sphere* and its value increases when both temperature and volume increase.

[4]The linear dimension of the containers considered is comparable with the thermal wavelength of the electron for low temperatures. This means that the electrons will feel the finiteness of the well and, therefore, the thermodynamic properties will change.

3.4 Ideal quantum gas on a torus knot

In the last years, the study of quantum mechanics in constrained systems has gained much attention acquiring diverse applications in both theoretical and experimental approaches [425, 426, 427, 428, 429, 430, 431, 411, 432, 433]. It was Jones [434] who examined knot invariants to address the connection between the physical world and pure mathematics. Afterwards, such an approach was linked to topological quantum field theory by Witten [435, 436]. It is worth mentioning that the connection of such invariant knots with statistical mechanics is also possible [437]. Another motivation to investigate the physical consequences of the torus topology ($\mathrm{T}^2 = S^1 \times S^1$) is its application to living beings, owing to their DNA [438, 439, 440, 441, 442]. Moreover, the fundamental group of the torus is

$$\pi_1(\mathrm{T}^2) = \pi_1(S^1) \times \pi_1(S^1) \cong \mathbb{Z}^1 \times \mathbb{Z}^1, \tag{3.21}$$

and its first homology group is isomorphic to the fundamental group [443]. Now, based on Ref. [411], where the spectral energy for the torus knot was calculated, and in the approach developed in Sec. 3.2 and Sec. 3.3, we propose to study how particles of different spins behave in such a scenario. Before providing numerical analyses, let us show again the spectral energy [411] as in Eq. (3.7d)

$$E_n = E_{0,n} F(\eta, \alpha), \tag{3.22}$$

where

$$E_{0,n} = \frac{n^2}{2\mathrm{M}\mathfrak{a}^2 p^2}, \quad F(\eta, \alpha) = \frac{\cosh^2 \eta}{\alpha^2 + \sinh^2 \eta - 1}. \tag{3.23}$$

Now we can insert the energy spectrum in Eqs. (3.9) and (3.19) and properly perform the following numerical analyses for both the energy and heat capacity. Since we are going to study how the thermal properties are modified for different values of winding numbers, for a better comprehension of the reader, we add Fig 3.3 in order to provide an illustration of how the path changes on a torus knot for distinct winding numbers.

We first study the behavior of the energy presented in Fig. 3.4. We can see that fermions and bosons behave differently. While the free energy of bosons increases with temperature and winding number, the fermions exhibits an "inversion point" at 3 K, e.g., before and after 3 K there exist different behaviors for diverse values of winding number. Moreover, for spin-less particles the Helmholtz free energy decreases with both temperature and winding number.

In Fig. 3.5, we present the heat capacity for different particle spins and different values of winding number. Let us start with the spin-less particles. In this case, we see that the

heat capacity increases with the winding number and tends to $0.5\ J/g \times K$ for larger values of the temperature. For bosons, we see that for a temperature below 0.3 K, the values of the heat capacity decreases when the winding number increases, while for temperatures above 0.3 K the value increases when α increases. It is worth mentioning that for large values of the temperature, the heat capacity tends to $8.0\ J/g \times K$. Finally, we observe an interesting behavior for fermions. We see that for temperatures below 1.0 K the heat capacity has a mound that becomes more evident when the winding number increases. Above 1.0 K the heat capacity increases with temperature until it reaches a value around $2.0\ J/g \times K$. It is interesting to see a system whose thermodynamic properties depend on a topological parameter. Thereby, the knowledge of such behaviors can be useful for future applications.

3.5 Further applications: noninteracting gases

In this section, we address possible future applications of our *noninteracting* model for quantum gases developed so far. In particular, we look toward the *Bose-Einstein condensate* and the *helium dimer*.

3.5.1 Bose-Einstein condensate

In Ref. [424], the grand canonical ensemble is also used to perform the calculations; the authors studied the asymptotic behavior of various thermodynamic and statistical quantities related to a confined ideal *Bose-Einstein* gas. In this case, the considered object is an arbitrary, finite, cubical enclosure subjected to periodic boundary conditions, i.e., thin-film, square-channel and cubic geometries.

Continuing the line of [424], our proposition is to probe how the thermal quantities are affected by spherical, cylindrical, ellipsoidal and toroidal geometries. This study can be useful within a possible future experimental scenario to be studied in material science.

3.5.2 Helium atoms - ^{3}He and ^{4}He

Taking the advantage of solving the Schrödinger equation numerically as well as the construction of suitable wavefunctions, in Refs. [444, 445], the binding of two helium atoms involving restricted and unrestricted geometries was studied in two and three dimensions. Such a model describes two atoms placed in a spherical potential (3.1a) with hard walls. As argued, one could insert a nontrivial interaction of the helium atoms with the walls [446, 447, 448, 449] and also some coupling between them, as presented in Sec. 3.6. Nevertheless, the interaction of the particles with the wall depends on the material of the cavity. Thereby,

it is feasible to propose a general investigation of these phenomena rather than being limited to individual cases.

In this sense, our proposal is as follows: based on the relevance of studying either helium liquids or helium dimer in solid matrices, a study of geometry influences the thermodynamic properties of such constrained systems might be relevant for future applications in condensed matter physics. Likewise, for the cylindrical shape (3.1b), it is notable to aim at investigating the thermal properties of shapes similar to that of carbon nanotubes [450, 451]. Also, using some approximations, the vortex-like shapes [452, 453] seem to reasonable to be examined as well.

3.6 Interacting gases: an analytical approach

3.6.1 The model

We intend now to take into account interactions between particles. To do so, we modify slightly the approach developed in Sec. 3.3 by introducing an interaction term $U(V,n)$. Here, we consider that such interaction energy has the dependency only on the particle density n and the volume V. As it is mentioned below, such type of interaction may be acquired by the mean field approximation which gives rise to the advantage of providing analytical results. Furthermore, as we shall verify, these solutions will allow us to recognize how the interactions can modify the thermal quantities of our system. It is important to highlight that the interaction term is a monotonically increasing function of the particle density. Thereby, if the density n is increased, the particles will come closer to each other and the respective interactions between them are supposed to increase. Analogously, the opposite behavior happens otherwise: if n decreases, $U(V,n)$ will have to decrease. Throughout this section, we adopt natural units where $k_B = 1$. Doing that, we get the following grand canonical partition function

$$\mathcal{Z}(T,V,\mu) = \sum_{\{N_\Omega\}=0}^{\{\infty/1\}} \exp\left\{-\beta\left[\sum_{\{\Omega\}} N_\Omega\left(E_\Omega - \mu\right) + U(V,n)\right]\right\}, \tag{3.24a}$$

where

$$z^N = \exp\{N\beta\mu\} = \exp\left\{\beta\sum_{\{\Omega\}} N_\Omega\mu\right\}. \tag{3.24b}$$

The sum index which appears in Eq. (3.24a), namely $\{\infty/1\}$, shows that infinitely many bosons may occupy the same quantum state Ω. On the other hand, if one considers instead of this, spin-half particles, only one fermion will be allowed due to the Pauli exclusion principle.

In a compact notation, we take the upper index ∞ for bosons and 1 for fermions. Let us now suppose that the interaction term has the form $U(V,n) = Vu(n)$. With this, we have

$$\mathcal{Z}(T,V,\mu) = \sum_{\{N_\Omega\}=0}^{\{\infty/1\}} \exp\left\{-\beta\left[\sum_{\{\Omega\}} N_\Omega\left(E_\Omega - \mu\right) + Vu(n)\right]\right\}. \tag{3.25}$$

For the sake of simplicity, in Eq. (3.25), we assume that $Vu(n)$ is linear in $\sum_\Omega N_\Omega = N$. Furthermore, the only appropriate manner to do so is to linearize $Vu(n)$. To do that, we use the Taylor series expansion of $u(n)$ around the mean value $\bar{n}$:

$$u(n) = u(\bar{n}) + u'(\bar{n})(n-\bar{n}) + \ldots. \tag{3.26}$$

More so, if one regards that the potential energy is dependent on the position that the particles occupy, Eq. (3.26) will account for the *molecular field approximation*. Such assumption is vastly employed in the literature concerning for instance condensed matter physics [454, 455, 456, 457, 458, 459]. Thereby, we can derive the energy of the quantum state Ω as being

$$E = \sum_{\{\Omega\}} N_\Omega\left[E_\Omega + u'(\bar{n})\right] + U(V,\bar{n}) - u'(\bar{n})\bar{N}, \tag{3.27}$$

and the solution of Eq. (3.25) can be evaluated

$$\begin{aligned}\mathcal{Z}(T,V,\mu) &= \exp\left\{-\beta\left[U(V,\bar{n}) - u'(\bar{n})\bar{N}\right]\right\} \\ &\quad\times\prod_{\Omega=1}^{\infty}\left(\sum_{N_\Omega=0}^{\{\infty/1\}}\exp\left\{-\beta\left[E_\Omega + u'(\bar{n}) - \mu\right]N_\Omega\right\}\right).\end{aligned} \tag{3.28}$$

After some algebraic manipulations, we can present the above expression as

$$\begin{aligned}\mathcal{Z}(T,V,\mu) &= \exp\left\{-\beta\left[U(V,\bar{n}) - u'(\bar{n})\bar{N}\right]\right\} \\ &\quad\times\prod_{\Omega=1}^{\infty}\left\{\begin{array}{c} 1+\exp\left[-\beta\left(E_\Omega + u'(\bar{n}) - \mu\right)\right], \text{fermions} \\ \left(1-\exp\left[-\beta\left(E_\Omega + u'(\bar{n}) - \mu\right)\right]\right)^{-1}, \text{bosons}\end{array}\right.,\end{aligned} \tag{3.29}$$

or in a more compact form

$$\begin{aligned}\mathcal{Z}(T,V,\mu) &= \exp\left\{-\beta\left[U(V,\bar{n}) - u'(\bar{n})\bar{N}\right]\right\} \\ &\quad\times\prod_{\Omega=1}^{\infty}\left(1+\chi\exp\left[-\beta\left(E_\Omega + u'(\bar{n}) - \mu\right)\right]\right)^{\chi},\end{aligned} \tag{3.30}$$

where $\chi = 1$ for fermions, and $\chi = -1$ for bosons.

3.6.2 Thermodynamic state quantities

Next, the derivation of the grand canonical potential is straightforward as follows

$$\begin{aligned}\Phi &= -T\ln\mathcal{Z} \\ &= -T\chi\sum_{\Omega}\ln\left(1+\chi\exp\left[-\beta\left(E_{\Omega}+u'\left(\bar{n}\right)-\mu\right)\right]\right)+U\left(V,\bar{n}\right)-u'\left(\bar{n}\right)\bar{N}. \end{aligned} \tag{3.31}$$

Based on this equation, the other thermodynamic functions can be calculated as well. In this sense, the mean particle number reads

$$\begin{aligned}\bar{N} &= -\left.\frac{\partial\Phi}{\partial\mu}\right|_{T,V}, \\ &= -V\left.\frac{\partial u\left(\bar{n}\right)}{\partial\mu}\right|_{T,V}+\bar{N}\left.\frac{\partial u'\left(\bar{n}\right)}{\partial\mu}\right|_{T,V}+u'\left(\bar{n}\right)\left.\frac{\partial\bar{N}}{\partial\mu}\right|_{T,V}+ \\ &+T\chi\sum_{\Omega}\frac{\chi\exp\left[-\beta\left(E_{\Omega}+u'\left(\bar{n}\right)-\mu\right)\right]}{1+\chi\exp\left[-\beta\left(E_{\Omega}+u'\left(\bar{n}\right)-\mu\right)\right]}\beta\left(1-\left.\frac{\partial u'\left(\bar{n}\right)}{\partial\mu}\right|_{T,V}\right), \end{aligned} \tag{3.32}$$

and from this,

$$\begin{aligned}\bar{N}\left(1-\left.\frac{\partial u\left(\bar{n}\right)}{\partial\mu}\right|_{T,V}\right) &= -V\left.\frac{\partial u\left(\bar{n}\right)}{\partial\mu}\right|_{T,V}+u'\left(\bar{n}\right)\left.\frac{\partial\bar{N}}{\partial\mu}\right|_{T,V} \\ &+\chi^2\beta T\left(1-\left.\frac{\partial u'\left(\bar{n}\right)}{\partial\mu}\right|_{T,V}\right)\sum_{\Omega}\frac{1}{\exp\left[\beta\left(E_{\Omega}+u'\left(\bar{n}\right)-\mu\right)\right]+\chi}. \end{aligned} \tag{3.33}$$

Since

$$\left.\frac{\partial u\left(\bar{n}\right)}{\partial\mu}\right|_{T,V}=u'\left(\bar{n}\right)\left.\frac{\partial\bar{n}}{\partial\mu}\right|_{T,V}=\frac{u'\left(\bar{n}\right)}{V}\left.\frac{\partial\bar{N}}{\partial\mu}\right|_{T,V}, \tag{3.34}$$

we get

$$\bar{N}=\sum_{\Omega}\frac{1}{\exp\left[\beta\left(E_{\Omega}+u'\left(\bar{n}\right)-\mu\right)\right]+\chi}. \tag{3.35}$$

The mean occupation number must be $\bar{N}=\sum_{\Omega}\bar{n}_{\Omega}$, where

$$\bar{n}_{\Omega}=\frac{1}{\exp\left[\beta\left(E_{\Omega}+u'\left(\bar{n}\right)-\mu\right)\right]+\chi}. \tag{3.36}$$

As we can also notice that the interaction modifies the mean particle number since the term $u'\left(\bar{n}\right)$ is present in Eq. (3.36). This modification is directly related to the fact that we chose the interaction energy as being a function of the particle density.

Next, the entropy is given by

$$\begin{aligned} S &= -\left.\frac{\partial \Phi}{\partial T}\right|_{\mu,V}, \\ &= -V\left.\frac{\partial u\left(\bar{n}\right)}{\partial T}\right|_{\mu,V} + \bar{N}\left.\frac{\partial u'\left(\bar{n}\right)}{\partial T}\right|_{\mu,V} + u'\left(\bar{n}\right)\left.\frac{\partial \bar{N}}{\partial T}\right|_{\mu,V} \\ &+ \chi\sum_{\Omega}\ln\left(1+\chi\exp\left[-\beta\left(E_{\Omega}+u'\left(\bar{n}\right)-\mu\right)\right]\right) \\ &+ \chi^{2}T\sum_{\Omega}\frac{\left(E_{\Omega}+u'\left(\bar{n}\right)-\mu\right)\left(-\frac{d\beta}{dT}\right)-\beta\left.\frac{\partial u'(\bar{n})}{\partial T}\right|_{\mu,V}}{\exp\left[\beta\left(E_{\Omega}+u'\left(\bar{n}\right)-\mu\right)\right]+\chi}, \end{aligned} \tag{3.37}$$

or in a more compact form,

$$\begin{aligned} S &= \chi\sum_{\Omega}\ln\left(1+\chi\exp\left[-\beta\left(E_{\Omega}+u'\left(\bar{n}\right)-\mu\right)\right]\right) \\ &+ \frac{1}{T}\sum_{\Omega}\bar{n}_{\Omega}\left(E_{\Omega}+u'\left(\bar{n}\right)-\mu\right). \end{aligned} \tag{3.38}$$

Moreover, the mean energy reads

$$\begin{aligned} \bar{E} &= \left.\frac{\partial\left(\beta\Phi\right)}{\partial\beta}\right|_{z,V}, \\ &= \left.\frac{\partial}{\partial\beta}\left[\beta V u\left(\bar{n}\right)-\beta\bar{N}u'\left(\bar{n}\right)\right]\right|_{z,V} \\ &- \chi\sum_{\Omega}\frac{\chi z\exp\left[-\beta\left(E_{\Omega}+u'\left(\bar{n}\right)\right)\right]}{1+\chi z\exp\left[-\beta\left(E_{\Omega}+u'\left(\bar{n}\right)\right)\right]}\left(-E_{\Omega}-\left.\frac{\partial}{\partial\beta}\left[\beta u'\left(\bar{n}\right)\right]\right|_{z,V}\right), \\ &= U\left(V,\bar{n}\right)+\beta V\left.\frac{\partial u\left(\bar{n}\right)}{\partial\beta}\right|_{z,V}-\bar{N}\left.\frac{\partial\left[\beta u'\left(\bar{n}\right)\right]}{\partial\beta}\right|_{z,V}-\beta u'\left(\bar{n}\right)\left.\frac{\partial\bar{N}}{\partial\beta}\right|_{z,V} \\ &+ \sum_{\Omega}\frac{E_{\Omega}}{z^{-1}\exp\left[\beta\left(E_{\Omega}+u'\left(\bar{n}\right)\right)\right]+\chi}+\bar{N}\left.\frac{\partial\left[\beta u'\left(\bar{n}\right)\right]}{\partial\beta}\right|_{z,V}. \end{aligned} \tag{3.39}$$

After some algebraic manipulations, one can rewrite this expression as

$$\bar{E} = \sum_{\Omega}\bar{n}_{\Omega}E_{\Omega}+U\left(V,\bar{n}\right). \tag{3.40}$$

This is a expected result since the energy is the average of the kinetic term plus the interactions energy. Finally, we derive the pressure of the system

$$p = -\left.\frac{\partial\Phi}{\partial V}\right|_{\mu,T},$$

$$= -u\left(\bar{n}\right) + u'\left(\bar{n}\right)\left.\frac{\partial \bar{N}}{\partial V}\right|_{\mu,T} + \frac{\chi T}{V}\sum_{\Omega}\ln\left(1+\chi\exp\left[-\beta\left(E_{\Omega}+u'\left(\bar{n}\right)-\mu\right)\right]\right), \tag{3.41}$$

$$= -\frac{\Phi}{V}, \tag{3.42}$$

where we have used Eq. (3.35) and the fact that the particle density does not depend on the volume. From Eq. (3.41), we can also realize how interaction plays an important role on the pressure. The first term in Eq. (3.41), - $u\left(\bar{n}\right)$, for instance, is responsible to reduce the pressure of the system, while the second one, $u'\left(\bar{n}\right)$, plays the role of increasing it instead. It is worth mentioning that such thermal functions were recently calculated in [460, 461, 462, 463, 464, 465, 466] for Lorentz-violating systems.

3.6.3 Analytical results for three-dimensional boxes

We exemplify our model constructed above for the three-dimensional box. The respective spectral energy is

$$E^{\mathrm{Box}}_{\eta_x,\eta_y,\eta_z} = \frac{\pi^2\hbar^2}{2\mathrm{M}}\left(\frac{\eta_x^2}{L_x^2}+\frac{\eta_y^2}{L_y^2}+\frac{\eta_z^2}{L_z^2}\right). \tag{3.43}$$

Here, the grand canonical potential of an *interacting* gas is

$$\Phi = -k_B T\chi\sum_{\left\{\eta_x,\eta_y,\eta_z\right\}}\ln\left\{1+\chi\exp\left[-\beta\left(E^{\mathrm{Box}}_{\eta_x,\eta_y,\eta_z}+u'\left(\bar{n}\right)-\mu\right)\right]\right\}+U\left(V,\bar{n}\right)-u'\left(\bar{n}\right)\bar{N}. \tag{3.44}$$

To proceed further, the *Euler-MacLaurin formula* [467, 147, 468] must be utilized,

$$\sum_{n}^{\infty}F\left(n\right) = \int_0^{\infty}F\left(n\right)dn+\frac{1}{2}F\left(0\right) - \frac{1}{2!}B_2F'\left(0\right)-\frac{1}{4!}B_4F'''\left(0\right)+\ldots, \tag{3.45}$$

which allows us to perform the calculation in an exact form, namely

$$\begin{aligned}\Phi = &-k_BT\chi\int_0^{\infty}\int_0^{\infty}\int_0^{\infty}d\eta_x d\eta_y d\eta_z\ln\left\{1+\chi_{\mathfrak{Z}}\exp\left[-\beta E^{\mathrm{Box}}_{\eta_x,\eta_y,\eta_z}\right]\right\}\\ &+\frac{k_BT\chi}{2}\int_0^{\infty}\int_0^{\infty}d\eta_y d\eta_z\ln\left\{1+\chi_{\mathfrak{Z}}\exp\left[-\beta E^{\mathrm{Box}}_{0,\eta_y,\eta_z}\right]\right\}\\ &+\frac{k_BT\chi}{2}\int_0^{\infty}\int_0^{\infty}d\eta_x d\eta_z\ln\left\{1+\chi_{\mathfrak{Z}}\exp\left[-\beta E^{\mathrm{Box}}_{\eta_x,0,\eta_z}\right]\right\}\\ &+\frac{k_BT\chi}{2}\int_0^{\infty}\int_0^{\infty}d\eta_x d\eta_y\ln\left\{1+\chi_{\mathfrak{Z}}\exp\left[-\beta E^{\mathrm{Box}}_{\eta_x,\eta_y,0}\right]\right\}\\ &+\frac{k_BT\chi}{4}\int_0^{\infty}d\eta_x\ln\left\{1+\chi_{\mathfrak{Z}}\exp\left[-\beta E^{\mathrm{Box}}_{\eta_x,0,0}\right]\right\}\end{aligned}$$

$$+\frac{k_BT\chi}{4}\int_0^\infty d\eta_y \ln\left\{1+\chi\mathfrak{z}\exp\left[-\beta E^{\text{Box}}_{0,\eta_y,0}\right]\right\}$$
$$+\frac{k_BT\chi}{4}\int_0^\infty d\eta_z \ln\left\{1+\chi\mathfrak{z}\exp\left[-\beta E^{\text{Box}}_{0,0,\eta_z}\right]\right\}$$
$$+\frac{k_BT\chi}{8}\ln\left(1+\chi\mathfrak{z}\right)+U\left(V,\bar{n}\right)-u'\left(\bar{n}\right)\bar{N}, \tag{3.46}$$

where we have defined $\mathfrak{z}=ze^{-\beta u'(\bar{n})}$. After performing the integrals, we obtain

$$\Phi=\frac{\mathcal{V}}{\lambda^3}h_{\frac{5}{2}}\left(\mathfrak{z}\right)-\frac{1}{4}\frac{\mathcal{S}}{\lambda^2}h_2\left(\mathfrak{z}\right)+\frac{1}{16}\frac{\mathcal{L}}{\lambda}h_{\frac{3}{2}}\left(\mathfrak{z}\right)-\frac{1}{8}h_1\left(\mathfrak{z}\right)+U\left(V,\bar{n}\right)-u'\left(\bar{n}\right)\bar{N}, \tag{3.47}$$

where $\lambda=h/\sqrt{2\pi \mathrm{M}k_BT}$ is the thermal wavelength, $\mathcal{V}=L_xL_yL_z$ is the volume, $\mathcal{S}=2\left(L_xL_y+L_yL_z+L_zL_x\right)$ the area of the surface, $\mathcal{L}=4\left(L_x+L_y+L_z\right)$ the total length of the side of the box and

$$h_\sigma\left(\mathfrak{z}\right)=\frac{1}{\Gamma\left(\sigma\right)}\int_0^\infty\frac{t^{\sigma-1}}{\mathfrak{z}^{-1}e^t+\chi}dt=\begin{cases} f_\sigma\left(\mathfrak{z}\right), \text{ for fermions } (\chi=1) \\ g_\sigma\left(\mathfrak{z}\right), \text{ for bosons } (\chi=-1)\end{cases}. \tag{3.48}$$

The boundary effects in Eq. (3.47) are represented by the second and third terms which are proportional to the perimeter $\mathcal{L}$ and to the surface $\mathcal{S}$. We note that these terms are modified by the interaction term $u'\left(\bar{n}\right)$. Also, we can carry out a similar calculation involving rather a two-dimensional box. Here, a straightforward question naturally arises: how are the thermal properties influenced if one considers spherical (3.1a), cylindrical (3.1b), ellipsoidal (3.1c) and toroidal (3.2) potentials instead? Despite being an intriguing question, it is challenging to perform such an analysis by analytical means. Nevertheless, this analysis will be performed numerically in an upcoming work.

As an application, let us use the result obtained from Eq. (3.47) to probe how interaction affects the Fermi energy. From that, we get

$$N=g\left[\frac{V}{\lambda^3}f_{\frac{3}{2}}\left(\mathfrak{z}\right)-\frac{1}{4}\frac{S}{\lambda^2}f_1\left(\mathfrak{z}\right)+\frac{L}{16\lambda}f_{\frac{1}{2}}\left(\mathfrak{z}\right)-\frac{1}{8}\frac{\mathfrak{z}}{\mathfrak{z}+1}\right], \tag{3.49}$$

where g is a weight factor that arises from the internal structure of the particles. The Fermi energy μ_0 is the energy of the topmost filled level in the ground state of an electron system. In this way,

$$N=g\left[\frac{V}{6\pi^2}\left(\frac{2m\mathfrak{X}}{\hbar^2}\right)^{\frac{3}{2}}-\frac{1}{4}\frac{S}{4\pi}\left(\frac{2m\mathfrak{X}}{\hbar^2}\right)+\frac{L}{16\pi}\left(\frac{2m\mathfrak{X}}{\hbar^2}\right)^{\frac{1}{2}}-\frac{1}{8}\right], \tag{3.50}$$

where $\mathfrak{X}=\mu_0-u'\left(n\right)$. The Fermi energy cannot be calculated from this equation until we conveniently choose the interaction $u(n)$ term. However, we can at least see how the interaction modifies the structure of the equation which determines the Fermi energy μ_0.

It is also possible to infer that the existence of a interaction enhances such energy level. Moreover, we realize that the interaction remarkably introduces a density-dependence on the Fermi energy. In order to have an idea of the interaction term, we can use the density of an ideal Fermi gas, which is given by [138]

$$n = \frac{g}{\lambda^3} f_{\frac{3}{2}}(z) \tag{3.51}$$

to estimate such energy. In possession with the above density, we can build an interaction term linear in n. Despite this, even with this simplest approximation, it is not possible to get analytical results.

3.6.4 Analytical results for angular constraints

The exact solutions for *interacting* gases in angular constraints can also be calculated with the help of the *Euler-MacLaurin* formula. Here, we consider an *interacting* quantum gas confined to a one-dimensional ring with radius R. The energy of the particle in such an angular scenario is determined by periodic boundary conditions:

$$E_\eta = \frac{\hbar^2}{2MR^2}\eta^2. \tag{3.52}$$

The grand canonical potential for this case is given by

$$\begin{aligned}\Phi &= -k_B T\chi \sum_{\eta=-\infty}^{\infty} \ln\left\{1+\chi_{\mathfrak{z}} \exp\left[-\frac{\beta\hbar^2}{2MR^2}\eta^2\right]\right\} + U(V,\bar{n}) - u'(\bar{n})\bar{N}, \qquad (3.53)\\ &= -2k_B T\chi \sum_{\eta=0}^{\infty} \ln\left\{1+\chi_{\mathfrak{z}} \exp\left[-\frac{\beta\hbar^2}{2MR^2}\eta^2\right]\right\} - k_B T\chi \ln\{1+\chi_{\mathfrak{z}}\} + U(V,\bar{n}) - u'(\bar{n})\bar{N}.\end{aligned}$$

The summation over the discrete parameter η can be converted into an integral which leads to

$$\Phi = \frac{\mathcal{L}}{\lambda} h_{\frac{3}{2}}(\mathfrak{z}) - h_1(\mathfrak{z}) + U(V,\bar{n}) - u'(\bar{n})\bar{N}. \tag{3.54}$$

where $\mathcal{L} = 2\pi R$ and $h_\sigma(\mathfrak{z})$ is the interaction. We can also notice that there is no boundary effect here. Notably, we could use these results to study the thermodynamic properties of a conducting ring and other similar systems. Moreover, if one does not consider interactions, the results presented in subsections 3.6.3 and 3.6.4 will reproduce those ones encountered in Ref. [143].

3.6.5 Analytical results for the torus

We can proceed as before to get an exact solution for the torus. The grand canonical potential for this case is given by

$$\begin{aligned}\Phi &= -T\chi \sum_{\delta=-\infty}^{\infty} \ln\left\{1+\chi\mathfrak{z}\exp\left[-\frac{\beta\hbar^2 F(\alpha,\eta)}{2M\mathfrak{a}^2p^2}\delta^2\right]\right\} + U(V,\bar{n}) - u'(\bar{n})\bar{N},\\ &= -2T\chi \sum_{\delta=1}^{\infty} \ln\left\{1+\chi\mathfrak{z}\exp\left[-\frac{\beta\hbar^2 F(\alpha,\eta)}{2M\mathfrak{a}^2p^2}\delta^2\right]\right\} - T\chi\ln\{1+\chi\mathfrak{z}\} + U(V,\bar{n}) - u'(\bar{n})\bar{N}.\end{aligned} \tag{3.55}$$

The summation over the discrete parameter δ can be rewritten as an integral, leading to

$$\Phi = \frac{\mathfrak{a}p^2}{F(\alpha,\eta)}\frac{\mathcal{L}}{\lambda}h_{\frac{3}{2}}(\mathfrak{z}) - h_1(\mathfrak{z}) + U(V,\bar{n}) - u'(\bar{n})\bar{N}. \tag{3.56}$$

where $\mathcal{L} = 2\pi a$ and again the interaction is also present in $h_\sigma(\mathfrak{z})$ function. We can also notice that here there is no boundary effects for the same reason encountered in the ring case. However, Eq.(3.56) is modified by the topological function $F(\alpha,\eta)$ given by Eq. (3.23).

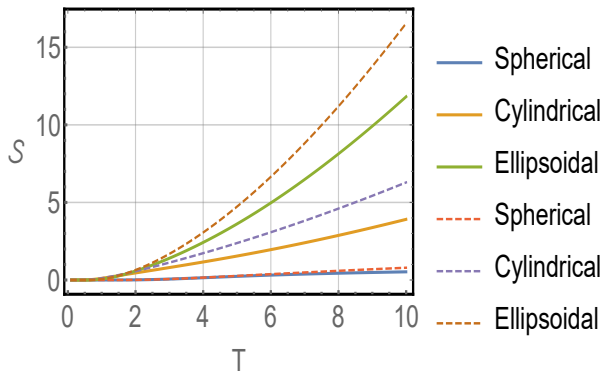

((a)) Entropy case 1

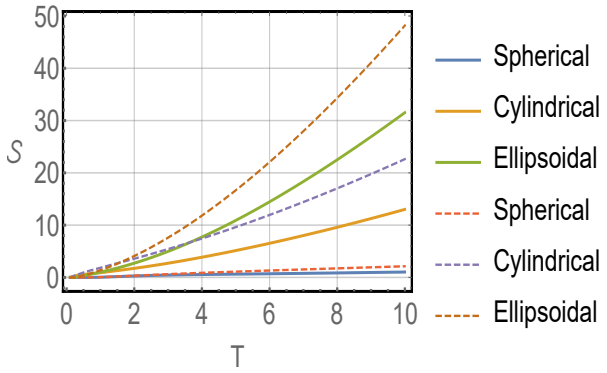

((b)) Entropy case 2

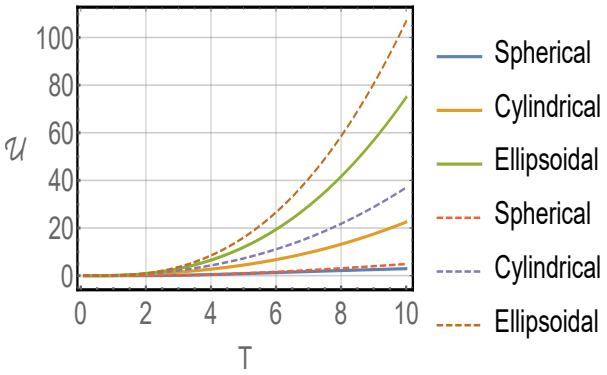

((c)) Energy case 1

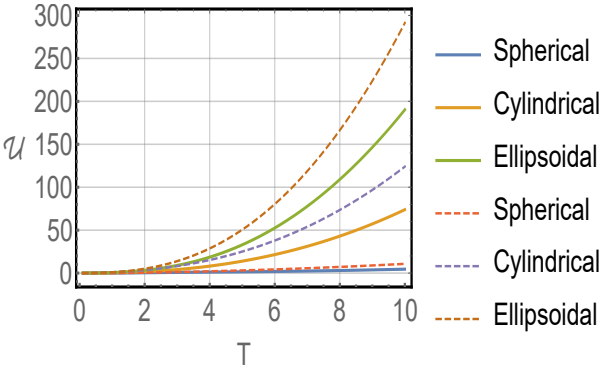

((d)) Energy case 2

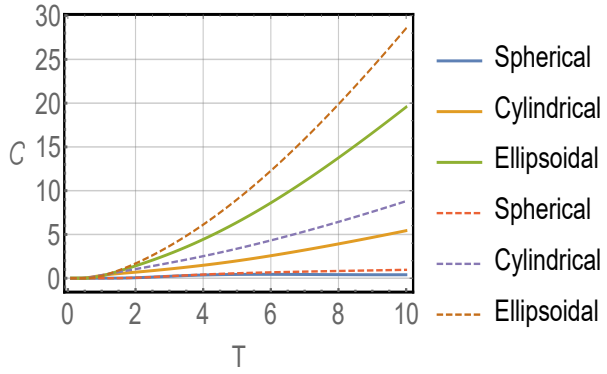

((e)) Heat capacity case 1

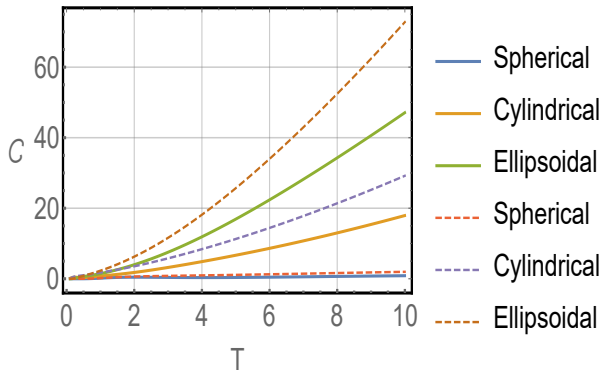

((f)) Heat capacity case 2

Fig. 3.2: The different behaviors for the entropy, mean energy and heat capacity, respactively

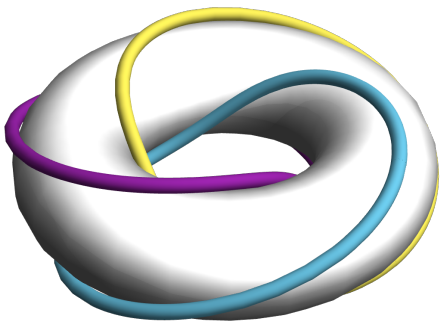

((a)) Winding number = 1

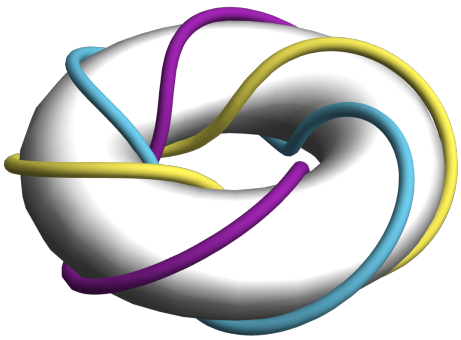

((b)) Winding number = 2

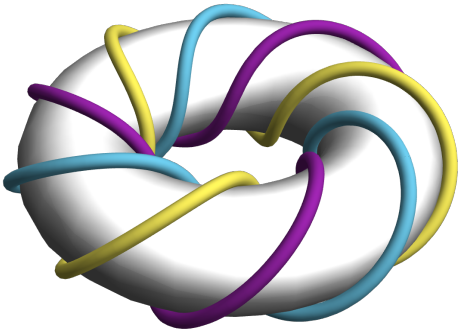

((c)) Winding number = 3

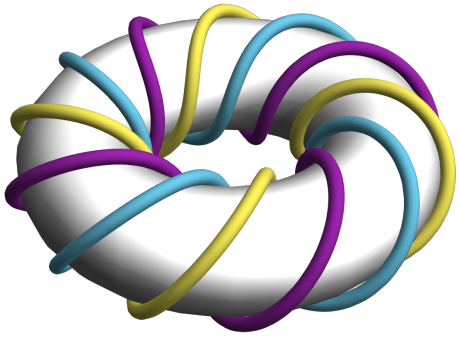

((d)) Winding number = 4

Fig. 3.3: Path behavior through a torus knot for different winding numbers

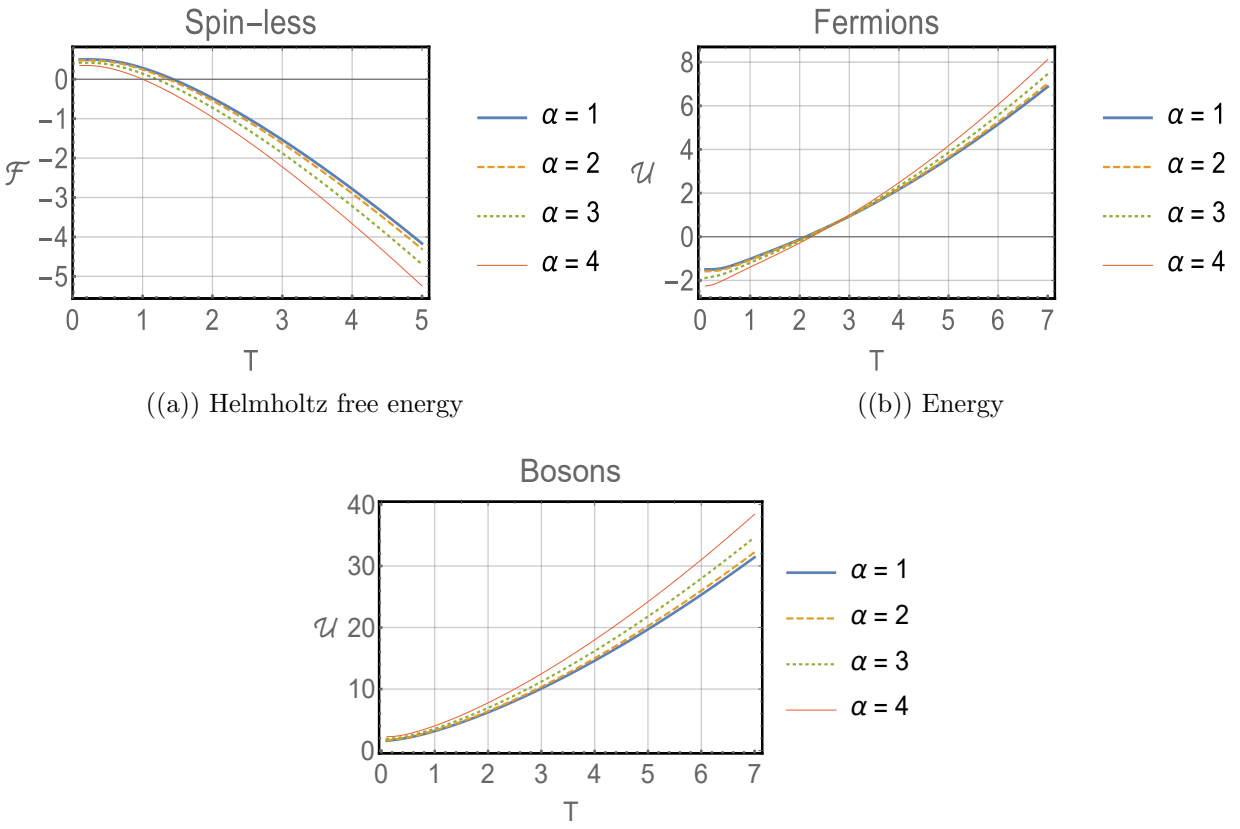

((a)) Helmholtz free energy

((b)) Energy

((c)) Energy

Fig. 3.4: Energy behavior in the low-temperature regime for different values of winding number α for the torus knot.

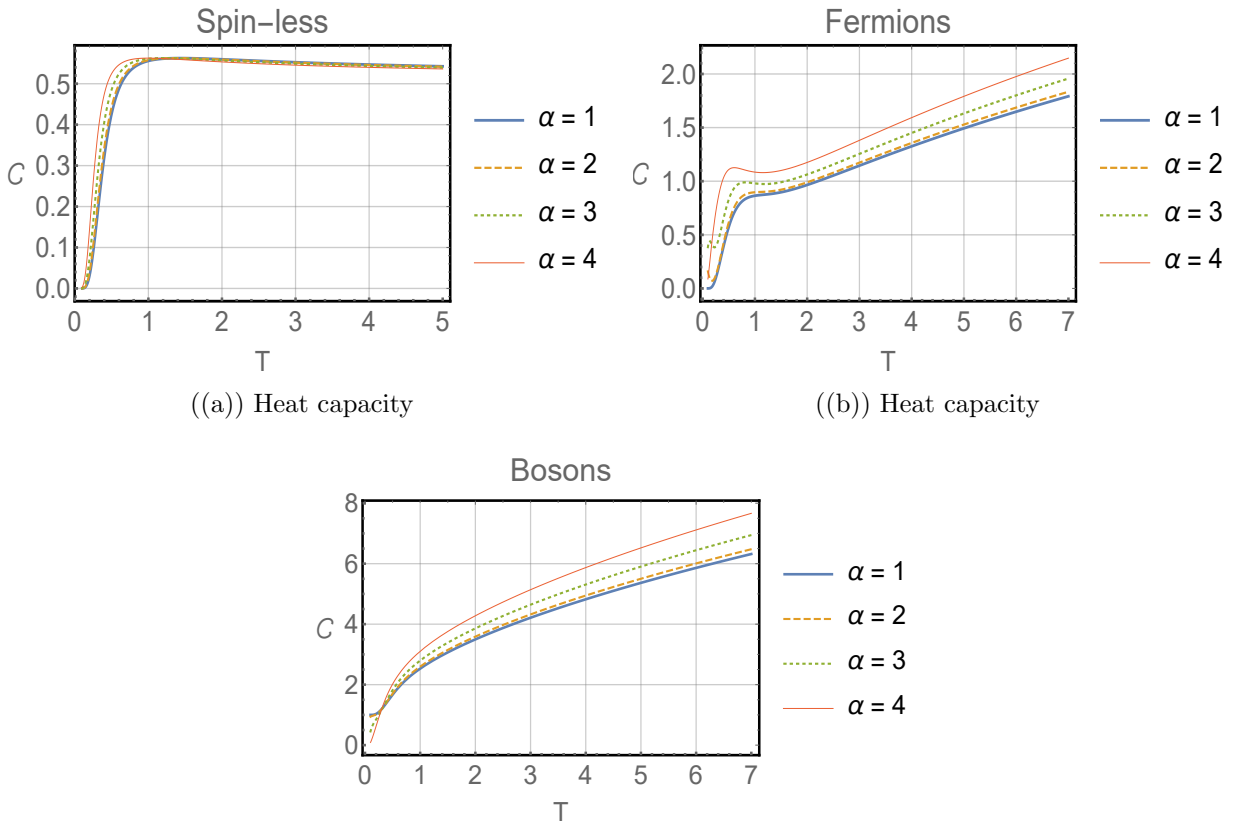

((a)) Heat capacity

((b)) Heat capacity

((c)) Heat capacity

Fig. 3.5: Heat capacity in the low-temperature regime for different values of winding number α for the torus knot.

4. FERMIONS ON A TORUS KNOT

4.1 Statistical mechanics of N particles in a torus knot subjected to a magnetic field

Let us consider an ensemble composed of N particles moving on a single torus in a prescribed path. For the situation that we are considering, the canonical ensemble theory is sufficient to describe this case. The partition function for the system of N particle is given by

$$\mathcal{Z} = \sum_{\{\Omega\}} \exp\left(-\beta E_{\Omega}\right), \tag{4.1}$$

where Ω is related to all accessible quantum states. Since we are dealing with noninteracting particles, the partition function (4.1) can be factorized, giving the following result below

$$\mathcal{Z} = \mathcal{Z}_1^N = \left\{ \sum_{\{\Omega\}} \exp\left(-\beta E_{\Omega}\right) \right\}^N, \tag{4.2}$$

where we have defined the single partition function as

$$\mathcal{Z}_1 = \sum_{\Omega} \exp\left(-\beta E_{\Omega}\right). \tag{4.3}$$

It is interesting to point out that, even though the underling geometry is not a simply connected one, there is no problem in regarding the factorization above, since there is no interaction potential generated by the geometry itself. This affirmation can naturally be checked by looking at the energy spectrum given by Eq. (4.8)[1]. The connection with macroscopic thermodynamic observables can be given by Helmholtz free energy

$$f = -\frac{1}{\beta} \lim_{N\to\infty} \frac{1}{N} \ln \mathcal{Z}, \tag{4.4}$$

[1]Note that the procedure used here to carried out the factorization is not a general result. It suits only for the results presented in this chapter.

where f stands for the Helmholtz free energy per particle. With this quantity, we can derive the following thermodynamic state functions

$$s = -\frac{\partial f}{\partial T}, \quad c = T\frac{\partial s}{\partial T}, \quad u = -\frac{\partial}{\partial \beta}\ln \mathcal{Z}, \tag{4.5}$$

where s, c, u represent entropy, heat capacity and energy per particle, respectively. We can also calculate magnetization $\mathfrak{m}$ and susceptibility χ with respect to the external magnetic B, as given by

$$\mathfrak{m} = -\frac{\partial f}{\partial B}, \quad \chi = \frac{\partial \mathfrak{m}}{\partial B}. \tag{4.6}$$

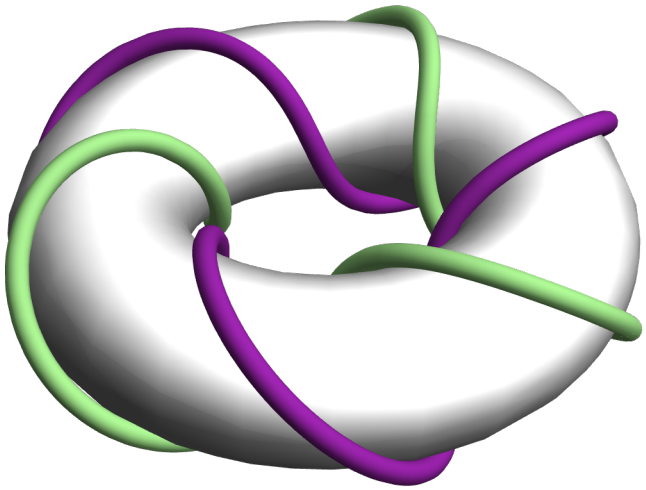

Fig. 4.1: A representation of a torus knot (2,3). The wire represents the path followed by the particles on its surface

The sum in Eq. (4.3) can be brought to a closed form by using the well-know *Euler-MacLaurin* formula [469, 470]

$$\sum_{n=0}^{\infty} F(n) = \int_0^{\infty} F(n)\, dn + \frac{1}{2}F(0) - \frac{1}{2!}B_2 F'(0) - \frac{1}{4!}B_4 F'''(0) + \ldots, \tag{4.7}$$

which allows us to perform the calculation exactly. The energy spectrum of a particle moving on a torus with dimensions a, d and submitted to a uniform magnetic field that points along

the $\hat{\boldsymbol{z}}$ direction is given by [182][2]

$$E_n = \frac{1}{2m}\left[\frac{n^2\hbar^2}{p^2d^2}\left(1-\frac{a^2q^2}{p^2d^2}\right)+\frac{eB}{p}n\hbar\left(1+\frac{a^2}{2d^2}-\frac{a^2q^2}{p^2d^2}\right)+\frac{e^2B^2d^2}{4}\left(1+\frac{a^2}{d^2}-\frac{a^2q^2}{p^2d^2}\right)\right], \tag{4.8}$$

where d is the outer radius and a the internal radius of the torus respectively with $(d > a)$ (see Fig. 4.1). The closed path is characterized by a (p,q)-knot with p and q denoting the toroidal and poloidal turns, respectively, so that it turns around d and a respectively. For a nontrivial torus knot, (p,q) are coprime numbers. The well known and simplest knot, a $(2,3)$ or trefoil knot, is depicted in Fig. 4.1.

Now, inserting the energy spectrum on the single partition function (4.1) and computing the sum, we are led to the following single particle partition function:

$$\begin{aligned}\mathcal{Z}_1 &= \sqrt{\frac{\pi m p^2 d^2}{2\beta\left(1-\mathcal{A}\right)}}\exp\left[\beta\frac{d\alpha^2\mathcal{A}}{32m\left(1-\mathcal{A}\right)}\xi\right]\times \\ &\times\left\{1+\mathrm{erf}\left[-\frac{\xi}{4}\sqrt{\frac{2\beta}{m\left(1-\mathcal{A}\right)}}\left(1-\mathcal{A}+\frac{\alpha^2}{2}\mathcal{A}\right)\right]\right\},\end{aligned} \tag{4.9}$$

where $\mathbf{erf}$ is the error function given by

$$\mathrm{erf}\left[z\right] = \frac{2}{\sqrt{\pi}}\int_0^z e^{-t^2}dt, \tag{4.10}$$

and we also have defined the following quantities

$$\xi = eB, \quad \mathcal{A} = \frac{a^2}{d^2}, \quad \alpha = \frac{q}{p}, \tag{4.11}$$

where $\mathcal{A}$ is a property of the torus whereas α characterises the knot of the particular path. The quantity α is called the "winding number" of the (p,q)-torus knot, and it is also a simple way of measuring the complexity of the knot. Notice that two different torus knots can have the same α. Nevertheless, α will be different if at least one of p or q differ. In this sense, α is regarded as a "unique" identity of a (p,q)-torus knot. It is worth mentioning that similar forms of partition function have appeared in very recent works in the literature considering different contexts [390, 471, 391, 359, 472].

[2]It should be noted that we have considered a magnetic field which, in technical terms, is referred as the solenoidal magnetic field (uniform magnetic field pointing in the $\hat{\boldsymbol{z}}$ direction). Nevertheless, for a particle on a torus knot, two other forms of magnetic field, referred to as toroidal (along the $\hat{\boldsymbol{\phi}}$ direction) and poloidal (along the $\hat{\boldsymbol{\theta}}$ direction) forms are also relevant. If one is interested in more details ascribed to them, please see Ref. [182].

Now substituting (4.9) in (4.4), we find

$$\begin{aligned} f &= -\frac{d\alpha^2\mathcal{A}}{32m\left(1-\mathcal{A}\right)}\xi - \frac{1}{\beta}\ln\sqrt{\frac{\pi m p^2 d^2}{2\beta\left(1-\mathcal{A}\right)}} \\ &\quad -\frac{1}{\beta}\ln\left\{1+\operatorname{erf}\left[-\frac{\xi}{4}\sqrt{\frac{2\beta}{m\left(1-\mathcal{A}\right)}}\left(1-\mathcal{A}+\frac{\alpha^2}{2}\mathcal{A}\right)\right]\right\}. \end{aligned} \tag{4.12}$$

From this expression, using previous relations (4.5), we can get the relevant thermodynamic variables. For instance, the internal energy is given by

$$\begin{aligned} u &= -\frac{1}{\beta^2}\left(\frac{1}{2}+\ln\sqrt{\frac{\pi m p^2 d^2}{2\beta\left(1-\mathcal{A}\right)}}\right) \\ &\quad -\frac{1}{\beta^2}\ln\left\{1+\operatorname{erf}\left[-\frac{\xi}{4}\sqrt{\frac{2\beta}{m\left(1-\mathcal{A}\right)}}\left(1-\mathcal{A}+\frac{\alpha^2}{2}\mathcal{A}\right)\right]\right\} \\ &\quad -\frac{\xi}{\beta^{\frac{3}{2}}}\sqrt{\frac{1}{8m\pi\left(1-\mathcal{A}\right)}}\frac{\left(1-\mathcal{A}+\frac{\alpha^2}{2}\mathcal{A}\right)\exp\left[-\frac{\xi^2}{8}\frac{\beta}{m(1-\mathcal{A})}\left(1-\mathcal{A}+\frac{\alpha^2}{2}\mathcal{A}\right)^2\right]}{1-\operatorname{erf}\left[\frac{\xi}{4}\sqrt{\frac{2\beta}{m(1-\mathcal{A})}}\left(1-\mathcal{A}+\frac{\alpha^2}{2}\mathcal{A}\right)\right]} \end{aligned} \tag{4.13}$$

Another important quantity is the magnetization, which reads

$$\mathfrak{m} = \frac{d\alpha^2\mathcal{A}}{32m\left(1-\mathcal{A}\right)} - \sqrt{\frac{1}{2\pi\beta m\left(1-\mathcal{A}\right)}}\frac{\left(1-\mathcal{A}+\frac{\alpha^2}{2}\mathcal{A}\right)\exp\left[-\frac{\xi^2}{8}\frac{\beta}{m(1-\mathcal{A})}\left(1-\mathcal{A}+\frac{\alpha^2}{2}\mathcal{A}\right)^2\right]}{1-\operatorname{erf}\left[\frac{\xi}{4}\sqrt{\frac{2\beta}{m(1-\mathcal{A})}}\left(1-\mathcal{A}+\frac{\alpha^2}{2}\mathcal{A}\right)\right]}. \tag{4.14}$$

The susceptibility can also be calculated and it is given by

$$\chi = -\frac{4}{\pi\beta}\frac{\mathcal{B}^2\exp\left(-2\mathcal{B}^2\xi^2\right)}{1-\operatorname{erf}\left(\mathcal{B}\xi\right)}\left\{\frac{1}{1-\operatorname{erf}\left(\mathcal{B}\xi\right)} - \sqrt{\pi}\mathcal{B}\xi\exp\left(\mathcal{B}^2\xi^2\right)\right\}, \tag{4.15}$$

where we have used the shorthand notation

$$\mathcal{B} = \frac{1}{4}\sqrt{\frac{2\beta}{m\left(1-\mathcal{A}\right)}}\left(1-\mathcal{A}+\frac{\alpha^2}{2}\mathcal{A}\right). \tag{4.16}$$

Since expressions of energy, magnetization and susceptibility are quite lengthy, instead of providing their explicit forms, we show their behavior pictorially. Similarly, in this way, for entropy and heat capacity in the low energy regime, we shall follow the same procedure. Let us explore some interesting features from the magnetization and the susceptibility for a particular configuration of magnetic field and temperature. Initially, we consider the

configuration in which $\xi = 0$. With this, we obtain the following results:

$$\mathfrak{m}_{\xi=0} = \frac{d\alpha^2\mathcal{A}}{32m\,(1-\mathcal{A})} - \frac{1-\mathcal{A}+\frac{\alpha^2}{2}\mathcal{A}}{\sqrt{2\pi\beta m\,(1-\mathcal{A})}}, \tag{4.17}$$

$$\chi_{\xi=0} = -\frac{4\mathcal{B}^2}{\pi\beta}. \tag{4.18}$$

Now, for both $\xi = 0$ and $T = 0$, we get

$$\mathfrak{m}_{\xi=0,T=0} = \frac{d\alpha^2\mathcal{A}}{32m\,(1-\mathcal{A})}, \tag{4.19}$$

$$\chi_{\xi=0,T=0} = -\frac{1}{2\pi}\frac{1}{m\,(1-\mathcal{A})}\left(1-\mathcal{A}+\frac{\alpha^2}{2}\mathcal{A}\right)^2. \tag{4.20}$$

It is interesting to note that in the above restricted cases, the topology of the path appears only through α whereas both a, d appear to represent geometry of the path. Furthermore, the residual magnetization and susceptibility are mainly characterized by its geometrical and topological aspects. For instance, if the topological parameter α increases, then both $\mathfrak{m}_{\xi=0,T=0}$ and $\chi_{\xi=0,T=0}$ increase as well their magnitude. Therefore, the residual magnetic properties will depend on the complexities of the path that the electrons follow.

In Figs. 4.2, 4.3 and 4.4, we have used the values $p = 2$ and $q = 3$, so that the first coprimes yielding the simplest and widely studied $(2,3)$-knot or the trefoil knot. The plots below exhibit the behavior of the thermodynamic functions with respect to the temperature. Moreover, we also compare the behavior of those functions for different values of the parameter ξ, which controls the intensity of the external magnetic field. Since our system consists of electrons, we need to take its mass into account in our numerical calculations.

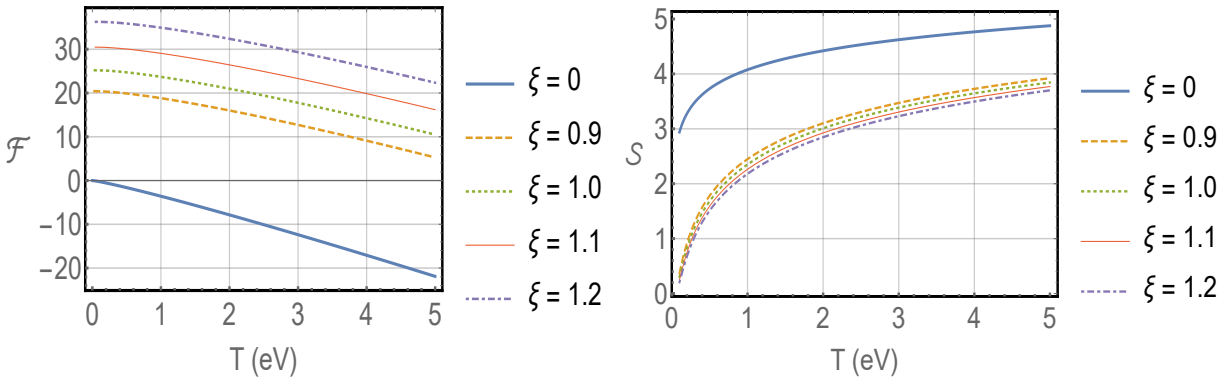

Fig. 4.2: Helmholtz free energy $(\mathcal{F})$ and entropy $(\mathcal{S})$ versus temperature (T)

In order to acquire a better understanding of the behavior of the thermodynamic functions for different combinations of toroidal and poloidal windings p and q, we display below the contour plot of such functions with respect to certain ranges of winding numbers, as

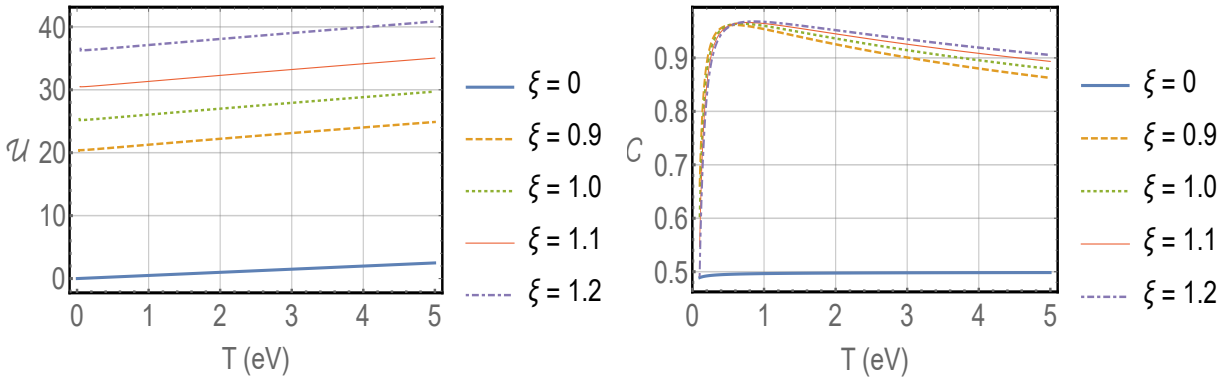

Fig. 4.3: Internal energy $(\mathcal{U})$ and Heat capacity $(\mathcal{C})$ versus temperature (T)

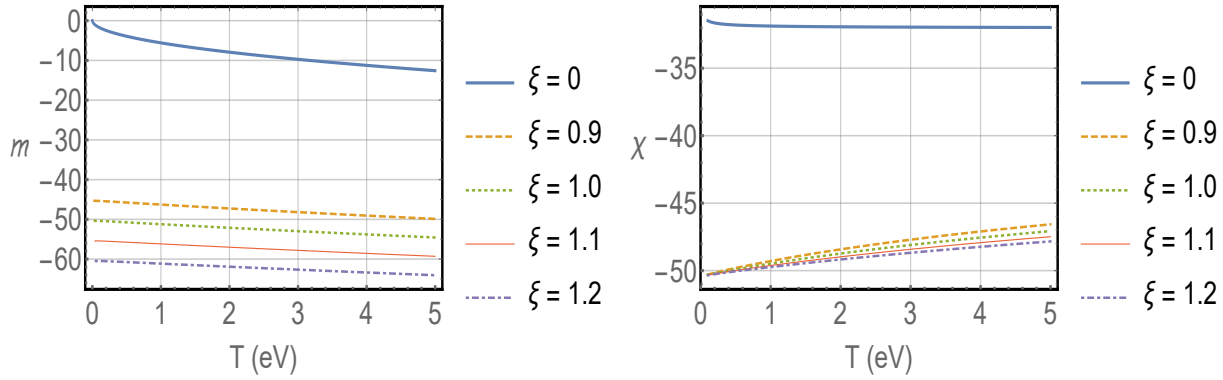

Fig. 4.4: Magnetization $(\mathcal{M})$ and Susceptibility $(\succ)$ versus temperature (T)

displayed in Figs. 4.5, 4.6, 4.7, 4.8, 4.9, and 4.10. Unlike the special cases of zero magnetic field and/or zero temperature, in general situations, the thermodynamic observables depend on both p, q individually (i.e. not only on α).

The plots mainly compare how those functions behave for a given temperature and magnetic field. Initially, in Fig. 4.5, we see the Helmholtz free energy for different fixed values of temperature and magnetic field – the variable combinations of winding numbers (p, q), including co-prime p, q, satisfy the knot condition. We see in all configurations that the larger the values of (p, q), the larger the Helmholtz energy becomes. In Fig. 4.6, we also investigate how entropy is modified for different configurations of temperature and magnetic field. It is shown the behavior of the entropy as a function of the winding numbers (p, q). In short, we verify that in all configurations when we increase values of (p, q), entropy increases. Next, in Fig. 4.7, we provide the contour plot for the mean energy regarding different configurations of temperature and magnetic field as well. We see that in all configurations when q is increased for fixed p, the mean energy decreases; on the other hand, when the values of p increase maintaining q fixed, the opposite behavior occurs. Fig. 4.8 displays contour plots to the heat capacity for different values of temperature and magnetic field. In these ones, we can naturally see the behavior of the heat capacity as a function of the

winding numbers (p, q). We see that in all configurations when we increase the values of q keeping p fixed, the heat capacity decreases its values; on the other hand, if we have the values of p increased maintaining q fixed, the opposite behavior also occurs. In Fig. 4.9, we also show the plots exhibiting how the magnetization is affected by different configurations of temperature and magnetic field. Here, we realize the behavior of the magnetization as a function of the winding numbers (p, q). Thereby, we see that in all configurations when we increase the values of (p, q), the larger the magnetization becomes. Finally, in Fig. 4.10, the plots exhibit how the the susceptibility is changed for different temperature and magnetic field. In this sense, we see the behavior of the susceptibility as a function of the winding numbers (p, q). Furthermore, we verify that in all configurations when we increase the values of (p, q), susceptibility becomes larger.

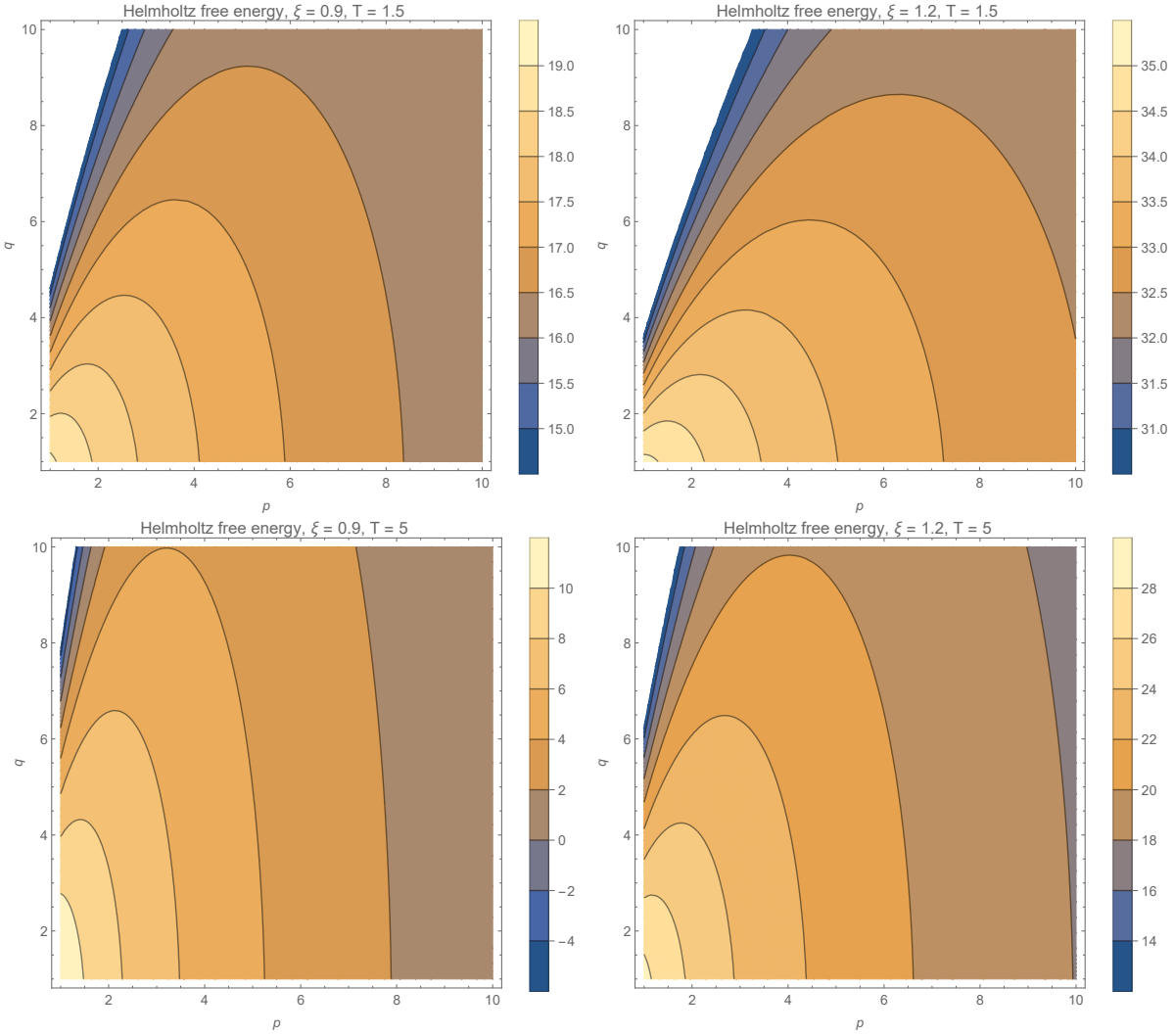

Fig. 4.5: These plots exhibit the Helmholtz free energy for different configurations of temperature and magnetic field. It also displays the behavior of Helmholtz energy as a function of the wind numbers (p, q). Note that Free energy increases when magnetic field increases and also when both p and q increases.

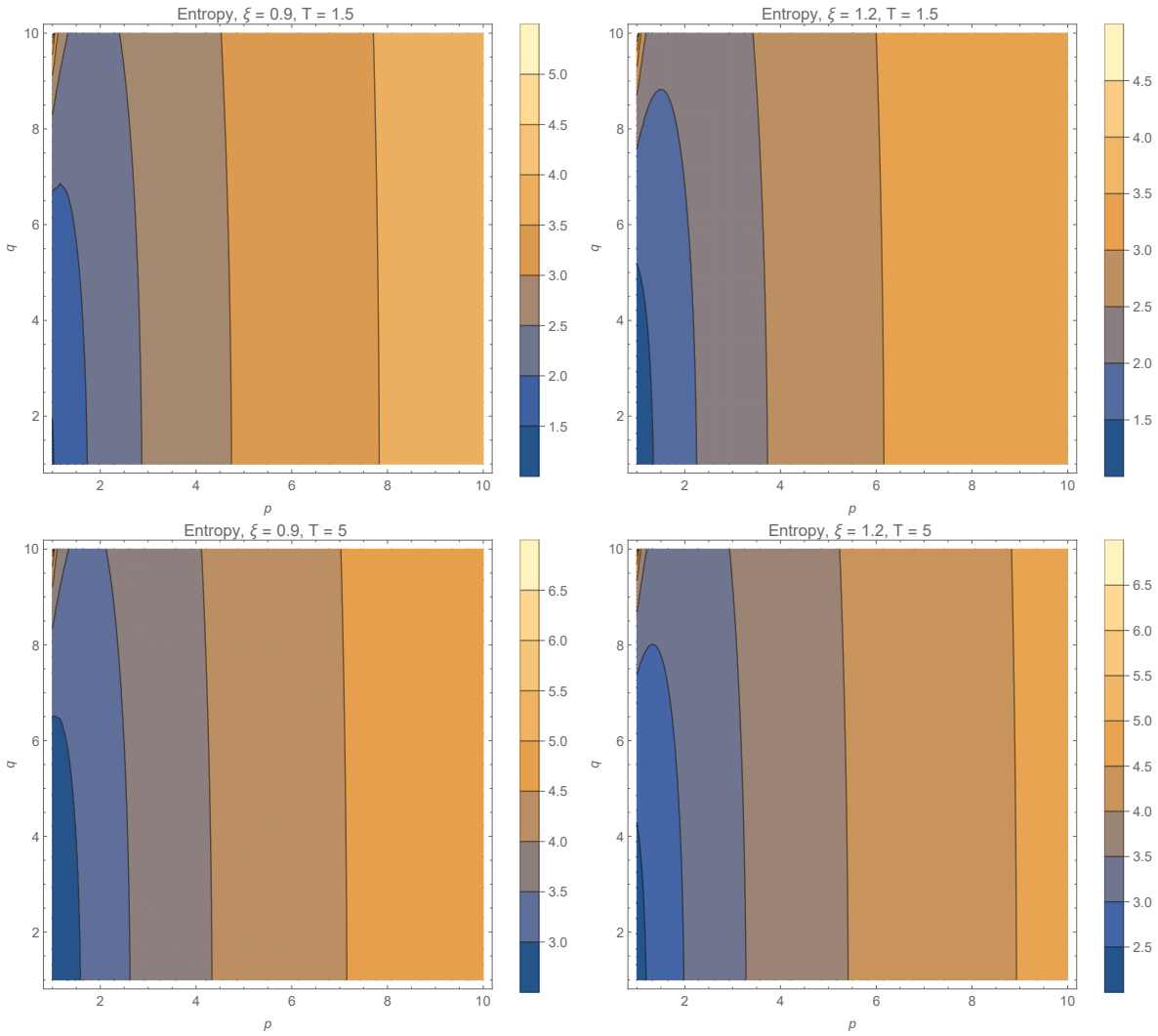

Fig. 4.6: These plots exhibit the entropy for different configurations of temperature and magnetic field. We also see its behavior as a function of the wind numbers (p, q). The behavior of the entropy is similar to the free energy, i.e. it increases with the parameters p and q.

4.1.1 Thin torus: the limit $a \to 0$

In this subsection, we focus on a particular case when the limit $a \to 0$ is taken into account. In other words, this means that we have a "circle" or a thin torus. Thereby, we get the following single particle partition function

$$\mathcal{Z}_1 = \sqrt{\frac{\pi m p^2 d^2}{2\beta}} \left\{ 1 + \text{erf}\left[-\frac{\xi}{4} \sqrt{\frac{2\beta}{m\,(1)}} \right] \right\}. \tag{4.21}$$

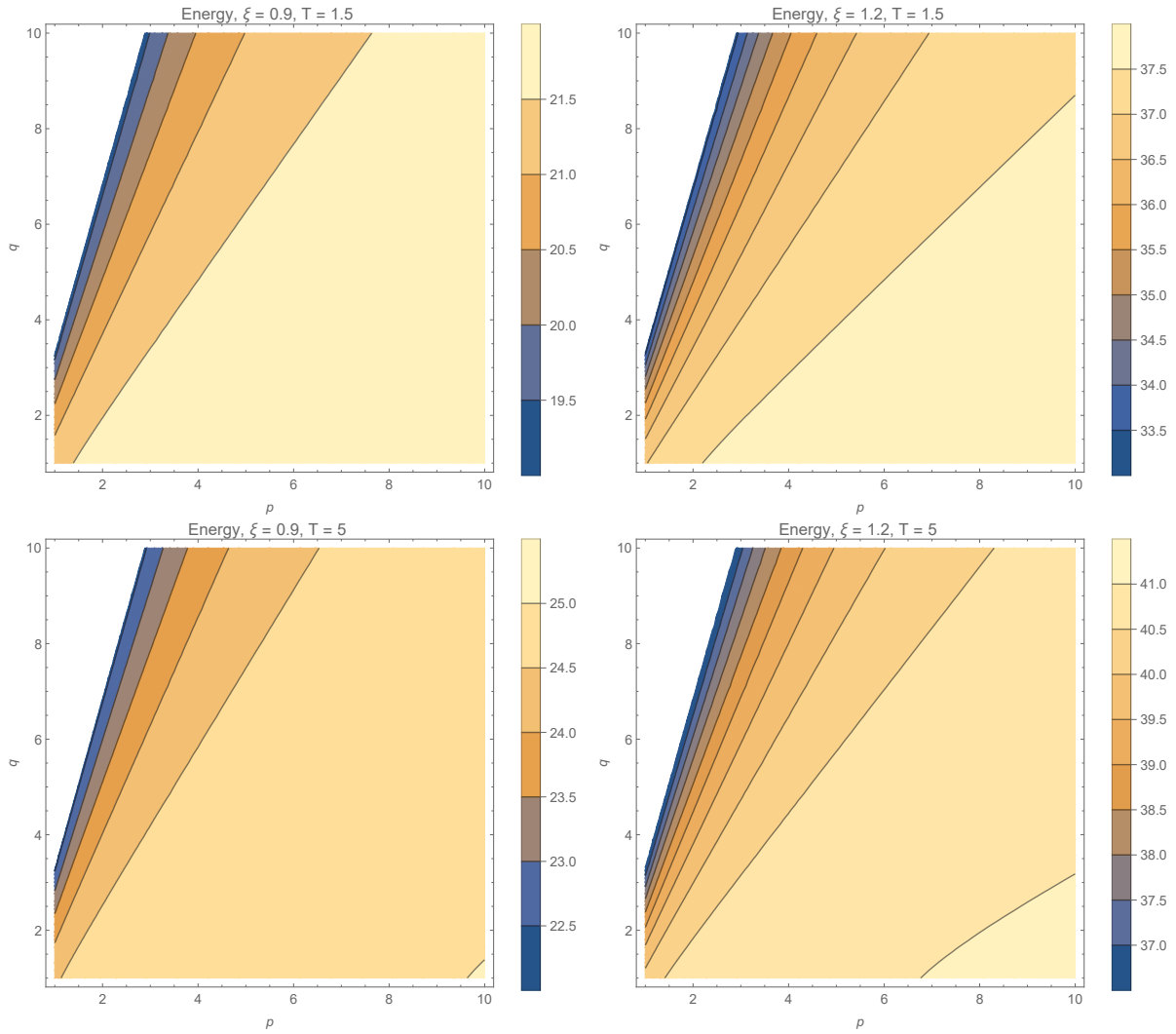

Fig. 4.7: These plots exhibit the contour plot for the mean energy for different configurations of temperature and magnetic field. In those plots we can see the behavior of the Energy as a function of the wind numbers (p, q).

Using the same methodology, we can also get from the above result the Helmholtz free energy

$$f = -\frac{1}{\beta}\ln\sqrt{\frac{\pi m p^2 d^2}{2\beta}} - \frac{1}{\beta}\ln\left\{1+\operatorname{erf}\left[-\frac{\xi}{4}\sqrt{\frac{2\beta}{m}}\right]\right\}, \tag{4.22}$$

and the internal energy per particle

$$\begin{aligned} u &= -\frac{1}{\beta^2}\left(\frac{1}{2}+\ln\sqrt{\frac{\pi m p^2 d^2}{2\beta}}\right) - \frac{1}{\beta^2}\ln\left\{1+\operatorname{erf}\left(-\frac{\xi}{4}\sqrt{\frac{2\beta}{m}}\right)\right\} \\ &\quad -\frac{\xi}{\beta^{\frac{3}{2}}}\sqrt{\frac{1}{8m\pi}}\frac{\exp\left(-\frac{\xi^2}{8}\frac{\beta}{m}\right)}{1-\operatorname{erf}\left(\frac{\xi}{4}\sqrt{\frac{2\beta}{m}}\right)}. \end{aligned} \tag{4.23}$$

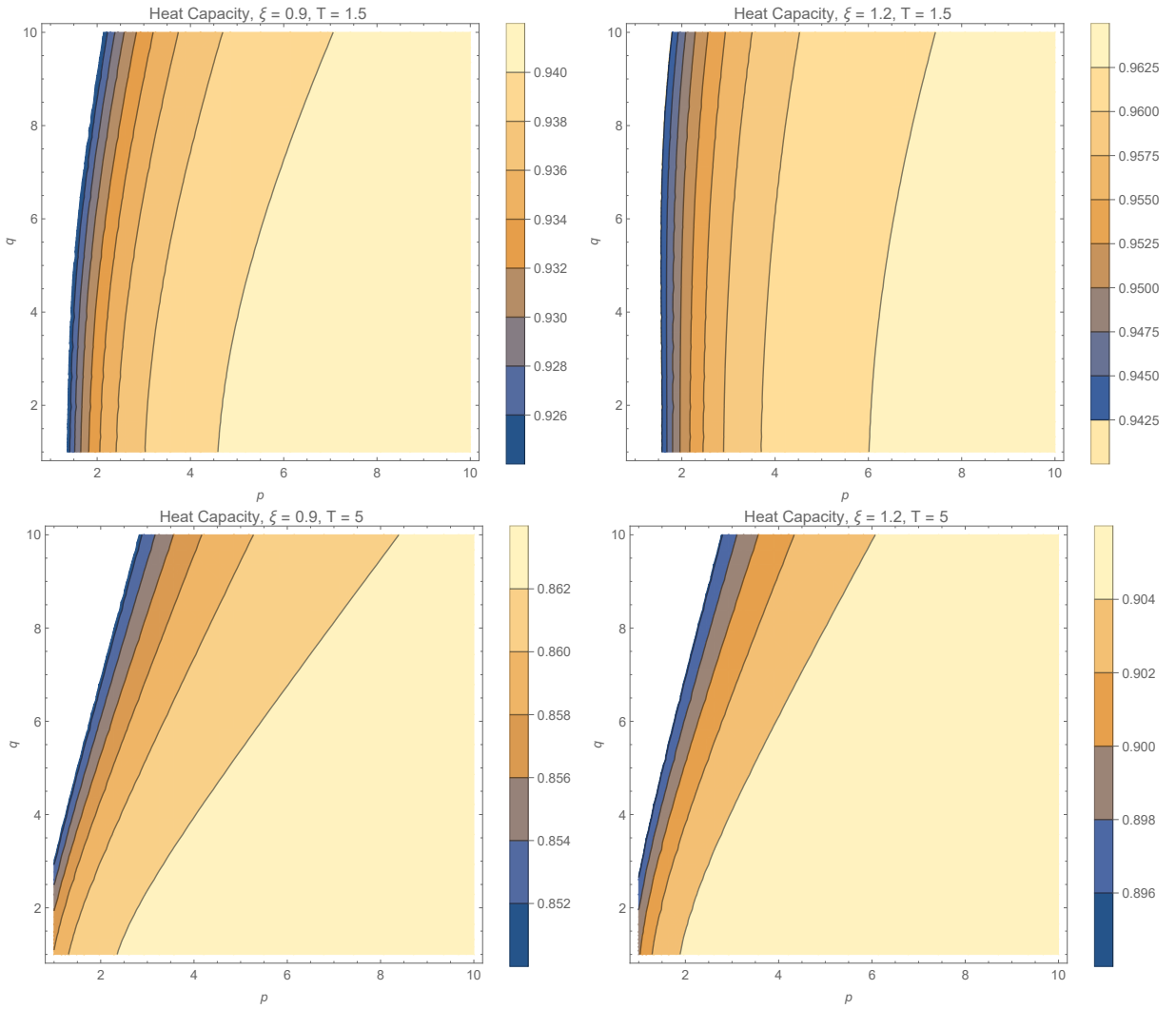

Fig. 4.8: The contour plots for the Heat Capacity for different configurations of temperature and magnetic field. In these ones, we can see the behavior of the Heat Capacity as a function of the wind numbers (p, q).

The magnetization and susceptibility, respectively, are displayed below:

$$\mathfrak{m} = -\sqrt{\frac{1}{2\pi\beta m}}\frac{\exp\left(-\frac{\xi^2}{8}\frac{\beta}{m}\right)}{1-\operatorname{erf}\left(\frac{\xi}{4}\sqrt{\frac{2\beta}{m}}\right)}, \tag{4.24}$$

$$\chi = -\frac{4}{\pi\beta}\frac{\mathcal{B}^2\exp\left(-2\mathcal{B}^2\xi^2\right)}{1-\operatorname{erf}\left(\mathcal{B}\xi\right)}\left\{\frac{1}{1-\operatorname{erf}\left(\mathcal{B}\xi\right)} - \sqrt{\pi}\mathcal{B}\xi\exp\left(\mathcal{B}^2\xi^2\right)\right\}, \tag{4.25}$$

where the parameter $\mathcal{B}$ assumes the form:

$$\mathcal{B} = \frac{1}{4}\sqrt{\frac{2\beta}{m}}. \tag{4.26}$$

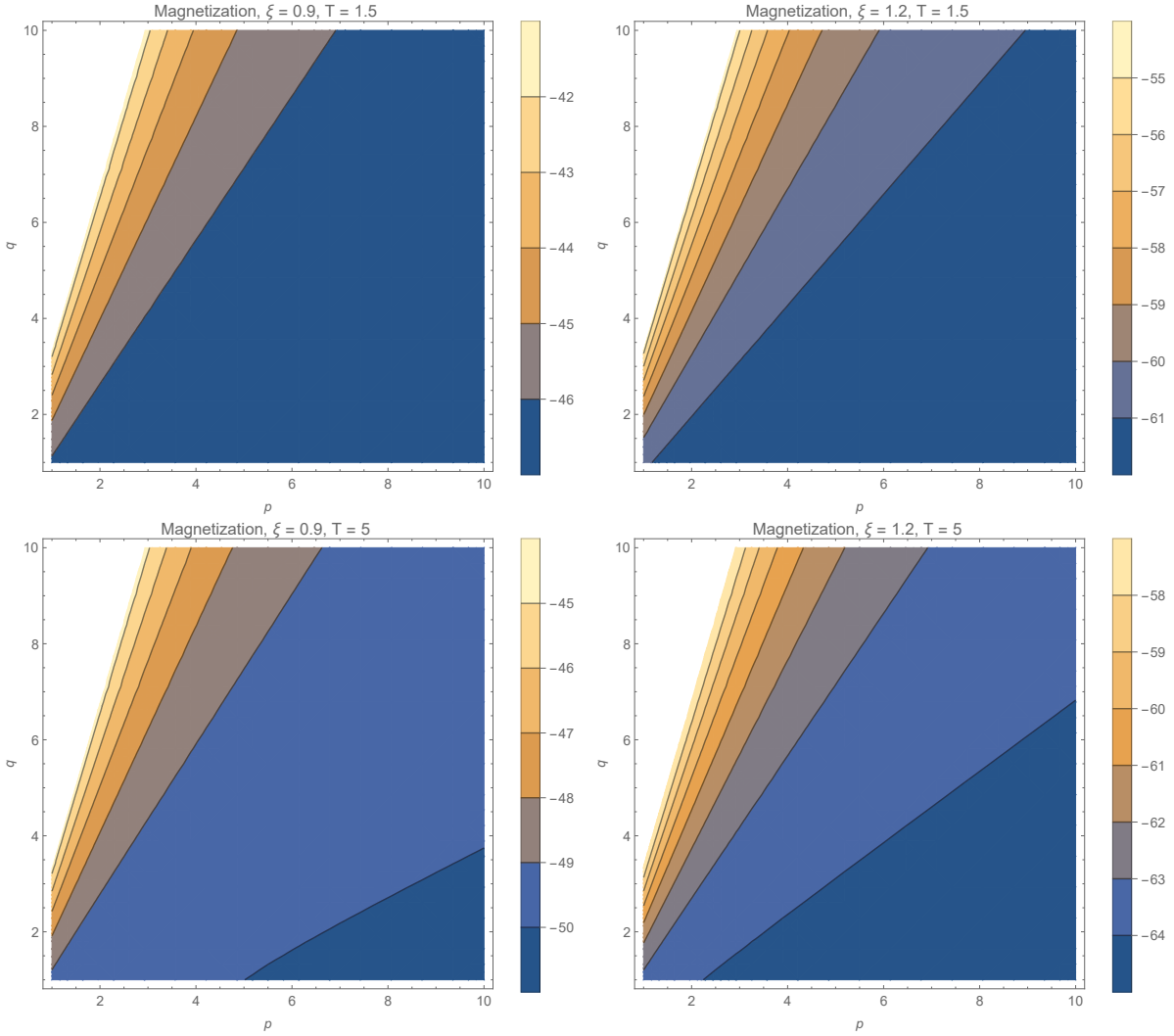

Fig. 4.9: These contour plots show the magnetization for different configurations of temperature and magnetic field. In these ones, we can see the behavior of the magnetization as a function of the wind numbers (p, q).

Let us now calculate the magnetization and the susceptibility for the same particular configuration of magnetic field and temperature as we did before. Initially, we consider a configuration in which $\xi = 0$. For this case, we obtain the following results:

$$\mathfrak{m}_{\xi=0} = -\frac{1}{\sqrt{2\pi\beta m}}, \quad \chi_{\xi=0} = -\frac{1}{2\pi m}. \tag{4.27}$$

Now, for both $\xi = 0$ and $T = 0$, we get

$$\mathfrak{m}_{\xi=0,T=0} = 0, \quad \chi_{\xi=0,T=0} = -\frac{1}{2\pi m}. \tag{4.28}$$

Here we notice that for $\xi = 0$ and $T = 0$, the magnetization turns out to be zero and

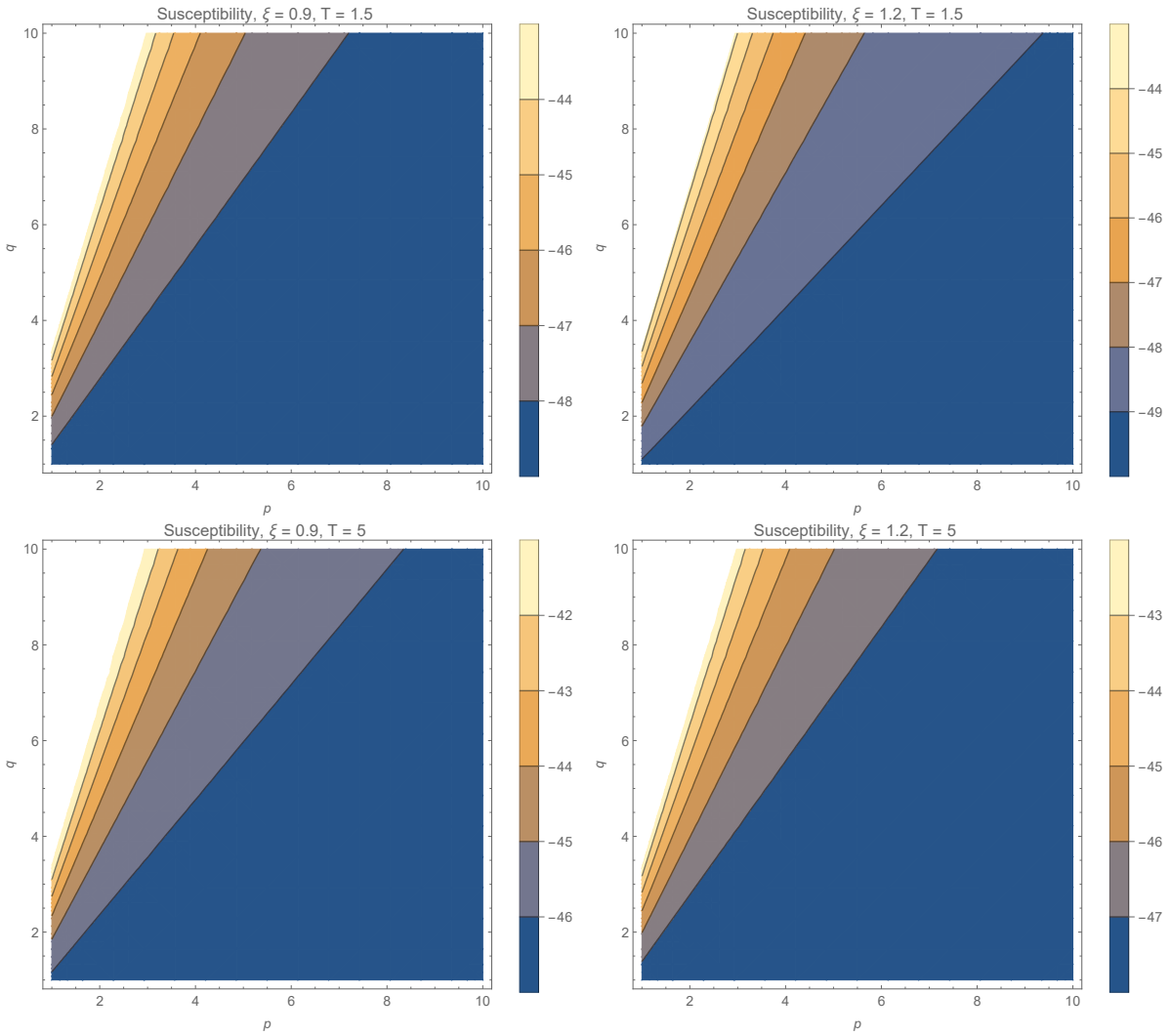

Fig. 4.10: The contour plots show how the susceptibility varies for different configurations of temperature and magnetic field. In these plots, we see the behavior of the Susceptibility as a function of the wind numbers (p, q).

we have a non-null constant susceptibility. On the other hand, considering the configuration where $\xi = 0$, both magnetization and susceptibility are non-zero. We have to pay attention in the fact that the magnetization (when $\xi = 0$) has the dependence on $T^{\frac{1}{2}}$. Another feature that is worth noticing is the fact that the mass ascribed to the fermions under consideration determines the magnitude of the susceptibility at zero magnetic field and also at zero temperature.

4.2 Fermions on a Torus Knot

We intend now to apply the grand canonical ensemble approach to understand the behavior of N noninteracting electrons moving in a prescribed torus knot on a single torus. Since

this formalism takes into account the Fermi-Dirac statistics, we can obtain more information on how the Pauli principle can modify the properties of the system.

The grand partition function for the present problem reads

$$\Xi = \sum_{N=0}^{\infty} \exp\left(\beta\mu N\right) \mathcal{Z}\left[N_\Omega\right], \tag{4.29}$$

where $\mathcal{Z}\left[N_\Omega\right]$ is the canonical partition function which is now a function of the occupation number N_Ω and Ω label a quantum state. Since we are dealing with fermions, we know that the occupation number allowed for each quantum state is restricted to $N_\Omega = \{0, 1\}$. So, for an arbitrary quantum state, the energy depends also on the occupation number as

$$E\left\{N_\Omega\right\} = \sum_{\{\Omega\}} N_\Omega E_\Omega$$

where we have the total fermion number N defined as

$$\sum_{\{\Omega\}} N_\Omega = N.$$

Thus the partition function becomes

$$\mathcal{Z}\left[N_\Omega\right] = \sum_{\{N_\Omega\}} \exp\left[-\beta \sum_{\{\Omega\}} N_\Omega E_\Omega\right]. \tag{4.30}$$

The grand partition function assumes the form

$$\Xi = \sum_{N=0}^{\infty} \exp\left(\beta\mu N\right) \sum_{\{N_\Omega\}} \exp\left[-\beta \sum_{\{\Omega\}} N_\Omega E_\Omega\right], \tag{4.31}$$

which can be rewritten as

$$\Xi = \prod_{\{\Omega\}} \left\{ \sum_{\{N_\Omega\}} \exp\left[-\beta N_\Omega \left(E_\Omega - \mu\right)\right] \right\}. \tag{4.32}$$

Performing the sum over the possible occupation numbers, we obtain

$$\Xi = \prod_{\{\Omega\}} \left\{1 + \exp\left[-\beta \left(E_\Omega - \mu\right)\right]\right\}, \tag{4.33}$$

The connection with thermodynamics is made using the grand potential given by

$$\Phi = -\frac{1}{\beta}\ln \Xi. \tag{4.34}$$

Replacing Ξ in the equation above, we get

$$\Phi = -\frac{1}{\beta}\sum_{\{\Omega\}} \ln\left\{1+\exp\left[-\beta\left(E_\Omega-\mu\right)\right]\right\}. \tag{4.35}$$

The entropy of the system can be cast in the following compact form, namely

$$S = -\frac{\partial\Phi}{\partial T} = -k_B\sum_{\{\Omega\}} \mathcal{N}_\Omega \ln\mathcal{N}_\Omega + \left(1-\mathcal{N}_\Omega\right)\ln\left(1-\mathcal{N}_\Omega\right)$$

where we explicitly use the Fermi-Dirac distribution function

$$\mathcal{N}_\Omega = \frac{1}{\exp\left[\beta\left(E_\Omega-\mu\right)\right]+1}.$$

We can also use the grand potential to calculate other important thermodynamics properties as mean particle number, energy, heat capacity and pressure using the following equation, respectively,

$$\mathcal{N} = -\frac{\partial\Phi}{\partial\mu}, \quad \mathcal{U} = -T^2\frac{\partial}{\partial T}\left(\frac{\Phi}{T}\right), \quad C_V = T\frac{\partial S}{\partial T}. \tag{4.36}$$

we can also calculate, as before, the magnetization and the susceptibility.

In order to calculate all thermodynamics quantities described above, we need to perform before the sum present in Eq. (4.35). Fortunately, it is possible to do it in a closed form using again the *Euler-MacLaurin* formula. Before performing the sum, we will rewrite the energy (4.8) in a more convenient form

$$E_n = \frac{1}{2m}\frac{\hbar^2\left(1-\mathcal{A}\right)}{p^2d^2}\left[n+\frac{\xi}{\hbar}\frac{pd^2}{\left(1-\mathcal{A}\right)}\left(1-\mathcal{A}+\frac{\alpha^2}{2}\mathcal{A}\right)\right]^2 - \frac{\xi^2\alpha^4\mathcal{A}^2d^2}{32m\left(1-\mathcal{A}\right)}. \tag{4.37}$$

Thereby, the grand partition function (4.35) can be rewritten as

$$\Phi = -\frac{2}{\beta}\int_0^\infty \mathrm{d}E\,\ln\left\{1+z\exp\left[-\beta E\left(n\right)\right]\right\}dn - \frac{1}{\beta}\ln\left\{1+ze^{-\beta\Upsilon}\right\}, \tag{4.38}$$

where

$$\Upsilon \equiv \frac{\xi^2}{2m}\frac{d^2}{\left(1-\mathcal{A}\right)}\left(1-\mathcal{A}+\frac{\alpha^2}{2}\mathcal{A}\right)^2 - \frac{\xi^2\alpha^4\mathcal{A}^2d^2}{32m\left(1-\mathcal{A}\right)}$$

Performing now the integration, we get

$$\Phi = \frac{\mathcal{L}}{\lambda} f_{\frac{3}{2}}(\Lambda, \mathfrak{X}) - f_1(\mathfrak{X}). \tag{4.39}$$

where $f_\sigma(\Lambda, \mathfrak{X})$

$$f_\sigma(\Lambda, \mathfrak{X}) = \frac{1}{\Gamma(\sigma)} \int_\Lambda^\infty \frac{t^{\sigma-1}}{\mathfrak{X}^{-1} e^t + 1} \mathrm{d}t, \tag{4.40}$$

is the incomplete Fermi-Dirac integral. We also define the quantities

$$\mathfrak{X} = z e^{\beta \Psi}, \tag{4.41}$$

$$\Psi = \frac{\xi^2 \alpha^4 \mathcal{A}^2 d^2}{32m(1-\mathcal{A})}, \tag{4.42}$$

$$\Lambda = \frac{\xi}{\hbar p} \frac{p^2 d^2}{(1-\mathcal{A})} \left(1 - \mathcal{A} + \frac{\alpha^2}{2}\mathcal{A}\right), \tag{4.43}$$

$$\mathcal{L} = \frac{p^2 d^2}{(1-\mathcal{A})}, \tag{4.44}$$

$$\lambda = \sqrt{\frac{2\pi\hbar^2}{m}} \beta. \tag{4.45}$$

For instance, the entropy is given by

$$S = \frac{\pi k_B \hbar^2}{m} \frac{\mathcal{L}}{\lambda^3} f_{\frac{3}{2}}(\Lambda, \mathfrak{X}) + k_B(\Psi + \mu) \frac{\mathcal{L}}{\lambda} f_{\frac{1}{2}}(\Lambda, \mathfrak{X}) - \frac{k_B(\Psi + \mu) z e^{-\beta \Upsilon}}{1 + z e^{-\beta \Upsilon}}. \tag{4.46}$$

In order to give an idea of the behavior of the thermodynamic functions, we display below, in Fig. 4.11, 4.12 and 4.13, some plots taking into account the same values as those presented in Sec. 4.1. Here, we see that for entropy, mean energy, heat capacity, and magnetization, when the temperature rises, the magnitude of their thermal properties increases; on the other hand, to the susceptibility the opposite behavior happened: when the temperature raised, the magnitude of such thermodynamic function decreased. On the other hand, when the magnetic field increases, the magnitude of entropy, mean energy and heat capacity decrease their values for a fixed temperature. However, the magnetization has an opposite behavior.

As an application, let us use the result obtained from the Eq. (4.39) to probe how interaction affects the Fermi energy. From Eq. (4.39) we get

$$N = g \left[\frac{\mathcal{L}}{\lambda} f_{\frac{1}{2}}(\Lambda, \mathfrak{X}) - \frac{\mathfrak{X}}{\mathfrak{X}+1}\right], \tag{4.47}$$

where g is a weight factor that arises from the internal structure of the particles. The Fermi

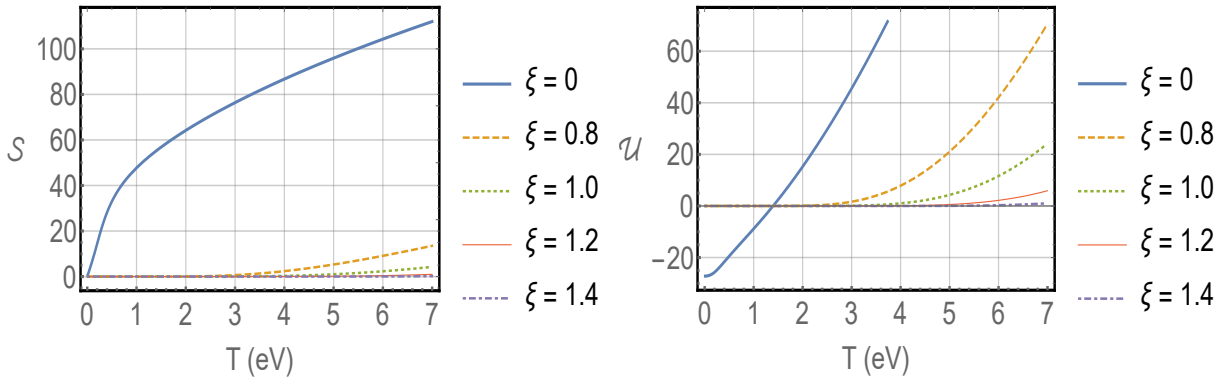

Fig. 4.11: Entropy and internal energy

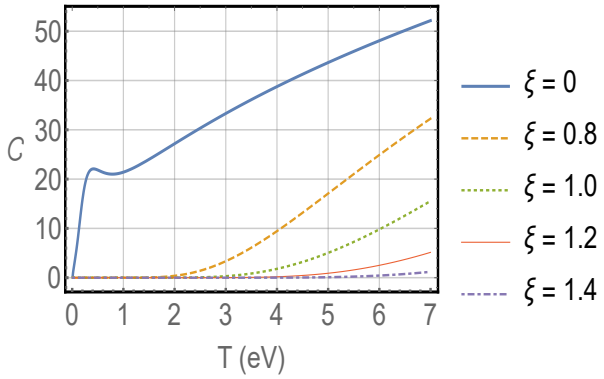

Fig. 4.12: Heat capacity

energy μ_0 is the energy of the topmost filled level in the ground state of the N electron system. In this way, we get

$$N = g\left\{\frac{4\mathcal{L}}{3}\left[\frac{m}{2\pi^2\hbar^2}\left(\Psi + \mu_0\right)\right]^{\frac{1}{2}} - 1\right\}. \tag{4.48}$$

Solving the above equation for μ_0, we get

$$\mu_0 = \frac{9\pi^2\hbar^2}{8m\mathcal{L}^2}\left(\frac{N}{g} + 1\right)^2 - \Psi. \tag{4.49}$$

It is interesting to notice that the Fermi energy μ_0 consists of two clearly divided parts. The first one contains the all information of a generic system; and all features of the specific torus (and torus-knot path) is encountered in the second part, Ψ. When we reduce the torus to a ring – when the limit $a \gg d$ is taken into account, we recover the well known result established in the literature [166, 167].

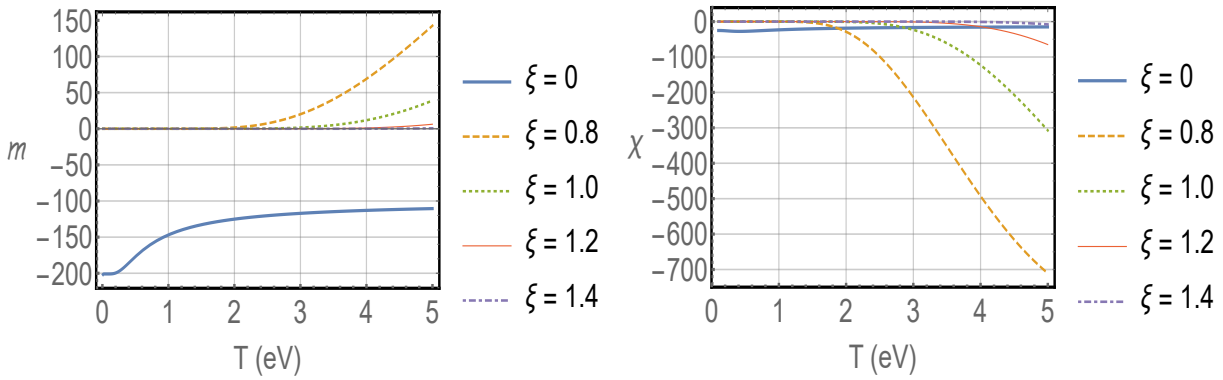

Fig. 4.13: Magnetization and Susceptibility

4.3 Interacting Fermions on a Torus Knot

Following the interacting approach developed in [54], we can derive the modified grand canonical potential taking into account the interaction between fermions, namely

$$\begin{aligned}\Phi &= -T\ln\mathcal{Z} \\ &= -T\sum_{\Omega}\ln\left(1+\exp\left[-\beta\left(E_{\Omega}+u'\left(\bar{n}\right)-\mu\right)\right]\right)+U\left(V,\bar{n}\right)-u'\left(\bar{n}\right)\bar{N}. \end{aligned} \quad (4.50)$$

The interaction is incorporated through $u'\left(\bar{n}\right)$ term. Based on this equation, the other thermodynamic functions can be calculated as well. Performing as before the *Euler-MacLaurin* formula we find

$$\Phi = \frac{\mathcal{L}}{\lambda}f_{\frac{3}{2}}\left(\Lambda,\mathfrak{Z}\right)-f_1\left(\mathfrak{Z}\right)+U\left(V,\bar{n}\right)-u'\left(\bar{n}\right)\bar{N}. \quad (4.51)$$

where we have now $\mathfrak{Z} = ze^{\beta\Psi}e^{-\beta u'(\bar{n})}$.

So, the correction for the Fermi energy in this context is given by:

$$\mu_0 = \frac{9\pi^2\hbar^2}{8m\mathcal{L}^2}\left(\frac{N}{g}+1\right)^2-\Psi+u'\left(\bar{n}\right). \quad (4.52)$$

In contrast to the result derived in Eq. (4.49), the interaction term appears as an additional term in the above equation. However, notice that such expression is a generic one. Although we got an analytical result, we cannot proceed further unless the structure of the interaction term is explicitly introduced.

5. THERMAL ASPECTS OF INTERACTING QUANTUM GASES IN LORENTZ-VIOLATING SCENARIOS

5.1 SME Fermion Sector

Initially, we introduce the Lagrange density for both minimal and nonminimal fermion sectors as being

$$\mathcal{L} = \frac{1}{2}\bar{\psi}\left(\gamma^{\mu}\mathrm{i}\partial_{\mu} - m_{\psi}\mathrm{I}_4 + \hat{\mathcal{Q}}\right)\psi + \mathrm{H.c.}, \tag{5.1}$$

where ψ is a Dirac spinor, $\bar{\psi} \equiv \psi^{\dagger}\gamma^0$ is the conjugate Dirac spinor and m_{ψ} is the fermion mass. Moreover, Lorentz-violating contributions are all contained in $\hat{\mathcal{Q}}$, which is a 4×4 matrix $\in SL(2,\mathbb{C})$ lying in spinor space $\mathbb{C}^2$. In nonminimal SME, $\hat{\mathcal{Q}}$ can be regarded as an expansion in either derivative ∂_{μ} or momenta $p_{\mu} = \mathrm{i}\partial_{\mu}$ operators. Besides, in the spinor space $\hat{\mathcal{Q}}$ can be decomposed into the 16 Dirac bilinear terms, namely

$$\hat{\mathcal{Q}} = \hat{\mathcal{S}}\mathrm{I}_4 + \hat{\mathcal{P}}\gamma^5 + \hat{\mathcal{V}}^{\mu}\gamma_{\mu} + \hat{\mathcal{A}}^{\mu}\gamma^5\gamma_{\mu} + \frac{1}{2}\hat{\mathcal{T}}^{\mu\nu}\sigma_{\mu\nu}\,, \tag{5.2}$$

where the scalar, pseudoscalar, vector, pseudovector and tensor operators are written in momentum space as follows

$$\hat{\mathcal{S}} = \sum_{d=3}^{\infty} \mathcal{S}^{(d)\alpha_1\alpha_2\ldots\alpha_{d-3}} p_{\alpha_1} p_{\alpha_2} \ldots p_{\alpha_{d-3}}, \tag{5.3a}$$

$$\hat{\mathcal{P}} = \sum_{d=3}^{\infty} \mathcal{P}^{(d)\alpha_1\alpha_2\ldots\alpha_{d-3}} p_{\alpha_1} p_{\alpha_2} \ldots p_{\alpha_{d-3}}, \tag{5.3b}$$

$$\hat{\mathcal{V}}^{\mu} = \sum_{d=3}^{\infty} \mathcal{V}^{(d)\mu\alpha_1\alpha_2\ldots\alpha_{d-3}} p_{\alpha_1} p_{\alpha_2} \ldots p_{\alpha_{d-3}}, \tag{5.3c}$$

$$\hat{\mathcal{A}}^{\mu} = \sum_{d=3}^{\infty} \mathcal{A}^{(d)\mu\alpha_1\alpha_2\ldots\alpha_{d-3}} p_{\alpha_1} p_{\alpha_2} \ldots p_{\alpha_{d-3}}, \tag{5.3d}$$

$$\hat{\mathcal{T}}^{\mu\nu} = \sum_{d=3}^{\infty} \mathcal{T}^{(d)\mu\nu\alpha_1\alpha_2\ldots\alpha_{d-3}} p_{\alpha_1} p_{\alpha_2} \ldots p_{\alpha_{d-3}}, \tag{5.3e}$$

These decompositions were first proposed in Ref. [263]. Here, we also point out that, having mass dimension $4-d$, the controlling coefficients $\mathcal{S}^{(d)\alpha_1\ldots\alpha_{d-3}}$, ..., $\mathcal{T}^{(d)\mu\nu\alpha_1\ldots\alpha_{d-3}}$ are spacetime independent in order to maintain the conservation of energy and momentum.

It is possible to obtain the dispersion relations directly from the determinant of the Dirac operator. According to [263], the first-order dispersion relation (for particle modes) related to the modified Dirac equation coming from Lagrangian (5.1) is

$$E \approx E_0 - \frac{m_\psi \hat{\mathcal{S}} + p \cdot \hat{\mathcal{V}}}{E_0} \pm \frac{\mathcal{Y}}{E_0}, \tag{5.4}$$

where $E_0 = \pm\sqrt{m_\psi^2 + \boldsymbol{p}^2}$ and $\mathcal{Y}$ is given by the following expression

$$\mathcal{Y}^2 = \left(p \cdot \hat{\mathcal{A}}\right)^2 - m_\psi^2 \hat{\mathcal{A}}^2 - 2m_\psi p \cdot \tilde{\hat{\mathcal{T}}} \cdot \hat{\mathcal{A}} + p \cdot \tilde{\hat{\mathcal{T}}} \cdot \tilde{\hat{\mathcal{T}}} \cdot p. \tag{5.5}$$

Here, we see that there exist two possible configurations for energy E_0. It suffices to describe both particles and antiparticles modes depending on the sign, i.e., positive for particles and negative for antiparticles respectively. Also, we observe that terms $\hat{\mathcal{S}}$, $\hat{\mathcal{V}}$ and $\mathcal{Y}$ displayed above depend on the 4-momentum, that at the leading order in Lorentz violation may be considered as $p^\mu \approx (E_0, -\mathbf{p})$ on the right hand side in Eq. (5.4). Thereby, in the existence of Lorentz violation, it is verified that such expression can have four non-degenerate solutions for each $\mathbf{p}$.

Additionally, an important remark which is worth taking into account is the case when the spin degeneracy of a Dirac fermion is broken. Thereby, being in contrast with the aspects encountered in scalar and vector cases, pseudovector and tensor operators no longer maintain the spin degeneracy as a consequence of nonzero $\mathcal{Y}$ term. Moreover, it is worth pointing out

that such degeneracy between either particles or antiparticles is no longer preserved when any of these Lorentz-violating operators have nonzero CPT-odd components. Besides, on the other hand, the pseudoscalar operator plays no role at the relevant order dispersion relation.

From Eq. (5.4), we can represent several deviations from the traditional Lorentz covariant approach concerning massive fermions. Many of them lie in anisotropy, dispersion, and birefringence cases, being analogous to those effects that arouse in the nonminimal photon sector of the SME [473, 474, 475, 476]. Next, we explore the consequences of scalar field in the context of Lorentz violation.

5.2 Lorentz-Violating Scalar Fields

Recently, in the literature it was proposed conjectures about Riemann-Finsler geometries ascribed to Lorentz-violating field theories [477]. In this sense, knowing how this novelty can be associated with the study of thermodynamic properties of interacting quantum gases is a remarkable question to be investigated. Looking toward to accomplish this, we initially introduce the respective model. Analogously to what was done in Ref. [477], we regard a complex scalar field $\phi(x^\mu)$ of mass m for $n = 4$. The effective quadratic Lagrangian for the scalar field is given by

$$\mathcal{L} = \partial^\mu \phi^\dagger \partial_\mu \phi - m\phi^\dagger \phi - \frac{1}{2}\left(i\phi^\dagger \left(\hat{k}_a\right)^\mu \partial_\mu \phi + \text{h.c.}\right) + \partial_\mu \phi^\dagger \left(\hat{k}_c\right)^{\mu\nu} \partial_\nu \phi, \tag{5.6}$$

where $\left(\hat{k}_a\right)^\mu$ and $\left(\hat{k}_c\right)^{\mu\nu}$ are operators constructed as series of even powers of the partial spacetime derivatives ∂_μ. In this way, since Lorentz violation is presumed to contain its effects around the Planck scale, both $\left(\hat{k}_a\right)^\mu$ and $\left(\hat{k}_c\right)^{\mu\nu}$ may be assumed to bring out only perturbations for ordinary physics. Again, we assume that these operators are independent quantities of spacetime position seeking to maintain the translational invariance, which accounts for the conservation of energy and momentum. The operators have the following structure in momentum space

$$\left(\hat{k}_a\right)^\kappa = \sum_{d\geq 3} (k_a)^{(d)\kappa\alpha_1\ldots\alpha_{(d-4)}}\, p_{\alpha_1}\ldots p_{\alpha_{(d-3)}}, \tag{5.7}$$

$$\left(\hat{k}_c\right)^{\kappa\xi} = \sum_{d\geq 4} (k_c)^{(d)\kappa\xi\alpha_1\ldots\alpha_{(d-4)}}\, p_{\alpha_1}\ldots p_{\alpha_{(d-4)}}. \tag{5.8}$$

Moreover, the respective dispersion relation for the theory encountered in Eq. (5.6) is given by

$$p^2 - m^2 - \left(\hat{k}_a\right)^\kappa p_k + \left(\hat{k}_c\right)^{\kappa\xi} p_\kappa p_\xi = 0, \tag{5.9}$$

whose first order dispersion relation is written as

$$E \approx E_0 + \frac{1}{2}\frac{\left(\hat{k}_a\right)^{\mu} p_{\mu}}{E_0} - \frac{\left(\hat{k}_c\right)^{\mu\nu} p_{\mu} p_{\nu}}{E_0}. \tag{5.10}$$

With all these features, it is verified that the boson sector has noteworthy properties and applications. Moreover, in Refs. [478, 479], the authors studied the scalar field in different scenarios as well. In Ref. [477], the authors proposed the correspondence between Riemann-Finsler geometries and effective field theories when spin-independent Lorentz violation is taken into account. Nevertheless, it is encountered a gap the literature looking toward to investigate the respective thermodynamic quantities for such case. In this way, we primarily present a model to derive the thermal quantities of interest, i.e., particle number, entropy, mean energy and pressure. For obtaining them, we utilize the so-called grand canonical partition function as well as the grand canonical potential. With these, the following procedure can be fully carried out.

5.3 Thermodynamic model

At the beginning, let us start our discussion considering a general quantum state φ of a free quantum gas, which is entirely determined when one specifies the occupation numbers, i.e, $\{n_1, n_2, ..., n_r, ...\}$, regarding a discrete quantum state r with energy ϵ_r. In this sense, the sum in φ must be carried out over all quantum states taking into account the restriction

$$\sum_r n_r = N, \tag{5.11}$$

where N is the particle number. Here, since there exist modifications in the relativistic particle dispersion relations due to Lorentz-violating terms, we can use the advantage of separating the energy of the quantum state φ as follows

$$E_{\varphi}^{free} = \sum_r n_r \epsilon_r + \sum_r n_r \delta_r, \tag{5.12}$$

where $\epsilon_r = \sqrt{\boldsymbol{p}_r^2 + m^2}$ is the usual relativistic energy and δ_r refers to Lorentz-violating contribution term that may assume a specific form depending on the case under consideration. Besides, it is worth pointing out that parameter δ_r is in general a function of the 3-momentum $\boldsymbol{p}_r$ that modifies the relativistic kinetic term only[1]. These and other features will be treated in what follows. Now, we derive the so-called grand canonical partition

[1]Here, we can still use the background coming from the standard Statistical Mechanics.

function, which is given by

$$\mathcal{Z}(T,V,z) = \sum_{N=0}^{\infty} z^N Z(T,V,N), \tag{5.13}$$

where $z = \exp(\beta\mu)$ is the fugacity of the system and the usual canonical partition function is written as

$$Z(T,V,N) = \sum_{\varphi} \exp\left(-\beta E_{\varphi}\right). \tag{5.14}$$

Here, using the general energy E_{φ}^{free}, we get the following grand canonical partition function

$$\mathcal{Z}(T,V,\mu) = \sum_{\{n_1,n_2,\ldots\}=0}^{\{\infty/1\}} \exp\left\{-\beta\left[\sum_r n_r\left(\epsilon_r + \delta_r - \mu\right) + U(V,n)\right]\right\}, \tag{5.15}$$

and

$$z^N = \exp\{N\beta\mu\} = \exp\left\{\beta\sum_r n_r\mu\right\}, \tag{5.16}$$

where we have considered $U(V,n)$ as being the interaction energy that depends only on the particle density n and the volume V. As we shall argue below, such type of interaction can be obtained through the well-know mean field approximation which can give us the advantage of obtaining analytical results. Moreover, these ones will allow us to identify how such type of interaction modifies the thermodynamic properties of the system. It is worth to mention that the interaction term is a monotonically increasing function of the density particle. In other words, if we increase the density n, the particles come closer to each other and the interactions between them are expected to increase. More so, the opposite behavior happens otherwise: when n decreases, $U(V,n)$ must decrease.

It is important to notice that the upper summation index in Eq. (5.15), namely $\{\infty/1\}$, indicates that despite having infinitely many bosons in the quantum state r, rather for the fermion case, only one fermion is allowed due to the Pauli exclusion principle. As an example, we regard the upper index "∞" for bosons and "1" for fermions. With this notation, we are able to treat both of them simultaneously without losing generality. Moreover, it is also convenient to assume that the total interaction energy can be written as $U(V,n) = Vu(n)$, where $n = N/V$ is the particle density. Such density-dependent interaction has applications in nuclear [480] and elementary particle physics [481, 482, 483]. Assuming this decomposition, we have

$$\mathcal{Z}(T,V,\mu) = \sum_{\{n_1,n_2,\ldots\}=0}^{\{\infty/1\}} \exp\left\{-\beta\left[\sum_r n_r\left(\epsilon_r + \delta_r - \mu\right) + Vu(n)\right]\right\}, \tag{5.17}$$

and, for further evaluation of the above expression, it is necessary that the exponential function be decomposed into factors of the form $\exp\{-\beta n_r(\ldots)\}$. It is noteworthy to mention that this assumption can be ensured if and only if the term $Vu(n)$ is linear in $\sum_r n_r = N$. However, for most cases this is not a straightforward procedure; $Vu(n)$ is a difficult function of N that has to be determined afterwards when the interaction is particularized. In this way, there is a traditional form in the literature to linearize $Vu(n)$ as a function of N, which is via Taylor series. We expand $u(n)$ around the mean value of the particle number density $\bar{n}$, that is

$$u(n) = u(\bar{n}) + u'(\bar{n})(n-\bar{n}) + \ldots. \tag{5.18}$$

Here, we choose only these two terms, since the other ones may be overlooked due to the fact that fluctuations $(n-\bar{n})$, close to the mean value of the particle number density, turn out to be tiny when one regards the thermodynamic limit (see Appendix 5.9 for further details).

Indeed, having splitted $U(V,n)$ into different terms, namely $U(V,\bar{n}) = Vu(\bar{n})$ and $Vu'(\bar{n})\bar{n} = u'(\bar{n})\bar{N}$ as well as into $Vu'(\bar{n})n = u'(\bar{n})N$, we are properly able to write down the total energy of the quantum state φ as follows

$$E_\varphi = \sum_r n_r\epsilon_r + \sum_r n_r\delta_r + \sum_r n_r u'(\bar{n}) + U(V,\bar{n}) - u'(\bar{n})\bar{N}, \tag{5.19}$$

where, up to these two latter terms, the energy of a particle in the quantum state r would be simply $\epsilon_r + \delta_r + u'(\bar{n})$. Certainly, it is worth mentioning that the mean energy $u'(\bar{n})$ of the respective ensemble of particles arouses from the fact that there exists interaction among them. Furthermore, we could suppose that such potential energy would come from a specified mean field[2] at the position of the particle, and consequently Eq. (5.18) would precisely address the widespread *molecular field approximation* which is massively used in condensed matter physics [454, 455, 456, 457, 458, 459]. Now, Eq. (5.17) can be rewritten in a straightforward manner as follows

$$\begin{aligned}\mathcal{Z}(T,V,\mu) &= \exp\left\{-\beta\left[U(V,\bar{n}) - u'(\bar{n})\bar{N}\right]\right\} \\ &\quad\times\prod_{r=1}^{\infty}\left(\sum_{n_r=0}^{\{\infty/1\}}\exp\left\{-\beta\left[\epsilon_r+\delta_r+u'(\bar{n})-\mu\right]n_r\right\}\right).\end{aligned} \tag{5.20}$$

Here, one may notice that in the latter line of the above expression there exists a sum

[2]Here, we are mentioning that the mean field approximation it is just one way to get such potential. However, our results are quite general and they are not restricted to the assumption of the validity of the *molecular field approximation*. Moreover, it is worth pointing out that such an approach is widely used to obtain many interactions in condensed-matter physics. Nevertheless, it is not the unique way to do so. Also, from the point of view of numerical results, the mean field approximation turns out to be convenient since we can find a lot of interesting results in the literature using the same procedure, as already mentioned in the manuscript.

in brackets which turns out to have merely two available values, namely $n_r = 0, 1$, if one considers either fermions or simply a geometric series when bosons are taken into account. In this way, we obtain

$$\begin{aligned}\mathcal{Z}(T,V,\mu) &= \exp\left\{-\beta\left[U(V,\bar{n}) - u'(\bar{n})\,\bar{N}\right]\right\} \\ &\quad \times \prod_{r=1}^{\infty} \begin{cases} 1+\exp\left[-\beta\left(\epsilon_r+\delta_r+u'(\bar{n})-\mu\right)\right], & \text{Fermions} \\ \left(1-\exp\left[-\beta\left(\epsilon_r+\delta_r+u'(\bar{n})-\mu\right)\right]\right)^{-1}, & \text{Bosons} \end{cases}, \end{aligned} \tag{5.21}$$

and, seeking for a generalized notation which can fit both of them, we provide the notation $\chi = +1$ for fermions and $\chi = -1$ for bosons respectively. Thus, we can rewrite such expression in a suitable way

$$\begin{aligned}\mathcal{Z}(T,V,\mu) &= \exp\left\{-\beta\left[U(V,\bar{n}) - u'(\bar{n})\,\bar{N}\right]\right\} \\ &\quad \times \prod_{r=1}^{\infty}\left(1+\chi\exp\left[-\beta\left(\epsilon_r+\delta_r+u'(\bar{n})-\mu\right)\right]\right)^{\chi}, \end{aligned} \tag{5.22}$$

which yields the so-called grand canonical potential

$$\begin{aligned}\Phi &= -T\ln\mathcal{Z} \\ &= -T\chi\sum_r \ln\left(1+\chi\exp\left[-\beta\left(\epsilon_r+\delta_r+u'(\bar{n})-\mu\right)\right]\right) + U(V,\bar{n}) - u'(\bar{n})\,\bar{N}, \end{aligned} \tag{5.23}$$

As we shall see, the grand canonical potential Φ will play a crucial role in deriving the following thermodynamic functions. Next, from these preliminaries, we will develop the thermal quantities, i.e., mean particle number, entropy, mean total energy as well as pressure, highlighting the contribution of parameters that account for Lorentz violation. In addition, it is important to notice that the derivation of such quantities is fully carried out in an analytical manner.

5.4 Thermodynamic state quantities

Certainly, whenever one considers the study of thermodynamic properties of a given system, one seeks the derivation of the main thermal parameters as a traditional procedure. Thereby, we devote our analysis to provide the development of mean particle number, entropy, mean total energy and finally pressure. As a matter of fact, the terms that account for the violation of Lorentz symmetry will be inferred for different cases. Moreover, if one takes the limit when such terms vanish, one will recover the usual case being in agreement with the literature [484, 485, 486] so that it corroborates our results. Now, we start off with

the mean particle number given by

$$\begin{aligned}\bar{N} &= -\left.\frac{\partial\Phi}{\partial\mu}\right|_{T,V}, \\ &= -V\left.\frac{\partial u\left(\bar{n}\right)}{\partial\mu}\right|_{T,V}+\bar{N}\left.\frac{\partial u'\left(\bar{n}\right)}{\partial\mu}\right|_{T,V}+u'\left(\bar{n}\right)\left.\frac{\partial\bar{N}}{\partial\mu}\right|_{T,V}+ \\ &\quad +T\chi\sum_{r}\frac{\chi\exp\left[-\beta\left(\epsilon_r+\delta_r+u'\left(\bar{n}\right)-\mu\right)\right]}{1+\chi\exp\left[-\beta\left(\epsilon_r+\delta_r+u'\left(\bar{n}\right)-\mu\right)\right]}\beta\left(1-\left.\frac{\partial u'\left(\bar{n}\right)}{\partial\mu}\right|_{T,V}\right), \quad (5.24)\end{aligned}$$

and, from it, we obtain

$$\begin{aligned}\bar{N}\left(1-\left.\frac{\partial u\left(\bar{n}\right)}{\partial\mu}\right|_{T,V}\right) &= -V\left.\frac{\partial u\left(\bar{n}\right)}{\partial\mu}\right|_{T,V}+u'\left(\bar{n}\right)\left.\frac{\partial\bar{N}}{\partial\mu}\right|_{T,V} \\ &\quad +\chi^2\beta T\left(1-\left.\frac{\partial u'\left(\bar{n}\right)}{\partial\mu}\right|_{T,V}\right) \\ &\quad \times\sum_{r}\frac{1}{\exp\left[\beta\left(\epsilon_r+\delta_r+u'\left(\bar{n}\right)-\mu\right)\right]+\chi}. \quad (5.25)\end{aligned}$$

Here, since u depends only on the particle number density, we obtain directly $du=\frac{du}{dn}dn$. In this sense,

$$\left.\frac{\partial u\left(\bar{n}\right)}{\partial\mu}\right|_{T,V}=u'\left(\bar{n}\right)\left.\frac{\partial\bar{n}}{\partial\mu}\right|_{T,V}=\frac{u'\left(\bar{n}\right)}{V}\left.\frac{\partial\bar{N}}{\partial\mu}\right|_{T,V}, \quad (5.26)$$

and it is worth pointing out that the first two terms in Eq. (5.25) cancel out each other. Regarding natural units, i.e., $\chi^2=\beta T=1$, then

$$\bar{N}=\sum_{r}\frac{1}{\exp\left[\beta\left(\epsilon_r+\delta_r+u'\left(\bar{n}\right)-\mu\right)\right]+\chi}. \quad (5.27)$$

We obtain such expression due to the fact that the brackets do not vanish in Eq. (5.25), since $u\left(n\right)$ can be an arbitrary function. Besides, the mean occupation number can be immediately written as

$$\bar{n}_r=\frac{1}{\exp\left[\beta\left(\epsilon_r+\delta_r+u'\left(\bar{n}\right)-\mu\right)\right]+\chi}. \quad (5.28)$$

Here, when compared to the usual case, Lorentz-violating parameters only modify the single-particle energy. Additionally, another further analysis can be done in such direction. Since Lorentz violation will be treated perturbatively, we can expand $\bar{n}_r$ at first order in δ_r, namely

$$\bar{n}_r\approx\frac{1}{\exp\left[\beta\left(\epsilon_r+u'\left(\bar{n}\right)-\mu\right)\right]+\chi}-\delta_r\frac{\beta\exp\left[-\beta\left(\epsilon_r+u'\left(\bar{n}\right)-\mu\right)\right]}{\left(\exp\left[\beta\left(\epsilon_r+u'\left(\bar{n}\right)-\mu\right)\right]+\chi\right)^2}, \quad (5.29)$$

and, seeking a shorter expression, we define the following useful quantity

$$\bar{\mathcal{N}}_r \equiv \frac{1}{\exp\left[\beta\left(\epsilon_r + u'\left(\bar{n}\right) - \mu\right)\right] + \chi}.$$

As a result, the mean occupation number can be written as

$$\bar{n}_r \approx \bar{\mathcal{N}}_r - \delta_r \beta \bar{\mathcal{N}}_r^2 \exp\left[-\beta\left(\epsilon_r + u'\left(\bar{n}\right) - \mu\right)\right]. \tag{5.30}$$

yielding therefore the mean particle number

$$\bar{N} \approx \sum_r \bar{\mathcal{N}}_r - \sum_r \delta_r \bar{\mathcal{N}}_r^2 \beta \exp\left[-\beta\left(\epsilon_r + u'\left(\bar{n}\right) - \mu\right)\right], \tag{5.31}$$

where the second term represents the deviation from the standard result highlighting the contribution due to the Lorentz violation. We can also notice that the interaction modifies the mean particle number since the term $u'\left(\bar{n}\right)$ is present in Eq. (5.28). This modification is directly related to the fact that we chose a interaction energy that is a function of the particle density.

Furthermore, looking toward to bring out the development to the calculation of the entropy, we proceed as follows

$$\begin{aligned} S &= -\left.\frac{\partial \Phi}{\partial T}\right|_{\mu,V} \\ &= -V\left.\frac{\partial u\left(\bar{n}\right)}{\partial T}\right|_{\mu,V} + \bar{N}\left.\frac{\partial u'\left(\bar{n}\right)}{\partial T}\right|_{\mu,V} + u'\left(\bar{n}\right)\left.\frac{\partial \bar{N}}{\partial T}\right|_{\mu,V} \\ &\quad +\chi\sum_r \ln\left(1+\chi\exp\left[-\beta\left(\epsilon_r+\delta_r+u'\left(\bar{n}\right)-\mu\right)\right]\right) \\ &\quad +\chi^2 T\sum_r \frac{\left(\epsilon_r+\delta_r+u'\left(\bar{n}\right)-\mu\right)\left(-\frac{d\beta}{dT}\right) - \beta\left.\frac{\partial u'(\bar{n})}{\partial T}\right|_{\mu,V}}{\exp\left[\beta\left(\epsilon_r+\delta_r+u'\left(\bar{n}\right)-\mu\right)\right]+\chi}, \end{aligned} \tag{5.32}$$

and, in agreement with what happened to Eq. (5.26), we also realize that the first and third terms cancel out each other. Now, regarding Eq. (5.27) in the numerator of the last sum, it follows that the second term cancels out the last term in the sum. Here, using the fact that $-\frac{d\beta}{dT} = \frac{1}{T^2}$, the result can be written as

$$\begin{aligned} S &= \chi\sum_r \ln\left(1+\chi\exp\left[-\beta\left(\epsilon_r+\delta_r+u'\left(\bar{n}\right)-\mu\right)\right]\right) \\ &\quad +\frac{1}{T}\sum_r \bar{n}_r\left(\epsilon_r+\delta_r+u'\left(\bar{n}\right)-\mu\right). \end{aligned} \tag{5.33}$$

Expanding the above expression up to the first order in δ_r, we yield

$$\begin{aligned} S &\approx \chi\sum_r \ln\left(1+\chi\exp\left[-\beta\left(\epsilon_r+u'\left(\bar{n}\right)-\mu\right)\right]\right)+\frac{1}{T}\sum_r\left(\epsilon_r+u'\left(\bar{n}\right)-\mu\right)\bar{\mathcal{N}}_r \\ &\quad -\sum_r\delta_r\beta\bar{\mathcal{N}}_r+\frac{1}{T}\sum_r\delta_r\bar{\mathcal{N}}_r\left\{1-\left(\epsilon_r+u'\left(\bar{n}\right)-\mu\right)\beta\exp\left[\beta\left(\epsilon_r+u'\left(\bar{n}\right)-\mu\right)\right]\bar{\mathcal{N}}_r\right\}, \end{aligned} \tag{5.34}$$

and, in particular, the last two terms represent the deviation from the standard result, exhibiting clearly the contribution of Lorentz-violating parameters. Following these approaches, we derive the mean total energy

$$\begin{aligned} \bar{E} &= \left.\frac{\partial\left(\beta\Phi\right)}{\partial\beta}\right|_{z,V}, \\ &= \left.\frac{\partial}{\partial\beta}\left[\beta V u\left(\bar{n}\right)-\beta\bar{N}u'\left(\bar{n}\right)\right]\right|_{z,V} \\ &\quad -\chi\sum_r\frac{\chi z\exp\left[-\beta\left(\epsilon_r+\delta_r+u'\left(\bar{n}\right)\right)\right]}{1+\chi z\exp\left[-\beta\left(\epsilon_r+\delta_r+u'\left(\bar{n}\right)\right)\right]}\left(-\epsilon_r-\delta_r-\left.\frac{\partial}{\partial\beta}\left[\beta u'\left(\bar{n}\right)\right]\right|_{z,V}\right), \\ &= U\left(V,\bar{n}\right)+\beta V\left.\frac{\partial u\left(\bar{n}\right)}{\partial\beta}\right|_{z,V}-\bar{N}\left.\frac{\partial\left[\beta u'\left(\bar{n}\right)\right]}{\partial\beta}\right|_{z,V}-\beta u'\left(\bar{n}\right)\left.\frac{\partial\bar{N}}{\partial\beta}\right|_{z,V} \\ &\quad +\sum_r\frac{\epsilon_r+\delta_r}{z^{-1}\exp\left[\beta\left(\epsilon_r+\delta_r+u'\left(\bar{n}\right)\right)\right]+\chi}+\bar{N}\left.\frac{\partial\left[\beta u'\left(\bar{n}\right)\right]}{\partial\beta}\right|_{z,V}. \end{aligned} \tag{5.35}$$

It is important to mention that because of

$$\left.\frac{\partial u\left(\bar{n}\right)}{\partial\beta}\right|_{z,V}=u'\left(\bar{n}\right)\left.\frac{\partial\bar{n}}{\partial\beta}\right|_{z,V}=\frac{u'\left(\bar{n}\right)}{V}\left.\frac{\partial\bar{N}}{\partial\beta}\right|_{z,V}, \tag{5.36}$$

the second term cancels out the fourth in Eq. (5.35) and, therefore we get

$$\bar{E}=\sum_r\bar{n}_r\left(\epsilon_r+\delta_r\right)+U\left(V,\bar{n}\right). \tag{5.37}$$

As expected, the energy is the average of the kinetic term plus the interactions energy. As an analogous procedure, we accomplish the expansion of the mean energy at first order in δ_r. This yields

$$\bar{E}\approx\sum_r\bar{\mathcal{N}}_r\epsilon_r+U\left(V,\bar{n}\right)+\sum_r\delta_r\bar{\mathcal{N}}_r\left\{1-\epsilon_r\beta\exp\left[\beta\left(\epsilon_r+u'\left(\bar{n}\right)-\mu\right)\right]\bar{\mathcal{N}}_r\right\}, \tag{5.38}$$

with the identification that the third term is the Lorentz-violating contribution that differs, thus, from the usual result. Finally, after all these features, we also provide the derivation

of pressure as follows

$$\begin{aligned}\mathcal{P} &= -\left.\frac{\partial\Phi}{\partial V}\right|_{\mu,T} \\ &= -u\left(\bar{n}\right)+u'\left(\bar{n}\right)\left.\frac{\partial\bar{N}}{\partial V}\right|_{\mu,T}+\frac{\chi T}{V}\sum_{r}\ln\left(1+\chi\exp\left[-\beta\left(\epsilon_r+\delta_r+u'\left(\bar{n}\right)-\mu\right)\right]\right) \\ &= -\frac{\Phi}{V'},\end{aligned} \tag{5.39}$$

where we have used Eq. (5.27), and the essential consideration that the respective particle number density is independent of the volume; as a result, $u\left(\bar{n}\right)$ and $u'\left(\bar{n}\right)$ do not depend on the volume as well, as shown in Appendix 5.9. From the Eq. (5.39), we can also realize how interaction plays an important role on the pressure. The first term in Eq. (5.39), - $u\left(\bar{n}\right)$, for instance, is responsible for reduce the pressure of the system, while the second one, $u'\left(\bar{n}\right)$, plays the rule of increasing it. Now, as we did before, let us expand the pressure at first order in δ_r. In doing so, we get

$$\mathcal{P}\approx-\frac{\Phi_{\text{Standard}}}{V}-\frac{T}{V}\sum_{r}\delta_r\beta\bar{\mathcal{N}}_r, \tag{5.40}$$

where conveniently we define

$$\Phi_{\text{Standard}}=-\chi T\sum_{r}\ln\left(1+\chi\exp\left[-\beta\left(\epsilon_r+u'\left(\bar{n}\right)-\mu\right)\right]\right). \tag{5.41}$$

Moreover, it is worth to point out that in Refs. [273, 272, 487], in the context of Lorentz violation, the authors also accomplished a similar analysis to the one encountered in this chapter. However, they brought out rather the advantage of using the accessible states of the system in order to derive the respective thermodynamic functions for higher-derivative electrodynamics. Besides, considering other viewpoints, the thermal quantities were calculated as well taking into account the canonical ensemble from its respective partition function [488, 489, 490, 491]. In the next sections, we will provide an analysis concerning different Lorentz-violating operators in order to verify their contributions when interacting quantum gases are regarded. Particularly, we examine both fermion and boson sectors respectively. For the first sector, we contemplate scalar, vector, pseudovector and tensor operators. On the other hand, for the latter one, we explore both $\left(\hat{k}_a\right)^{\kappa}$ and $\left(\hat{k}_c\right)^{\kappa\xi}$ operators to complete our discussion. We also point out that such analysis will bring out the behavior of the thermodynamic functions that we have calculated so far. Furthermore, as we could verify, the mathematical structure of those functions are quite complicated to explain in a phenomenological manner. Nevertheless, we overtake this situation performing a numerical analysis where we display the plots for the thermodynamic functions under consideration.

5.5 Interacting fermions

In this section, we devoted our attention to study fermions concerning the minimal sector of the Standard Model Extension. In doing so, we seek this analysis for knowing how such coupling terms affect the interaction energy when a quantum gas is taken into account. In order to carry out such investigation, we assume scalar, vector, pseudovector and tensor operators respectively. Moreover, we summarize them in Table 5.1 for the sake of bringing about a better comprehension to the reader. Now, we are on the verge of showing some interesting dispersion relations that can be used from the background established in the previous sections. Thereby, the general dispersion relation has the following structure for both fermions and bosons

$$E \approx E_0 + \frac{\delta_r}{E_0}. \tag{5.42}$$

Particularly, the subsequent specifications of δ_r are displayed in Table 5.1. In the last column on the right hand, we have used the definition $\bar{p}_\alpha \equiv (E_0, -\boldsymbol{p})$ so that it allows to obtain the first order dispersion relation in a covariant way.

Operator	δ_r	Definition
Scalar	$-m_\psi \hat{\mathcal{S}}$	$\hat{\mathcal{S}} = \mathcal{S}^{(d)\alpha_1\ldots\alpha_{(d-3)}}\bar{p}_{\alpha_1}\ldots\bar{p}_{\alpha_{(d-3)}}$
Vector	$-\bar{p}\cdot\hat{\mathcal{V}}$	$\hat{\mathcal{V}}^\kappa = \mathcal{V}^{(d)\kappa\alpha_1\ldots\alpha_{(d-3)}}\bar{p}_{\alpha_1}\ldots\bar{p}_{\alpha_{(d-3)}}$
Pseudovector	$\pm\sqrt{\left(\bar{p}\cdot\hat{\mathcal{A}}\right)^2 - m_\psi^2\hat{\mathcal{A}}^2}$	$\hat{\mathcal{A}}^\kappa = \mathcal{A}^{(d)\kappa\alpha_1\ldots\alpha_{(d-3)}}\bar{p}_{\alpha_1}\ldots\bar{p}_{\alpha_{(d-3)}}$
Tensor	$\pm\sqrt{p\cdot\tilde{\hat{\mathcal{T}}}\cdot\tilde{\hat{\mathcal{T}}}\cdot p.}$	$\hat{\mathcal{T}}^{\kappa\xi} = \mathcal{T}^{(d)\kappa\xi\alpha_1\ldots\alpha_{(d-3)}}\bar{p}_{\alpha_1}\ldots\bar{p}_{\alpha_{(d-3)}}$

Tab. 5.1: This table summarizes four particular cases of δ_r, namely, scalar, vector, pseudovector and tensor operators for the fermion sector. Their respective definitions are shown as well.

In order to carry out the study of the main thermal properties discussed in section 5.4, we need to perform the thermodynamic limit of Eqs. (5.31), (5.38) and (5.34) as developed in detail in appendix 5.9. Since such limits give rise to complicated integrals in momentum space, we provide numerical calculations for some particular backgrounds. Furthermore, with the purpose of offering a better arrangement to this chapter, we display all numerical outputs in Appendix 5.10.

Now, we start with a simple configuration for the scalar operator, namely $\mathcal{S}^{(4)0}p_0 = \mathcal{S}^{(4)0}E_0$. This configuration belongs to the minimal SME and yields the following dispersion relation

$$E \approx E_0 - m_\psi \mathcal{S}^{(4)0}.$$

Now, with the dispersion relation above, we can replace the results encountered in the Eqs.

(5.31), (5.38) as well as (5.34), and perform integrations over the momenta. In Table 5.3, we exhibit numerical evaluations for different values of β.

The second case taken into account has a vector operator whose non null controlling coefficient is $\mathcal{V}^{(4)33}$. With it, we can obtain the following dispersion relation, namely

$$E \approx E_0 - \frac{\mathcal{V}^{(4)33} p_3 p_3}{E_0}. \tag{5.43}$$

Now, we need to perform numerical integrations in order to find out the contribution to vector operator. The respective results are displayed in Table 5.4.

Another interesting case is the one related to pseudovector operators. We choose $\mathcal{A}^{(3)0}$ as the only non null controlling coefficient, which yields the following dispersion relation

$$E \approx E_0 \pm \frac{\sqrt{\left(E_0 \mathcal{A}^{(3)0}\right)^2 - m_\psi^2 \left(\mathcal{A}^{(3)0}\right)^2}}{E_0}. \tag{5.44}$$

Here, we notice that we have two different values to be considered. By inserting this result in the expression involving mean particle number, energy and entropy, we get the results shown in Table 5.5.

On the other hand, we will treat the tensor operator whose non null controlling coefficient chosen is $\tilde{\tilde{\mathcal{T}}}^{(4)010}$. This configuration gives rise to the dispersion relation given below

$$E \approx E_0 \pm E_0 \tilde{\tilde{\mathcal{T}}}^{(4)010} \tag{5.45}$$

Likewise, we need to perform numerical integrations for the sake of obtaining the information about the quantities of interest. Table 5.6 shows how the thermodynamic quantities change with β.

Although the previous Tables are quite useful to afford quantitatively our results, they do not give us a reasonable visualization of what happens. In this sense, seeking to overtake this situation, we display the plots for the mean particle number for all dispersion relations treated in this section. In Fig. 5.1, it is interesting to notice that we have two different solutions whenever we contemplate pseudovector and tensor operators. This occurs because these operators break the spin degeneracy. In other words, it turns out that spin-up $(+)$ particles propagate differently if compared with spin-down $(-)$ ones. This feature leads to a remarkable consequence: the mean particle number of a full interacting quantum gas of spin-down particles becomes greater in comparison with spin-up ones when we consider high temperature regime, as shown in Fig. 5.1(c) and 5.1(d) . In addition, the other equation of state will exhibit the same property.

Another important feature to mention is that independently of the configuration that we have chosen for the spin-degenerate case, the global behavior remains the same as we can

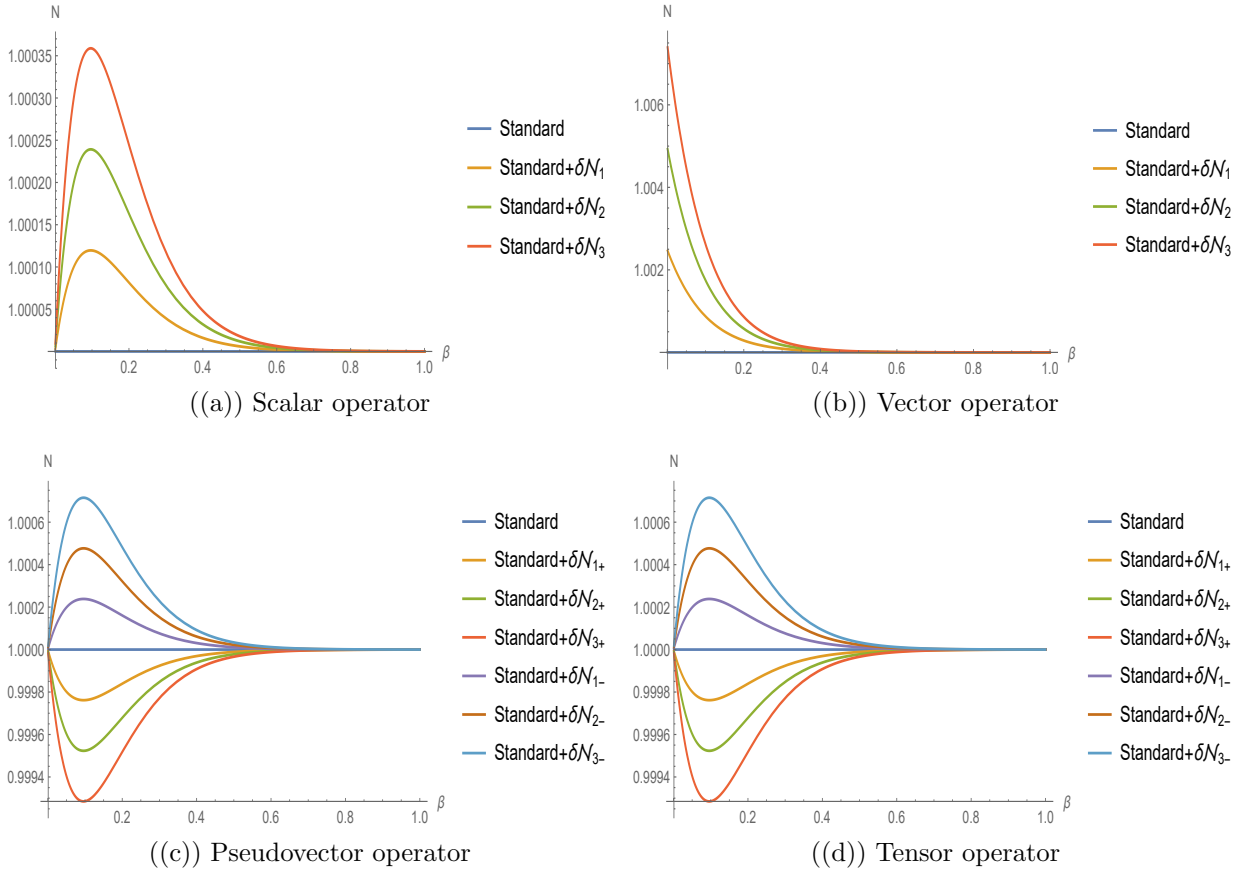

((a)) Scalar operator ((b)) Vector operator

((c)) Pseudovector operator ((d)) Tensor operator

Fig. 5.1: This figure shows a comparison between mean particle number for different background configurations. These plots are normalized by the standard result, which means that the value 1 is the behavior regardless Lorentz violation. In order to clarify the notation, we should notice that $\delta\mathcal{N}_i$ means the deviation from the standard result using the values 10^{-3}, 10^{-5} and 10^{-7} for the controlling coefficient respectively.

check in Fig. 5.2. Analogously, the same behavior is shown for the spin-nondegenerate case exhibited in Fig. 5.3.

5.6 Interacting bosons

Now, we perform a similar analysis that was done for fermions. In Table 5.2, we summarize some definitions used from now on. The first case considered is related to a vector coupling, whose non-null controlling coefficient is $\left(\hat{k}_a\right)^0$. The dispersion relation associated with it is given below

$$E \approx E_0 + \frac{1}{2}\left(\hat{k}_a\right)^0. \tag{5.46}$$

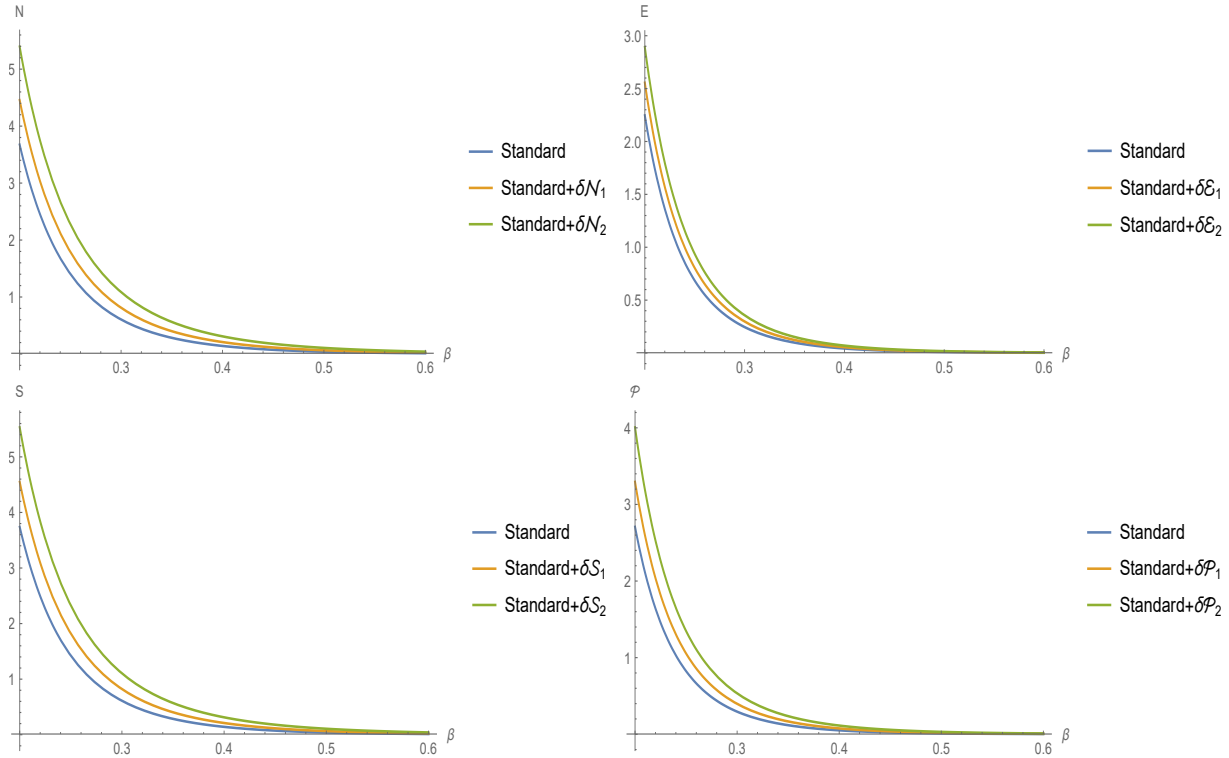

Fig. 5.2: This figure shows the general behavior of spin-degenerate case for fermions, where the same notation as in Fig. 5.1 is used. As one can see, the deviation from the standard results become relevant for high energy regime, which means small β. Here, it is worth to remember that temperature is given in eV.

Operator	δ_r	Definition
Vector	$\frac{1}{2}\left(\hat{k}_a\right)^{\mu}\bar{p}_\mu$	$\left(\hat{k}_a\right)^{\kappa} = (k_a)^{(d)\kappa\alpha_1\ldots\alpha_{(d-4)}}\,\bar{p}_{\alpha_1}\ldots\bar{p}_{\alpha_{(d-3)}}$
Tensor	$-\left(\hat{k}_c\right)^{\mu\nu}\bar{p}_\mu\bar{p}_\nu$	$\left(\hat{k}_c\right)^{\kappa\xi} = (k_c)^{(d)\kappa\xi\alpha_1\ldots\alpha_{(d-4)}}\,\bar{p}_{\alpha_1}\ldots\bar{p}_{\alpha_{(d-4)}}$

Tab. 5.2: This table summarizes two particular cases of δ_r, i.e., vector and tensor operators for the boson sector. The respective definitions are exhibited as well.

Here, we can perform a numerical study for such configuration. In this sense, we proceed analogously to what was accomplished in Sec. 5.5. In doing so, we obtain the results displayed in Table 5.7.

Furthermore, the second case is the modification due to a symmetric tensor operator. We choose the non-null controlling coefficient $\left(\hat{k}_c\right)^{00}$, which gives rise to the following dispersion relation shown below

$$E \approx E_0 - \left(\hat{k}_c\right)^{00} E_0. \tag{5.47}$$

With it, we can perform again a numerical analysis that produces the respective values displayed in Table 5.8. Besides, we also show in Fig. 5.4 the behavior of the particle number

for both cases considered above.

5.7 Results and discussions

We focused on displaying the main aspects encountered in the study of relativistic interacting quantum gases for both fermion and boson sectors when Lorentz violation was taken into account. We provided some discussions based on the graphics exhibited throughout this manuscript. In a complementary way, some tables were shown as well in order to offer the reader a better comprehension of our results in Appendix 5.10. Here, we pointed out some noteworthy remarks as proceeded.

Initially, we verified that only at high temperature regime, when Lorentz violation was considered, there existed a change in the results in comparison with the standard ones. Besides, if we had considered an opposite regime, the same behavior presented in the usual case would be expected (without considering Lorentz violation). Furthermore, interesting phenomena occurred when we took into account the analysis of the particle number as we could see in Fig. 5.1. We realized that for the spin-degenerate operators the mean particle number aroused when the temperature increased. The same occurred when Lorentz-violating coefficients increased. Now, with the nondegenerate spin operators for a fermion gas, we obtained an intriguing result. For spin-down particles, the mean particle number raised when the temperature reached high values. However, if instead the spin-up particles were regarded, the mean particle number would reach values below to the usual one at the same temperature regime. Also, in this context of nondegenerate spin operators, we acquired another remarkable feature. As a result, the spin-up modes had lower energy values in contrast with those presented in spin-down cases, as seen in Fig. 5.3. It is also worth to mention that these differences do not imply a disbalance between spin-up and spin-down particles; it means that if we have a gas with spin-down particles, we will find a different result encountered in spin-up ones. On the other hand, if we have a gas made of a mixture of both, the effects turn out to be suppressed; this is because, in average, we have the same amount of spin-up and spin-down modes.

In general, the behavior of all quantities converged to the standard values when low temperature regime was regarded. Nevertheless, they differed from each other in the case of high temperature scenario. Here, it is important to mention that these behaviors were expected, since the Lorentz-violating coefficients are suppressed in low temperature cases. In a complementary manner, the tables were displayed exhibiting the first order corrections, which aroused from the deviations of the standard result. As a matter of fact, if we took the non-relativistic and the non-interacting limits of our calculations, we would recover the well-established results in the literature [283].

Moreover, concerning boson modes, we saw that the mean particle number for the vector case decreased, whereas increased for the tensor case at high temperatures. This could be checked by examining the plot displayed in Fig. 5.4. A similar analysis was also accomplished in Tables 5.7 and 5.7 to energy, entropy and pressure. Definitely, for our case, we noticed that the dispersion relation emerged from a genuine scalar theory. On the contrary, in Ref. [283], a spin-0 boson gas was described by combining two fermions into a singlet representation of the spin group.

Furthermore, we analyzed the fermion case in the minimal SME regarding a system having instead scalar, vector, pseudovector and tensor operators. Thereby, we observed that the pseudoscalar operator played no role in the leading-order dispersion relation. From the discussion above, it emerges a straightforward question: in which manner the parameters of nonminimal SME could modify those respective thermal properties? We do not provide the answer to this question because such investigation lies beyond the scope of the current chapter. Nonetheless, we shall address it in an upcoming manuscript.

Here, since we were dealing with Lorentz and CPT violations, it is worth pointing out that we can use the previous descriptions to address a study considering rather the analysis of antiparticles. It is well known that the degeneracy between particles and antiparticles is broken when any of these operators have nonzero CPT-odd components. Then, we expect that there can be modifications of all properties studied previously for the antiparticle case. Nevertheless, such analysis lies beyond the scope of the current chapter and will be addressed in an upcoming one. Here we also would like to emphasize that the Eqs. (5.27), (5.33), (5.37) and (5.39) were valid for different types of kinematic modifications[3], like the ones that come from the *Very Special Relativity* [492], for instance.

Now, we estimate the magnitude of Lorentz-violating background. To do that, we can use the experimental data from [493]. In this reference, in the context of pions, we find the fluctuations for both particle density and mean energy. Here, we chose $u(n) = \bar{n}$, which is the simplest interaction energy function to estimate our results. Particularly, we use the following respective values to the temperature $T = 115\ \mathrm{MeV}$, the chemical potential $\mu = 134.9\ \mathrm{MeV}$ and the pion mass $m_\pi = 139\ \mathrm{MeV}$. To get the bounds, we first calculate the value of the thermodynamics functions that comes from our boson model considering the background coefficients as free variables. Then, we are able to compare our outputs with the available data[4]. In this direction, we can estimate the upper bound from the fluctuations of the thermodynamic functions. Thereby, we look toward to obtain the relative mean-square

[3]It is important to mention that the only requirement is that δ_r can be written in terms of momenta.

[4]Here we point out that all the results below were calculated numerically. So, to avoid a plethora of numerical terms, we decide to omit them and show just the important results.

fluctuation in the particle density [486]:

$$\frac{\overline{(\Delta n)^2}}{\bar{n}^2} = \frac{kT}{\bar{N}^2}\left(\frac{\partial \bar{N}}{\partial \mu}\right)_{T,V}. \tag{5.48}$$

Inserting Eq. (5.27) and the dispersion relation (5.46) in the above equation and comparing the results with the experimental data present in [493], we get the following upper bound for the vector background $\left(\hat{k}_a\right)^0$

$$|\left(\hat{k}_a\right)^0| < 1.2 \times 10^{-10}. \tag{5.49}$$

Now, we shall examine fluctuations for the energy of a system modified by the dispersion relation (5.47). Following the usual procedure, we obtain

$$\overline{(\Delta E)^2} = kT^2\left(\frac{\partial U}{\partial T}\right)_{z,V}. \tag{5.50}$$

Inserting now Eq. (5.35) into the above equation and comparing it with the available data in [493], we obtain the following upper bound for the configuration $\left(\hat{k}_c\right)^{00}$, namely,

$$|\left(\hat{k}_c\right)^{00}| < 1.8 \times 10^{-8}. \tag{5.51}$$

As we can see from both bounds obtained so far, the contribution that arises due to Lorentz-violating coefficients are very slight. Such contribution becomes even smaller when one takes into account a quadratic interaction energy $u(n) = \bar{n}^2$.

5.8 Applications

Here, we propose some feasible applications for our model concerning the quantum gases developed in this manuscript. It is important to highlight that the only requirement established is that the term δ_r, in Eq. (5.12), be dependent only on the momenta. In this way, we can apply our model to address such applications. Particularly, we look forward to two different scenarios involving *phosphorene*, and *spin precession*.

At the beginning, when one considers the measurements of some experimental physics, inevitable one stumbles upon the observable operators. In our case, following the ideas shown in Ref. [263], we consider the Hamiltonian operator in order to perform the following investigations. In doing so, we implement the decomposition of the Hamiltonian in terms of the spherical harmonics. With this, we can perform a coherent categorization of those pre-

vious coefficients which influenced the dynamic of particle modes studied so far. Moreover, it is opportune because rotation violations are a key signature of Lorentz violation.

Nevertheless, an exact expression to Hamiltonian is a challenge since we are dealing with higher-order derivative operators. To overtake this situation, we consider the Hamiltonian as being

$$\mathcal{H} = \mathcal{H}_0 + \delta\mathcal{H}, \tag{5.52}$$

where the nonpertubatibed form of the Hamiltonian is

$$\mathcal{H}_0 = \gamma_0(\mathbf{p}\cdot\mathbf{fl} + m_\psi) \tag{5.53}$$

and its respective perturbated version is written as

$$\begin{aligned}\delta\mathcal{H} = \frac{1}{E_0}\Bigg[&m_\psi\hat{\mathcal{S}}\gamma_5 - E_0\hat{\mathcal{V}}^0 - \hat{\mathcal{V}}^j p^j\gamma_5 + \hat{\mathcal{A}}^0 p^j\gamma^j\gamma_0 + m_\psi\hat{\mathcal{A}}^j\gamma^j\gamma_0\gamma_5 + \frac{\hat{\mathcal{A}}^j p^j p^k\gamma^k\gamma_0\gamma_5}{E_0+m_\psi} \\ &+ip^j\hat{\mathcal{T}}^{0k}\gamma^j\gamma^k + i\hat{\mathcal{T}}^{0j}p^j - E_0\tilde{\hat{\mathcal{T}}}^{0j}\gamma_0 + \frac{\tilde{\hat{\mathcal{T}}}^{0j}p^j p^k\gamma^k\gamma_0}{E_0+m_\psi}\Bigg]\end{aligned}. \tag{5.54}$$

It is important to note that the, from the above expression, we shall only consider the leading order, namely, $\delta\mathfrak{h}$. In this way, we can obtain therefore

$$\begin{aligned}\delta\mathfrak{h} &= \mathfrak{h}_a + \mathfrak{h}_c + \mathfrak{h}_g + \mathfrak{h}_H, \\ &= \frac{1}{E_0}\left(\hat{a}^\nu_{\text{eff}} - \hat{c}^\nu_{\text{eff}} - \tilde{\hat{g}}^{\mu\nu}_{\text{eff}}\tau_\mu + \tilde{\hat{H}}^{\mu\nu}_{\text{eff}}\tau_\mu\right)p_\nu,\end{aligned} \tag{5.55}$$

where the explicit definitions of $\hat{a}^\nu_{\text{eff}}$, $\hat{c}^\nu_{\text{eff}}$, $\tilde{\hat{g}}^{\mu\nu}_{\text{eff}}$ and $\tilde{\hat{H}}^{\mu\nu}_{\text{eff}}$ can properly be encountered in Ref. [263]. In the subsection 5.8.2, we take into account the advantage of using such approach to address an application involving the Lamor-like precession. As we shall see in what follows, the components $\mathfrak{h}_g$ and $\mathfrak{h}_H$ gives rise to a remarkable phenomenon due to the Lorentz violation, the birefringence.

5.8.1 Phosphorene

In this case, we can encompass both particle modes, namely, fermions (electrons) and bosons (phonons), in order to address our possible applications. Given the existence of some well-known approximations, the electrons of a metal can be assumed to be a gas, as they are effectively free particles [131, 458, 133, 134, 135, 459]. Therefore, our model, concerning the theory of ensembles, fits pretty well to this case.

Moreover, there can exist a promising aspect to be investigated in condensed matter physics, which is the thermal properties of anisotropic systems considering Lorentz viola-

tion. Such anisotropy may reveal new phenomena which might be in principle confronted with experimental physics. In the case of *phosphorene*, one can assume electrons to have an anisotropic effective mass [494], which raises many possibilities: if we confine these electrons in a box, collisions with the walls will depend on the angle that the wall makes with anisotropy direction. More so, *phonons* behave likewise in such systems.

Therefore, our proposal is to investigate how the coefficients, which triggers the Lorentz violation pointed out in Eqs. (5.3a - 5.3e), (5.7) and (5.8), can disturb the system in order to uncover some fingerprints of any signal of the Lorentz violation in the context of phosphorene.

5.8.2 Spin precession

Taken into account the expansion in terms of spherical harmonics as argued previously, the application involving spin precession seems to be viable as well. Here, we aim at displaying the group velocity, and the fermion spin precession in order to provide additional information (parameters/data) for helping the detection of the Lorentz violation in the context of quantum gases.

For a fermion wave packet, we can write its group velocity $\mathfrak{v}_{\mathbf{g}}$ as

$$|\mathfrak{v}_g| = \frac{|\mathbf{p}|}{E_0} + \sum_n (p^2 + nm_\psi^2) E_0^{-1-n} |\mathbf{p}|^{n-1} \times \left[a_n^{(d)} \mp m_\psi g_n^{(d+1)} - c_n^{(d)} \pm m_\psi H_n^{(d+1)} \right], \quad (5.56)$$

which might possibly be measured by the future experiments. Moreover, it is worth mentioning that the components h_g and h_H of the perturbative Hamiltonian also brings about a new phenomenon, the so-called birefringence [495, 344, 263, 473, 496]. This means that, depending on the direction under consideration, our system configuration may behave differently; it entails that there can possibly exist some modifications in its respective thermal properties.

Furthermore, it can also be perceived in another remarkable way; we shall interpret such aspect as being a Larmor-like precession of the spin operator $\hat{\mathbf{S}}$. Thereby, its dynamics is given by

$$\frac{\mathrm{d}}{\mathrm{d}t} \langle \psi_i | \, \hat{\mathbf{S}} \, | \psi_j \rangle = -i \, \langle \psi_i | \, [h, \hat{\mathbf{S}}] \, | \psi_j \rangle \approx 2(h_g + h_H) \times \langle \psi_i | \, \hat{\mathbf{S}} \, | \psi_j \rangle \,, \quad (5.57)$$

where we can interpret the term in the parenthesis $2(h_g + h_H)$ as precession frequency ω [263]. Therefore, based on the advantage of using our thermodynamic model of quantum gases, we propose the investigation of such frequency for the sake of probing the existence of Lorentz violation.

5.9 Are they still extensive state quantities?

Here, to corroborate our results, we proceed further for the sake of verifying the validity of the derived relations in the thermodynamic limit. Indeed, we need to take $N \to \infty$, $V \to \infty$ and $N/V = \text{const}$. Being proportional to the volume, the mean particle number, the entropy and the mean energy turn out to be extensive quantities in the ordinary case. Nevertheless, knowing whether the Lorentz violation removes such extensive property or not is an intriguing question to be checked. With this purpose, we proceed making the substitution in the following way

$$\sum_r \to \frac{gV}{(2\pi)^3}\int d^3\boldsymbol{p}, \tag{5.58}$$

where g is the degeneracy factor. Now, let us make some comments. Taking the thermodynamic limit is only reasonably supported when $u'(\bar{n})$ and $u(\bar{n})$ do not depend upon the volume. Additionally, this also entails that the particle number density $\bar{n} = \bar{N}/V$ must not depend upon it. Now, let us verify this assumption starting with

$$\left.\frac{\partial \bar{n}}{\partial V}\right|_{\mu,T} = \left.\frac{\partial}{\partial V}\left(\frac{\bar{N}}{V}\right)\right|_{\mu,T} = \frac{1}{V}\left(\left.\frac{\partial \bar{N}}{\partial V}\right|_{\mu,T} - \frac{\bar{N}}{V}\right), \tag{5.59}$$

which yields

$$\begin{aligned}\left.\frac{\partial \bar{N}}{\partial V}\right|_{\mu,T} &= \frac{gV}{(2\pi)^3}\int d^3\boldsymbol{p}\frac{1}{\exp\left\{\beta\left[\epsilon_r(\boldsymbol{p}) + \delta_r(\boldsymbol{p}) + u'(\bar{n}) - \mu\right]\right\} + \chi} \\ &+ \frac{gV}{(2\pi)^3}\int d^3\boldsymbol{p}\left\{-\left[\frac{1}{\exp\left\{\beta\left[\epsilon_r(\boldsymbol{p}) + \delta_r(\boldsymbol{p}) + u'(\bar{n}) - \mu\right]\right\} + \chi}\right]^2\right\} \times \\ &\times \exp\left\{\beta\left[\epsilon_r(\boldsymbol{p}) + \delta_r(\boldsymbol{p}) + u'(\bar{n}) - \mu\right]\right\}\beta\left.\frac{\partial u'(\bar{n})}{\partial V}\right|_{\mu,T}.\end{aligned} \tag{5.60}$$

In this sense, we identify the first term as $\bar{N}/V$; the second term we rewrite using

$$\left.\frac{\partial u'(\bar{n})}{\partial V}\right|_{\mu,T} = u''(\bar{n})\left.\frac{\partial \bar{n}}{\partial V}\right|_{\mu,T} = \frac{u''(\bar{n})}{V}\left(\left.\frac{\partial \bar{N}}{\partial V}\right|_{\mu,T} - \frac{\bar{N}}{V}\right), \tag{5.61}$$

as

$$-\sum_r \bar{n}_r \frac{\beta}{V}u''(\bar{n})\left(\left.\frac{\partial \bar{N}}{\partial V}\right|_{\mu,T} - \frac{\bar{N}}{V}\right)\exp\left\{\beta\left[\epsilon_r(\boldsymbol{p}) + \delta_r(\boldsymbol{p}) + u'(\bar{n}) - \mu\right]\right\},$$

and to finish we obtain

$$\begin{aligned}\left.\frac{\partial\bar{n}}{\partial V}\right|_{\mu,T} &= \frac{1}{V}\left(\left.\frac{\partial\bar{N}}{\partial V}\right|_{\mu,T}-\frac{\bar{N}}{V}\right)\\ &= \frac{1}{V}\left(-\sum_r \bar{n}_r\frac{\beta}{V}u''\left(\bar{n}\right)\exp\left\{\beta\left[\epsilon_r\left(\boldsymbol{p}\right)+\delta_r\left(\boldsymbol{p}\right)+u'\left(\bar{n}\right)-\mu\right]\right\}\right)\times\\ &\quad\times\left(\left.\frac{\partial\bar{N}}{\partial V}\right|_{\mu,T}-\frac{\bar{N}}{V}\right).\end{aligned} \tag{5.62}$$

Additionally, this relation is verified if

$$1=-\sum_r \bar{n}_r\frac{\beta}{V}\exp\left\{\beta\left[\epsilon_r\left(\boldsymbol{p}\right)+\delta_r\left(\boldsymbol{p}\right)+u'\left(\bar{n}\right)-\mu\right]\right\}u''\left(\bar{n}\right). \tag{5.63}$$

Nevertheless, in a general case, this is not true for the reason that $u\left(n\right)$ is an absolutely arbitrary interaction potential density. As a matter of fact, it must hold that

$$\left.\frac{\partial\bar{N}}{\partial V}\right|_{\mu,T}=\frac{\bar{N}}{V}, \tag{5.64}$$

i.e., $\left.\frac{\partial\bar{n}}{\partial V}\right|_{\mu,T}$ must vanish. Finally, we should notice that, since $\delta_r\left(\boldsymbol{p}\right)$ is a function only of $\boldsymbol{p}$, it does not mess up the extensive property. Therefore, for such thermal properties, even in the presence of Lorentz violation, the extensive characteristic of the system is maintained as well.

5.10 Numerical analyses

Here, we provide such Appendix to exhibit a concise explanation for the numerical calculations encountered throughout this manuscript. We show the thermal quantities, namely, the energy, the mean particle number and the entropy per volume, for different values of β. Besides, $\mathcal{E}$, $\mathfrak{N}$ and $\mathfrak{S}$ are quantities representing the energy, the mean particle number as well as the entropy per volume respectively. The outputs for fermions and bosons modes are displayed as follows:

β	$\mathcal{E}$	$\delta\mathcal{E}_1$	$\delta\mathcal{E}_2$	$\delta\mathcal{E}_3$	$\mathfrak{N}$	$\delta\mathfrak{N}_1$	$\delta\mathfrak{N}_2$	$\delta\mathfrak{N}_3$	$\mathfrak{S}$	$\delta\mathfrak{S}_1$	$\delta\mathfrak{S}_2$	$\delta\mathfrak{S}_3$
0.1	3231.95	0.104598	0.00104598	0.0000104598	104.543	-0.0000416498	-4.16498×10^{-7}	-4.16498×10^{-9}	734.947	0.00522714	0.0000522714	$5.22714\,10^{-7}$
0.2	112.314	0.00736482	0.0000736482	7.36482×10^{-7}	7.34833	-1.99713×10^{-7}	-1.99713×10^{-8}	-1.99713×10^{-10}	51.5659	0.000734833	7.34833×10^{-6}	7.34833×10^{-8}
0.3	12.2594	0.00121608	0.0000121608	1.21608×10^{-7}	1.20978	-1.58032×10^{-7}	-1.58032×10^{-9}	-1.58032×10^{-11}	8.48027	0.000181467	1.81467×10^{-6}	1.81467×10^{-8}
0.4	2.13516	0.000284015	2.84015×10^{-6}	2.84015×10^{-8}	0.28138	-1.50433×10^{-8}	-1.50433×10^{-10}	-1.50433×10^{-12}	1.97117	0.0000562759	5.62759×10^{-7}	5.62759×10^{-9}
0.5	0.480237	0.0000801838	8.01838×10^{-7}	8.01838×10^{-9}	0.0790277	-1.5763×10^{-9}	-1.5763×10^{-11}	-1.5763×10^{-13}	0.553427	0.0000197569	1.97569×10^{-7}	1.97569×10^{-9}
0.6	0.126973	0.000025527	2.5527×10^{-7}	2.5527×10^{-9}	0.0250043	-1.75433×10^{-10}	-1.75433×10^{-12}	-1.75433×10^{-14}	0.17507	7.50128×10^{-6}	7.50128×10^{-8}	7.50128×10^{-10}
0.7	0.0375352	8.83081×10^{-6}	8.83081×10^{-8}	8.83081×10^{-10}	0.00858928	-2.03663×10^{-11}	-2.03663×10^{-13}	-2.03663×10^{-15}	0.0601324	3.00625×10^{-6}	3.00625×10^{-8}	3.00625×10^{-10}
0.8	0.0120401	3.24695×10^{-6}	3.24695×10^{-8}	3.24695×10^{-10}	0.00313348	-2.4398×10^{-12}	-2.4398×10^{-14}	-2.4398×10^{-16}	0.0219358	1.25339×10^{-6}	1.25339×10^{-8}	1.25339×10^{-10}
0.9	0.0041105	1.25082×10^{-6}	1.25082×10^{-8}	1.25082×10^{-10}	0.00119682	-2.99456×10^{-13}	-2.99456×10^{-15}	-2.99456×10^{-17}	0.00838577	3.70143×10^{-6}	3.70143×10^{-8}	3.70143×10^{-10}
1.0	0.00147396	4.99909×10^{-7}	4.99909×10^{-9}	4.99909×10^{-11}	0.000473931	-3.74665×10^{-14}	-3.74665×10^{-16}	-3.74665×10^{-18}	0.00331758	2.36965×10^{-7}	2.36965×10^{-9}	2.36965×10^{-11}

Tab. 5.3: The scalar operator concerning the fermion sector.

β	$\mathcal{E}$	$\delta\mathcal{E}_1$	$\delta\mathcal{E}_2$	$\delta\mathcal{E}_3$	$\mathfrak{N}$	$\delta\mathfrak{N}_1$	$\delta\mathfrak{N}_2$	$\delta\mathfrak{N}_3$	$\mathfrak{S}$	$\delta\mathfrak{S}_1$	$\delta\mathfrak{S}_2$	$\delta\mathfrak{S}_3$
0.1	3231.95	3.23195	0.0323195	0.000323195	104.543	-0.00030446	-3.0446×10^{-6}	-3.0446×10^{-8}	734.947	0.107691	0.00107691	0.0000107691
0.2	112.314	0.112314	0.00112314	0.0000112314	7.34833	-7.03273×10^{-6}	-7.03273×10^{-8}	-7.03273×10^{-10}	51.5659	0.00747586	0.0000747586	7.47586×10^{-7}
0.3	12.2594	0.0122594	0.000122594	1.22594×10^{-6}	1.20978	-3.62361×10^{-7}	-3.62361×10^{-9}	-3.62361×10^{-11}	8.48027	0.00122158	0.0000122158	1.22158×10^{-7}
0.4	2.13516	0.00213516	0.0000213516	2.13516×10^{-7}	0.28138	-2.55114×10^{-8}	-2.55114×10^{-10}	-2.55114×10^{-12}	1.97117	0.000282896	2.82896×10^{-6}	2.82896×10^{-8}
0.5	0.480237	0.000480237	4.80237×10^{-6}	4.80237×10^{-8}	0.0790277	-2.12168×10^{-9}	-2.12168×10^{-11}	-2.12168×10^{-13}	0.553427	0.0000792604	7.92604×10^{-7}	7.92604×10^{-9}
0.6	0.126973	0.000126973	1.26973×10^{-6}	1.26973×10^{-8}	0.0250043	-1.95919×10^{-10}	-1.95919×10^{-12}	-1.95919×10^{-14}	0.17507	0.0000250442	2.50442×10^{-7}	2.50442×10^{-9}
0.7	0.0375352	0.0000375352	3.75352×10^{-7}	3.75352×10^{-9}	0.00858928	-1.94491×10^{-11}	-1.94491×10^{-13}	-1.94491×10^{-15}	0.0601324	8.59669×10^{-6}	8.59669×10^{-8}	8.59669×10^{-10}
0.8	0.0120401	0.0000120401	1.20401×10^{-7}	1.20401×10^{-9}	0.00313348	-2.0361×10^{-12}	-2.0361×10^{-14}	-2.0361×10^{-16}	0.0219358	3.13493×10^{-6}	3.13493×10^{-8}	3.13493×10^{-10}
0.9	0.0041105	4.1105×10^{-6}	4.1105×10^{-8}	4.1105×10^{-10}	0.00119682	-2.21989×10^{-13}	-2.21989×10^{-15}	-2.21989×10^{-17}	0.00837801	1.19711×10^{-6}	1.19711×10^{-8}	1.19711×10^{-10}
1.0	0.00147396	1.47396×10^{-6}	1.47396×10^{-8}	1.47396×10^{-10}	0.000473931	-2.49878×10^{-14}	-2.49878×10^{-16}	-2.49878×10^{-18}	0.00331758	4.739949×10^{-7}	4.73994×10^{-9}	4.73994×10^{-11}

Tab. 5.4: The vector operator concerning the fermion sector.

β	$\mathcal{E}$	$\delta\mathcal{E}_1$	$\delta\mathcal{E}_2$	$\delta\mathcal{E}_3$	$\mathfrak{N}$	$\delta\mathfrak{N}_1$	$\delta\mathfrak{N}_2$	$\delta\mathfrak{N}_3$	$\mathfrak{S}$	$\delta\mathfrak{S}_1$	$\delta\mathfrak{S}_2$	$\delta\mathfrak{S}_3$
0.1	3231.95	-0.209193	-0.00209193	-0.0000209193	104.543	0.0000829947	8.29947×10^{-7}	8.29947×10^{-9}	734.947	-0.010449	-0.00010449	-1.0449×10^{-6}
0.2	112.314	-0.014728	-0.00014728	-1.4728×10^{-6}	7.34833	3.93882×10^{-6}	3.93882×10^{-8}	3.93882×10^{-10}	51.5659	-0.00146669	-0.0000146669	-1.46669×10^{-7}
0.3	12.2594	-0.00243122	-0.0000243122	-2.43122×10^{-7}	1.20978	3.07031×10^{-7}	3.07031×10^{-9}	3.07031×10^{-11}	8.48027	-0.000361314	-3.61314×10^{-6}	-3.61314×10^{-8}
0.4	2.13516	-0.000567521	-5.67521×10^{-6}	-5.67521×10^{-8}	0.28138	2.87129×10^{-8}	2.87129×10^{-10}	2.87129×10^{-12}	1.97117	-0.000111689	-1.11689×10^{-6}	-1.11689×10^{-8}
0.5	0.480237	-0.000160098	-1.60098×10^{-6}	-1.60098×10^{-8}	0.0790277	2.95182×10^{-9}	2.95182×10^{-11}	2.95182×10^{-13}	0.553427	-0.000039061	-3.9061×10^{-7}	-3.9061×10^{-9}
0.6	0.126973	-0.0000509137	-5.09137×10^{-7}	-5.09137×10^{-9}	0.0250043	3.22144×10^{-10}	3.22144×10^{-12}	3.22144×10^{-14}	0.17507	-0.0000147665	-1.47665×10^{-7}	-1.47665×10^{-9}
0.7	0.0375352	-0.000017589	-1.7589×10^{-7}	-1.7589×10^{-9}	0.00858928	3.66682×10^{-11}	3.66682×10^{-13}	3.66682×10^{-15}	0.0601324	-5.8899×10^{-6}	-5.8899×10^{-8}	-5.8899×10^{-10}
0.8	0.0120401	-6.45643×10^{-6}	-6.45643×10^{-8}	-6.45643×10^{-10}	0.00313348	4.30756×10^{-12}	4.30756×10^{-14}	4.30756×10^{-16}	0.0219358	-2.44322×10^{-6}	-2.44322×10^{-8}	-2.44322×10^{-10}
0.9	0.0041105	-2.48233×10^{-6}	-2.48233×10^{-8}	-2.48233×10^{-10}	0.00119682	5.18591×10^{-13}	5.18591×10^{-15}	5.18591×10^{-17}	0.00837801	-1.04421×10^{-6}	-1.04421×10^{-8}	-1.04421×10^{-10}
1.0	0.00147396	-9.8986×10^{-7}	-9.8986×10^{-9}	-9.8986×10^{-11}	0.000473931	6.36654×10^{-14}	6.36654×10^{-16}	6.36654×10^{-18}	0.00331758	-4.56876×10^{-7}	-4.56876×10^{-9}	-4.56876×10^{-11}

Tab. 5.5: The pseudovector operator for fermions.

β	$\mathcal{E}$	$\delta\mathcal{E}_1$	$\delta\mathcal{E}_2$	$\delta\mathcal{E}_3$	$\mathfrak{N}$	$\delta\mathfrak{N}_1$	$\delta\mathfrak{N}_2$	$\delta\mathfrak{N}_3$	$\mathfrak{S}$	$\delta\mathfrak{S}_1$	$\delta\mathfrak{S}_2$	$\delta\mathfrak{S}_3$
0.1	3231.95	-9.6971	-0.096971	-0.00096971	104.543	-0.000916101	9.16101×10^{-6}	9.16101×10^{-8}	734.947	-0.323195	-0.00323195	-0.0000323195
0.2	112.314	-0.33712	-0.0033712	-0.000033712	7.34833	0.0000213616	2.13616×10^{-7}	2.13616×10^{-9}	51.5659	-0.0224627	-0.000224627	-2.24627×10^{-6}
0.3	12.2594	-0.0368236	-0.000368236	-3.68236×10^{-6}	1.20978	1.11777×10^{-6}	1.11777×10^{-8}	1.11777×10^{-10}	8.48027	-0.00367781	-0.0000367781	-3.67781×10^{-7}
0.4	2.13516	-0.00641989	-0.0000641989	-6.41989×10^{-7}	0.28138	8.02973×10^{-8}	8.02973×10^{-10}	8.02973×10^{-12}	1.97117	-0.000854066	-8.54066×10^{-6}	-8.54066×10^{-8}
0.5	0.480237	-0.00144586	-0.0000144586	-1.44586×10^{-7}	0.0790277	6.83726×10^{-9}	6.83726×10^{-11}	6.83726×10^{-13}	0.553427	-0.000240119	-2.40119×10^{-6}	-2.40119×10^{-8}
0.6	0.126973	-0.000382907	-3.82907×10^{-6}	-3.82907×10^{-8}	0.0250043	6.47963×10^{-10}	6.47963×10^{-12}	6.47963×10^{-14}	0.17507	-0.0000761841	-7.61841×10^{-7}	-7.61841×10^{-9}
0.7	0.0375352	-0.000113414	-1.13414×10^{-6}	-1.13414×10^{-8}	0.00858928	6.61241×10^{-11}	6.61241×10^{-13}	6.61241×10^{-15}	0.0601324	-0.0000262746	-2.62746×10^{-7}	-2.62746×10^{-9}
0.8	0.0120401	-0.0000364624	-3.64624×10^{-7}	-3.64624×10^{-9}	0.00313348	7.12401×10^{-12}	7.12401×10^{-14}	7.12401×10^{-16}	0.0219358	-9.63211×10^{-6}	-9.63211×10^{-8}	-9.63211×10^{-10}
0.9	0.0041105	-0.0000124805	-1.24805×10^{-7}	-1.24805×10^{-9}	0.00119682	7.99893×10^{-13}	7.99893×10^{-15}	7.99893×10^{-17}	0.00837801	-3.69945×10^{-6}	-3.69945×10^{-8}	-3.69945×10^{-10}
1.0	0.00147396	-4.48836×10^{-6}	-4.48836×10^{-8}	-4.48836×10^{-10}	0.000473931	9.27651×10^{-14}	9.27651×10^{-16}	9.27651×10^{-18}	0.00331758	-1.47396×10^{-6}	-1.47396×10^{-8}	-1.47396×10^{-10}

Tab. 5.6: The tensor operator for fermions.

β	$\mathcal{E}$	$\delta\mathcal{E}_1$	$\delta\mathcal{E}_2$	$\delta\mathcal{E}_3$	$\mathfrak{N}$	$\delta\mathfrak{N}_1$	$\delta\mathfrak{N}_2$	$\delta\mathfrak{N}_3$	$\mathfrak{S}$	$\delta\mathfrak{S}_1$	$\delta\mathfrak{S}_2$	$\delta\mathfrak{S}_3$
0.1	3465.22	-0.12049	-0.0012049	-0.000012049	120.39	0.000110936	1.10936×10^{-6}	1.10936×10^{-8}	837.793	-0.0060195	-0.000060195	-6.0195×10^{-7}
0.2	116.632	-0.00794586	0.0000794586	-794586×10^{-7}	7.92365	3.31996×10^{-6}	3.31996×10^{-8}	3.31996×10^{-10}	55.3038	-0.000792365	-7.92365×10^{-6}	-7.92365×10^{-8}
0.3	12.5142	-0.00126748	-0.0000126748	-126748×10^{-7}	1.26011	2.07175×10^{-7}	2.07175×10^{-9}	2.07175×10^{-11}	8.80739	-0.000189017	-1.89017×10^{-6}	-1.89017×10^{-8}
0.4	2.15927	-0.000290522	-2.90522×10^{-6}	-2.90522×10^{-8}	0.287658	1.73861×10^{-8}	1.73861×10^{-10}	1.73861×10^{-12}	2.01198	-0.0000575316	-5.75316×10^{-7}	-5.75316×10^{-9}
0.5	0.483186	-0.0000811842	-8.11842×10^{-7}	-8.11842×10^{-9}	0.0799761	1.70289×10^{-9}	1.70289×10^{-11}	1.70289×10^{-13}	0.559591	-0.000019994	-1.9994×10^{-7}	-1.9994×10^{-9}
0.6	0.127398	-0.0000257007	-2.57007×10^{-7}	-2.57007×10^{-9}	0.0251657	1.82797×10^{-10}	1.82797×10^{-12}	1.82797×10^{-14}	0.176119	-7.5497×10^{-6}	-7.5497×10^{-8}	-7.5497×10^{-10}
0.7	0.0376033	-8.8636×10^{-6}	-8.8636×10^{-8}	-8.8636×10^{-10}	0.00861908	2.08159×10^{-11}	2.08159×10^{-13}	2.08159×10^{-15}	0.060326	-3.01668×10^{-6}	-3.01668×10^{-8}	-3.01668×10^{-10}
0.8	0.012052	-3.25352×10^{-6}	-3.25352×10^{-8}	-3.25352×10^{-10}	0.00313931	2.4682×10^{-12}	2.4682×10^{-14}	2.4682×10^{-16}	0.0219737	-1.25572×10^{-6}	-1.25572×10^{-8}	-1.25572×10^{-10}
0.9	0.00411269	-1.2522×10^{-6}	-1.2522×10^{-8}	-1.2522×10^{-10}	0.00119801	3.01294×10^{-13}	3.01294×10^{-15}	3.01294×10^{-17}	0.00838577	-5.39104×10^{-7}	-5.39104×10^{-9}	-5.39104×10^{-11}
1.0	0.00147439	-5.00208×10^{-7}	-5.00208×10^{-9}	-5.00208×10^{-11}	0.000474184	3.75879×10^{-14}	3.75879×10^{-16}	3.75879×10^{-18}	0.00331922	-2.37092×10^{-7}	-2.37092×10^{-9}	-2.37092×10^{-11}

Tab. 5.7: The vector operator in the boson sector.

β	$\mathcal{E}$	$\delta\mathcal{E}_1$	$\delta\mathcal{E}_2$	$\delta\mathcal{E}_3$	$\mathfrak{N}$	$\delta\mathfrak{N}_1$	$\delta\mathfrak{N}_2$	$\delta\mathfrak{N}_3$	$\mathfrak{S}$	$\delta\mathfrak{S}_1$	$\delta\mathfrak{S}_2$	$\delta\mathfrak{S}_3$
0.1	3465.22	10.3973	0.103973	0.00103973	120.39	-0.00189399	-0.0000189399	-1.89399×10^{-7}	837.793	0.346522	0.00346522	0.0000346522
0.2	116.632	0.350106	0.00350106	0.0000350106	7.92365	-0.0000313526	-3.13526×10^{-7}	-3.13526×10^{-9}	55.3038	0.0233264	0.000233264	2.33264×10^{-6}
0.3	12.5142	0.037592	0.00037592	3.7592×10^{-6}	1.26011	-1.37484×10^{-6}	-1.37484×10^{-8}	-1.37484×10^{-10}	8.80739	0.00375425	0.0000375425	3.75425×10^{-7}
0.4	2.15927	0.00649289	-0.0000649289	6.49289×10^{-7}	0.287658	-8.98141×10^{-8}	-8.98141×10^{-10}	-8.98141×10^{-12}	2.01198	0.000863707	8.63707×10^{-6}	8.63707×10^{-8}
0.5	0.483186	0.00145484	0.0000145484	1.45484×10^{-7}	0.0799761	-7.26379×10^{-9}	-7.26379×10^{-11}	-7.26379×10^{-13}	0.559591	0.000241593	2.41593×10^{-6}	2.41593×10^{-8}
0.6	0.127398	0.000384207	3.84207×10^{-6}	3.84207×10^{-8}	0.0251657	-6.6944×10^{-10}	-6.6944×10^{-12}	-6.6944×10^{-14}	0.176119	0.0000764385	7.64385×10^{-7}	7.64385×10^{-9}
0.7	0.0376033	-8.8636×10^{-6}	-8.8636×10^{-8}	-8.8636×10^{-10}	0.00861908	2.08159×10^{-11}	2.08159×10^{-13}	2.08159×10^{-15}	0.060326	-3.01668×10^{-6}	-3.01668×10^{-8}	-3.01668×10^{-10}
0.8	0.0376033	0.000113624	1.13624×10^{-6}	1.13624×10^{-8}	0.00861908	-6.7293×10^{-11}	-6.7293×10^{-13}	-6.7293×10^{-15}	0.0219737	9.64159×10^{-6}	9.64159×10^{-8}	9.64159×10^{-10}
0.9	0.00411269	0.0000124874	1.24874×10^{-7}	1.24874×10^{-9}	0.00119801	-8.03919×10^{-13}	-8.03919×10^{-15}	-8.03919×10^{-17}	0.00838577	3.70143×10^{-6}	3.70143×10^{-8}	3.70143×10^{-10}
1.0	0.00147439	4.48971×10^{-6}	4.48971×10^{-8}	4.48971×10^{-10}	0.000474184	-9.30139×10^{-14}	-9.30139×10^{-16}	-9.30139×10^{-18}	0.00331922	1.47439×10^{-6}	1.47439×10^{-8}	-2.37092×10^{-10}

Tab. 5.8: The tensor operator for the boson sector.

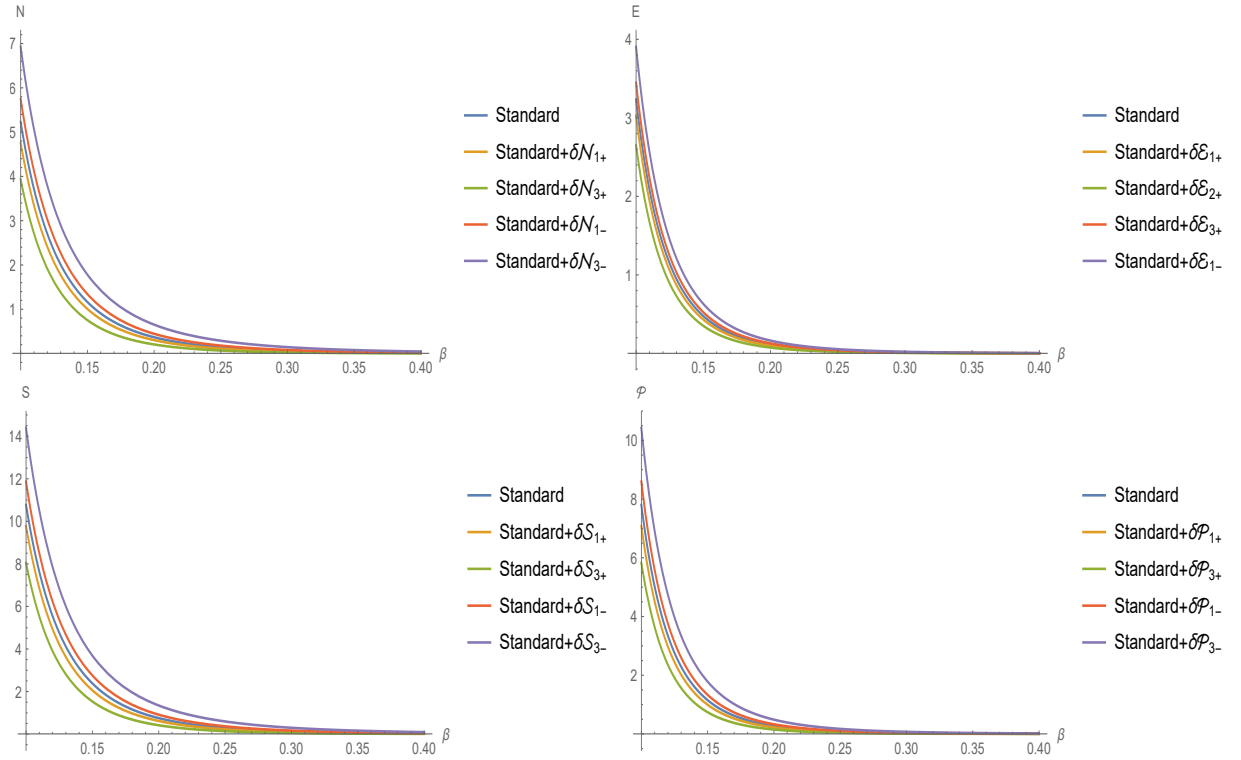

Fig. 5.3: These plots exhibit the general behavior to spin-nondegenerate case for fermions.

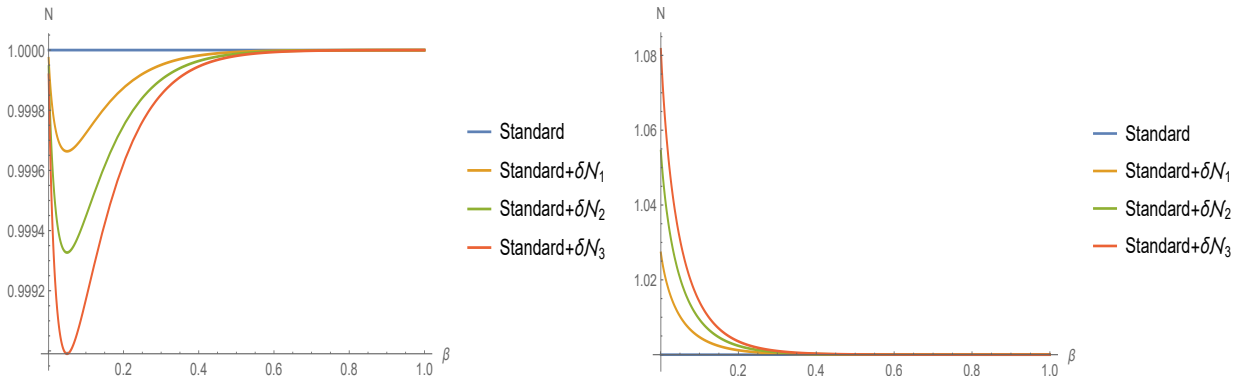

((a)) $\hat{k}_a$ operator ((b)) $\hat{k}_c$ operator

Fig. 5.4: This figure shows a comparison between particle number to different background configurations for bosons. Here, the normalization is also applied.

6. THERMODYNAMIC PROPERTIES IN HIGHER-DERIVATIVE ELECTRODYNAMICS

6.1 Podolsky electrodynamics

6.1.1 The model

The four-dimensional Lagrangian density of the Podolsky electrodynamics is written as [296, 320, 321]

$$\mathcal{L} = -\frac{1}{4}F_{\mu\nu}F^{\mu\nu} + \frac{\theta^2}{2}\partial_\alpha F^{\alpha\beta}\partial_\lambda F^{\lambda}{}_{\beta} - A_\mu J^\mu, \tag{6.1}$$

where $F_{\mu\nu} = \partial_\mu A_\nu - \partial_\nu A_\mu$ is the usual Maxwell field strength, A_μ is the vector field and θ is the Podolsky's parameter with mass dimension -1, and J^μ is a conserved current. In addition, in Refs. [322, 325] the authors accomplished remarkable classical analyzes of this theory i.e., they studied interparticle potential between sources, quantization, generalization of such theory in the framework of Dirac's theory of constrained systems and others. From Eq. (6.1), the equation of motion can be written as

$$\left(1 + \theta^2\Box\right)\partial_\mu F^{\mu\nu} = J^\nu. \tag{6.2}$$

Here, it must be pointed out that there exists a distinguishing characteristic if compared with the Proca's theory which is the generation of a massive mode without losing its gauge symmetry. Thereby, by adding a gauge fixing term to Eq. (6.1), namely $-\frac{1}{2\varsigma}(\partial_\mu A^\mu)^2$, with ς being the gauge-fixing parameter, we can immediately derive the propagator in the momentum space as follows

$$\Delta_{\mu\nu}(k) = -\frac{1}{k^2(1-\theta^2k^2)}\left\{\theta_{\mu\nu} + \varsigma(1-\theta^2k^2)\omega_{\mu\nu}\right\}, \tag{6.3}$$

where $\theta_{\mu\nu} \equiv \eta_{\mu\nu} - \omega_{\mu\nu}$ and $\omega_{\mu\nu} \equiv k_\mu k_\nu/k^2$ are the transverse and longitudinal projectors respectively. Here, $\eta_{\mu\nu}$ is the Minkowski metric with signature $(+.-,-,-)$. Clearly, from above expression, we verify the presence of both Maxwell $k^2 = 0$ and Podolsky $1 - \theta^2k^2 = 0$

poles. From the pole of the propagator encountered in Eq. (6.3), we have

$$k_\mu k^\mu (1 - \theta^2 k^\alpha k_\alpha) = 0. \tag{6.4}$$

Furthermore, note that when one considers $\theta \to 0$, the standard dispersion relation is recovered i.e., $k^2 = 0$. Besides, Eq. (6.4) may be rewritten simply as

$$\mathbf{k}^2 = \frac{2E^2\theta^2 - 1 \mp 1}{2\theta^2}, \tag{6.5}$$

where this equation shows that we have a different state equation which must change the thermodynamic properties of our system due to the fact that the relation between energy and momentum is no longer ascribed to be the usual one. It is worth to note that from Eq. (8.19), we choose the -1 configuration, since otherwise we will not have the contribution of parameter θ. Moreover, in what follows, we examine a photon gas in a volume Γ and instead of dealing with a quantizing momentum due to the boundary conditions, rather we assume a continuous momentum spectrum as it is commonly used in the literature [497, 498, 273]. We use the fact that the statistical mechanics tells us that the relation between energy and momentum has a remarkable aspect in evaluating the dependence of the pressure as a function of the energy density. In the next subsection, we proceed with the purpose of obtaining the accessible states of the system in order to calculate the partition function which suffices to address all thermodynamic properties. In addition, it is noteworthy that in different contexts the thermodynamic functions were calculated as well [489, 488, 499, 490, 500].

6.1.2 Thermodynamic properties

We start with the construction of the partition function for the sake of obtaining the following thermodynamic properties i.e., Helmholtz free energy, mean energy, entropy heat capacity. In this sense, we use the traditional method for doing so; we use the concept of the number of accessible states of the system [497]. Generically, it can be written as

$$\Omega(E) = \frac{\zeta}{(2\pi)^3} \int\int \mathrm{d}^3\mathbf{x}\, \mathrm{d}^3\mathbf{k}, \tag{6.6}$$

where ζ is the spin multiplicity which in our case will be considered as the photon sector i.e., $\zeta = 2$. However, for the sake of simplicity, the above equation may be rewritten as follows

$$\Omega(E) = \frac{\Gamma}{\pi^2} \int_0^\infty \mathrm{d}\mathbf{k} |\mathbf{k}|^2, \tag{6.7}$$

where Γ is considered the volume of the thermal bath and $\mathbf{dk}$ being given by

$$\mathbf{dk} = \frac{\theta E}{\sqrt{E^2\theta^2 - 1}}\mathrm{d}E. \tag{6.8}$$

After substituting (8.19) and (6.8) in (6.7), we obtain

$$\Omega(E) = \frac{\Gamma}{\pi^2}\int_0^\infty \frac{E(E^2\theta^2 - 1)}{\theta\sqrt{E^2\theta^2 - 1}}\,\mathrm{d}E, \tag{6.9}$$

and therefore we are properly able to write down the partition function analogously to what the authors did in Ref. [273] as follows

$$\ln\left[Z(\beta,\Gamma)\right] = -\frac{\Gamma}{\pi^2}\int_0^\infty \frac{E(E^2\theta^2 - 1)}{\theta\sqrt{E^2\theta^2 - 1}}\ln\left(1 - e^{-\beta E}\right)\mathrm{d}E, \tag{6.10}$$

where $\beta = 1/k_B T$. Using Eq.(7.10), we can obtain the thermodynamic functions per volume Γ, namely, Helmholtz free energy $F(\beta,\theta)$, mean energy $U(\beta,\theta)$, entropy $S(\beta,\theta)$ and heat capacity $C_V(\beta,\theta)$ defined as follows:

$$\begin{aligned}
F(\beta,\theta) &= -\frac{1}{\beta}\ln\left[Z(\beta,\theta)\right], \\
U(\beta,\theta) &= -\frac{\partial}{\partial\beta}\ln\left[Z(\beta,\theta)\right], \\
S(\beta,\theta) &= k_B\beta^2\frac{\partial}{\partial\beta}F(\beta,\theta), \\
C_V(\beta,\theta) &= -k_B\beta^2\frac{\partial}{\partial\beta}U(\beta,\theta).
\end{aligned} \tag{6.11}$$

At the beginning, let us consider the mean energy

$$U(\beta,\theta) = \frac{1}{\pi^2}\int_0^\infty \frac{E^2\sqrt{E^2\theta^2 - 1}\,e^{-\beta E}}{\theta\left(1 - e^{-\beta E}\right)}\mathrm{d}E, \tag{6.12}$$

which follows the spectral radiance defined by:

$$\chi(\theta,\nu) = \frac{(h\nu)^2\sqrt{(h\nu)^2\theta^2 - 1}\,e^{-\beta h\nu}}{\pi^2\theta\left(1 - e^{-\beta h\nu}\right)}, \tag{6.13}$$

with $E = h\nu$ where h is the Planck constant and ν is the frequency. Here, it is reasonable to investigate how the parameter θ affects our theory in the spectral radiation. Additionally, it has to be noted that, even though we explicit the constants h, k_B, for performing the following calculations, we set them $h = k_B = 1$. In this way, the plot of this configuration is

shown in Fig. 6.1. Here, we notice that the black body radiation spectra for different values of θ are greater than one exhibited in the Maxwell case. On the other hand, when $\theta \to 0$, we recover the usual Maxwell electrodynamics. Physically, such result reflects the existence of an additional massive mode presented in Podolsky electrodynamics.

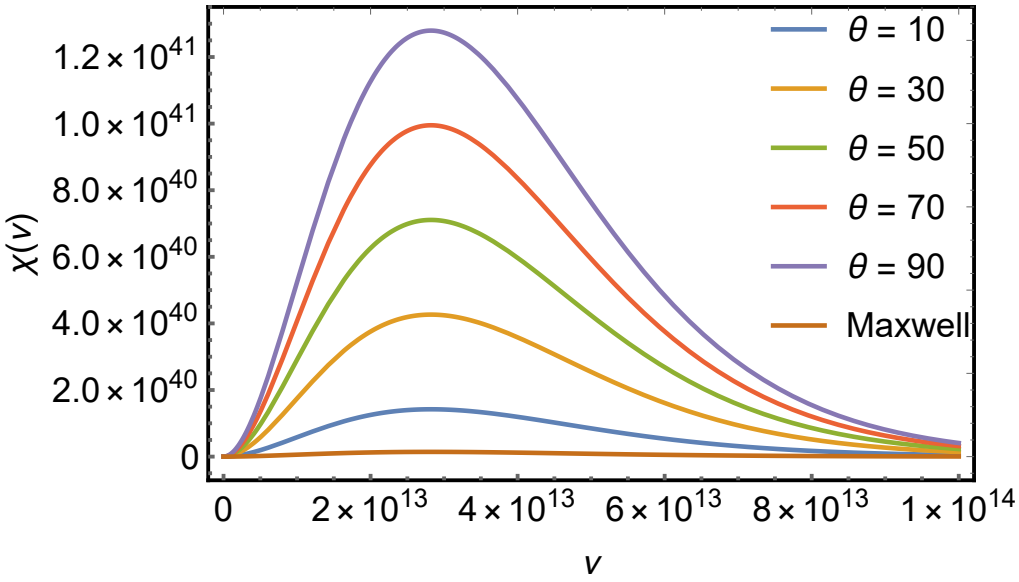

Fig. 6.1: The figure shows the behavior of the black body radiation as a function of the frequency ν for different values of θ within Podolsky electrodynamics considering $h = 1$.

For the sake of obtaining the well-established radiation constant of the *Stefan- Boltzmann* energy density i.e., $u_S = \alpha T^4$, we consider $(E\theta)^2 \gg 1$ which leads to

$$\alpha = \frac{1}{\pi^2}\int_0^\infty \frac{E^3\, e^{-\beta E}}{\left(1 - e^{-\beta E}\right)} \mathrm{d}E = \frac{\pi^2}{15}, \tag{6.14}$$

reproducing the well-established result in the literature [150]. On the other hand, in order to check how the coupling constant θ affects the new radiation constant, we proceed as follows:

$$\tilde{\alpha} \equiv U(\beta, \theta)\beta^4. \tag{6.15}$$

The analysis will be accomplished via numerical calculations. The plots are shown in Fig.6.2 taking into account three different circumstances i.e., when θ is either a small or a huge number. Furthermore, the aspect of examining the limit when $E^2\sqrt{E^2\theta^2 - 1} \gg \theta$ is also regarded. The latter can be handily associated with the primordial inflationary universe, since we may deal with high temperature regime i.e., $\beta = 10^{-13}$ GeV^{-1}. Another interesting approach which it is worth being investigated is whether the thermodynamics functions bear with CMB (Cosmic Microwave Background) analysis. Nevertheless, this approach lies beyond the scope of the current chapter and will be addressed in a future upcoming

manuscript though.

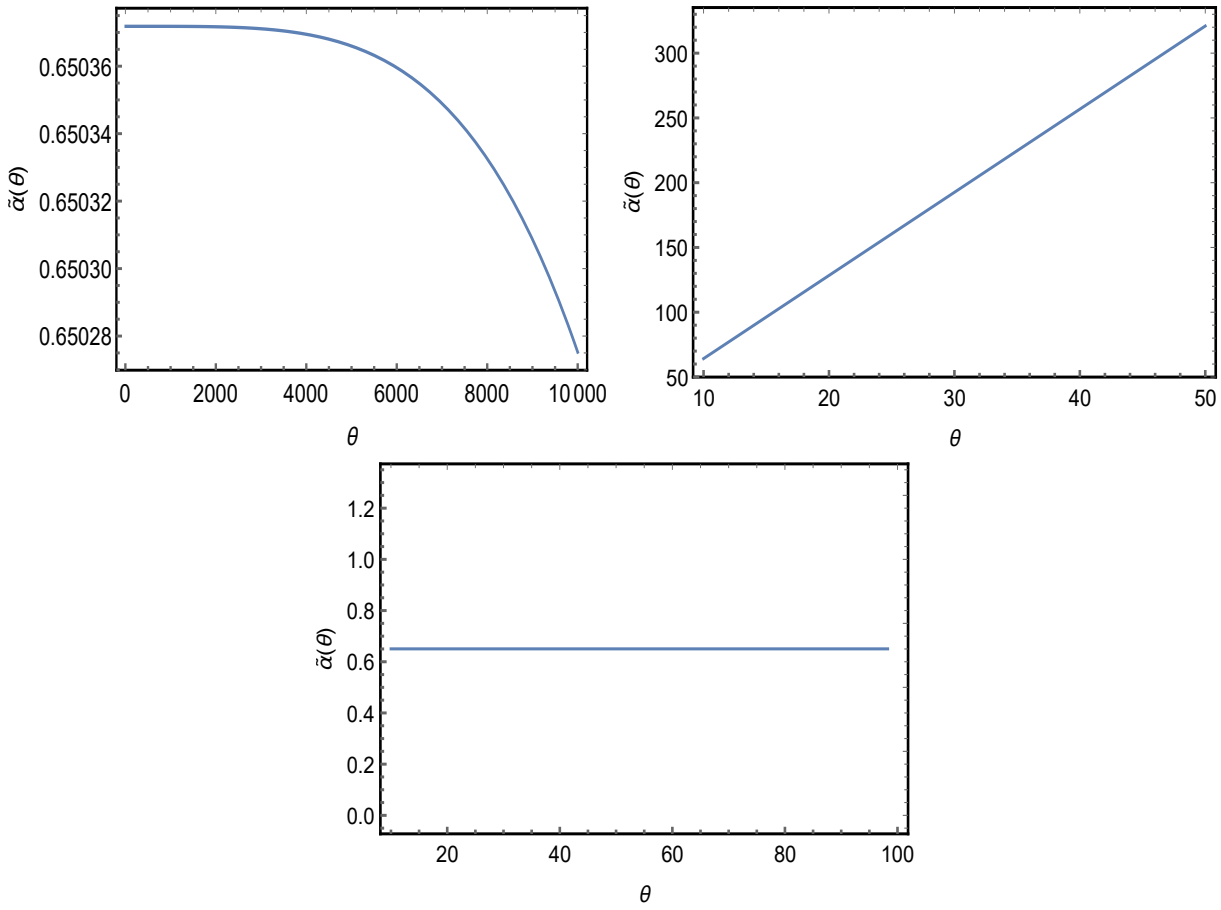

Fig. 6.2: The figure shows the correction to the *Stefan–Boltzmann* law represented by parameter $\tilde{\alpha}$ as a function of θ considering $k_B = 1$ and the temperature in the early inflationary universe i.e., $\beta = 10^{-13}$ GeV^{-1}.

Analogously, the remaining thermodynamic functions can be explicitly computed:

$$F(\beta,\theta) = \frac{1}{\theta\pi^2\beta}\int_0^\infty E\sqrt{E^2\theta^2-1}\ln\left(1-e^{-\beta E}\right)\mathrm{d}E, \tag{6.16}$$

$$S(\beta,\theta) = \frac{k_B}{\theta\pi^2}\left(-\int_0^\infty E\sqrt{E^2\theta^2-1}\ln\left(1-e^{-\beta E}\right)+\beta\int_0^\infty \frac{E^2\sqrt{E^2\theta^2-1}\,e^{-\beta E}}{1-e^{-\beta E}}\right)\mathrm{d}E, \tag{6.17}$$

$$C_V(\beta,\theta) = \frac{k_B\beta^2}{\theta\pi^2}\left(+\int_0^\infty \frac{E^3\sqrt{E^2\theta^2-1}\,e^{-2\beta E}}{\left(1-e^{-\beta E}\right)^2}+\int_0^\infty \frac{E^3\sqrt{E^2\theta^2-1}\,e^{-\beta E}}{1-e^{-\beta E}}\right)\mathrm{d}E, \tag{6.18}$$

and the following results ascribed to them are displayed in Figs. 6.3, 6.4 and 6.5 respectively.

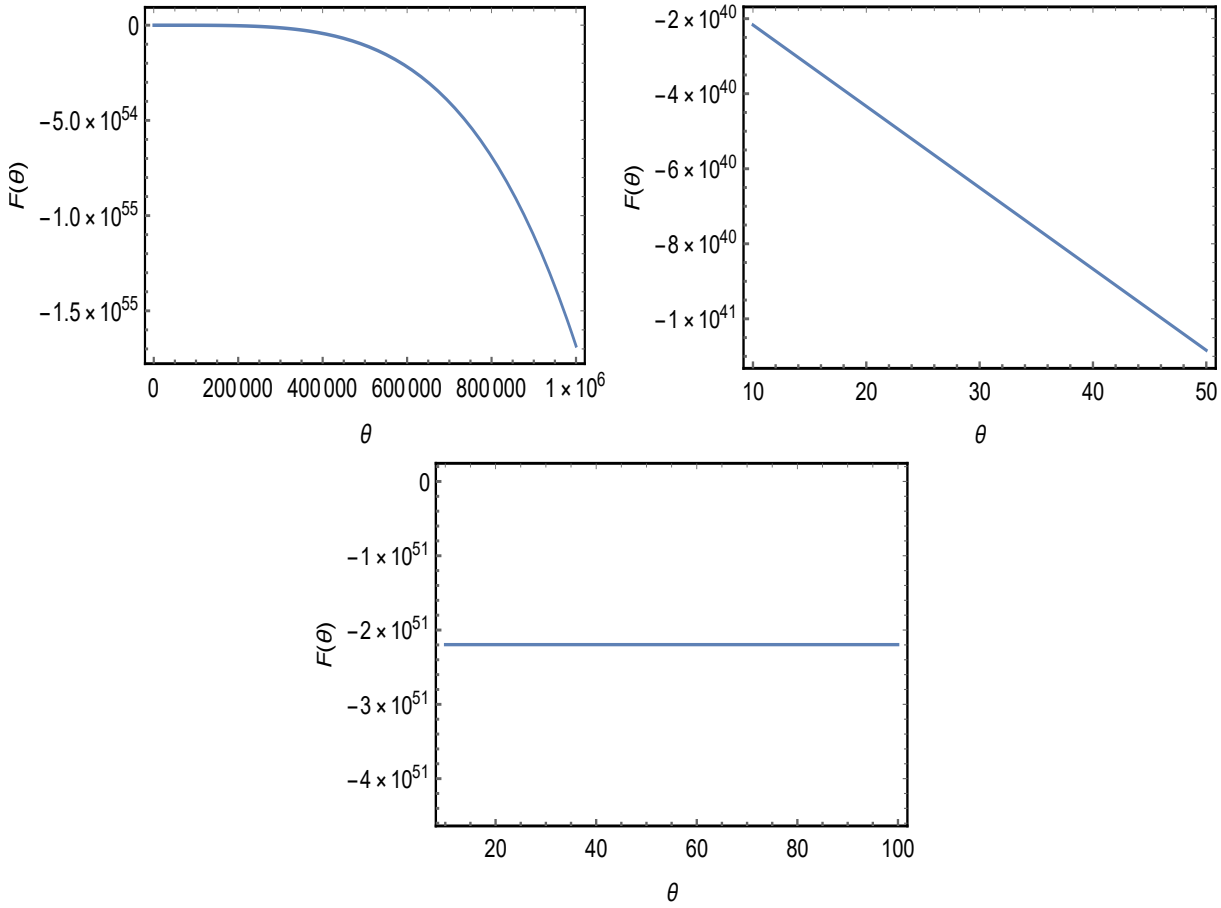

Fig. 6.3: The figure exhibits the solutions to Helmholtz free energy $F(\theta)$ at high temperature regime considering $k_B = 1$.

6.2 Podolsky with Lorentz violation

6.2.1 The model

Here, we study the Podolsky electrodynamics modified by the traceless LV dimension-6 term presented in Ref.[271]. In this work, the authors analyzed the classical aspects of such theory taking into account unitariry and causality from the study of the respective propagator proceeding analogously to it is already established in the literature [501, 502]. They consider the construction of a closed algebra using the prescription $D_{\mu\nu} = (B_\mu C_\nu - B_\nu C_\mu)/2$, where B_μ and C_ν are constant background vectors which accounts for LV. In this sense, the Lagrangian density which represents this model is given by

$$\mathcal{L} = -\frac{1}{4}F_{\mu\nu}F^{\mu\nu} + \frac{\theta^2}{2}\partial_\alpha F^{\alpha\beta}\partial_\lambda F^{\lambda}{}_{\beta} + \eta^2 D_{\beta\alpha}\partial_\sigma F^{\sigma\beta}\partial_\lambda F^{\lambda\alpha} + \frac{1}{2\xi}(\partial_\mu A^\mu)^2, \tag{6.19}$$

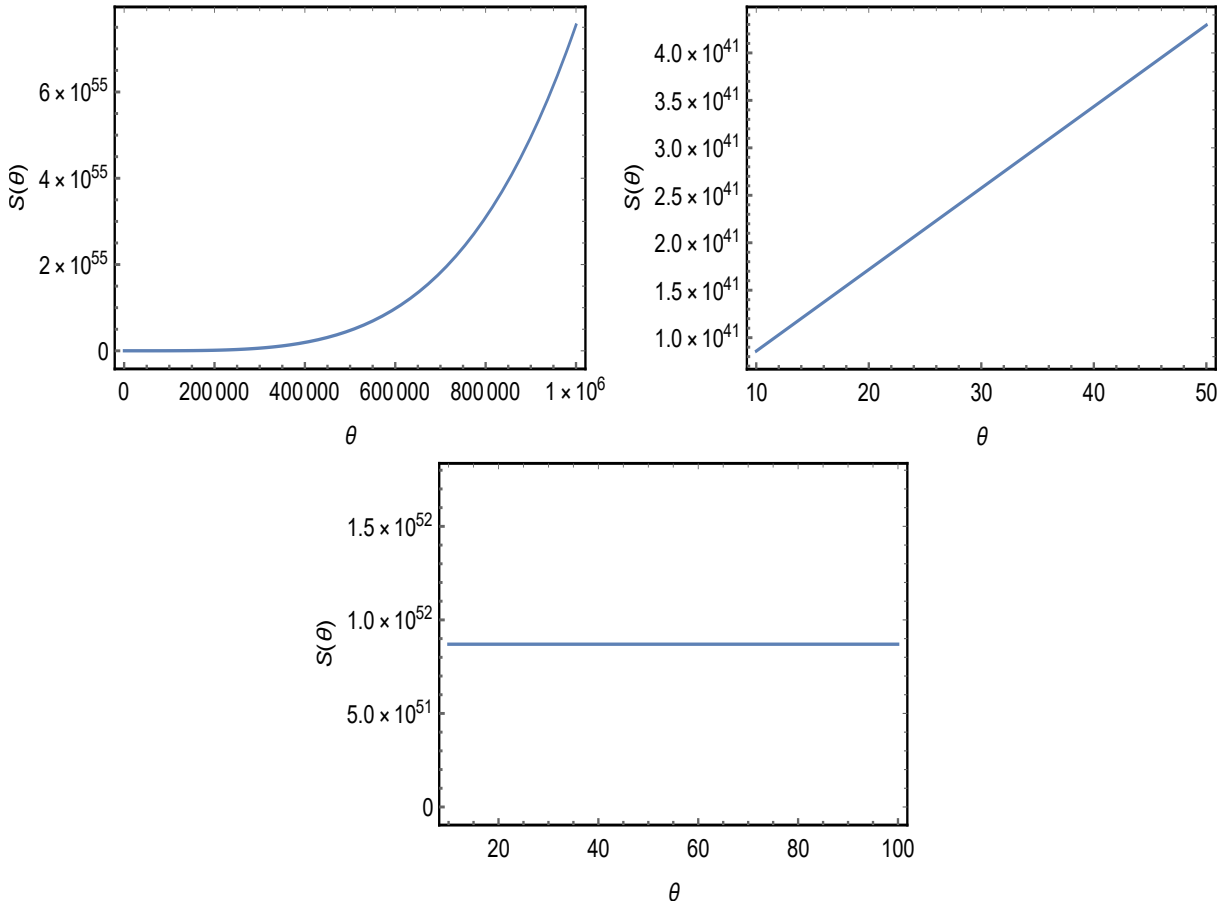

Fig. 6.4: These three graphics exhibit the behavior of the entropy $S(\theta)$ considering the temperature in the primitive inflationary universe where $k_B = 1$.

where θ is the same parameter defined previously, η is the constant coupling with dimension of mass $[m]^{-1}$ and ξ is the gauge fixing parameter required to evaluate the respective propagator. Nevertheless, we focus only on the investigation of its dispersion relation presented in the poles of the propagator for the sake of calculating the following thermodynamic functions. Therefore, the poles are given by

$$k^2(1-\theta^2k^2)\gamma(k) = 0, \tag{6.20}$$

where $\gamma(k) = \eta^4[(B\cdot k)^2 - B^2k^2][(C\cdot k)^2 - C^2k^2] - \left[1 - \theta^2k^2 - \eta^2(B\cdot C)k^2 + \eta^2(B\cdot k)(C\cdot k)\right]^2$. Considering the complete isotropic sector in this theory, i.e., $D_{\mu\nu} = -D_{00}\times \mathbf{diag}(3,1,1,1)_{\mu\nu}$, Eq. (6.20) turns out to be written as

$$E = \sqrt{\left(1 - \frac{8\eta^2 D_{00}}{\theta^2 + 2\eta^2 D_{00}}\right)\mathbf{k}^2 + \frac{1}{\theta^2 + 2\eta^2 D_{00}}}. \tag{6.21}$$

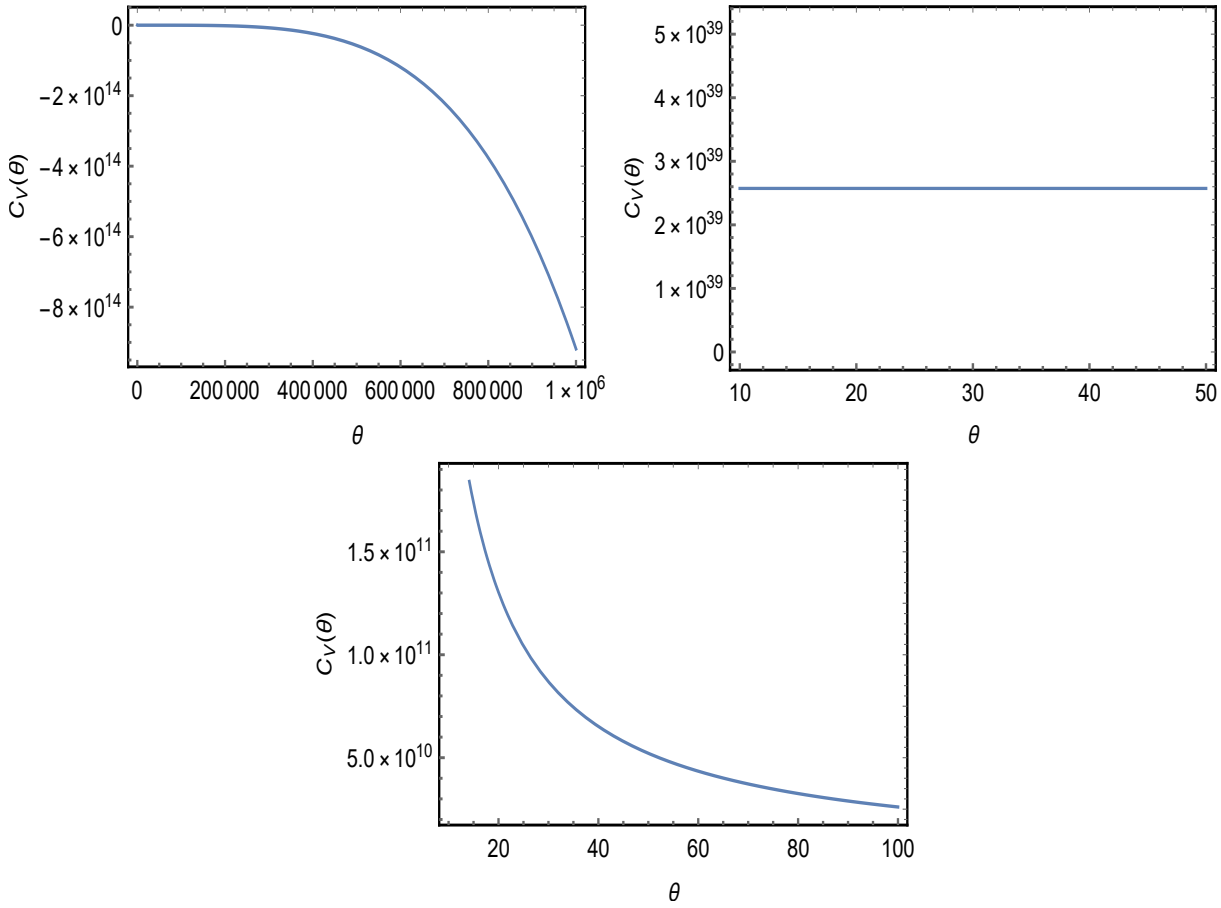

Fig. 6.5: The plots exhibit solutions to the heat capacity $C_V(\theta)$ considering $k_B = 1$ and the temperature at the beginning inflationary universe.

As it was accomplished in the last section, in what follows, we calculate the accessible states for this configuration which accounts for the Lorentz violation. Next, we proceed likewise.

6.2.2 Thermodynamic properties

The number of accessible states per volume is

$$\bar{\Omega}(E) = \frac{1}{\pi^2}\int_0^\infty E\left(1-\frac{8\eta^2 D_{00}}{\theta^2+2\eta^2 D_{00}}\right)^{-3/2}\left[\frac{E^2(\theta^2+2\eta^2 D_{00})-1}{\theta^2+2\eta^2 D_{00}}\right]^{1/2} \mathrm{d}E, \tag{6.22}$$

and, from it, we can construct the respective partition function for such theory which follows

$$\ln[\bar{Z}(\beta,\eta,\theta,D_{00})] = -\frac{1}{\pi^2}\int_0^\infty E\left(1-\frac{8\eta^2 D_{00}}{\theta^2+2\eta^2 D_{00}}\right)^{-3/2}\left[\frac{E^2(\theta^2+2\eta^2 D_{00})-1}{\theta^2+2\eta^2 D_{00}}\right]^{1/2} \ln\left(1-e^{-\beta E}\right) \mathrm{d}E \tag{6.23}$$

and using the definitions established in (9.8), we calculate Helmholtz free energy, mean energy, entropy, and heat capacity. At the beginning, we devote our attention to the spectral

radiance as we did before. The respective plot of $\bar{\chi}$ as a function of frequency ν for different values of η is shown in Fig. 6.6. In agreement with the previous section, in which we accomplished the correction to the *Stefan–Boltzmann* law exhibited in Eq. (8.25), we step forward likewise

$$\bar{\alpha} \equiv \bar{U}(\beta, \eta, \theta, D_{00})\beta^4. \tag{6.24}$$

Again, this analysis will be performed via numerical approach in the context of primordial temperature of the universe. To perform such calculation, we need to obtain the behavior of the mean energy. In this way,

$$\bar{U}(\beta, \eta, \theta, D_{00}) = \frac{1}{\pi^2}\int_0^\infty E^2\left(1 - \frac{8\eta^2 D_{00}}{\theta^2 + 2\eta^2 D_{00}}\right)^{-3/2}\left[\frac{E^2(\theta^2 + 2\eta^2 D_{00}) - 1}{\theta^2 + 2\eta^2 D_{00}}\right]^{1/2}\frac{e^{-\beta E}}{1 - e^{-\beta E}}\,\mathrm{d}E, \tag{6.25}$$

with the spectral radiance (plotted in Fig. 6.6) being given by

$$\bar{\chi}(\beta, \eta, \theta, D_{00}) = \frac{1}{\pi^2}E^2\left(1 - \frac{8\eta^2 D_{00}}{\theta^2 + 2\eta^2 D_{00}}\right)^{-3/2}\left[\frac{E^2(\theta^2 + 2\eta^2 D_{00}) - 1}{\theta^2 + 2\eta^2 D_{00}}\right]^{1/2}\frac{e^{-\beta E}}{1 - e^{-\beta E}}. \tag{6.26}$$

Here, the remaining thermodynamics functions are provided bellow: the Helmholtz free energy

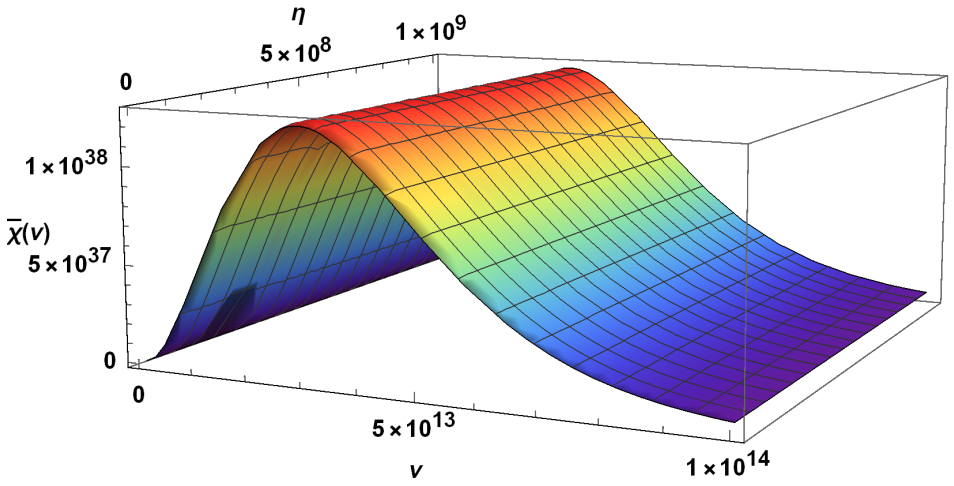

Fig. 6.6: The figure shows the behavior of the black body radiation in the generalized Podolsky electrodynamics with Lorentz violation for fixed values of $\theta = 10$ and $D_{00} = 1$.

$$\bar{F}(\beta, \eta, \theta, D_{00}) = \frac{1}{\pi^2\beta^2}\int_0^\infty E\left(1 - \frac{8\eta^2 D_{00}}{\theta^2 + 2\eta^2 D_{00}}\right)^{-3/2}\left[\frac{E^2(\theta^2 + 2\eta^2 D_{00}) - 1}{\theta^2 + 2\eta^2 D_{00}}\right]^{1/2}\ln\left(1 - e^{-\beta E}\right)\,\mathrm{d}E, \tag{6.27}$$

the entropy

$$\bar{S}(\beta,\eta,\theta,D_{00}) = -\frac{1}{\pi^2}\int_0^\infty E\left(1-\frac{8\eta^2 D_{00}}{\theta^2+2\eta^2 D_{00}}\right)^{-3/2}\left[\frac{E^2(\theta^2+2\eta^2 D_{00})-1}{\theta^2+2\eta^2 D_{00}}\right]^{1/2}\ln\left(1-e^{-\beta E}\right)\,\mathrm{d}E$$
$$+\frac{\beta}{\pi^2}\int_0^\infty E^2\left(1-\frac{8\eta^2 D_{00}}{\theta^2+2\eta^2 D_{00}}\right)^{-3/2}\left[\frac{E^2(\theta^2+2\eta^2 D_{00})-1}{\theta^2+2\eta^2 D_{00}}\right]^{1/2}\frac{e^{-\beta E}}{1-e^{-\beta E}}\mathrm{d}E, \tag{6.28}$$

and finally, the heat capacity

$$\bar{C}_V(\beta,\eta,\theta,D_{00}) = +\frac{\beta^2}{\pi^2}\int_0^\infty E^3\left(1-\frac{8\eta^2 D_{00}}{\theta^2+2\eta^2 D_{00}}\right)^{-3/2}\left[\frac{E^2(\theta^2+2\eta^2 D_{00})-1}{\theta^2+2\eta^2 D_{00}}\right]^{1/2}\frac{e^{-2\beta E}}{\left(1-e^{-\beta E}\right)^2}\mathrm{d}E$$
$$+\frac{\beta^2}{\pi^2}\int_0^\infty E^3\left(1-\frac{8\eta^2 D_{00}}{\theta^2+2\eta^2 D_{00}}\right)^{-3/2}\left[\frac{E^2(\theta^2+2\eta^2 D_{00})-1}{\theta^2+2\eta^2 D_{00}}\right]^{1/2}\frac{e^{-\beta E}}{1-e^{-\beta E}}\mathrm{d}E. \tag{6.29}$$

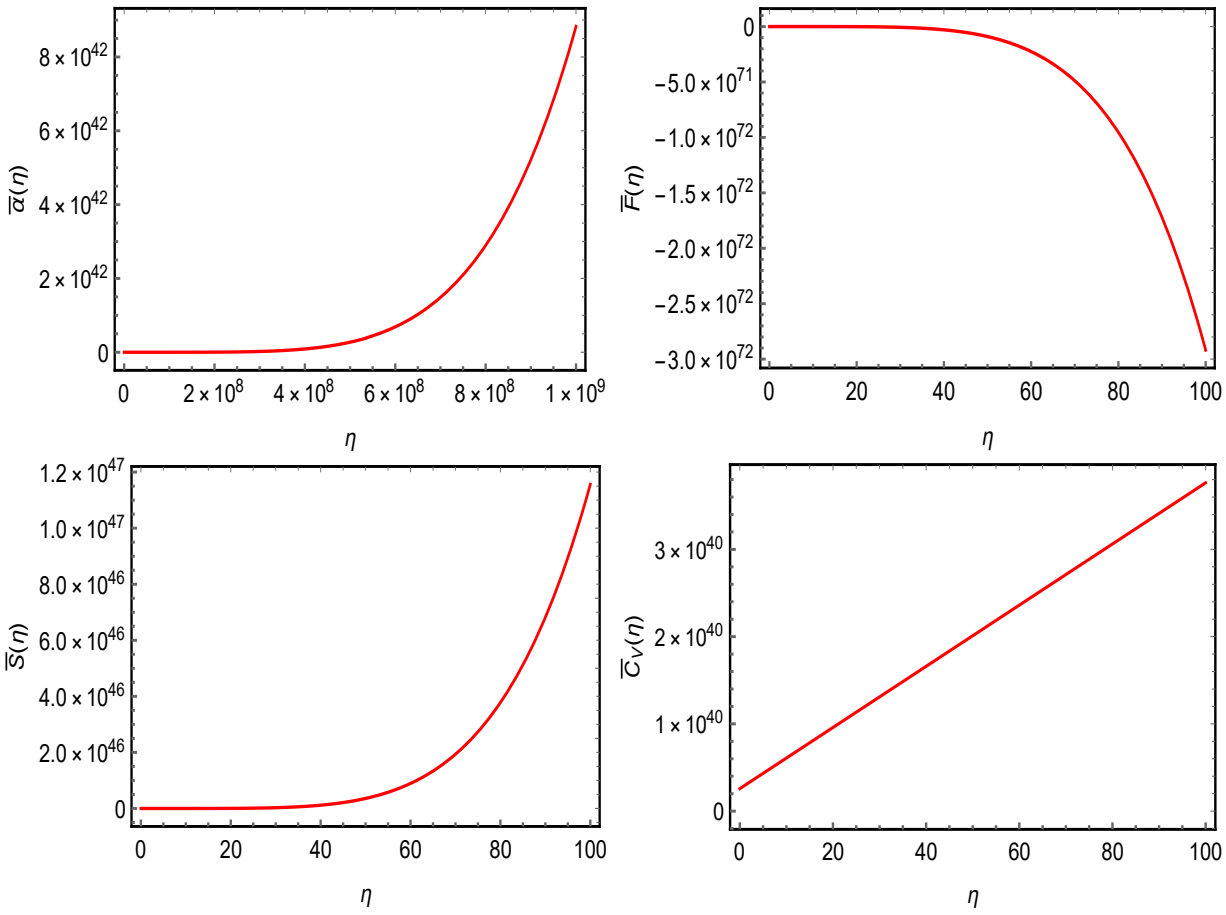

Fig. 6.7: The graphics show the correction to the *Stefan–Boltzmann* law $\bar{\alpha}(\eta)$, entropy $\bar{S}(\eta)$, Helmholtz free energy $\bar{F}(\eta)$ and heat capacity $\bar{C}_V(\eta)$ regarding $k_B = 1$.

6.3 Results and discussions

Initially, let us focus our attention on the pure Podolsky electrodynamics. Indeed, we determined the expression of the spectral radiance $\chi(\nu)$ exhibited in (8.23) with its plot displayed in Fig. 6.1. From it, we could see that $\chi(\nu)$ was sensitive to changes of θ i.e., θ= 10, θ= 30, θ= 50, θ= 70, θ= 90. We made a comparison of these different values to the black body radiation with the Maxwell theory. We noted that the latter had its spectral radiance smaller than the Podolsky one. It is important to note that to accomplish such analysis, we needed to consider the limit where $E^2\sqrt{E^2\theta^2-1} \gg \theta$. Next, we did the plot of Fig. 6.2 which showed the correction to the *Stefan–Boltzmann* law represented by parameter $\tilde{\alpha}(\theta)$ considering the temperature in the early inflationary universe i.e., $\beta = 10^{-13}$ GeV^{-1}. The upper graph in the left side exhibited a very slow variation of $\tilde{\alpha}(\theta)$ when θ varied. Moreover, we considered small variations of θ, which entailed a constant behavior (it was displayed in the lower graphic). On the other hand, we considered instead of the condition in which $E^2\sqrt{E^2\theta^2-1} \gg \theta$ and, therefore, we obtained a linear behavior of such graphic which was shown in the upper graph in the right side.

In Fig 6.3, a similar analysis could be done. In this sense, we have exhibited three configurations to Helmholtz free energy $F(\beta,\theta)$, considering the primitive temperature in the early universe. The top left exhibited a very slow variation of $F(\beta,\theta)$ when θ changed. Besides, we considered small variations of θ, and the graphic exhibited a constant behavior, as shown in the bottom graphic. On the other hand, we rather regarded a situation where $E^2\sqrt{E^2\theta^2-1} \gg \theta$. Thereby, we had a linear behavior with a negative angular coefficient, though which was displayed in the top right.

Likewise, Figs. 6.4 and 6.5 exhibited different behaviors of entropy $S(\theta)$ and heat capacity $C_V(\theta)$ for diverse values of θ analogously to what we did in the analysis accomplished for $\tilde{\alpha}(\theta)$ and $F(\theta)$ considering high temperature regime. Specifically, in Fig. 6.4 the upper graph on the left hand showed a variation of $S(\beta,\theta)$ when θ started to increase. Moreover, having regarded rather a situation where there existed the limit when $E^2\sqrt{E^2\theta^2-1} \gg \theta$, one possessed a linear behavior with a positive angular coefficient which was shown in the upper graph on the right hand. In addition, the bottom one exhibited how entropy $S(\beta,\theta)$ behaved for close values of θ. Furthermore, in Fig. 6.5, the top left showed a variation of $C_V(\beta,\theta)$ when θ started to increase drastically and if one rather regarded a situation where there was the limit when $E^2\sqrt{E^2\theta^2-1} \gg \theta$, one would have a constant behavior which was shown in the top right. Besides, the bottom one revealed how heat capacity $C_V(\beta,\theta)$ behaved for close values of θ.

Now, let us focus on the generalization of the Podolsky electrodynamics with the Lorentz-symmetry violation. Fig. 6.6 displayed the behavior of the black body radiation as a function

of η and ν for fixed values of θ and D_{00} i.e., $\theta = 10$ and $D_{00} = 1$, in the generalized Podolsky electrodynamics. Next, we analyzed Fig. 6.7, which was the compilation of all thermodynamic functions in order to provide a concise discussion on this recent electrodynamics. Considering the plot to $\bar{\alpha}(\eta)$ for huge values of η, we obtained a strong positive inclination of such curve, which differed from the pure Podolsky theory due to its increasing characteristic. A similar analysis was shown in $\bar{S}(\eta)$, but for a different range of η though i.e., $0 \leq \eta \leq 100$. Additionally, it had the same behavior encountered in the plot of $S(\theta)$. In the same range of η, we verified that there existed a negative curve for Helmholtz free energy $\bar{F}(\eta)$ as well being in agreement with the usual Podolsky case. Next, for the case of heat capacity $\bar{C}_V(\eta)$, it was displayed a linear increase with a positive angular coefficient when η started to increase. Also, the behavior of this curve was completely different from heat capacity $C_V(\theta)$ exhibited in the Podolsky electrodynamics.

7. LORENTZ-VIOLATING SCENARIOS IN A THERMAL RESERVOIR

7.1 Graviton with Lorentz violation

In this section, we begin with the action responsible for the dynamics of the bumblebee field B_μ written as

$$S_B = \int \mathrm{d}^4x\sqrt{-g}\left[-\frac{1}{4}B^{\mu\nu}B_{\mu\nu} + \frac{2\xi}{\kappa^2}B^\mu B^\nu R_{\mu\nu} - V(B^\mu B_\mu \mp b^2)\right], \tag{7.1}$$

where $B_{\mu\nu} = \partial_\mu B_\nu - \partial_\nu B_\mu$, ξ is a positive parameter which allows the nonminimal coupling between the bumblebee field and the Ricci tensor $R_{\mu\nu}$, and $\kappa^2 = 32\pi G$ is the gravitational coupling constant. Here, it is worth mentioning that, considering the natural units, the mass dimension of such fields and parameters are $[B^\mu] = 1$, $[B^{\mu\nu}] = 2$, $[\kappa^2] = -2$, $[\xi] = -2$. Next, seeking for simplicity, we adopt the smooth quadratic potential which triggers the spontaneous Lorentz symmetry breaking

$$V = \frac{\lambda}{2}\left(B_\mu B^\mu \mp b^2\right)^2, \tag{7.2}$$

where the vector b_μ is the vacuum expectation value of the bumblebee field B_μ having its minimum when $g_{\mu\nu}B^\mu B^\nu \pm b^2 = 0$. In Ref. [503], regardless torsion, the authors examined the graviton spectrum using the weak field approximation for the Einstein-Hilbert gravity in the context of Lorentz violation. For the sake of obtaining its respective Feynman propagator, we focus only on the kinetic part

$$\mathcal{L}_{kin} = -\frac{1}{2}h^{\mu\nu}\hat{\mathcal{O}}_{\mu\nu,\alpha\beta}h^{\alpha\beta}, \tag{7.3}$$

where $\hat{\mathcal{O}}^{\mu\nu}{}_{\lambda\sigma}$ is the wave operator associated to the theory. Following the definitions encountered in Ref. [504], the graviton propagator is defined as follows

$$\langle 0|T[h_{\mu\nu}(x)h_{\alpha\beta}(y)]|0\rangle = D_{\mu\nu,\alpha\beta}(x-y). \tag{7.4}$$

Here, the main issue is finding a closed tensor algebra in order to obtain such operator $D_{\mu\nu,\alpha\beta}(x-y)$ which satisfies the Green's function

$$\hat{\mathcal{O}}^{\mu\nu}{}_{\lambda\sigma}D^{\lambda\sigma,\alpha\beta}(x-y) = i\mathcal{I}^{\mu\nu,\alpha\beta}\delta^4(x-y), \tag{7.5}$$

where $\mathcal{I}^{\mu\nu,\alpha\beta}$ plays the role of the identity operator being defined as $\mathcal{I}^{\mu\nu,\alpha\beta} = \frac{1}{2}(\eta^{\mu\alpha}\eta^{\nu\beta} + \eta^{\mu\beta}\eta^{\nu\alpha})$. Now, after many algebraic manipulations seeking the inversion of the wave operator $\hat{\mathcal{O}}^{\mu\nu}{}_{\lambda\sigma}$, we get

$$\begin{aligned} D_{\mu\nu,\alpha\beta} =& \frac{i}{\boxplus(k)}\left\{\frac{N_1}{\kappa^2\xi^2(b\cdot k)^2\boxdot}\mathrm{P}^{(1)}_{\mu\nu,\alpha\beta} + \mathrm{P}^{(2)}_{\mu\nu,\alpha\beta} - \frac{1}{2}\mathrm{P}^{(0-\theta)}_{\mu\nu,\alpha\beta} + \frac{N_4}{2\lambda\kappa^2\xi^2(b\cdot k)^2\boxdot^2}\mathrm{P}^{(0-\omega)}_{\mu\nu,\alpha\beta}\right. \\ &+\frac{k^2}{\boxdot}\Pi^{(2)}_{\mu\nu,\alpha\beta} + \frac{N_5}{2\xi(b\cdot k)^2\boxdot}\tilde{\mathrm{P}}^{(0-\theta\omega)}_{\mu\nu,\alpha\beta} + \frac{k^2}{\xi(b\cdot k)\boxdot}\tilde{\Pi}^{(1)}_{\mu\nu,\alpha\beta} + \frac{N_8}{4\xi(b\cdot k)\boxdot}\tilde{\Pi}^{(\theta\Sigma)}_{\mu\nu,\alpha\beta} \\ &-\frac{\sqrt{3}k^2}{2\boxdot}\tilde{\Pi}^{(\theta\Lambda)}_{\mu\nu,\alpha\beta} + \frac{k^4}{2\boxdot^2}\tilde{\Pi}^{(\Lambda\Lambda)}_{\mu\nu,\alpha\beta} + \frac{N_{11}}{8\xi^2(b\cdot k)^2\boxdot^2}\tilde{\Pi}^{(\omega\Lambda-a)}_{\mu\nu,\alpha\beta} \\ &\left.+\frac{N_{12}}{2\xi(b\cdot k)^2\boxdot^2}\tilde{\Pi}^{(\omega\Lambda-b)}_{\mu\nu,\alpha\beta} + \frac{N_{13}}{4\kappa^2\xi^2(b\cdot k)^3\boxdot^2}\tilde{\Pi}^{(\omega\Sigma)}_{\mu\nu,\alpha\beta} + \frac{N_{14}}{4\xi(b\cdot k)\boxdot^2}\tilde{\Pi}^{(\Lambda\Sigma)}_{\mu\nu,\alpha\beta}\right\}, \end{aligned} \tag{7.6}$$

with $\boxplus(k)$ and $\boxdot(k)$ being given by

$$\boxplus(k) = k^2 + \xi(b\cdot k)^2, \tag{7.7}$$

and

$$\boxdot(k) = (b\cdot k)^2 - b^2k^2, \tag{7.8}$$

where our attention will be devoted. Moreover, such propagator[1] was verified to be physical reasonable, since it is in agreement with causality and unitarity. Nevertheless, there is no necessity of working with the full expression in our case, since all we need is fully contained in the pole of the propagator, i.e., $\boxplus(k)$. More so, it is important to mention that the pole $\boxdot(k)$ will be overlook due to the fact that it does not represent a physical mode, since it gives rise to nonunitary dispersion relation in the spacelike configuration, and it has no positive defined energy in the timelike configuration as well.

In possession of this, the following calculations will be performed in order to derive all the main thermodynamic functions. For doing so, we proceed further seeking the number of the available states of the system in order to build up the so-called partition function. Here, we start with the following dispersion relation given by

$$k^2 + \xi(b\cdot k)^2 = 0,$$

[1]If one is interested in any missing definitions of Eq. (7.6), see Ref. [503] for further details.

and, in this sense, we take the unitary time like configuration for b_μ, namely $b_\mu = (1, \mathbf{0})$, which yields the accessible states of the system written as

$$\Omega(\xi) = \frac{\overset{\sim}{\Gamma}}{\pi^2} \int_0^\infty (1+\xi)^{3/2} E^2 \, \mathrm{d}E, \tag{7.9}$$

where $\overset{\sim}{\Gamma}$ is the volume of the thermal reservoir. Now, let us remind here that the link between the thermal behavior and the macroscopic world is carried out by the partition function. Then, we are properly able to write it down

$$\ln\left[Z(\beta,\Gamma)\right] = -\frac{\overset{\sim}{\Gamma}}{\pi^2} \int_0^\infty (1+\xi)^{3/2} E^2 \ln\left(1 - e^{-\beta E}\right) \mathrm{d}E, \tag{7.10}$$

where $\beta = 1/\kappa_B T$ and T is the temperature of the Universe. The above expression is similar to Bose-Einstein statistics but rather having a modification due to parameter ξ. In a straightforward manner, using the advantage of taking into account Eq.(7.10), we can obtain the thermodynamic functions per volume $\overset{\sim}{\Gamma}$, namely, the Helmholtz free energy $F(\beta,\xi)$, the mean energy $U(\beta,\xi)$, the entropy $S(\beta,\xi)$ and the heat capacity $C_V(\beta,\xi)$, defined as follows:

$$\begin{aligned}
F(\beta,\xi) &= -\frac{1}{\beta}\ln\left[Z(\beta,\xi)\right], \\
U(\beta,\xi) &= -\frac{\partial}{\partial\beta}\ln\left[Z(\beta,\xi)\right], \\
S(\beta,\xi) &= k_B\beta^2\frac{\partial}{\partial\beta}F(\beta,\xi), \\
C_V(\beta,\xi) &= -k_B\beta^2\frac{\partial}{\partial\beta}U(\beta,\xi).
\end{aligned} \tag{7.11}$$

At the beginning, let us consider the mean energy

$$U(\beta,\xi) = \frac{1}{\pi^2}\int_0^\infty \frac{(1+\xi)^{3/2}E^3\, e^{-\beta E}}{\left(1-e^{-\beta E}\right)}\mathrm{d}E, \tag{7.12}$$

which follows the spectral radiance given by:

$$\chi(\xi,\nu) = \frac{(h\nu)^3(1+\xi)^{3/2}\, e^{-\beta h\nu}}{\pi^2\left(1-e^{-\beta h\nu}\right)}, \tag{7.13}$$

where we have regarded $E = h\nu$, as h being the Planck constant and ν the frequency. The plot of the above equation is exhibited in Fig. 7.1 concerning three different cases when parameters ξ and β vary. This and other comments are better explained and discussed in Section 7.3. Looking towards to recover the radiation constant of the *Stefan-Boltzmann*

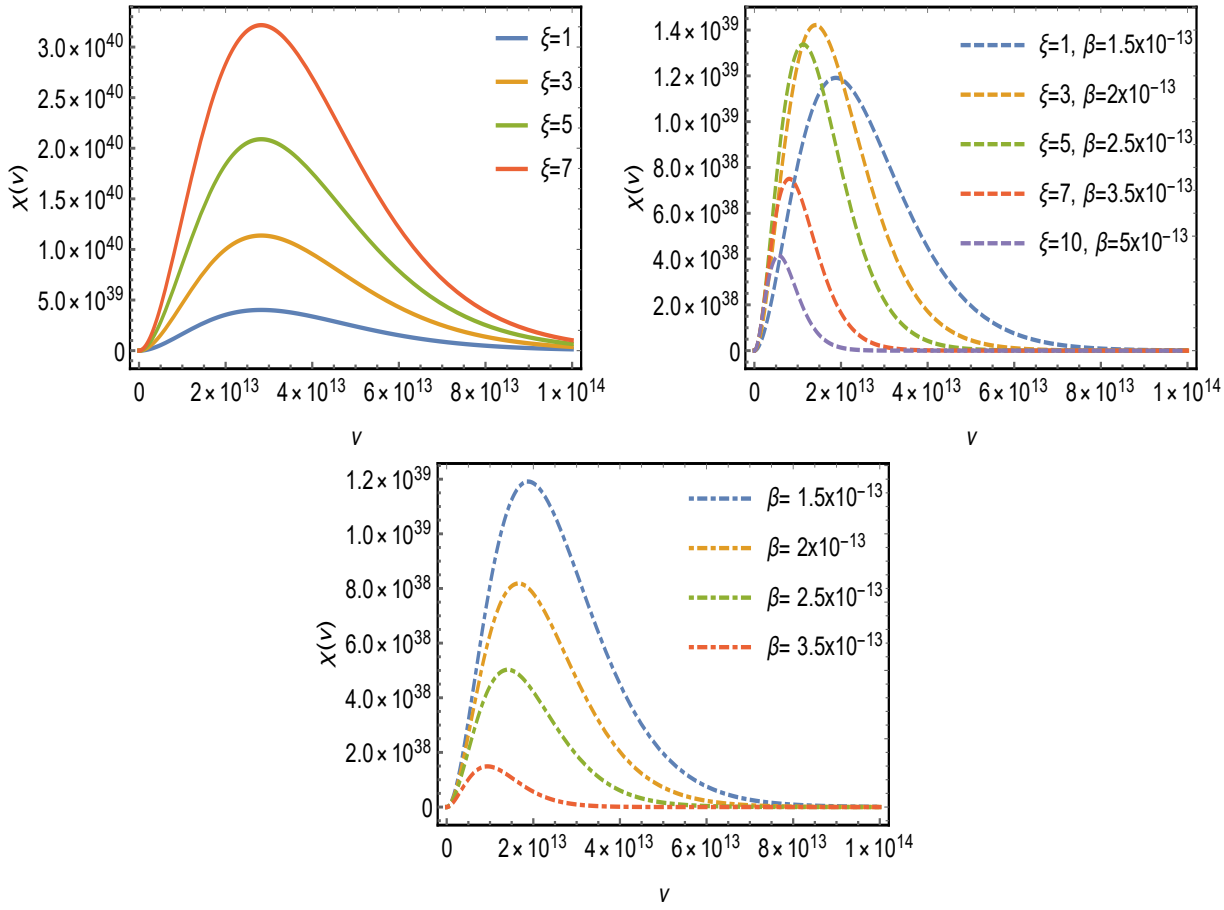

Fig. 7.1: The plots exhibit how the spectral radiance $\chi(\nu)$ changes as a function of frequency ν for different scenarios with $h = 1$.

energy, i.e., $u_S = \alpha T^4$, we consider $\xi \longrightarrow 0$ leading to

$$\alpha = \frac{1}{\pi^2}\int_0^\infty \frac{E^3\, e^{-\beta E}}{\left(1 - e^{-\beta E}\right)} \mathrm{d}E = \frac{\pi^2}{15}, \tag{7.14}$$

which reproduces the well-established result in the literature [505]. Now, for the sake of completeness, it is important to point out that hereafter, unless stated otherwise, all the following computations will be performed having the temperature $\beta = 10^{-13}\,\mathrm{GeV}^{-1}$, $\kappa_B = 1$, as well as the density per volume $\overset{\sim}{\Gamma}$ approach. In this sense, in order to check how the coupling constant ξ affects the new radiation constant and all the remaining thermodynamic functions, we proceed as follows:

$$\tilde{\alpha} \equiv U(\beta, \xi)\beta^4, \tag{7.15}$$

and we calculate the Helmholtz free energy

$$F(\beta, \xi) = \frac{1}{\pi^2\beta}\int_0^\infty (1+\xi)^{3/2} E^2 \ln\left(1 - e^{-\beta E}\right) \mathrm{d}E, \tag{7.16}$$

the entropy

$$S(\beta,\xi)=\frac{\kappa_B}{\pi^2}\left(-\int_0^\infty (1+\xi)^{3/2}E^2\ln\left(1-e^{-\beta E}\right)+\beta\int_0^\infty \frac{(1+\xi)^{3/2}E^3\,e^{-\beta E}}{1-e^{-\beta E}}\right)\mathrm{d}E, \quad (7.17)$$

and the heat capacity

$$C_V(\beta,\xi)=\frac{\kappa_B\beta^2}{\pi^2}\left(\int_0^\infty \frac{(1+\xi)^{3/2}E^4\,e^{-2\beta E}}{\left(1-e^{-\beta E}\right)^2}+\int_0^\infty \frac{(1+\xi)^{3/2}E^4\,e^{-\beta E}}{1-e^{-\beta E}}\right)\mathrm{d}E. \quad (7.18)$$

Now, having obtained these expressions, we can solve them and their following results are displayed in Fig. 7.2. Notably, within the context of a linearized theory of gravity, there exists a corresponding intrinsic entropy ascribed to any distribution of gravitational radiation [506] and a well-behavior conjecture having the absence of an ultraviolet catastrophe [507].

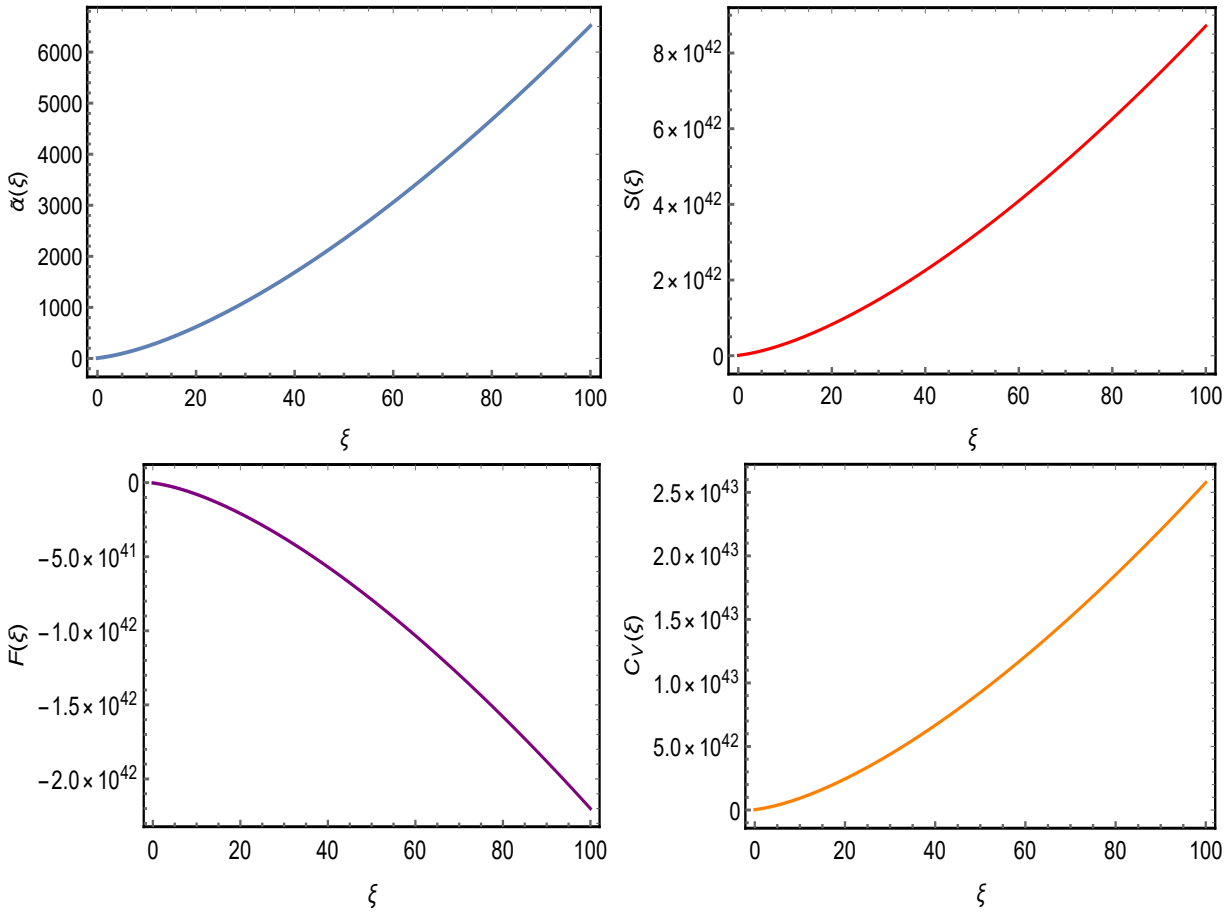

Fig. 7.2: The figure shows the correction to the so-called *Stefan–Boltzmann* law represented by parameter $\tilde{\alpha}(\xi)$, the entropy $S(\xi)$, the Helmholtz free energy $F(\xi)$ and the heat capacity $C_V(\xi)$, considering $\kappa_B=1$ in the high temperature regime of the universe, namely, $\beta=10^{-13}$ GeV^{-1}.

7.2 Generalized model with Podolsky and Lee-Wick terms

Recently, in the literature, the authors proposed an effective model of higher-derivative electrodynamics in the context of Lorentz violation which studies some classical aspects regarding unitarity and causality from the propagator, i.e., it is proposed a generalized model involving anisotropic Podolsky and Lee-Wick terms [271]. In such reference, it is used the advantage of regarding the spin-projection operators [502, 239], seeking a closed algebra in order to calculate the propagator of this respective theory. For doing so, the prescription of a rank-2 symmetric tensor $D_{\beta\alpha} = (B_\beta C_\alpha - B_\alpha C_\beta)/2$ (where B_β and C_α are constant background four-vectors which account for Lorentz violation) has been invoked. In this sense, it was considered a more general dimension-6 higher-derivative Lagrangian

$$\mathcal{L} = -\frac{1}{4}F^{\mu\nu}F_{\mu\nu} + \frac{\theta^2}{2}\partial_\alpha F^{\alpha\beta}\partial_\lambda F^\lambda{}_\beta + \eta_1^2 D_{\beta\alpha}\partial_\sigma F^{\sigma\beta}\partial_\lambda F^{\lambda\alpha} + \eta_2^2 D^{\beta\alpha}\partial_\sigma F^{\sigma\lambda}\partial_\beta F_{\alpha\lambda} + \frac{1}{2\tilde{\xi}}(\partial_\mu A^\mu)^2 \tag{7.19}$$

where θ, η_1 and η_2 are coupling constants with positive defined values and $\tilde{\xi}$ is the gauge fixing parameter to invert the wave operator associated with the Lagrangian of this theory. Besides, Eq. (7.19) leads to the corresponding propagator[2]

$$\begin{aligned}\tilde{\Xi}_{\nu\alpha}(k) = -\frac{i}{k^2\Delta(k)}\{&\tilde{\Gamma}(k)\Theta_{\nu\alpha} + [b' - \tilde{\xi}\Delta(k)]\Omega_{\nu\alpha} - i\tilde{F}(k)(B_\nu k_\alpha + B_\alpha k_\nu) \\ &- 2\eta_1^2 D_{\nu\alpha}k^2\tilde{\Pi}(k) - i\tilde{H}(k)(C_\nu k_\alpha + C_\alpha k_\nu) \\ &+ \eta_1^4 B_\nu B_\alpha[(C\cdot k)^2 - C^2k^2]k^2 + \eta_1^4 C_\nu C_\alpha[(B\cdot k)^2 - B^2k^2]k^2\},\end{aligned} \tag{7.20}$$

where $\tilde{\Gamma}(k) = \eta_1^4[(B\cdot k)^2 - B^2k^2][(C\cdot k)^2 - C^2k^2] - \{1 - \theta^2k^2 - \eta_1^2k^2(B\cdot C) + [\eta_1^2 - 2\eta_2^2]$ $\times (B\cdot k)(C\cdot k)\}^2$ and $\Delta(k) = [1 - \theta^2k^2 - \eta_2^2(B\cdot k)(C\cdot k)]\,\tilde{\Gamma}(k)$. In addition, Eq. (7.19) gives rise to the following dispersion relation

$$k^2\left[1 - \theta^2k^2 - \eta_2^2(B\cdot k)(C\cdot k)\right]\tilde{\Gamma}(k) = 0. \tag{7.21}$$

Here, let us regard a timelike isotropic configuration characterized by $B_\mu = (B_0, \mathbf{0})$ and $C_\mu = (C_0, \mathbf{0})$. This assumption gives rise to three *independent* dispersion relations to Eq. (7.21) [271] as follows

$$E_1^2 = \frac{1}{1 + 2\eta_2^2B_0C_0/\theta^2}\mathbf{k}^2 + \frac{1}{\theta^2 + 2\eta_2^2B_0C_0}, \tag{7.22}$$

[2]Likewise in the previous section, for any missing definitions of Eq. (7.20), see Ref.[271] for further details.

$$E_2^2 = \frac{\theta^2}{\theta^2 + 2\eta_2^2 B_0 C_0}\mathbf{k}^2 + \frac{1}{\theta^2 + 2\eta_2^2 B_0 C_0}, \tag{7.23}$$

and

$$E_3^2 = \frac{\theta^2 + 2\eta_1^2 B_0 C_0}{\theta^2 + 2\eta_2^2 B_0 C_0}\mathbf{k}^2 + \frac{1}{\theta^2 + 2\eta_2^2 B_0 C_0}, \tag{7.24}$$

where, notably, the term $1 + 2\eta_2^2 B_0 C_0/\theta^2$ may be identified as a dielectric constant modifying the usual Podolsky electrodynamics. In order to perform a complete analysis of the thermal aspects of this theory displayed in Eq. (7.21), we shall examine our system considering all dispersion relations shown in Eqs. (7.22), (7.23), and (7.24). To do so, we consider the following approach to acquire our results, namely, $E^2 = E_1^2 + E_2^2 + E_3^2$.

In possession of Eqs. (7.22), (7.23), (7.24) and considering a photon gas in a thermal bath, the number of available states can be derived in a straightforward way:

$$\bar{\Omega}(\theta, \eta_1, \eta_2, B_0, C_0) = \frac{1}{\pi^2}\int_0^\infty E\left(\frac{2\theta^2 + 2\eta_1^2 B_0 C_0}{\theta^2 + 2\eta_2^2 B_0 C_0}\right)^{-3/2}\sqrt{E^2 - \frac{3}{\theta^2 + 2\eta_2^2 B_0 C_0}}\,\mathrm{d}E, \tag{7.25}$$

yielding the partition function, which may be properly written as

$$\ln[\bar{Z}(\theta, \beta, \eta_1, \eta_2, B_0, C_0)] = -\frac{1}{\pi^2}\int_0^\infty E\left(\frac{2\theta^2 + 2\eta_1^2 B_0 C_0}{\theta^2 + 2\eta_2^2 B_0 C_0}\right)^{-3/2}\sqrt{E^2 - \frac{3}{\theta^2 + 2\eta_2^2 B_0 C_0}}\ln\left(1 - e^{-\beta E}\right)\mathrm{d}E, \tag{7.26}$$

Additionally, it is important to mention that in different contexts, many works have been made in such direction [272, 490, 489, 488, 356, 384] and a Podolsky term can be generated if quantum corrections are taken into account regarding a condensation of topological defects [332]. Here, from Eq. (7.26), an analogous process to calculate all those thermodynamic quantities presented in the previous section can be performed as well. In this way, we have the mean energy

$$\bar{U}(\theta, \beta, \eta_1, \eta_2, B_0, C_0) = \frac{1}{\pi^2}\int_0^\infty E^2\left(\frac{2\theta^2 + 2\eta_1^2 B_0 C_0}{\theta^2 + 2\eta_2^2 B_0 C_0}\right)^{-3/2}\sqrt{E^2 - \frac{3}{\theta^2 + 2\eta_2^2 B_0 C_0}}\left(\frac{e^{-\beta E}}{1 - e^{-\beta E}}\right)\mathrm{d}E, \tag{7.27}$$

which follows the spectral radiance

$$\bar{\chi}(\theta, \beta, \eta_1, \eta_2, B_0, C_0) = \frac{1}{\pi^2}E^2\left(\frac{2\theta^2 + 2\eta_1^2 B_0 C_0}{\theta^2 + 2\eta_2^2 B_0 C_0}\right)^{-3/2}\sqrt{E^2 - \frac{3}{\theta^2 + 2\eta_2^2 B_0 C_0}}\left(\frac{e^{-\beta E}}{1 - e^{-\beta E}}\right), \tag{7.28}$$

plotted in Fig. 7.3 for different values of η_2. Again, the same procedure of inferring how the new radiation constant of the *Stefan–Boltzmann* law behaves, namely $\bar{\alpha}(\theta, \beta, \eta_1, \eta_2, B_0, C_0)$, is performed as well in what follows. Next, we derive all the remaining ones: the Helmholtz

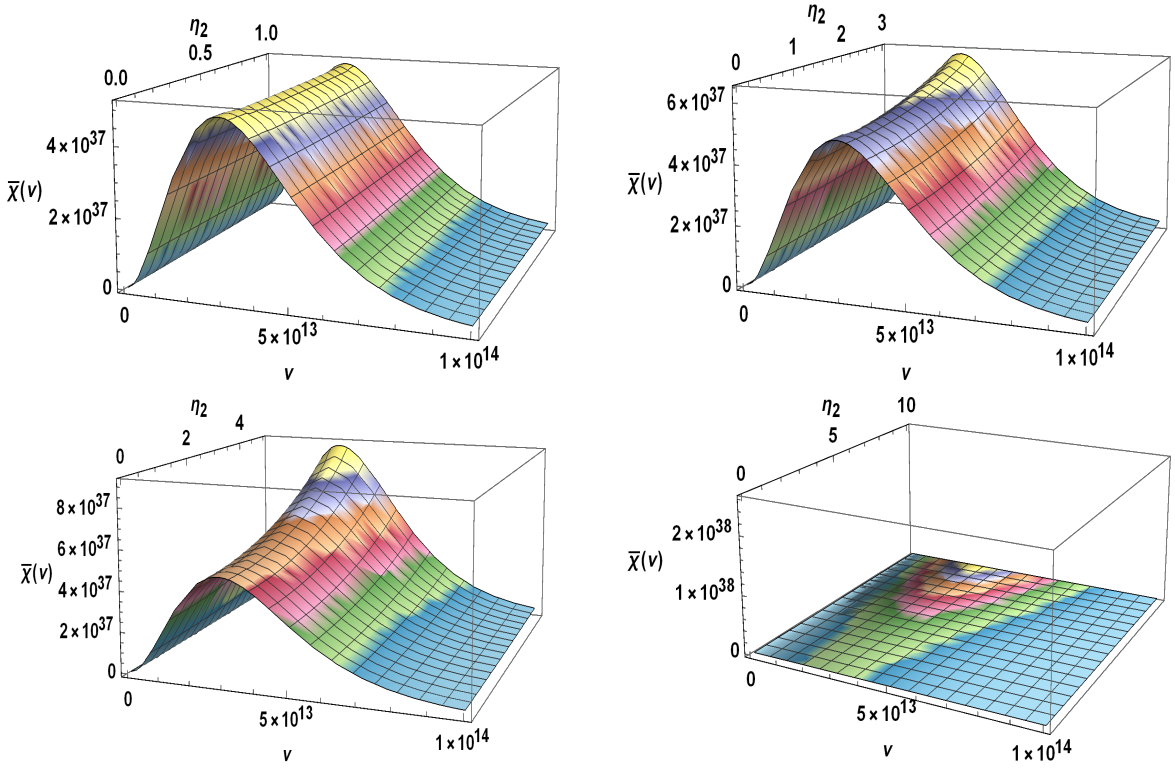

Fig. 7.3: This figure shows the behavior of the spectral radiance $\bar{\chi}(\nu)$ for different values of η_2 and ν. We consider fixed values of B_0, C_0 and θ, i.e., $\eta_1 = B_0 = C_0 = 1$ and $\theta = 10$, in the context of the temperature in the inflationary era of the universe, i.e., $\beta = 10^{-13}$ GeV^{-1}.

free energy

$$\bar{F}(\theta,\beta,\eta_1,\eta_2,B_0,C_0) = \frac{1}{\beta^2\pi^2}\int_0^\infty E\left(\frac{2\theta^2+2\eta_1^2B_0C_0}{\theta^2+2\eta_2^2B_0C_0}\right)^{-3/2}\sqrt{E^2-\frac{3}{\theta^2+2\eta_2^2B_0C_0}}\ln\left(1-e^{-\beta E}\right)\mathrm{d}E, \tag{7.29}$$

the entropy

$$\begin{aligned}\bar{S}(\theta,\beta,\eta_1,\eta_2,B_0,C_0) = &-\frac{1}{\pi^2}\int_0^\infty E\left(\frac{2\theta^2+2\eta_1^2B_0C_0}{\theta^2+2\eta_2^2B_0C_0}\right)^{-3/2}\sqrt{E^2-\frac{3}{\theta^2+2\eta_2^2B_0C_0}}\ln\left(1-e^{-\beta E}\right)\mathrm{d}E\\ &+\frac{\beta}{\pi^2}\int_0^\infty E^2\left(\frac{2\theta^2+2\eta_1^2B_0C_0}{\theta^2+2\eta_2^2B_0C_0}\right)^{-3/2}\sqrt{E^2-\frac{3}{\theta^2+2\eta_2^2B_0C_0}}\left(\frac{e^{-\beta E}}{1-e^{-\beta E}}\right)\mathrm{d}E,\end{aligned} \tag{7.30}$$

and, finally, the heat capacity

$$\bar{C}_V(\theta,\beta,\eta_1,\eta_2,B_0,C_0) = +\frac{\beta^2}{\pi^2}\int_0^\infty E^3\left(\frac{2\theta^2+2\eta_1^2B_0C_0}{\theta^2+2\eta_2^2B_0C_0}\right)^{-3/2}\sqrt{E^2-\frac{3}{\theta^2+2\eta_2^2B_0C_0}}\left[\frac{e^{-2\beta E}}{\left(1-e^{-\beta E}\right)^2}\right]\mathrm{d}E$$
$$+\frac{\beta^2}{\pi^2}\int_0^\infty E^3\left(\frac{2\theta^2+2\eta_1^2B_0C_0}{\theta^2+2\eta_2^2B_0C_0}\right)^{-3/2}\sqrt{E^2-\frac{3}{\theta^2+2\eta_2^2B_0C_0}}\left(\frac{e^{-\beta E}}{1-e^{-\beta E}}\right)\mathrm{d}E. \tag{7.31}$$

Furthermore, the graphics of these quantities are displayed in Fig. 7.4. It is worth mentioning that even though there exists the appearance of a minus sign in all those square roots, as long as the positive defined values of θ and η_2 are considered, the theory does not possess any disturbing issues ascribed to imaginary energies. In addition, considering also the CPT-even scenario, the authors calculated the contribution to the free energy in the rotationally invariant Lorentz-violating quantum electrodynamics as well as the correction to the pressure for one-and two-loop approximations at high temperature regime [508].

7.3 Results and discussions

At the beginning, we started off with the subsequent discussion regarding the thermodynamic aspects of the graviton with Lorentz violation. In this sense, we proceeded the calculations seeking the number of available states of the system which came from the given dispersion relation exhibited in Eq. (7.7). From it, the so-called partition function was built up in Eq. (7.10) which sufficed to provide all the required thermodynamic functions, i.e., the spectral radiance $\chi(\beta,\xi)$, the mean energy $U(\beta,\xi)$, the Helmholtz free energy $F(\beta,\xi)$, the entropy $S(\beta,\xi)$ and the heat capacity $C_V(\beta,\xi)$.

Next, in Fig 7.1, the spectral radiance was plotted for three different cases, namely, on the top left, the graphic exhibited how $\chi(\nu)$ changed as a function of ν for a fixed temperature $\beta = 10^{-13}\ \mathrm{GeV}^{-1}$; on the top right, it was shown how $\chi(\nu)$ evolved for diverse values of ξ and β; on the other hand, on the bottom one, the plot presented the behavior of $\chi(\nu)$ for distinct temperatures considering $\xi = 1$. Besides, in Fig 7.2, it was displayed the modification to the *Stefan–Boltzmann* law represented by parameter $\tilde{\alpha}(\xi)$ exhibiting the characteristic of a monotonically increasing function. The same behavior was also presented when one considered the entropy $S(\beta,\xi)$ and the heat capacity $C_V(\beta,\xi)$. However, having a different behavior from the other ones, the Helmholtz free energy $F(\beta,\xi)$ showed a monotonically decreasing function when ξ started to increase.

Now, let us take into account the theory of generalized Podolsky with Lee-Wick terms. Likewise, we calculated the same thermodynamic functions for this case. In Fig. 7.3 is

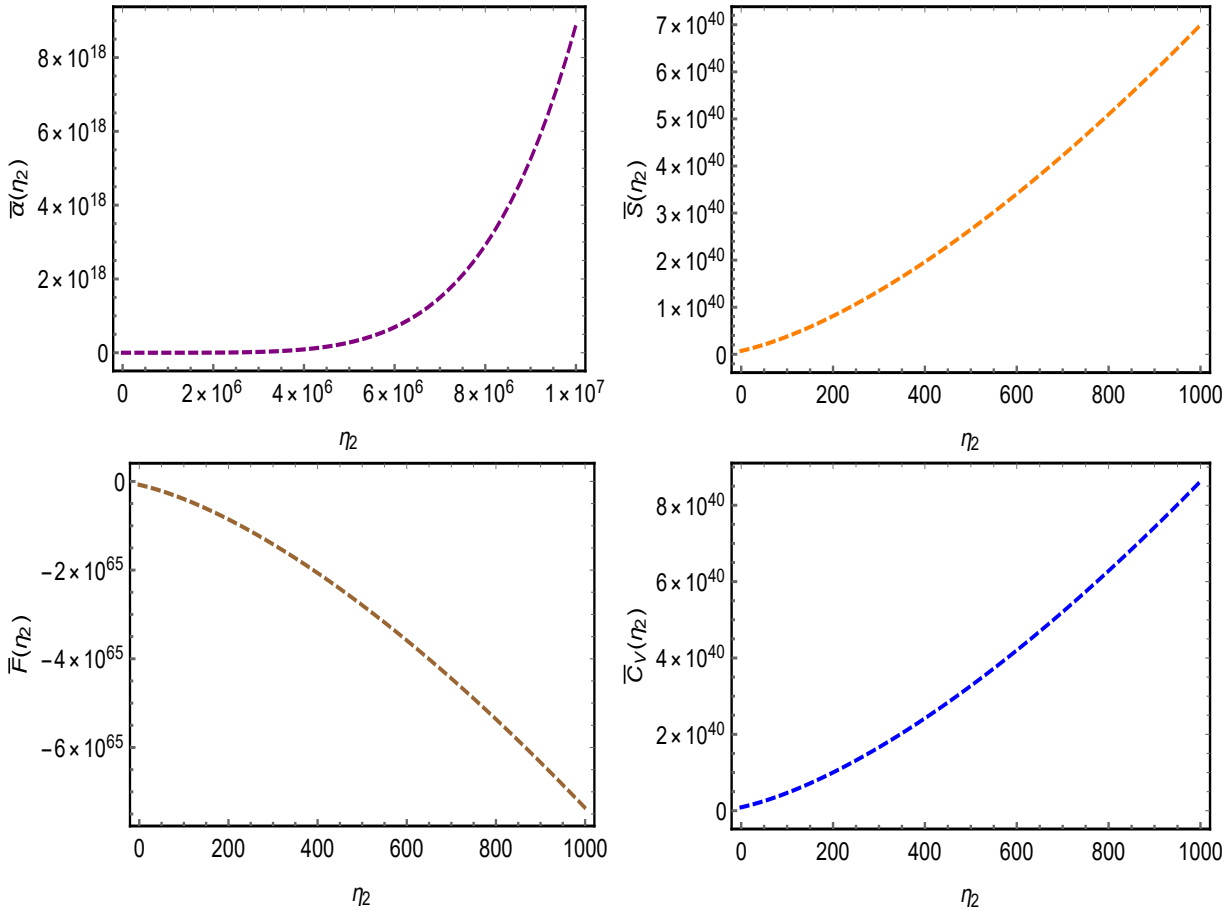

Fig. 7.4: The figure displays the correction to the so-called *Stefan–Boltzmann* law represented by parameter $\bar{\alpha}(\eta_2)$, the entropy $\bar{S}(\eta_2)$, the Helmholtz free energy $\bar{F}(\eta_2)$ and the heat capacity $\bar{C}_V(\eta_2)$ considering $\kappa_B = 1$ in the inflationary epoch of the universe, i.e., $\beta = 10^{-13}$ GeV^{-1}.

displayed how the spectral radiance evolved when η_2 and ν changed for fixed values of β, B_0, C_0 and θ, i.e., $\beta = 10^{-13}$ GeV^{-1}, $\eta_1 = B_0 = C_0 = 1$ and $\theta = 10$ respectively. In such direction, it is worth mentioning that there was an intriguing point due to the fact that when one considered $\eta_2 > 9$, one obtained a sudden behavior of such plot, namely, the flatness characteristic of the spectral radiance $\bar{\chi}(\eta_2, \nu)$.

Furthermore, in Fig. 7.4, the correction to the *Stefan–Boltzmann* law characterized by $\bar{\alpha}(\eta_2)$ was shown to have an expressive positive curvature of such curve for huge values of η_2. This differed from the analysis accomplished by the study of the graviton modified by Lorentz violation, since the latter showed a very smooth curvature. Now, considering both the entropy $\bar{S}(\eta_2)$ and the heat capacity $\bar{C}_V(\eta_2)$, we verified that they presented a monotonically increasing function with a very smooth curvature when η_2 changed, being similar to those aspects concerning the study of the thermodynamic properties of the graviton in the context of Lorentz violation. Finally, having an analogous behavior of such theory, the

Helmholtz free energy $\bar{F}(\eta_2)$, showed a monotonically decreasing curve when η_2 changed.

8. HIGHER-DERIVATIVE LORENTZ-BREAKING DISPERSION RELATIONS: A THERMAL DESCRIPTION

8.1 Thermodynamical aspects of CPT-even higher-derivative LV theory

Here, let us consider the higher-derivative LV theories. To study their thermodynamical aspects, we will define the dispersion relations of these theories in which are generally sufficient to obtain various related quantities such as free energy [353]. Our first example is the following dispersion relation [509]:

$$E^2 = \mathbf{k}^2 + \sigma^4 \mathbf{k}^6. \tag{8.1}$$

Clearly, if we consider $\sigma \to 0$, the usual dispersion relation $E^2 = \mathbf{k}^2$ is recove. Physically, such a relation can arise in Horava-Lifshitz-like theories involving both $z = 1$ and $z = 3$ terms in the spatial sector, e.g. in a scalar field model characterized by the Lagrangian $\mathcal{L} = \frac{1}{2}\phi(\Box + \sigma^4(\nabla^2)^3)\phi$, in a spinor model involving terms with these values of z [510], and perhaps for some degrees of freedom of a certain LV gauge theory or, a Horava-Lifshitz-like gravity model involving $z = 3$ and $z = 1$ terms [511]. Let us briefly discuss the possible physical significance of these relations. It must be noted that the usual Lorentz-breaking extensions of various field theory models conside within phernomenological context – their full list is given in [344] – have rather a different form since they involve the same orders in space and time derivatives until we choose the special form of Lorentz-breaking parameters. More so, the models involving the dispersion relations like (8.1) can also be regarded for studies of various physical problems; for instance, one of the most important applications of this model has been developed in [512] where it was used for an investigation of gamma-ray bursts in the Lorentz-breaking context and allowed to estimate the characteristic energy of quantum gravity mass. It is easy to see that the dispersion relation in Eq. (8.1) gives rise to six solutions. Nevertheless, only one of them allows us to work on a positive defined real

spatial momentum. In this sense, we can write the solution of Eq. (8.1) as being

$$\mathbf{k}=\left(\frac{\sqrt[3]{\sqrt{3}\sqrt{4\sigma^{12}+27\sigma^{16}E^4}+9\sigma^8E^2}}{\sqrt[3]{2}\,3^{2/3}\sigma^4}-\frac{\sqrt[3]{\frac{2}{3}}}{\sqrt[3]{\sqrt{3}\sqrt{4\sigma^{12}+27\sigma^{16}E^4}+9\sigma^8E^2}}\right)^{1/2}. \tag{8.2}$$

Next, we take the advantage of using the formalism of the partition function in order to derive all relevant thermodynamic quantities i.e., Helmholtz free energy, mean energy, entropy and heat capacity. Initially, we calculate the number of accessible states of the system [513, 56, 53, 514]. By definition, it can be represented as

$$\Omega(E)=\frac{\zeta}{(2\pi)^3}\int\int \mathrm{d}^3\mathbf{x}\,\mathrm{d}^3\mathbf{k}, \tag{8.3}$$

where ζ is the spin multiplicity whose magnitude in the photon sector is $\zeta=2$ [357]. More so, Eq. (8.3) can be rewritten as

$$\Omega(E)=\frac{V}{\pi^2}\int_0^\infty \mathrm{d}\mathbf{k}|\mathbf{k}|^2, \tag{8.4}$$

where V is the volume of the thermal reservoir and the integral measure $\mathbf{dk}$ is given by

$$\mathrm{d}\mathbf{k}=\frac{\frac{\sqrt[3]{\frac{2}{3}}\left(\frac{54\sqrt{3}\sigma^{16}E^3}{\sqrt{4\sigma^{12}+27\sigma^{16}E^4}}+18\sigma^8E\right)}{3\left(\sqrt{3}\sqrt{4\sigma^{12}+27\sigma^{16}E^4}+9\sigma^8E^2\right)^{4/3}}+\frac{\frac{54\sqrt{3}\sigma^{16}E^3}{\sqrt{4\sigma^{12}+27\sigma^{16}E^4}}+18\sigma^8E}{3\sqrt[3]{2}3^{2/3}\sigma^4\left(\sqrt{3}\sqrt{4\sigma^{12}+27\sigma^{16}E^4}+9\sigma^8E^2\right)^{2/3}}}{2\sqrt{\frac{\sqrt[3]{\sqrt{3}\sqrt{4\sigma^{12}+27\sigma^{16}E^4}+9\sigma^8E^2}}{\sqrt[3]{2}3^{2/3}\sigma^4}-\frac{\sqrt[3]{\frac{2}{3}}}{\sqrt[3]{\sqrt{3}\sqrt{4\sigma^{12}+27\sigma^{16}E^4}+9\sigma^8E^2}}}}\mathrm{d}E. \tag{8.5}$$

Next, we substitute (8.2) and (8.5) in (8.4), which yields

$$\begin{aligned}\Omega(\sigma)=\frac{V}{\pi^2}\int_0^\infty&\left(\frac{\sqrt[3]{\frac{2}{3}}\left(\frac{54\sqrt{3}\sigma^{16}E^3}{\sqrt{4\sigma^{12}+27\sigma^{16}E^4}}+18\sigma^8E\right)}{3\left(\sqrt{3}\sqrt{4\sigma^{12}+27\sigma^{16}E^4}+9\sigma^8E^2\right)^{4/3}}\right.\\&\left.+\frac{\frac{54\sqrt{3}\sigma^{16}E^3}{\sqrt{4\sigma^{12}+27\sigma^{16}E^4}}+18\sigma^8E}{3\sqrt[3]{2}3^{2/3}\sigma^4\left(\sqrt{3}\sqrt{4\sigma^{12}+27\sigma^{16}E^4}+9\sigma^8E^2\right)^{2/3}}\right)\\&\times\sqrt{\frac{\sqrt[3]{\sqrt{3}\sqrt{4\sigma^{12}+27\sigma^{16}E^4}+9\sigma^8E^2}}{\sqrt[3]{2}3^{2/3}\sigma^4}-\frac{\sqrt[3]{\frac{2}{3}}}{\sqrt[3]{\sqrt{3}\sqrt{4\sigma^{12}+27\sigma^{16}E^4}+9\sigma^8E^2}}}\,\mathrm{d}E,\end{aligned} \tag{8.6}$$

and, therefore, we can explicitly write down the partition function in a manner similar to Refs. [357, 515] as follows:

$$\ln\left[Z(\beta,\Gamma,\sigma)\right]=-\frac{V}{\pi^2}\int_0^{\infty}\left(\frac{\sqrt[3]{\frac{2}{3}}\left(\frac{54\sqrt{3}\sigma^{16}E^3}{\sqrt{4\sigma^{12}+27\sigma^{16}E^4}}+18\sigma^8E\right)}{3\left(\sqrt{3}\sqrt{4\sigma^{12}+27\sigma^{16}E^4}+9\sigma^8E^2\right)^{4/3}}\right.$$
$$\left.+\frac{\frac{54\sqrt{3}\sigma^{16}E^3}{\sqrt{4\sigma^{12}+27\sigma^{16}E^4}}+18\sigma^8E}{3\sqrt[3]{2}3^{2/3}\sigma^4\left(\sqrt{3}\sqrt{4\sigma^{12}+27\sigma^{16}E^4}+9\sigma^8E^2\right)^{2/3}}\right)\times\ln\left(1-e^{-\beta E}\right)$$
$$\times\sqrt{\frac{\sqrt[3]{\sqrt{3}\sqrt{4\sigma^{12}+27\sigma^{16}E^4}+9\sigma^8E^2}}{\sqrt[3]{2}3^{2/3}\sigma^4}-\frac{\sqrt[3]{\frac{2}{3}}}{\sqrt[3]{\sqrt{3}\sqrt{4\sigma^{12}+27\sigma^{16}E^4}+9\sigma^8E^2}}}\,\mathrm{d}E,\tag{8.7}$$

where $\beta=1/(k_BT)$ is the inverse of the temperature. From Eq. (8.7), the thermodynamic functions can be derived. It is important to mention that all our calculations will provide the values of these functions per volume V. The thermal functions of interest are defined as

$$\begin{aligned}
F(\beta,\sigma)&=-\frac{1}{\beta}\ln\left[Z(\beta,\sigma)\right],\\
U(\beta,\sigma)&=-\frac{\partial}{\partial\beta}\ln\left[Z(\beta,\sigma)\right],\\
S(\beta,\sigma)&=k_B\beta^2\frac{\partial}{\partial\beta}F(\beta,\sigma),\\
C_V(\beta,\sigma)&=-k_B\beta^2\frac{\partial}{\partial\beta}U(\beta,\sigma).
\end{aligned}\tag{8.8}$$

Primarily, let us focus on the mean energy

$$\begin{aligned}
U(\beta,\sigma) &= \frac{V}{\pi^2}\int_0^{\infty}\mathrm{d}E\,E\left(\frac{\sqrt[3]{\frac{2}{3}}\left(\frac{54\sqrt{3}\sigma^{16}E^3}{\sqrt{4\sigma^{12}+27\sigma^{16}E^4}}+18\sigma^8E\right)}{3\left(\sqrt{3}\sqrt{4\sigma^{12}+27\sigma^{16}E^4}+9\sigma^8E^2\right)^{4/3}}\right.\\
&+\left.\frac{\frac{54\sqrt{3}\sigma^{16}E^3}{\sqrt{4\sigma^{12}+27\sigma^{16}E^4}}+18\sigma^8E}{3\sqrt[3]{2}3^{2/3}\sigma^4\left(\sqrt{3}\sqrt{4\sigma^{12}+27\sigma^{16}E^4}+9\sigma^8E^2\right)^{2/3}}\right)\times\frac{e^{-\beta E}}{\left(1-e^{-\beta E}\right)}\\
&\times\sqrt{\frac{\sqrt[3]{\sqrt{3}\sqrt{4\sigma^{12}+27\sigma^{16}E^4}+9\sigma^8E^2}}{\sqrt[3]{2}\cdot3^{2/3}\sigma^4}-\frac{\sqrt[3]{\frac{2}{3}}}{\sqrt[3]{\sqrt{3}\sqrt{4\sigma^{12}+27\sigma^{16}E^4}+9\sigma^8E^2}}}
\end{aligned}\tag{8.9}$$

which implies the following spectral radiance:

$$\begin{aligned}\chi(\sigma,\nu) &= \frac{h\nu}{\pi^2}\left(\frac{\sqrt[3]{\frac{2}{3}}\left(\frac{54\sqrt{3}\sigma^{16}(h\nu)^3}{\sqrt{4\sigma^{12}+27\sigma^{16}(h\nu)^4}}+18\sigma^8(h\nu)\right)}{3\left(\sqrt{3}\sqrt{4\sigma^{12}+27\sigma^{16}(h\nu)^4}+9\sigma^8(h\nu)^2\right)^{4/3}}\right. \\ &+ \left.\frac{\frac{54\sqrt{3}\sigma^{16}(h\nu)^3}{\sqrt{4\sigma^{12}+27\sigma^{16}(h\nu)^4}}+18\sigma^8(h\nu)}{3\sqrt[3]{2}3^{2/3}\sigma^4\left(\sqrt{3}\sqrt{4\sigma^{12}+27\sigma^{16}(h\nu)^4}+9\sigma^8(h\nu)^2\right)^{2/3}}\right)\times\frac{e^{-\beta(h\nu)}}{\left(1-e^{-\beta(h\nu)}\right)} \\ &\times\sqrt{\frac{\sqrt[3]{\sqrt{3}\sqrt{4\sigma^{12}+27\sigma^{16}(h\nu)^4}+9\sigma^8(h\nu)^2}}{\sqrt[3]{2}3^{2/3}\sigma^4}-\frac{\sqrt[3]{\frac{2}{3}}}{\sqrt[3]{\sqrt{3}\sqrt{4\sigma^{12}+27\sigma^{16}(h\nu)^4}+9\sigma^8(h\nu)^2}}}.\end{aligned} \tag{8.10}$$

Here, $E = h\nu$ where h is the well-known Planck constant and ν is the frequency. Now, let us examine how the parameter σ affects the spectral radiance of our theory. In addition, it must be noted that, despite of showing explicitly the constants h, k_B, to obtain the following calculations, we choose them as being $h = k_B = 1$. At the beginning, we examine how the black body spectra can be modified by the parameter σ. Moreover, we consider three different configurations of temperatures for our system, namely, CMB ($T = 10^{-13}$ GeV), electroweak epoch ($T = 10^3$ GeV) and inflationary era ($T = 10^{13}$ GeV).

The results displayed at Fig. 8.1 show that the only one configuration of the black body radiation took a proper place in a prominent manner (in terms of shape of the curve) – it was with the CMB temperature. Furthermore, taking into account the electroweak scenario, we see that the graphics started to increase reaching maxima peaks and, then, tended to attenuate their values until having a constant behavior. On the other hand, to the inflationary temperature, the plots show a behavior closer to Wien's energy density distribution [176].

Another interesting aspect to be verified is the correction to the *Stefan–Boltzmann* law ascribed to the parameter σ. In order to do this, let us define the constant:

$$\tilde{\alpha} \equiv U(\beta,\sigma)\beta^4. \tag{8.11}$$

As it can easily be noted, the above expressions are unsolvable analytically. Thereby, the calculations will be performed numerically. Analogously, we regard the same previous configurations of temperature and the plots are exhibited in Fig. 8.2. For the CMB temperature, the curve exhibits a constant behavior of α. Moreover, to the electroweak epoch, we have a decreasing function $\tilde{\alpha}$ when σ started to increase. The inflationary era, on the other hand, shows an increasing function of $\tilde{\alpha}$ for positive changes of σ. To this latter case, for $\tilde{\alpha} < 20$, the system seems to show instability. Next, we shall acquire all the remaining

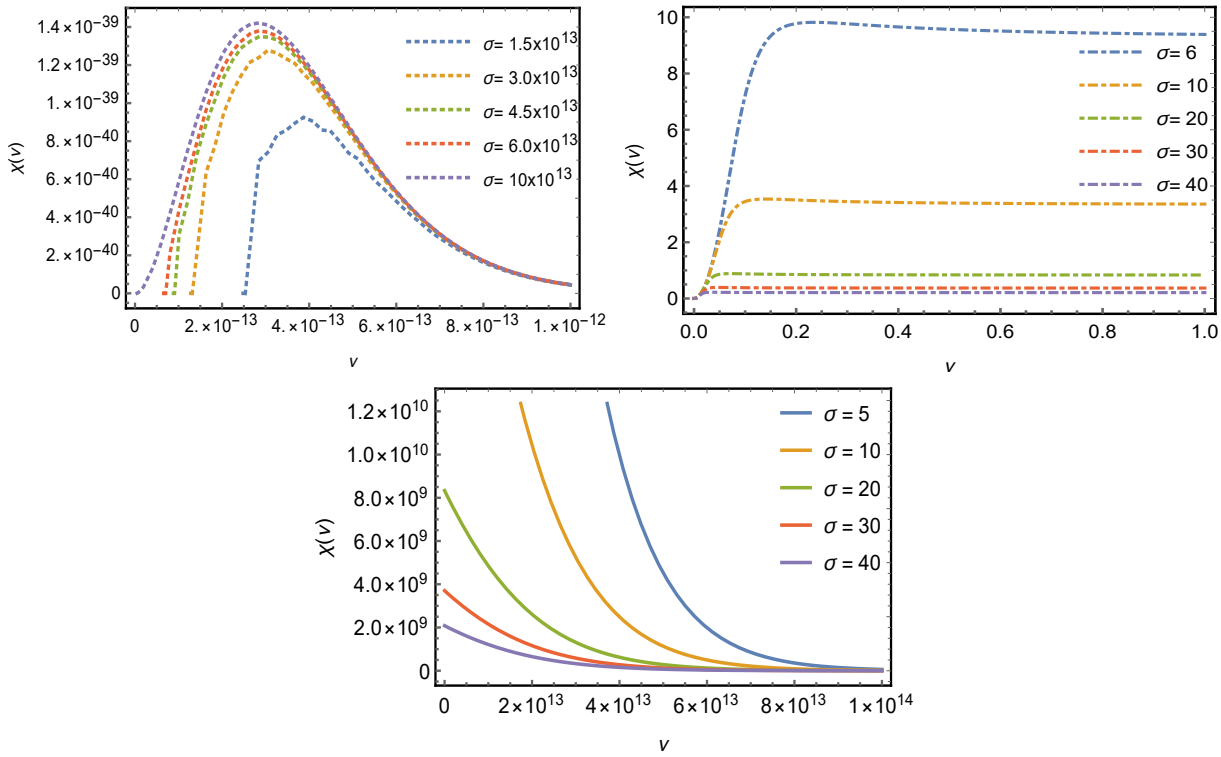

Fig. 8.1: The plots exhibit the spectral radiance $\chi(\nu)$ changing for different values of frequency ν and the Lorentz-breaking parameter σ (its unit is GeV^{-1}). The top left (dotted) is the configuration to the cosmic microwave background, i.e., $\beta = 10^{13}\ \mathrm{GeV}^{-1}$; the top right (dot-dashed) is ascribed to the electroweak configuration, i.e., $\beta = 10^{-3}\ \mathrm{GeV}^{-1}$; the bottom plot shows the black body radiation to the inflationary period of the Universe, i.e., $\beta = 10^{-13}\ \mathrm{GeV}^{-1}$.

thermodynamic properties in what follows.

Using the expressions above, we can first obtain the Helmholtz free energy as being

$$
\begin{aligned}
F(\beta,\sigma) \;=\; & \frac{V}{\beta\pi^2}\int_0^\infty \left(\frac{\sqrt[3]{\frac{2}{3}}\left(\frac{54\sqrt{3}\sigma^{16}E^3}{\sqrt{4\sigma^{12}+27\sigma^{16}E^4}}+18\sigma^8E\right)}{3\left(\sqrt{3}\sqrt{4\sigma^{12}+27\sigma^{16}E^4}+9\sigma^8E^2\right)^{4/3}} \right. \\
& \left. + \frac{\frac{54\sqrt{3}\sigma^{16}E^3}{\sqrt{4\sigma^{12}+27\sigma^{16}E^4}}+18\sigma^8E}{3\sqrt[3]{2}3^{2/3}\sigma^4\left(\sqrt{3}\sqrt{4\sigma^{12}+27\sigma^{16}E^4}+9\sigma^8E^2\right)^{2/3}} \right) \times \ln\left(1-e^{-\beta E}\right) \\
& \times \sqrt{\frac{\sqrt[3]{\sqrt{3}\sqrt{4\sigma^{12}+27\sigma^{16}E^4}+9\sigma^8E^2}}{\sqrt[3]{2}3^{2/3}\sigma^4} - \frac{\sqrt[3]{\frac{2}{3}}}{\sqrt[3]{\sqrt{3}\sqrt{4\sigma^{12}+27\sigma^{16}E^4}+9\sigma^8E^2}}}\,\mathrm{d}E,
\end{aligned}
\tag{8.12}
$$

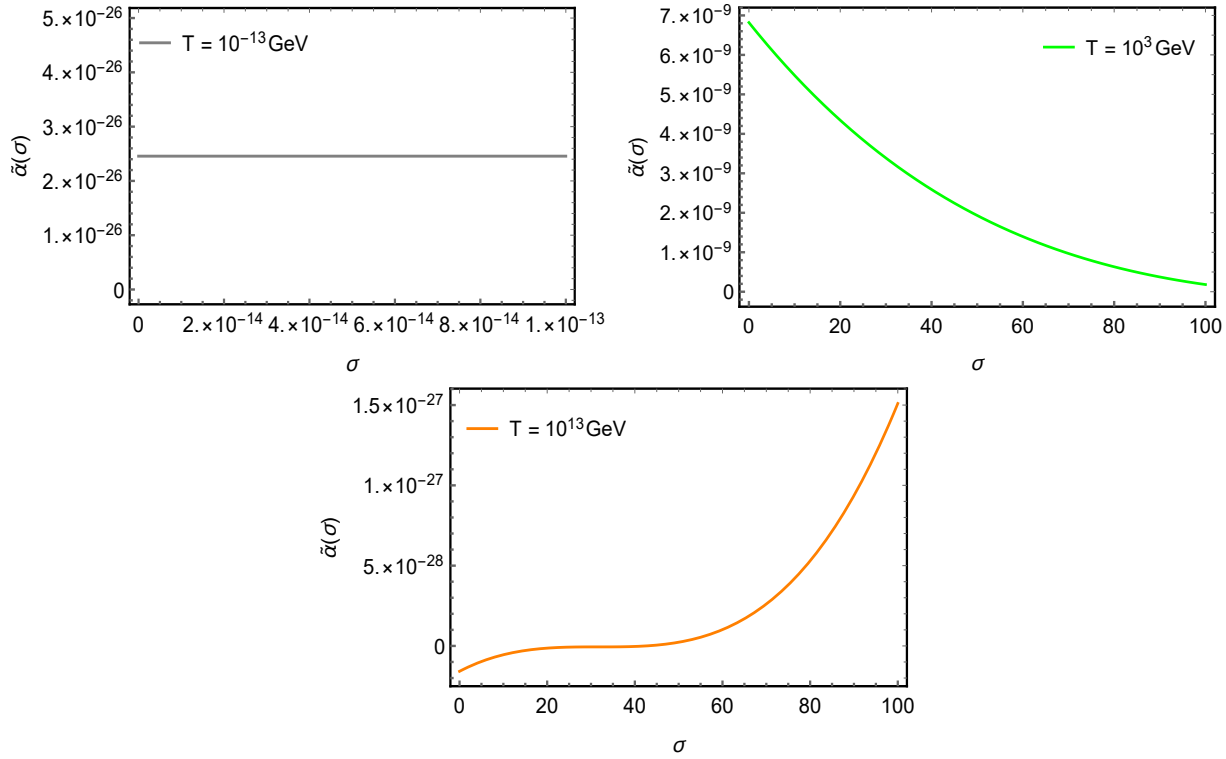

Fig. 8.2: The figure shows the correction to the *Stefan–Boltzmann* law ascribed to parameter $\tilde{\alpha}$ as a function of σ (its unit is GeV^{-1}) for the temperatures of cosmic microwave background (top left), electroweak scenario (top right) and the early inflationary universe (bottom).

the entropy

$$
\begin{aligned}
S(\beta,\sigma) \;=\; & -\frac{V k_B}{\pi^2}\int_0^\infty \left(\frac{\sqrt[3]{\frac{2}{3}}\left(\frac{54\sqrt{3}\sigma^{16}E^3}{\sqrt{4\sigma^{12}+27\sigma^{16}E^4}}+18\sigma^8 E\right)}{3\left(\sqrt{3}\sqrt{4\sigma^{12}+27\sigma^{16}E^4}+9\sigma^8E^2\right)^{4/3}}\right. \\
& \left. + \frac{\frac{54\sqrt{3}\sigma^{16}E^3}{\sqrt{4\sigma^{12}+27\sigma^{16}E^4}}+18\sigma^8 E}{3\sqrt[3]{2}3^{2/3}\sigma^4\left(\sqrt{3}\sqrt{4\sigma^{12}+27\sigma^{16}E^4}+9\sigma^8E^2\right)^{2/3}}\right)\times\ln\left(1-e^{-\beta E}\right) \\
& \times\sqrt{\frac{\sqrt[3]{\sqrt{3}\sqrt{4\sigma^{12}+27\sigma^{16}E^4}+9\sigma^8E^2}}{\sqrt[3]{2}3^{2/3}\sigma^4}-\frac{\sqrt[3]{\frac{2}{3}}}{\sqrt[3]{\sqrt{3}\sqrt{4\sigma^{12}+27\sigma^{16}E^4}+9\sigma^8E^2}}} \\
& + \frac{V\beta k_B}{\pi^2}\int_0^\infty E\left(\frac{\sqrt[3]{\frac{2}{3}}\left(\frac{54\sqrt{3}\sigma^{16}E^3}{\sqrt{4\sigma^{12}+27\sigma^{16}E^4}}+18\sigma^8 E\right)}{3\left(\sqrt{3}\sqrt{4\sigma^{12}+27\sigma^{16}E^4}+9\sigma^8E^2\right)^{4/3}}\right. \\
& \left. + \frac{\frac{54\sqrt{3}\sigma^{16}E^3}{\sqrt{4\sigma^{12}+27\sigma^{16}E^4}}+18\sigma^8 E}{3\sqrt[3]{2}3^{2/3}\sigma^4\left(\sqrt{3}\sqrt{4\sigma^{12}+27\sigma^{16}E^4}+9\sigma^8E^2\right)^{2/3}}\right)\times\frac{e^{-\beta E}}{1-e^{-\beta E}} \\
& \times\sqrt{\frac{\sqrt[3]{\sqrt{3}\sqrt{4\sigma^{12}+27\sigma^{16}E^4}+9\sigma^8E^2}}{\sqrt[3]{2}3^{2/3}\sigma^4}-\frac{\sqrt[3]{\frac{2}{3}}}{\sqrt[3]{\sqrt{3}\sqrt{4\sigma^{12}+27\sigma^{16}E^4}+9\sigma^8E^2}}}\,\mathrm{d}E,
\end{aligned}
\tag{8.13}
$$

and, lastly, the heat capacity

$$
\begin{aligned}
C_V(\beta,\sigma) &= \frac{Vk_B\beta^2}{\pi^2}\int_0^\infty E^2\left(\frac{\sqrt[3]{\frac{2}{3}}\left(\frac{54\sqrt{3}\sigma^{16}E^3}{\sqrt{4\sigma^{12}+27\sigma^{16}E^4}}+18\sigma^8E\right)}{3\left(\sqrt{3}\sqrt{4\sigma^{12}+27\sigma^{16}E^4}+9\sigma^8E^2\right)^{4/3}}\right. \\
&+ \left.\frac{\frac{54\sqrt{3}\sigma^{16}E^3}{\sqrt{4\sigma^{12}+27\sigma^{16}E^4}}+18\sigma^8E}{3\sqrt[3]{2}3^{2/3}\sigma^4\left(\sqrt{3}\sqrt{4\sigma^{12}+27\sigma^{16}E^4}+9\sigma^8E^2\right)^{2/3}}\right)\times\frac{e^{-2\beta E}}{(1-e^{-\beta E})^2} \\
&\times\sqrt{\frac{\sqrt[3]{\sqrt{3}\sqrt{4\sigma^{12}+27\sigma^{16}E^4}+9\sigma^8E^2}}{\sqrt[3]{2}3^{2/3}\sigma^4}-\frac{\sqrt[3]{\frac{2}{3}}}{\sqrt[3]{\sqrt{3}\sqrt{4\sigma^{12}+27\sigma^{16}E^4}+9\sigma^8E^2}}} \\
&+ \frac{Vk_B\beta^2}{\pi^2}\int_0^\infty E^2\left(\frac{\sqrt[3]{\frac{2}{3}}\left(\frac{54\sqrt{3}\sigma^{16}E^3}{\sqrt{4\sigma^{12}+27\sigma^{16}E^4}}+18\sigma^8E\right)}{3\left(\sqrt{3}\sqrt{4\sigma^{12}+27\sigma^{16}E^4}+9\sigma^8E^2\right)^{4/3}}\right. \\
&+ \left.\frac{\frac{54\sqrt{3}\sigma^{16}E^3}{\sqrt{4\sigma^{12}+27\sigma^{16}E^4}}+18\sigma^8E}{3\sqrt[3]{2}3^{2/3}\sigma^4\left(\sqrt{3}\sqrt{4\sigma^{12}+27\sigma^{16}E^4}+9\sigma^8E^2\right)^{2/3}}\right)\times\frac{e^{-\beta E}}{1-e^{-\beta E}} \\
&\times\sqrt{\frac{\sqrt[3]{\sqrt{3}\sqrt{4\sigma^{12}+27\sigma^{16}E^4}+9\sigma^8E^2}}{\sqrt[3]{2}3^{2/3}\sigma^4}-\frac{\sqrt[3]{\frac{2}{3}}}{\sqrt[3]{\sqrt{3}\sqrt{4\sigma^{12}+27\sigma^{16}E^4}+9\sigma^8E^2}}}\,\mathrm{d}E.
\end{aligned}
\tag{8.14}
$$

Their behaviors are shown in Figs. 8.5, 8.6, and 8.7 respectively. Moreover, the thermal quantities were also calculated [469, 470, 384, 516, 517, 518] into different contexts. In the context of CMB, all of them turned out to have no contribution to our calculations. For Helmholtz free energy, we obtained decreasing curves with an expressive curvature when σ increases for both electroweak and inflationary cases. The entropy, on the other hand, showed a decreasing behavior for different values of σ for both electroweak and inflationary cases. It is worth mentioning that such behavior does not imply an instability since the entropy is still an increasing function when it is analyzed against the temperature for fixed values of σ – as it should be. Lastly, the heat capacity exhibited a strong increasing behavior when σ started to change for both cases as well, i.e., the CMB and the inflationary temperatures. In principle, this fact might signalize the possibility of some phase transition at some large σ; nevertheless, this hypothesis requires further investigation.

Whenever we are dealing with the thermodynamic systems, one question naturally arises: what is the form of the equation of state when the parameter σ, which characterizes the magnitude of Lorentz symmetry breaking, is taken into account? To answer such a question,

we must start with the following relation:

$$\mathrm{d}F = -S\,\mathrm{d}T - p\,\mathrm{d}V, \tag{8.15}$$

which, immediately, implies

$$\begin{aligned} p = -\left(\frac{\partial F}{\partial V}\right)_T &= -\frac{1}{\beta\pi^2}\int_0^\infty \left(\frac{\sqrt[3]{\frac{2}{3}}\left(\frac{54\sqrt{3}\sigma^{16}E^3}{\sqrt{4\sigma^{12}+27\sigma^{16}E^4}}+18\sigma^8 E\right)}{3\left(\sqrt{3}\sqrt{4\sigma^{12}+27\sigma^{16}E^4}+9\sigma^8E^2\right)^{4/3}} \right. \\ &+ \left. \frac{\frac{54\sqrt{3}\sigma^{16}E^3}{\sqrt{4\sigma^{12}+27\sigma^{16}E^4}}+18\sigma^8E}{3\sqrt[3]{2}3^{2/3}\sigma^4\left(\sqrt{3}\sqrt{4\sigma^{12}+27\sigma^{16}E^4}+9\sigma^8E^2\right)^{2/3}} \right) \times \ln\left(1-e^{-\beta E}\right) \\ &\times \sqrt{\frac{\sqrt[3]{\sqrt{3}\sqrt{4\sigma^{12}+27\sigma^{16}E^4}+9\sigma^8E^2}}{\sqrt[3]{2}3^{2/3}\sigma^4} - \frac{\sqrt[3]{\frac{2}{3}}}{\sqrt[3]{\sqrt{3}\sqrt{4\sigma^{12}+27\sigma^{16}E^4}+9\sigma^8E^2}}}\,\mathrm{d}E. \end{aligned} \tag{8.16}$$

Here, we focus on the study of the behavior of pressure – which leads to the equation of states. After introducing new dimensionless variable $t = \sigma E$, we get

$$\begin{aligned} p &= \frac{1}{\sigma^3\beta\pi^2}\int_0^\infty \mathrm{d}t\,\ln(1-e^{-\frac{\beta}{\sigma}t})F(t); \\ F(t) &= -2^{1/6}3^{-7/6}\frac{t}{\sqrt{4+27t^4}}\left[(\chi(t))^{-1/3}+\frac{1}{\sqrt[3]{18}}(\chi(t))^{1/3}\right]\cdot\sqrt{\frac{(\chi(t))^{2/3}-12^{1/3}}{(\chi(t))^{1/3}}}; \\ \chi(t) &= \sqrt{3}\cdot\sqrt{4+27t^4}+9t^2. \end{aligned} \tag{8.17}$$

With these above expressions, let us examine some limits. Initially, at the very high temperature limit, namely $\frac{\beta}{\sigma} = \frac{1}{\sigma T} \ll 1$, we perform the expansion in the Taylor series. After that, only the first two terms are considered, which yields $p = \frac{1}{\sigma^3\beta\pi^2}\frac{\beta}{\sigma}\int_0^\infty \mathrm{d}tF(t)t = \frac{c_h}{\sigma^4\pi^2}$, where $c_h = \int_0^\infty \mathrm{d}tF(t)t$, i.e., at $T\to\infty$ ($\beta\to 0$), the pressure tends to a constant. Such behavior is displayed in Fig. 8.3; next, at the natural limit of low Lorentz symmetry breaking or low temperature, one has $\frac{\beta}{\sigma} \gg 1$. In this case, the exponential is strongly suppressed, and one has $p = \frac{c_l}{\sigma^3\beta\pi^2}$, where $c_l = \int_0^\infty \mathrm{d}tF(t)$, i.e., the pressure grows linearly with the temperature. Thereby, its corresponding behavior is shown in Fig. 8.4.

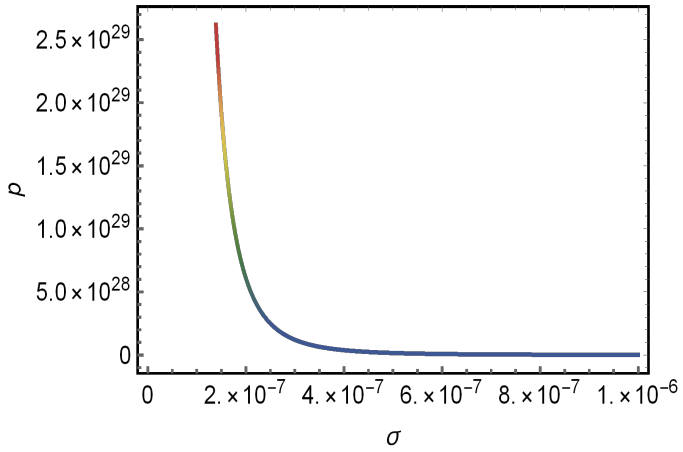

Fig. 8.3: This figure shows the behavior of the equation of states when the high temperature limit, namely $\frac{\beta}{\sigma} \ll 1$, is taken into account.

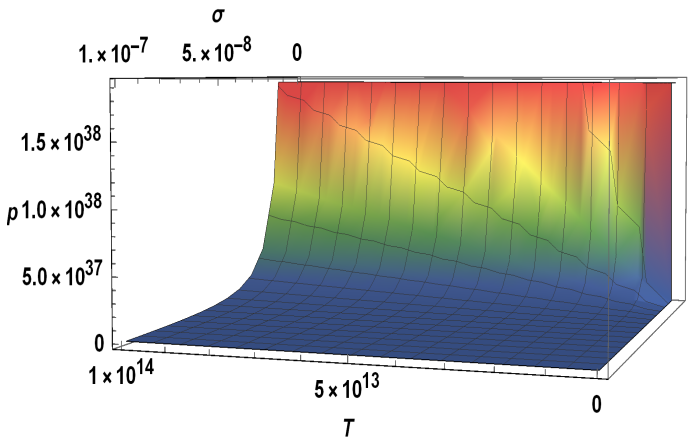

Fig. 8.4: This figure shows the behavior of the equation of states when the low temperature limit, namely $\frac{\beta}{\sigma} \gg 1$, is taken into account.

8.2 Thermodynamical aspects of CPT-odd higher-derivative LV theory

In this section, let us consider the theory described by the following dispersion relation [519]:

$$E^2 + \alpha l E^3 + \beta l E \mathbf{k}^2 = \mathbf{k}^2 + m^2. \tag{8.18}$$

where l is a parameter characterizing the intensity of the Lorentz symmetry breaking. It is clear that in the limit $l \to 0$, the standard massive dispersion relation $E^2 = \mathbf{k}^2 + m^2$ is recovered. Such a relation, being similar to relations studied in Ref. [377], can arise e.g. in a scalar field theory with the higher-derivative quadratic Lagrangian of the scalar field looking like $\mathcal{L} = \frac{1}{2}\phi(\Box + m^2 + \rho^{\mu\nu\lambda}\partial_\mu\partial_\nu\partial_\rho)\phi$, with $\rho^{\mu\nu\lambda}$ being a completely symmetric third-rank

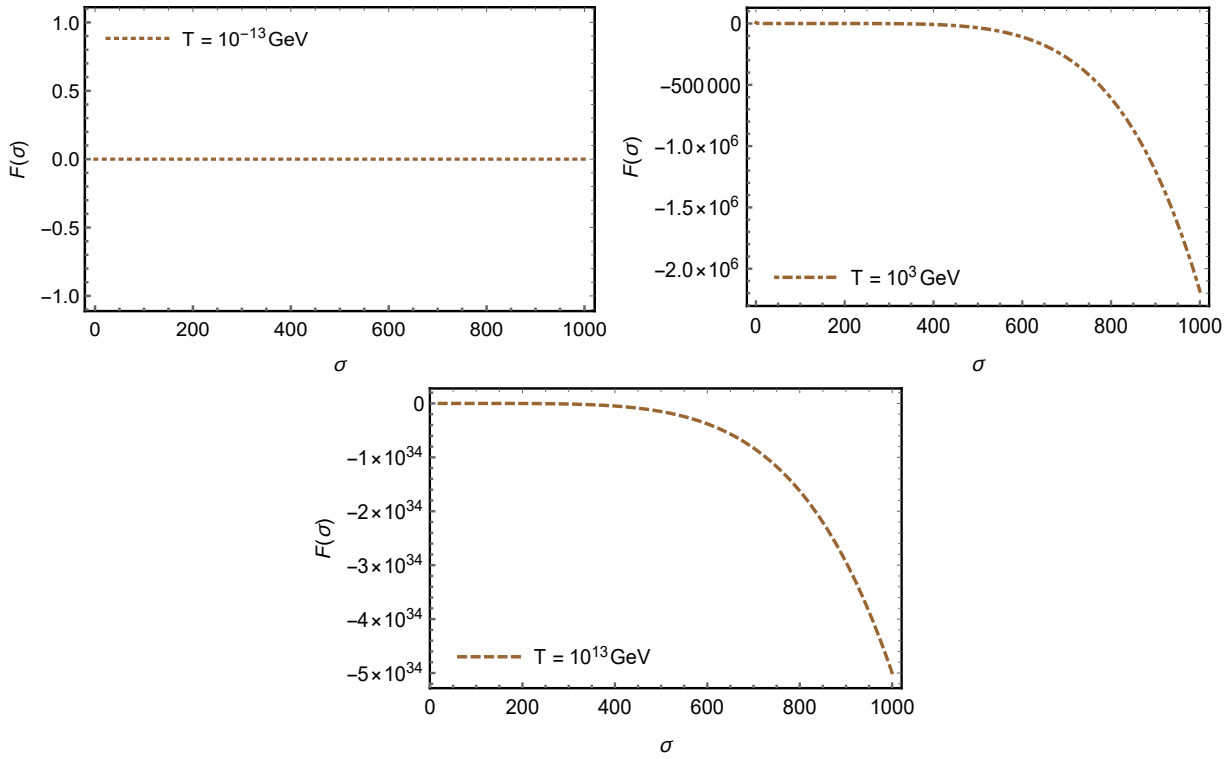

Fig. 8.5: The figure shows the modification of the Helmholtz free energy $F(\sigma)$ due to the parameter σ (its unit is GeV^{-1}) considering the temperatures of cosmic microwave background (top left), electroweak scenario (top right) and the early inflationary universe (bottom).

tensor whose only non-zero components are $\rho^{000} = \beta l$, and $\rho^{0ij} = \frac{1}{3}\alpha l \delta^{ij}$. In principle, it is natural to expect that such a relation, in the massless case, can also arise in a specific higher-derivative LV extension of QED. In particular, the dispersion relation displayed in Eq. (8.18) can be applied to understand how Planck-scale effects may affect translation transformations. This is relevant due to the fact that it carries the information on the distance between source and detector, and it factors in the interplay between quantum-spacetime effects and the curvature of spacetime [520, 519]. In the literature, some propositions are addressed in the context of gamma-ray-burst neutrinos and photons [521], and IceCube and GRB neutrinos [520].

Thereby, we restrict ourselves to a particular massless case, i.e., we set $m = 0, \alpha = 1$ and $\beta = 1$. In this sense, it is convenient to rewrite Eq. (8.18) as

$$\mathbf{k}^2 = \frac{E^2 + lE^3}{1 - lE}, \tag{8.19}$$

where, analogously with the previous section, the accessible states can be derived:

$$\bar{\Omega}(l) = \frac{\Gamma}{2\pi^2} \int_0^\infty \left(\frac{E^2 + lE^3}{1 - lE} \right)^{1/2} \left[\frac{(2E + 3lE^2)(1 - lE) + l(E^2 + lE^3)}{(1 - lE)^2} \right] \mathrm{d}E. \tag{8.20}$$

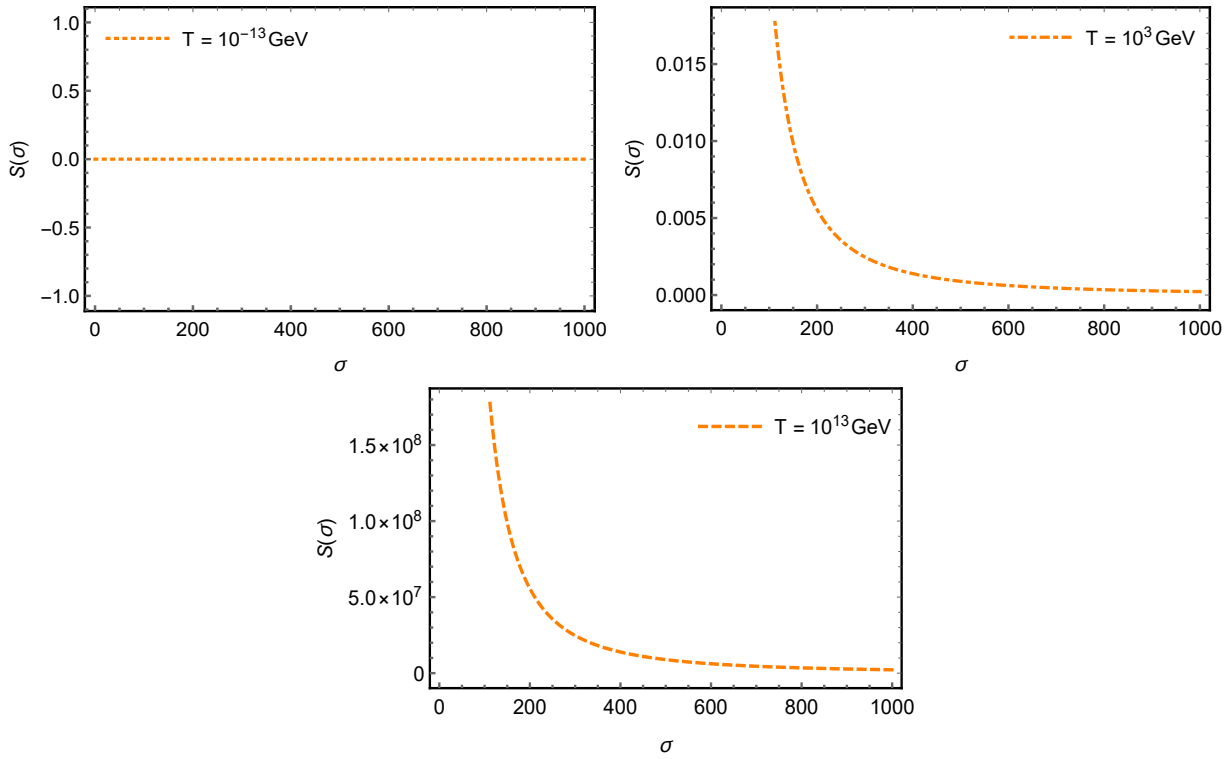

Fig. 8.6: The plots show the modification to the entropy $S(\sigma)$ as a function of σ (its unit is GeV^{-1}) considering the temperatures of cosmic microwave background (top left), electroweak scenario (top right), and the early inflationary universe (bottom).

With this, we are able to write down the corresponding partition function as follows

$$\begin{aligned} &\ln\left[\bar{Z}(\beta,l)\right] = \\ &= -\frac{\Gamma}{\pi^2}\int_0^\infty \left(\frac{E^2+lE^3}{1-lE}\right)^{1/2}\left[\frac{(2E+3lE^2)(1-lE)+l(E^2+lE^3)}{(1-lE)^2}\right]\ln\left(1-e^{-\beta E}\right)\mathrm{d}E. \end{aligned} \tag{8.21}$$

Using Eq. (8.22), we can obtain the thermodynamic functions per volume Γ as well. Here, we provide the calculation of Helmholtz free energy $\bar{F}(\beta,l)$, mean energy $\bar{U}(\beta,l)$, entropy $\bar{S}(\beta,l)$, and heat capacity $\bar{C}_V(\beta,l)$. Let us start with the mean energy

$$\bar{U}(\beta,l) = \frac{1}{\pi^2}\int_0^\infty E\left(\frac{E^2+lE^3}{1-lE}\right)^{1/2}\left[\frac{(2E+3lE^2)(1-lE)+l(E^2+lE^3)}{(1-lE)^2}\right]\frac{e^{-\beta E}}{\left(1-e^{-\beta E}\right)}\mathrm{d}E, \tag{8.22}$$

which implies the spectral radiance given by:

$$\begin{aligned} \bar{\chi}(l,\nu) &= (h\nu)\left(\frac{(h\nu)^2+l(h\nu)^3}{1-l(h\nu)}\right)^{1/2}\left[\frac{(2(h\nu)+3l(h\nu)^2)(1-l(h\nu))+l((h\nu)^2+l(h\nu)^3)}{(1-l(h\nu))^2}\right]\times \\ &\times \frac{e^{-\beta(h\nu)}}{\left(1-e^{-\beta(h\nu)}\right)}. \end{aligned} \tag{8.23}$$

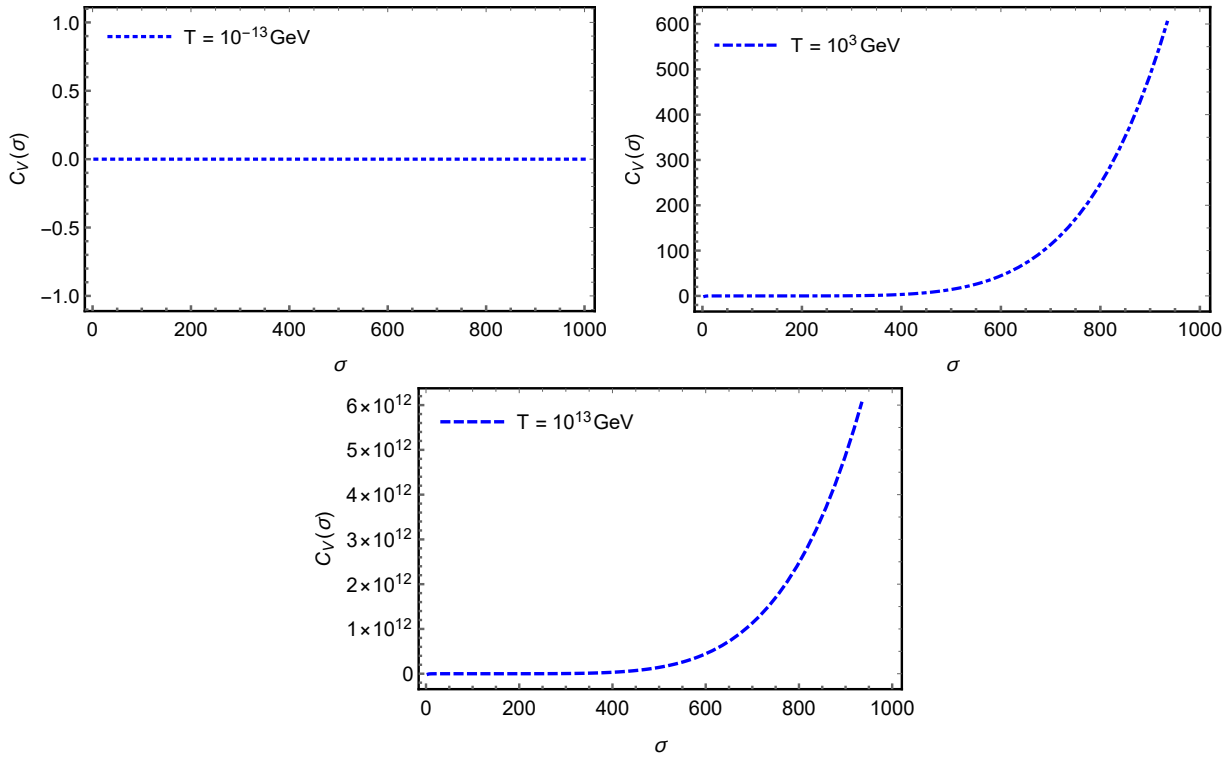

Fig. 8.7: The plots show the modification to the heat capacity $C_V(\sigma)$ as a function of σ (its unit is GeV^{-1}) considering the temperatures of cosmic microwave background (top left), electroweak scenario (top right), and the early inflationary universe (bottom).

The respective plots of these thermal quantities are presented in Fig. 8.8. Here, we show the black body radiation spectra for different values of l corresponding to the Cosmic Microwave Background, electroweak epoch and inflationary era of the Universe. Moreover, the black body radiation shape is maintained for the three of them, differently what happened in our first example in the previous section. Note that when $l \to 0$, we recover the usual radiation constant of the *Stefan–Boltzmann* law, namely, $u_{SB} = \alpha T^4$. In other words, we have

$$\alpha = \frac{1}{\pi^2}\int_0^\infty \frac{E^3\, e^{-\beta E}}{\left(1 - e^{-\beta E}\right)}\mathrm{d}E = \frac{\pi^2}{15}. \tag{8.24}$$

Furthermore, for the sake of examining how the parameter l affects the correction to the *Stefan–Boltzmann* law, we also consider

$$\bar{\alpha} \equiv U(\beta, l)\beta^4. \tag{8.25}$$

The plots are exhibited in Fig. 8.9 taking differently into account three scenarios, i.e., the temperatures of: CMB, electroweak epoch and the early inflationary era of the universe. Furthermore, the high-energy limit $2E + 3lE^2 \gg 1 - lE$ is also regarded. Here, when the CMB temperature is considered, we see a constant behavior of the curve. On the other hand,

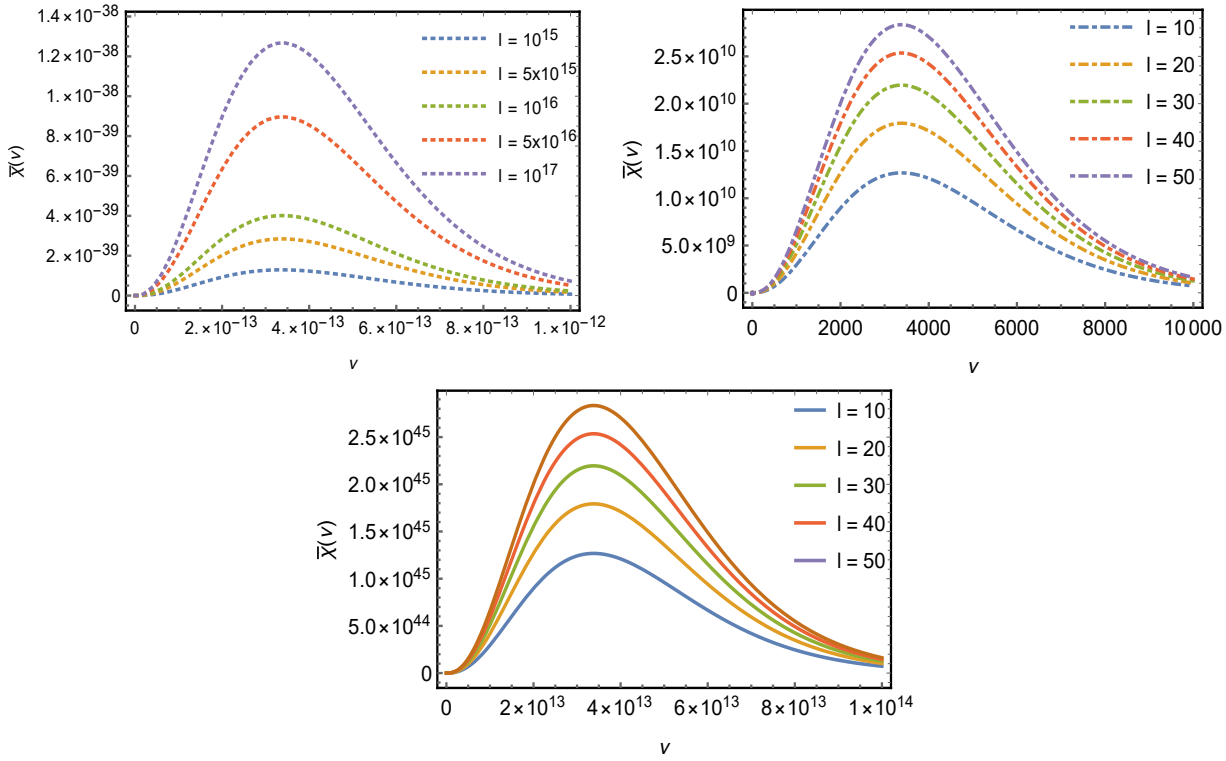

Fig. 8.8: The plots show how the spectral radiance $\bar{\chi}(\nu)$ changes as a function of frequency ν and l(whose dimension is $m \cdot kg^{-1/2} \cdot s^{-1}$) for three different cases. The top left (dotted) is configuration to the cosmic microwave background, i.e., $\beta = 10^{13}$ GeV^{-1}; the top right (dot-dashed) is ascribed to the electroweak configuration, i.e., $\beta = 10^{-3}$ GeV^{-1}; the bottom plot shows the black body radiation to the inflationary period of the Universe, i.e., $\beta = 10^{-13}$ GeV^{-1}.

to the electroweak scenario, we obtain a monotonically increasing function as l changes. Finally, in the inflationary era, we also have a stable model showing a rising behavior when l increases.

In the same manner, the remaining thermodynamic functions can be explicitly computed:

$$\bar{F}(\beta,l) = \frac{1}{\pi^2\beta}\int_0^\infty \left(\frac{E^2+lE^3}{1-lE}\right)^{1/2}\left[\frac{(2E+3lE^2)(1-lE)+l(E^2+lE^3)}{(1-lE)^2}\right]\ln\left(1-e^{-\beta E}\right)\mathrm{d}E, \tag{8.26}$$

$$\bar{S}(\beta,l) = \frac{k_B}{\pi^2}\int_0^\infty \left\{-\left(\frac{E^2+lE^3}{1-lE}\right)^{1/2}\left[\frac{(2E+3lE^2)(1-lE)+l(E^2+lE^3)}{(1-lE)^2}\right]\ln\left(1-e^{-\beta E}\right)\right.$$
$$\left.+E\left(\frac{E^2+lE^3}{1-lE}\right)^{1/2}\left[\frac{(2E+3lE^2)(1-lE)+l(E^2+lE^3)}{(1-lE)^2}\right]\frac{e^{-\beta E}}{1-e^{-\beta E}}\right\}\mathrm{d}E,$$

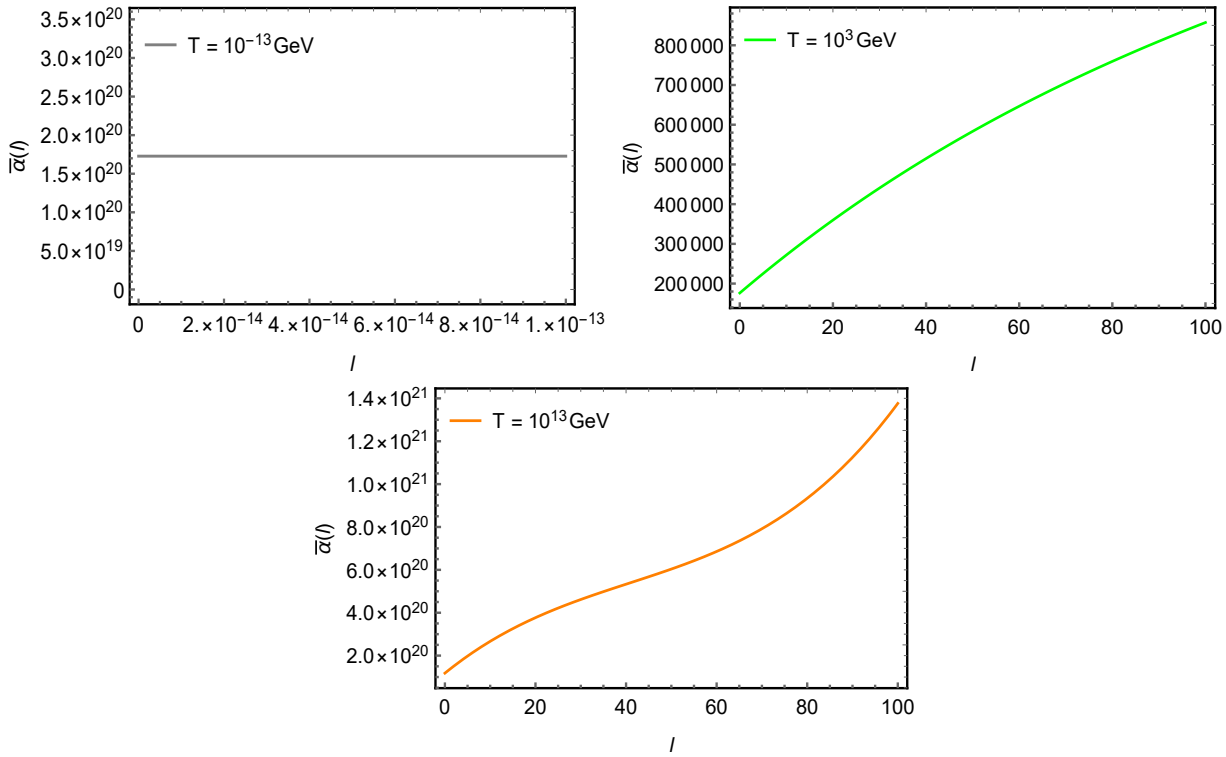

Fig. 8.9: The figure shows the correction to the *Stefan–Boltzmann* law represented by parameter $\bar{\alpha}$ as a function of l(whose dimension is $m \cdot kg^{-1/2} \cdot s^{-1}$) considering the temperatures of cosmic microwave background (top left), electroweak scenario (top right), and the early inflationary universe (bottom).

$$\begin{aligned}\bar{C}_V(\beta,l) &= \frac{k_B\beta^2}{\pi^2}\int_0^\infty dE \times \\ &\times \left\{E^2\left(\frac{E^2+lE^3}{1-lE}\right)^{1/2}\left[\frac{(2E+3lE^2)(1-lE)+l(E^2+lE^3)}{(1-lE)^2}\right]\frac{e^{-2\beta E}}{\left(1-e^{-\beta E}\right)^2}\right. \\ &+ \left. E^2\left(\frac{E^2+lE^3}{1-lE}\right)^{1/2}\left[\frac{(2E+3lE^2)(1-lE)+l(E^2+lE^3)}{(1-lE)^2}\right]\frac{e^{-\beta E}}{1-e^{-\beta E}}\right\}.\end{aligned} \tag{8.27}$$

Initially, we provide the analysis of the Helmholtz free energy displayed in Eq. (8.26); it is considered within three different scenarios of the Universe: CMB, primordial electroweak epoch, and inflationary era. All these results are demonstrated in Fig. 8.10, which displays a trivial contribution to the first case, and a decreasing characteristic for the latter two ones. Next, we examined the entropy which was shown in Eq. (9.9); we investigated such thermal function in the same different scenarios of the Universe. All these considerations were shown in Fig. 8.11, which exhibited the same trivial contribution to the first case, despite of showing an increase characteristic to the latter two ones. Finally, we studied the heat capacity exhibited in Eq. (8.28); we also examined this thermal function in the same different scenarios of the Universe. All these considerations were shown in Fig. 8.12,

exhibiting a trivial contribution to the first case as well, and increasing curves for the next two ones.

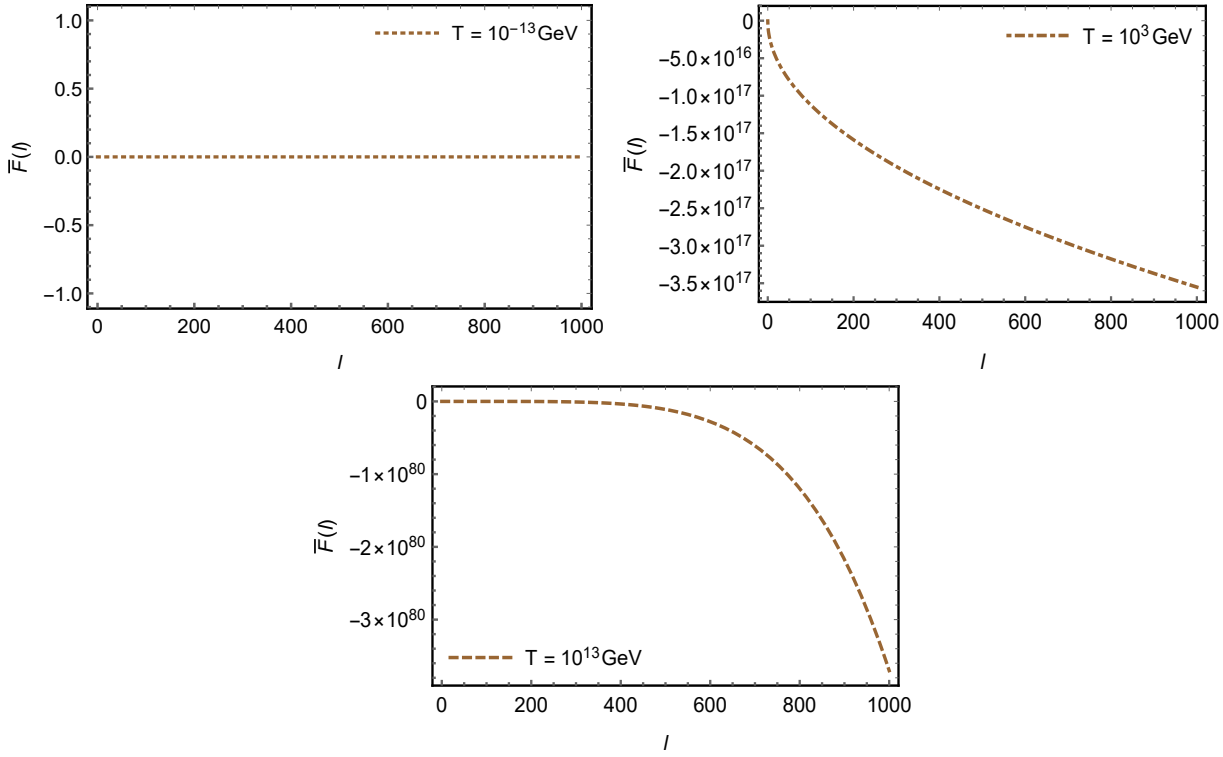

Fig. 8.10: The figure shows the modification of the Helmholtz free energy $\bar{F}$ as a function of l(whose dimension is $m \cdot kg^{-1/2} \cdot s^{-1}$) considering the temperatures of cosmic microwave background (top left), electroweak scenario (top right), and the early inflationary universe (bottom).

Here, just as we did in the previous section, we also present the analysis of the equation of state. Moreover, since there is no analytical solution to perform our analysis, we have to consider a particular limit to obtain its magnitude as we did before. The limit that we study is $(E^2 + lE^3)^{1/2}/(1 - lE)^2 \ll 1$. With it, we obtain the following expression

$$p = \frac{1}{45\pi^2} T^6 \left[270 l^2 \zeta(5) + 4\pi^4 \frac{l}{T} + 90 \frac{1}{T^2} \zeta(3) \right], \tag{8.28}$$

where $\zeta(s)$ is the Riemann zeta function defined by

$$\zeta(s) = \sum_{n=1}^{\infty} \frac{1}{n^s} = \frac{1}{\Gamma(s)} \int_0^{\infty} \frac{x^{s-1}}{e^x - 1} \mathrm{d}x, \quad \Gamma(s) = \int_0^{\infty} x^{s-1} e^{-x} \mathrm{d}x. \tag{8.29}$$

The behavior of Eq. (8.28) is displayed in Fig 8.13. Differently with what happens to the model involving σ, the dispersion relation coming from Eq. (8.18) has a fascinating feature: the shape exhibited to the equation of states turns out to be sensitive to the modification of

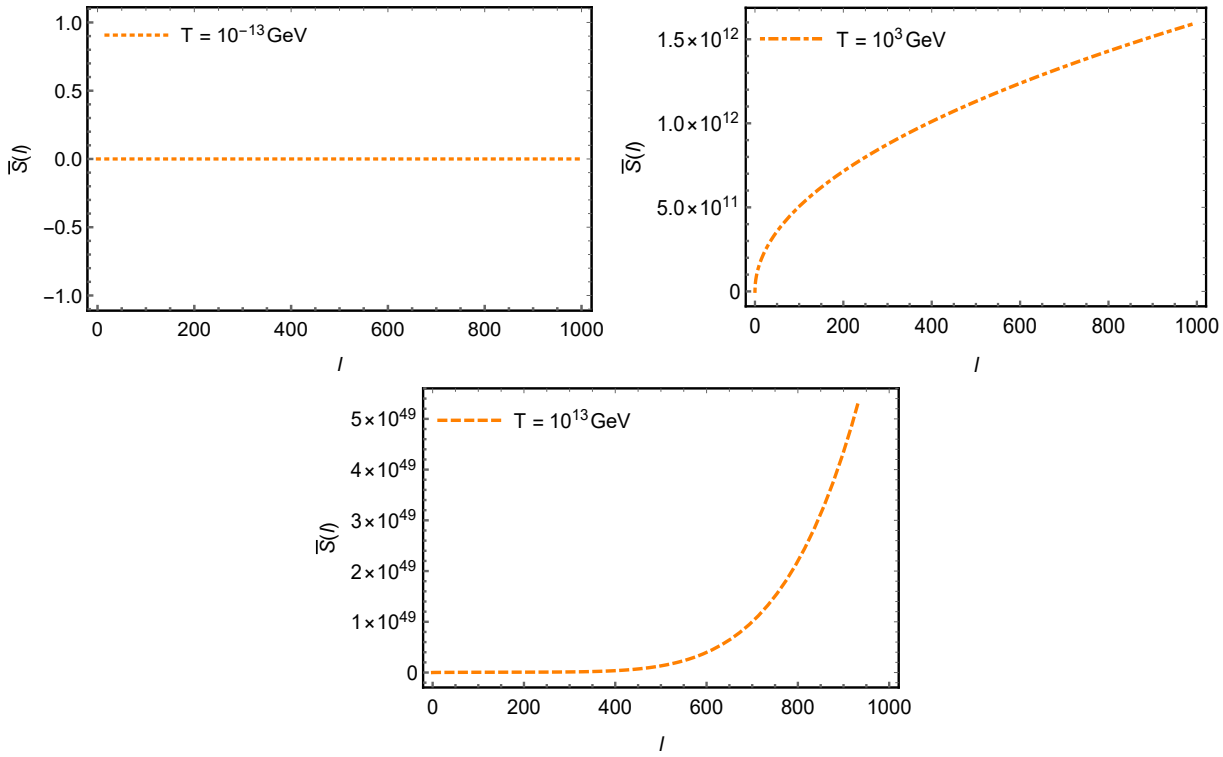

Fig. 8.11: The figure shows the modification of the entropy $\bar{S}$ as a function of l(whose dimension is $m \cdot kg^{-1/2} \cdot s^{-1}$) considering the temperatures of cosmic microwave background (top left), electroweak scenario (top right) and the early inflationary universe (bottom).

the values of l. Furthermore, note that, if we consider $l \to 0$, we obtain

$$p = \frac{90\zeta(3)}{45\pi^2} T^4. \tag{8.30}$$

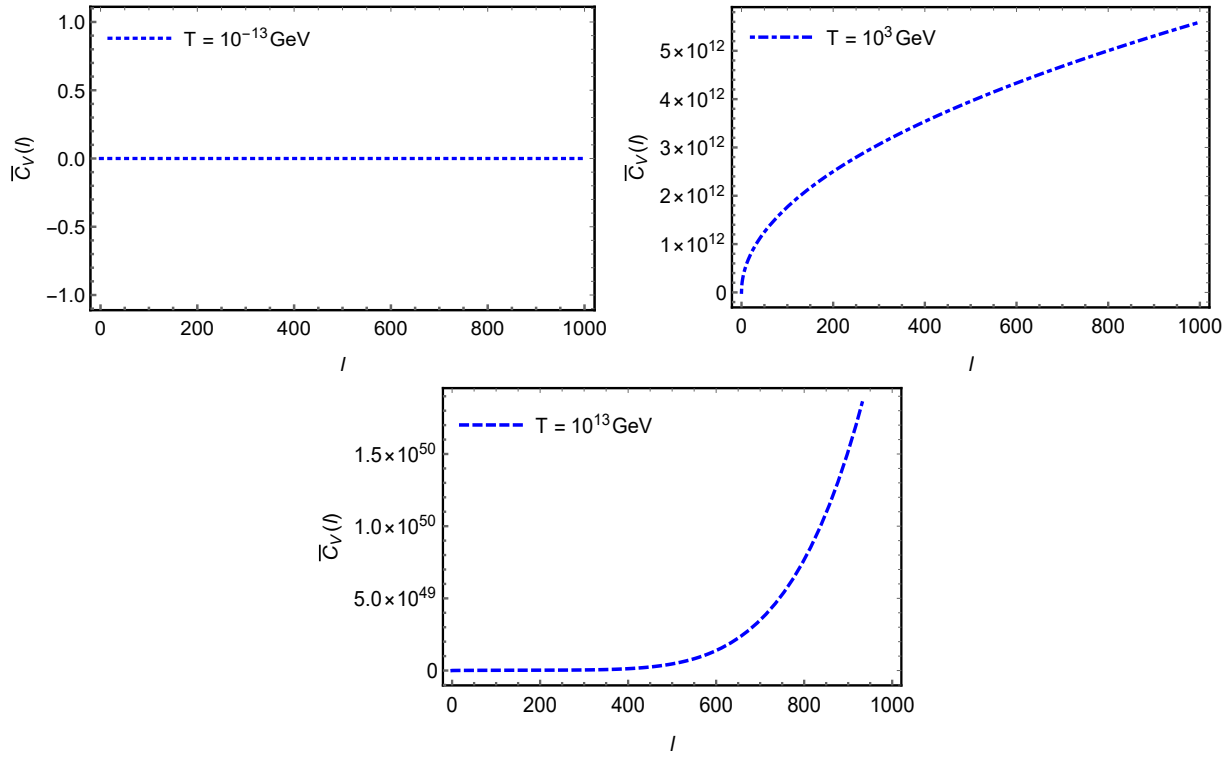

Fig. 8.12: The figure shows the modification of the heat capacity $\bar{C}_V$ as a function of l(whose dimension is $m \cdot kg^{-1/2} \cdot s^{-1}$) considering the temperatures of cosmic microwave background (top left), electroweak scenario (top right) and the early inflationary universe (bottom).

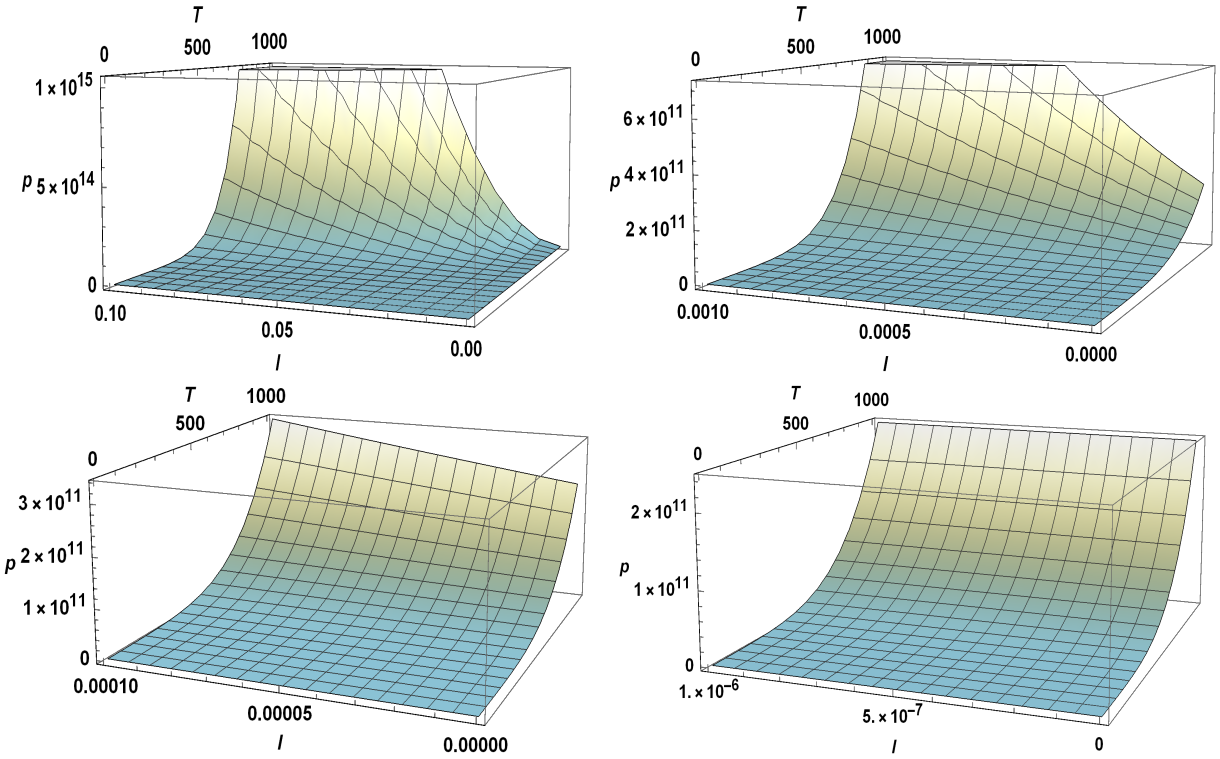

Fig. 8.13: The figure shows the equation of states for different values of p, T, and l(whose dimension is $m \cdot kg^{-1/2} \cdot s^{-1}$).

9. BOUNCING UNIVERSE IN A HEAT BATH

9.1 Modified dispersion relations and their thermodynamical impacts

Here, we start from a general modified dispersion relation in the context of *doubly special relativity* (DSR) [522, 523, 524, 525]

$$E^2 f^2(l_P E) = k^2 g^2(l_P E) + m^2 \tag{9.1}$$

where E is the energy, l_P is the Planck length, defining the fundamental energy scale playing the key role within the DSR, and m is the mass; more so, $f(l_P E)$, $g(l_P E)$ are arbitrary functions and k is the momentum of the particle. The key idea of this concept (for motivations and more detailed discussions, see f.e. [522]) is that the dispersion relations are assumed to be characterized by an additional constant, describing the characteristic energy scale – the Planck energy. As a result, the dispersion relations, at small energies, behave as usual ones, while at higher energies, their deformation, and consequent difference from the usual relativistic scenario, becomes to be the crucial effect. Due to the presence of two constants, that is, the speed of light and the energy scale, this concept was defined as doubly special relativity. It is worth mentioning that the modified dispersion relation coming from Eq. (9.1) has been used as a basis for investigations of black holes [376] and rainbow spacetimes [526, 527, 528]. Note that, if one considers the limit where $f(l_P E) = g(l_P E) \approx 1$, i.e., within a low energy domain $1 \gg l_P E$, one naturally recovers the usual massive dispersion relation $E^2 - k^2 = m^2$. An example of a specific choice of the parameters $f(l_P E)$ and $g(l_P E)$, was done in Ref. [362, 529], explicitly,

$$g(l_P E) = 1, \quad f(l_P E) = \sqrt{\frac{\sin^2(\eta^2 l_P E)}{\eta^2 l_P^2 E^2}} \tag{9.2}$$

which implies

$$\frac{1}{\eta^2 l_P} \sin(\eta^2 l_P E) = \sqrt{k^2 + m^2} \tag{9.3}$$

where η is a dimensionless parameter. The specific choices of the functions $g(l_P E)$, and $f(l_P E)$ presented in Eq. (9.2), as well as in the modified dispersion relation (9.3) are mainly motivated by the study of black hole thermodynamics [527, 530, 531]. Furthermore, as argued in [362], such a choice of the modified dispersion relation can generate bouncing solutions through a thermodynamical approach of general relativity with an apparent horizon. With this, the accessible state of the system, namely, $\Omega(E)$, can properly derived as

$$\Omega(E) = \frac{\Gamma}{\pi^2} \int \frac{1}{\eta^2 l_P^2} \sin^2(\eta^2 l_P E) \cos(\eta^2 l_P E)\, \mathrm{d}E \tag{9.4}$$

where Γ is the volume of the reservoir[1]. Here, we are able to proceed with calculations derived from Eq. (9.4) in a *analytical* manner. It is worth mentioning that such *analytical* studies involving thermodynamic properties in the context of Lorentz symmetry violation were performed only in rare cases. Moreover, from Figs. 9.1, 9.2, 9.3, we accomplish an analysis taking into account low through high-energy temperatures to the accessible states of the system, e.g., we consider three distinct periods of the universe: the inflationary period ($T = 10^{13}$ GeV), the electroweak epoch ($T = 10^{3}$ GeV), and cosmic microwave background radiation ($T = 10^{-13}$ GeV).

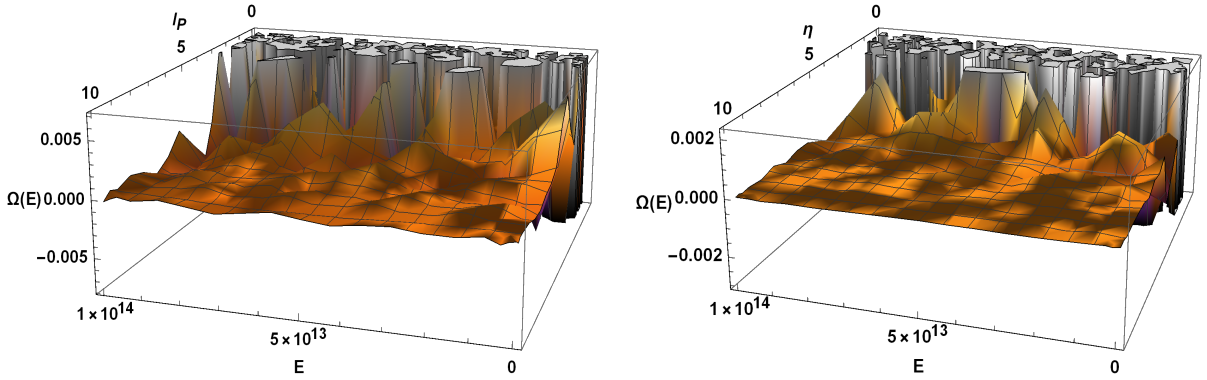

Fig. 9.1: The accessible states of the system to the inflationary period.

We see that the plots displayed in Figs. 9.1, and 9.2 have a similar behavior differing from each other mainly in the energy scale. On the other hand, in the CMB scenario exhibited in Fig. 9.3, the accessible states of the system turn out to be sheets having, therefore, their behavior less complex than the two previous cases. Here, for a better comprehension, let us introduce a generic definition of the partition function for an indistinguishable spinless gas [53]:

$$Z(T, \Gamma, N) = \frac{1}{N! h^{3N}} \int \mathrm{d}q^{3N} \mathrm{d}p^{3N} e^{-\beta H(q,p)} \equiv \int \mathrm{d}E\, \Omega(E) e^{-\beta E}, \tag{9.5}$$

where q is the generalized coordinates, p is the generalized momenta, N is the number of

[1]For the sake of simplicity, hereafter, we will consider the following calculations in a per volume approach.

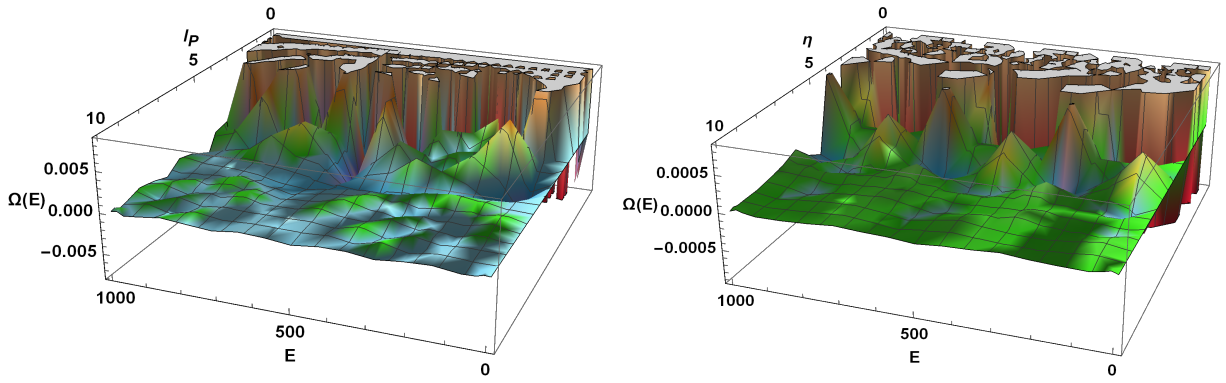

Fig. 9.2: The accessible states of the system to the electroweak period.

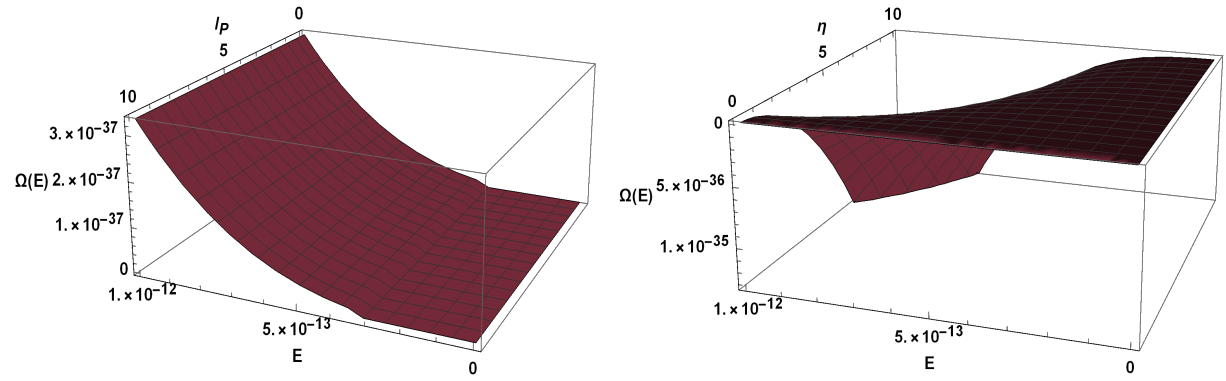

Fig. 9.3: The accessible states of the system to the cosmic microwave background.

particles, H is the Hamiltonian of the system, h is the Planck's constant. Nevertheless, Eq. (9.5), does not account for the spin of the particles that we are dealing with. In our case, we have considered photons (bosons) which reads:

$$\ln[Z] = \int \mathrm{d}E\, \Omega(E) \ln[1 - e^{-\beta E}], \tag{9.6}$$

where the factor $\ln[1 - e^{-\beta E}]$ accounts for the Bose-Einstein statistics. Next, after using Eq.

(9.4), the partition function can be written in a straightforward manner as

$$\begin{aligned}
\ln[Z(\beta,\eta,l_P)] =& -\frac{1}{\pi^2}\int_0^\infty \frac{1}{\eta^2 l_P^2}\sin^2(\eta^2 l_P E)\cos(\eta^2 l_P E)\ln\left(1-e^{-\beta E}\right)\,\mathrm{d}E \\
=& -\frac{\pi^2}{\eta^2 l_P^2}\left\{\frac{\beta e^{\beta E+i\eta^2 l_P E}\,{}_2F_1\left(1,\frac{il_P\eta^2+\beta}{\beta};\frac{il_P\eta^2+2\beta}{\beta};e^{\beta E}\right)}{-8\eta^4 l_P^2+8i\beta\eta^2 l_P}\right. \\
&+\frac{1}{72 l_P^2\eta^4}\left[+\frac{3i\beta\eta^2 l_P e^{E\left(\beta+3i\eta^2 l_P\right)}\,{}_2F_1\left(1,\frac{3il_P\eta^2}{\beta}+1;\frac{3il_P\eta^2}{\beta}+2;e^{\beta E}\right)}{\beta+3i\eta^2 l_P}\right. \\
&-\frac{9\beta\eta^2 l_P e^{E\left(\beta-i\eta^2 l_P\right)}\,{}_2F_1\left(1,1-\frac{il_P\eta^2}{\beta};2-\frac{il_P\eta^2}{\beta};e^{\beta E}\right)}{\eta^2 l_P+i\beta} \\
&-\frac{3i\beta\eta^2 l_P e^{E\left(\beta-3i\eta^2 l_P\right)}\,{}_2F_1\left(1,1-\frac{3il_P\eta^2}{\beta};2-\frac{3il_P\eta^2}{\beta};e^{\beta E}\right)}{\beta-3i\eta^2 l_P} \\
&-18\beta\cos\left(\eta^2 l_P E\right)+2\beta\cos\left(3\eta^2 l_P E\right)+18\eta^2 l_P\ln\left(1-e^{-\beta E}\right)\sin\left(\eta^2 l_P E\right) \\
&\left.\left.-6\eta^2 l_P\ln\left(1-e^{-\beta E}\right)\sin\left(3\eta^2 l_P E\right)\right]\right\}\Bigg|_0^\infty \\
=& -\frac{\pi^2\left\{8\beta+3\pi\eta^2 l_P\left[\coth\left(\frac{3\pi\eta^2 l_P}{\beta}\right)-3\coth\left(\frac{\pi\eta^2 l_P}{\beta}\right)\right]\right\}}{72\eta^6 l_P^4},
\end{aligned} \tag{9.7}$$

where $\beta = 1/\kappa_B T$ and F_1 is the hypergeometric function. Here, with the partition function, all quantities of interest can be derived using the definitions below:

$$\begin{aligned}
F(\beta,\eta,l_P) &= -\frac{1}{\beta}\ln\left[Z(\beta,\eta,l_P)\right], \\
U(\beta,\eta,l_P) &= -\frac{\partial}{\partial\beta}\ln\left[Z(\beta,\eta,l_P)\right], \\
S(\beta,\eta,l_P) &= k_B\beta^2\frac{\partial}{\partial\beta}F(\beta,\eta,l_P), \\
C_V(\beta,\eta,l_P) &= -k_B\beta^2\frac{\partial}{\partial\beta}U(\beta,\eta,l_P).
\end{aligned} \tag{9.8}$$

It is worth mentioning that regarding the thermal aspects, other previous studies were derived in different scenarios [469, 470, 532, 533, 384, 360] as well. In other to accomplish

our investigation, we begin to analyze the mean energy which takes the form

$$
\begin{aligned}
U(\beta,\eta,l_P) &= \frac{1}{\pi^2}\int_0^\infty \frac{1}{\eta^2 l_P^2}\sin^2(\eta^2 l_P E)\cos(\eta^2 l_P E)\frac{e^{-\beta E}}{1-e^{-\beta E}}\,\mathrm{d}E \\
=&\frac{1}{72 l_P^4\pi^2\eta^6} \\
&\times\left\{\left(-9\sin\left(E\eta^2 l_P\right)-9i\cos\left(E\eta^2 l_P\right)\right)\left[E\eta^2 l_P\,{}_2F_1\left(1,-\frac{il_P\eta^2}{\beta};1-\frac{il_P\eta^2}{\beta};\cosh(\beta E)+\sinh(\beta E)\right)\right.\right. \\
&\left.-i\,{}_3F_2\left(1,-\frac{il_P\eta^2}{\beta},-\frac{il_P\eta^2}{\beta};1-\frac{il_P\eta^2}{\beta},1-\frac{il_P\eta^2}{\beta};\cosh(\beta E)+\sinh(\beta E)\right)\right]+\left(-9\sin\left(E\eta^2 l_P\right)\right. \\
&\left.+9i\cos\left(E\eta^2 l_P\right)\right)\left[i\,{}_3F_2\left(1,\frac{il_P\eta^2}{\beta},\frac{il_P\eta^2}{\beta};\frac{il_P\eta^2}{\beta}+1,\frac{il_P\eta^2}{\beta}+1;\cosh(\beta E)+\sinh(\beta E)\right)\right. \\
&\left.+E\eta^2 l_P\,{}_2F_1\left(1,\frac{il_P\eta^2}{\beta};\frac{il_P\eta^2}{\beta}+1;\cosh(\beta E)+\sinh(\beta E)\right)\right] \\
&+\left(\cos\left(3E\eta^2 l_P\right)+i\sin\left(3E\eta^2 l_P\right)\right) \\
&\times\left[{}_3F_2\left(1,\frac{3il_P\eta^2}{\beta},\frac{3il_P\eta^2}{\beta};\frac{3il_P\eta^2}{\beta}+1,\frac{3il_P\eta^2}{\beta}+1;\cosh(\beta E)+\sinh(\beta E)\right)\right. \\
&\left.-3iE\eta^2 l_P\,{}_2F_1\left(1,\frac{3il_P\eta^2}{\beta};\frac{3il_P\eta^2}{\beta}+1;\cosh(\beta E)+\sinh(\beta E)\right)\right]+ \\
&\left(\cos\left(3E\eta^2 l_P\right)-i\sin\left(3E\eta^2 l_P\right)\right) \\
&\times\left[{}_3F_2\left(1,-\frac{3il_P\eta^2}{\beta},-\frac{3il_P\eta^2}{\beta};1-\frac{3il_P\eta^2}{\beta},1-\frac{3il_P\eta^2}{\beta};\cosh(\beta E)+\sinh(\beta E)\right)\right. \\
&\left.\left.+3iE\eta^2 l_P\,{}_2F_1\left(1,-\frac{3il_P\eta^2}{\beta};1-\frac{3il_P\eta^2}{\beta};\cosh(\beta E)+\sinh(\beta E)\right)\right]\right\}\Bigg|_0^\infty = 0.
\end{aligned}
\tag{9.9}
$$

Here, notice that this expression displays a fascinating effect: after considering the limits of integration, the mean energy does not yield any contribution besides the trivial one. Moreover, from Eq. (9.9), we immediately obtain the spectral radiance given by

$$
\chi(\eta,l_P,\nu) = \frac{1}{\pi^2\eta^2 l_P^2}\sin^2(\eta^2 l_P h\nu)\cos(\eta^2 l_P h\nu)\frac{e^{-\beta h\nu}}{1-e^{-\beta h\nu}}, \tag{9.10}
$$

where we have considered $E = h\nu$, being h the Planck constant[2] and ν the frequency. The plots of such a radiance are displayed in Figs. 9.4, and 9.5. Specifically, for the Fig. 9.4, we examine how the parameter l_P modifies the accessible states of the system. Further, in Fig. 9.5, we perform the same examination for the parameter η though. Intriguing, for

[2]For the sake of simplicity, we shall consider $\kappa_B = h = 1$.

both scenarios, the behavior of the spectral radiance turned out to be unusual. This occurs because they exhibited a fluctuation between positive and negative values of frequency as a mirror. Moreover, this might indicate instability from the starting model mainly perhaps due to the periodic characteristic of the dispersion relation of Eq. (9.3).

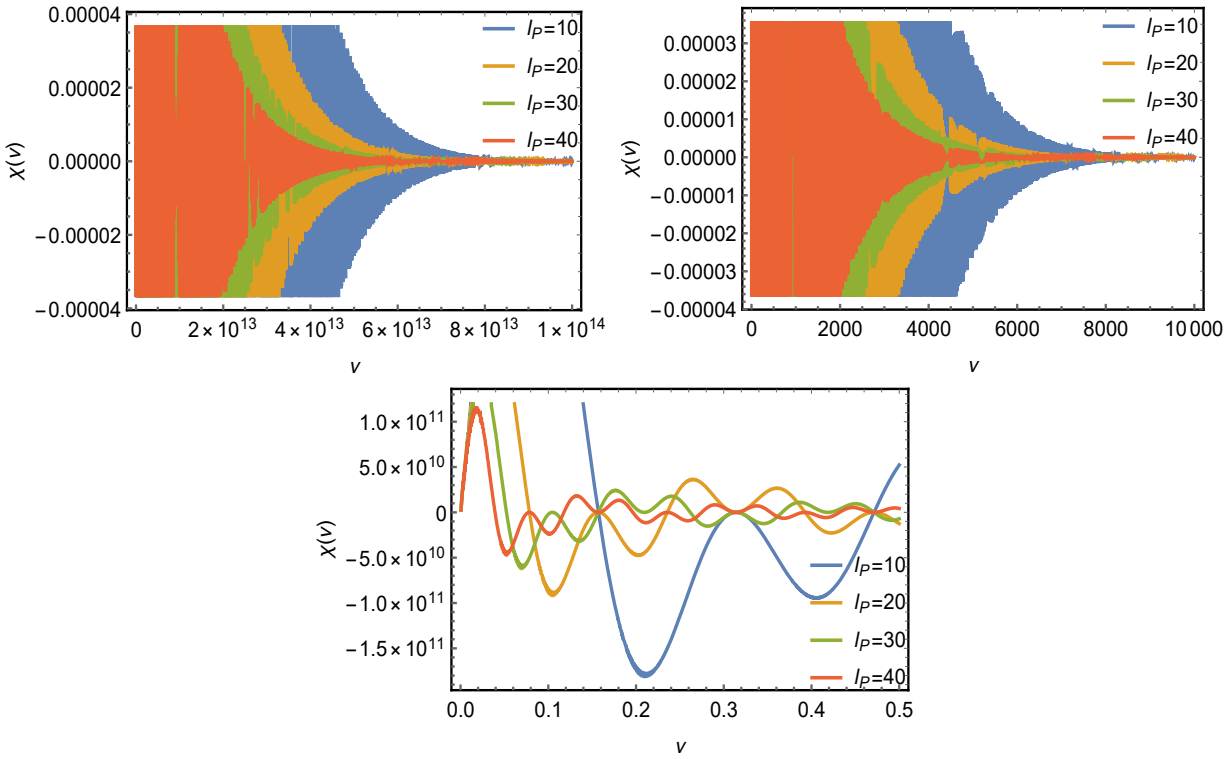

Fig. 9.4: The spectral radiance to inflationary (top left), electroweak (top right) and cosmic microwave back ground (the bottom) periods of the universe for different values of l_P.

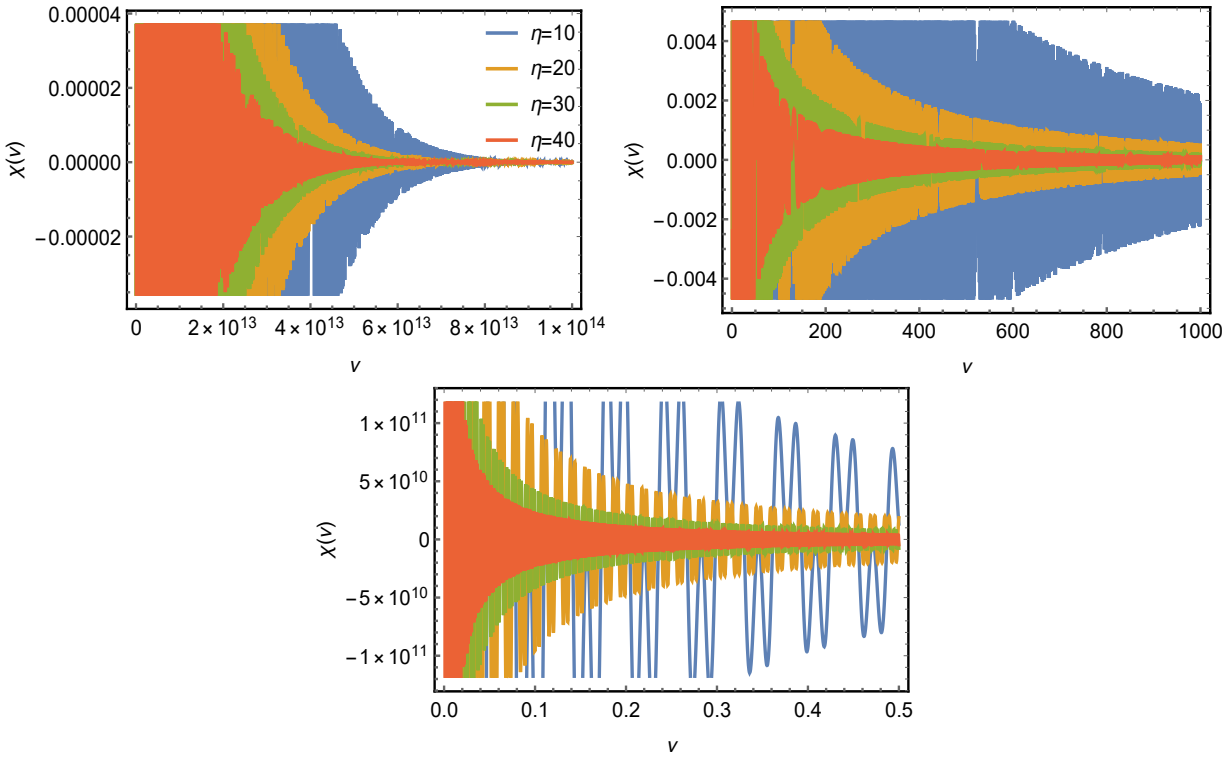

Fig. 9.5: The spectral radiance to inflationary (top left), electroweak (top right) and cosmic microwave back ground (the bottom) periods of the universe for different values of η.

Next, we calculate the Helmholtz free energy

$$
\begin{aligned}
F(\beta,\eta,l_P) &= \frac{1}{\beta\pi^2}\int_0^\infty \frac{1}{\eta^2 l_P^2}\sin^2(\eta^2 l_P E)\cos(\eta^2 l_P E)\ln\left(1-e^{-\beta E}\right)\,\mathrm{d}E \\
&= \frac{\pi^2}{\beta\eta^2 l_P^2}\left\{\frac{\beta e^{\beta E+i\eta^2 l_P E}\,{}_2F_1\left(1,\frac{il_P\eta^2+\beta}{\beta};\frac{il_P\eta^2+2\beta}{\beta};e^{\beta E}\right)}{-8\eta^4 l_P^2+8i\beta\eta^2 l_P}\right. \\
&\quad+\frac{1}{72l_P^2\eta^4}\left[+\frac{3i\beta\eta^2 l_P e^{E\left(\beta+3i\eta^2 l_P\right)}\,{}_2F_1\left(1,\frac{3il_P\eta^2}{\beta}+1;\frac{3il_P\eta^2}{\beta}+2;e^{\beta E}\right)}{\beta+3i\eta^2 l_P}\right. \\
&\quad-\frac{9\beta\eta^2 l_P e^{E\left(\beta-i\eta^2 l_P\right)}\,{}_2F_1\left(1,1-\frac{il_P\eta^2}{\beta};2-\frac{il_P\eta^2}{\beta};e^{\beta E}\right)}{\eta^2 l_P+i\beta} \\
&\quad-\frac{3i\beta\eta^2 l_P e^{E\left(\beta-3i\eta^2 l_P\right)}\,{}_2F_1\left(1,1-\frac{3il_P\eta^2}{\beta};2-\frac{3il_P\eta^2}{\beta};e^{\beta E}\right)}{\beta-3i\eta^2 l_P} \\
&\quad-18\beta\cos\left(\eta^2 l_P E\right)+2\beta\cos\left(3\eta^2 l_P E\right)+18\eta^2 l_P\ln\left(1-e^{-\beta E}\right)\sin\left(\eta^2 l_P E\right) \\
&\quad\left.\left.-6\eta^2 l_P\ln\left(1-e^{-\beta E}\right)\sin\left(3\eta^2 l_P E\right)\right]\right\}\Bigg|_0^\infty \\
&= \frac{\pi^2\left\{8\beta+3\pi\eta^2 l_P\left[\coth\left(\frac{3\pi\eta^2 l_P}{\beta}\right)-3\coth\left(\frac{\pi\eta^2 l_P}{\beta}\right)\right]\right\}}{72\beta\eta^6 l_P^4}.
\end{aligned}
\tag{9.11}
$$

Differently from the result encountered in the mean energy, for the case of the Helmholtz free energy, we arrive at a nontrivial solution after substituting the limits of integration. The behavior of such thermodynamic function is displayed in Fig. 9.6 and Fig. 9.7. In Fig. 9.6, we plot such thermal function for different values of l_P. Likewise, in Fig. 9.7, we study the behavior for rather distinct values of the parameter η.

In general, these curves totally agree with the known results, except in the case when we consider the temperature of the cosmic microwave background, i.e., T = 10^{-13} GeV. The graphics indicate that there exist oscillations between positive and negative values. In this case, it might indicate that our system is close to the bouncing region and, therefore, some disturbing/unusual consequences might take place.

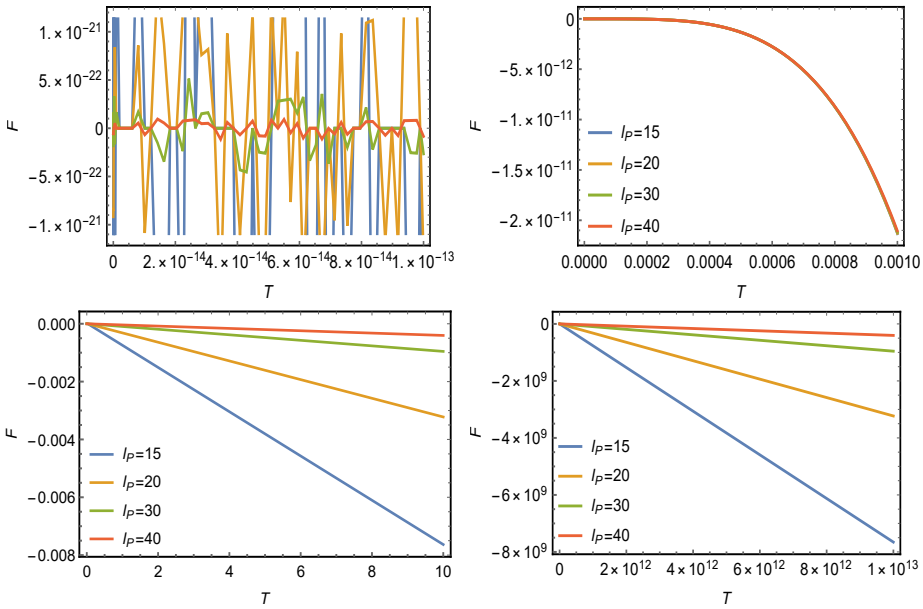

Fig. 9.6: The Helmholtz free energy for different values of l_P.

Furthermore, one important thermodynamic function to be taken into account is the

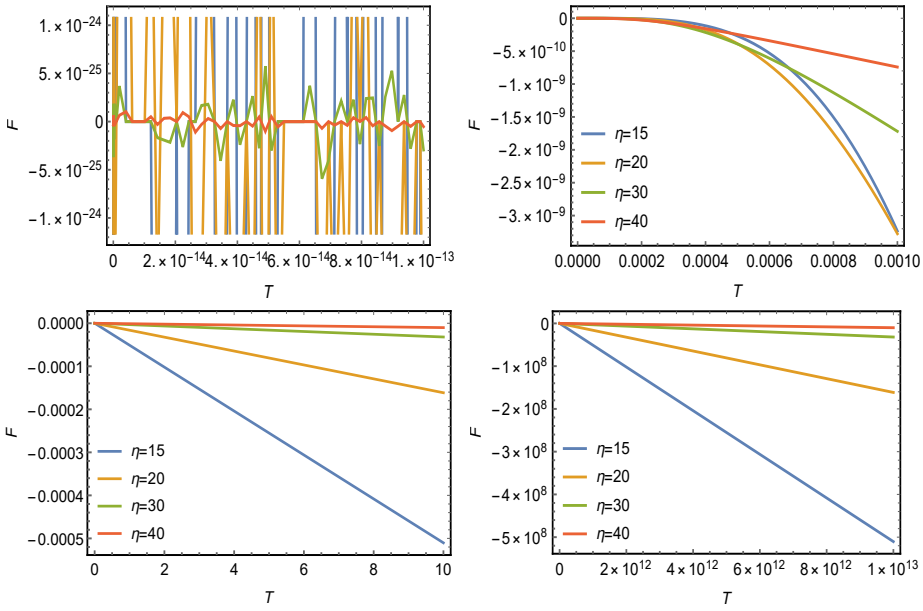

Fig. 9.7: The Helmholtz free energy for different values of η.

entropy. In this sense,

$$
\begin{aligned}
S(\beta,\eta,l_P) &= \frac{\kappa_B}{\pi^2}\int_0^\infty \frac{1}{\eta^2 l_P^2}\sin^2(\eta^2 l_P E)\cos(\eta^2 l_P E)\ln\left(1-e^{-\beta E}\right)\,\mathrm{d}E \\
&+\frac{\kappa_B\beta}{\pi^2}\int_0^\infty \frac{E}{\eta^2 l_P^2}\sin^2(\eta^2 l_P E)\cos(\eta^2 l_P E)\frac{e^{-\beta E}}{1-e^{-\beta E}}\,\mathrm{d}E \\
&= \frac{1}{72\pi^2\eta^6 l_P^4}\left\{9\beta e^{iE\eta^2 l_P}\left[\left(1+iE\eta^2 l_P\right)\,{}_2F_1\left(1,\frac{il_P\eta^2}{\beta};\frac{il_P\eta^2}{\beta}+1;e^{\beta E}\right)\right.\right. \\
&-{}_3F_2\left(1,\frac{il_P\eta^2}{\beta},\frac{il_P\eta^2}{\beta};\frac{il_P\eta^2}{\beta}+1,\frac{il_P\eta^2}{\beta}+1;e^{\beta E}\right)\Big] \\
&+\beta e^{3iE\eta^2 l_P}\left[{}_3F_2\left(1,\frac{3il_P\eta^2}{\beta},\frac{3il_P\eta^2}{\beta};\frac{3il_P\eta^2}{\beta}+1,\frac{3il_P\eta^2}{\beta}+1;e^{\beta E}\right)\right. \\
&+\left(-1-3iE\eta^2 l_P\right)\,{}_2F_1\left(1,\frac{3il_P\eta^2}{\beta};\frac{3il_P\eta^2}{\beta}+1;e^{\beta E}\right)\Big] \\
&+9\beta e^{-iE\eta^2 l_P}\left[\left(1-iE\eta^2 l_P\right)\,{}_2F_1\left(1,-\frac{il_P\eta^2}{\beta};1-\frac{il_P\eta^2}{\beta};e^{\beta E}\right)\right. \\
&-{}_3F_2\left(1,-\frac{il_P\eta^2}{\beta},-\frac{il_P\eta^2}{\beta};1-\frac{il_P\eta^2}{\beta},1-\frac{il_P\eta^2}{\beta};e^{\beta E}\right)\Big] \\
&+\beta e^{-3iE\eta^2 l_P}\left[{}_3F_2\left(1,-\frac{3il_P\eta^2}{\beta},-\frac{3il_P\eta^2}{\beta};1-\frac{3il_P\eta^2}{\beta},1-\frac{3il_P\eta^2}{\beta};e^{\beta E}\right)\right. \\
&+\left(-1+3iE\eta^2 l_P\right)\,{}_2F_1\left(1,-\frac{3il_P\eta^2}{\beta};1-\frac{3il_P\eta^2}{\beta};e^{\beta E}\right)\Big] \\
&-24\eta^2 l_P\ln\left(e^{\beta E}-1\right)\sin^3\left(E\eta^2 l_P\right)-18\eta^2 l_P\left[\ln\left(1-e^{-\beta E}\right)\right. \\
&\left.\left.-\ln\left(e^{\beta E}-1\right)\right]\sin\left(E\eta^2 l_P\right)+6\eta^2 l_P\left(\ln\left(1-e^{-\beta E}\right)\right.\right. \\
&\left.\left.\left.-\ln\left(e^{\beta E}-1\right)\right)\sin\left(3E\eta^2 l_P\right)\right\}\right|_0^\infty = \frac{3\pi\eta^2 l_P\left[3\coth\left(\frac{\pi\eta^2 l_P}{\beta}\right)-\coth\left(\frac{3\pi\eta^2 l_P}{\beta}\right)\right]-8\beta}{72\pi^2\eta^6 l_P^4}.
\end{aligned}
\tag{9.12}
$$

The behavior of the entropy agrees with the previously known results from low through high-temperature regimes; in other words, this means that the second law of the thermodynamics is maintained, as it is natural to expect. Nevertheless, additionally of what was discussed in Refs. [362, 524], a confusing behavior was also revealed in Figs. 9.8 and 9.9 for the very low temperatures (the cosmic microwave background temperature): negative values of the entropy aroused. This might also be related to the bouncing region.

The critical temperature for both configuration of entropy and Helmholtz free energy was $T \leq 3.5 \times 10^{-5}$ GeV. In this regime, the system seems to display instability since the thermal quantities entropy and Helmholtz free energy showed fluctuation between negative and positive values.

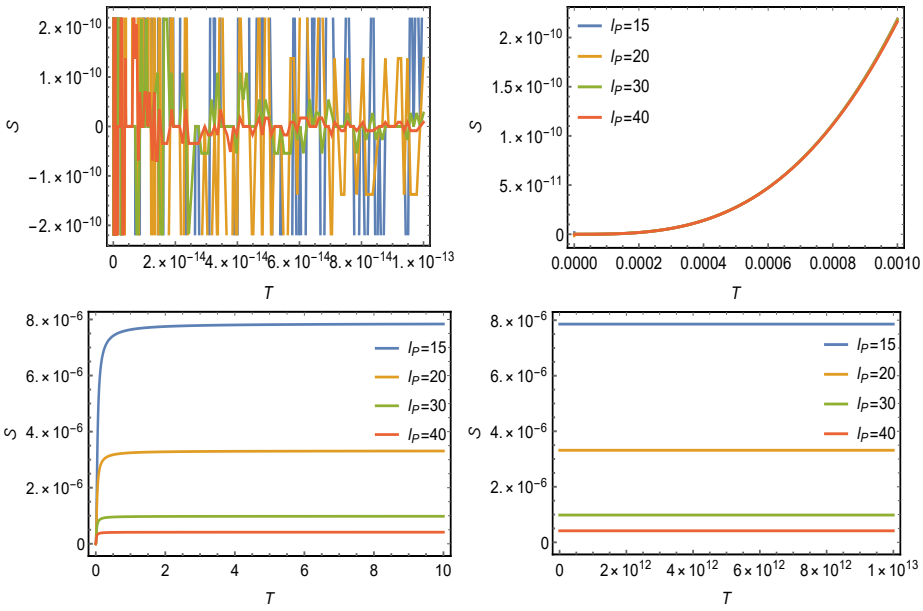

Fig. 9.8: Entropy for different values of l_P.

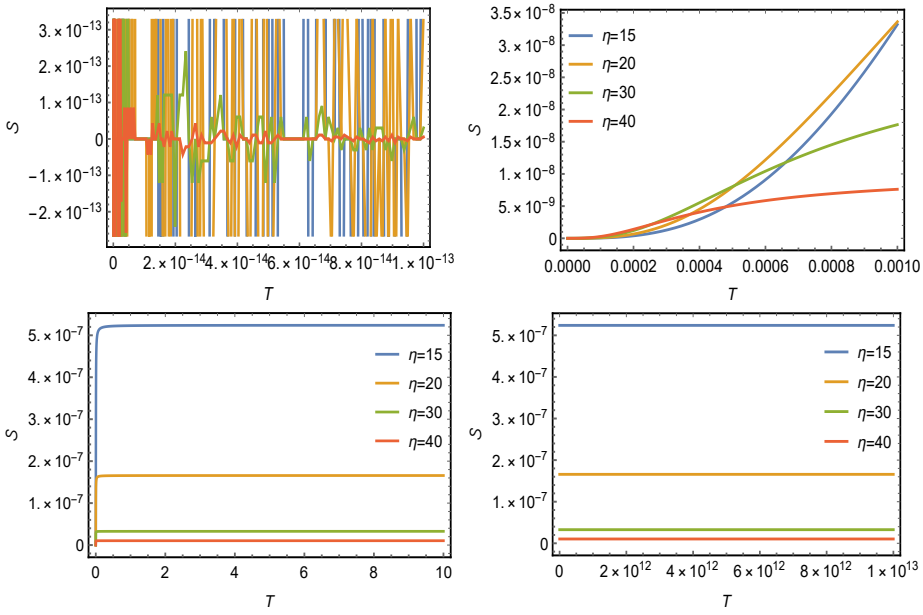

Fig. 9.9: Entropy for different values of η.

Finally, the heat capacity is found to look like

$$
\begin{aligned}
&C_V(\beta,\eta,l_P) = \frac{\kappa_B\beta^2}{\pi^2}\int_0^\infty \frac{E^2}{\eta^2 l_P^2}\sin^2(\eta^2 l_P E)\cos(\eta^2 l_P E)\frac{e^{-2\beta E}}{(1-e^{-\beta E})^2}\,\mathrm{d}E \\
&+\frac{\kappa_B\beta}{\pi^2}\int_0^\infty \frac{E^2}{\eta^2 l_P^2}\sin^2(\eta^2 l_P E)\cos(\eta^2 l_P E)\frac{e^{-\beta E}}{1-e^{-\beta E}}\,\mathrm{d}E \\
=&\frac{\beta}{72\pi^2\eta^2 l_P^2}\left\{\frac{18E^2\cos\left(3E\eta^2 l_P\right)}{e^{\beta E}-1}\right. \\
&9\left[-\frac{2E^2\cos\left(E\eta^2 l_P\right)}{e^{\beta E}-1}+\frac{1}{\eta^4 l_P^2}e^{-iE\eta^2 l_P}\left[-l_P E\eta^2\left(E\eta^2 l_P+2i\right){}_2F_1\left(1,-\frac{il_P\eta^2}{\beta};1-\frac{il_P\eta^2}{\beta};e^{\beta E}\right)\right.\right. \\
&+\left(-2+2iE\eta^2 l_P\right){}_3F_2\left(1,-\frac{il_P\eta^2}{\beta},-\frac{il_P\eta^2}{\beta};1-\frac{il_P\eta^2}{\beta},1-\frac{il_P\eta^2}{\beta};e^{\beta E}\right) \\
&\left.\left.+2\,{}_4F_3\left(1,-\frac{il_P\eta^2}{\beta},-\frac{il_P\eta^2}{\beta},-\frac{il_P\eta^2}{\beta};1-\frac{il_P\eta^2}{\beta},1-\frac{il_P\eta^2}{\beta},1-\frac{il_P\eta^2}{\beta};e^{\beta E}\right)\right]\right] \\
&-\frac{e^{iE\eta^2 l_P}}{\eta^4 l_P^2}\left[E\eta^2 l_P\left(E\eta^2 l_P-2i\right){}_2F_1\left(1,\frac{il_P\eta^2}{\beta};\frac{il_P\eta^2}{\beta}+1;e^{\beta E}\right)\right. \\
&+\left(2+2iE\eta^2 l_P\right){}_3F_2\left(1,\frac{il_P\eta^2}{\beta},\frac{il_P\eta^2}{\beta};\frac{il_P\eta^2}{\beta}+1,\frac{il_P\eta^2}{\beta}+1;e^{\beta E}\right) \\
&\left.-2\,{}_4F_3\left(1,\frac{il_P\eta^2}{\beta},\frac{il_P\eta^2}{\beta},\frac{il_P\eta^2}{\beta};\frac{il_P\eta^2}{\beta}+1,\frac{il_P\eta^2}{\beta}+1,\frac{il_P\eta^2}{\beta}+1;e^{\beta E}\right)\right] \\
&+\frac{e^{-3iE\eta^2 l_P}}{\eta^4 l_P^2}\left[3E\eta^2 l_P\left(3E\eta^2 l_P+2i\right){}_2F_1\left(1,-\frac{3il_P\eta^2}{\beta};1-\frac{3il_P\eta^2}{\beta};e^{\beta E}\right)\right. \\
&+\left(2-6iE\eta^2 l_P\right){}_3F_2\left(1,-\frac{3il_P\eta^2}{\beta},-\frac{3il_P\eta^2}{\beta};1-\frac{3il_P\eta^2}{\beta},1-\frac{3il_P\eta^2}{\beta};e^{\beta E}\right) \\
&\left.+2\,{}_4F_3\left(1,-\frac{3il_P\eta^2}{\beta},-\frac{3il_P\eta^2}{\beta},-\frac{3il_P\eta^2}{\beta};1-\frac{3il_P\eta^2}{\beta},1-\frac{3il_P\eta^2}{\beta},1-\frac{3il_P\eta^2}{\beta};e^{\beta E}\right)\right] \\
&+\frac{e^{3iE\eta^2 l_P}}{\eta^4 l_P^2}\left[3E\eta^2 l_P\left(3E\eta^2 l_P-2i\right){}_2F_1\left(1,\frac{3il_P\eta^2}{\beta};1+\frac{3il_P\eta^2}{\beta};e^{\beta E}\right)\right. \\
&+\left(2+6iE\eta^2 l_P\right){}_3F_2\left(1,\frac{3il_P\eta^2}{\beta},+\frac{3il_P\eta^2}{\beta};1+\frac{3il_P\eta^2}{\beta},1+\frac{3il_P\eta^2}{\beta};e^{\beta E}\right) \\
&\left.\left.+2\,{}_4F_3\left(1,\frac{3il_P\eta^2}{\beta},\frac{3il_P\eta^2}{\beta},\frac{3il_P\eta^2}{\beta};1+\frac{3il_P\eta^2}{\beta},1+\frac{3il_P\eta^2}{\beta},1+\frac{3il_P\eta^2}{\beta};e^{\beta E}\right)\right]\right\}\Bigg|_0^\infty = 0.
\end{aligned}
\tag{9.13}
$$

Therefore, just as occurred for the mean energy, the heat capacity turned out to yield only the trivial contribution after performing the limits of integration.

10. CONCLUSION AND PERSPECTIVES

This thesis was aimed at investigating the thermodynamic properties of diverse field theories concerning high-energy and condensed matter physics. More so, we used the theory of ensembles to derive our calculations. Initially, we provide the thermodynamic properties based on the formalism of canonical ensemble to the Aharonov-Bohm quantum ring. Next, we constructed a model in order to study quantum gases. In this context, we studied bosons, fermions and spinless particles within the grand-canonical ensemble taking into account two different approaches: *interacting* and *noninteracting* particles. To corroborate our results, we applied them to the Bose-Einstein condensate and to the helium dimmers ^{3}He and ^{4}He. The same model was applied considering rather the Lorentz violation. Moreover, to the latter case, we also proposed two applications to support our theoretical calculations: *phosphorene* and *spin precession*. Next, the thermal aspects were investigated as well to a variety of models/theories (regarding different dispersion relations) when the Lorentz symmetry was no longer maintained within the canonical ensemble. To these cases, three distinct scenarios were consider to the universe: the cosmic microwave background, the electroweak epoch, and the inflationary period. Particularly, all these features are precisely highlighted as follows:

In chapter 2, we had the purpose of investigating the thermodynamic properties of an Aharonov-Bohm quantum ring in a heat bath regarding both relativistic and non-relativistic cases in the canonical ensemble at finite temperature. Initially, we calculated the energy spectrum and the eigenfunctions for the relativistic case, and we took a low-energy limit where the nonrelativistic energy spectrum was recovered. In both cases, the energy spectrum turned out to be non-degenerate. Since the exact partition function did not have a closed form for carrying out our calculations, we assumed the strong field approximation and we employed the Euler-Mclaurin summation formula to evaluate numerically the partition function. Once determined the partition function, all the main thermodynamic quantities could be derived, namely the Helmholtz free energy F, the mean energy U, the entropy S and the heat capacity C_V. Their respective graphics were plotted for several values of T and different magnetic fluxes Φ's. As a result, we noticed that the well-known Dulong-Petit law was satisfied and the relativistic specific heat was twice in comparison with the non-relativistic limit. Finally, we expect that our results may be used as a useful tool to study these thermal properties in agreement with experiments.

In chapter 3, we examined the behavior of the thermodynamic functions for different geometries, i.e., spherical, cyllindrical, ellipsoidal and toroidal ones; we primarily used the canonical ensemble for spinless particles. Moreover, *noninteracting* gases were also taken into account for the same geometries with the usage of the grand canonical ensemble description. A study of how geometry affected the system of spinless particles, fermions and bosons was provided as well. Moreover, two applications were given to corroborate our results: the *Bose-Einstein condensate* and the *helium dimer*. Furthermore, for the bosonic sector, independently of the geometry, the entropy and internal energy turned out to be greater than for the fermionic case; a standard ordering of the sizes of the computed quantities repeatedly occurred for both systems: *Ellipsoid* > *Cylinder* > *Sphere*. Also, it is worth mentioning that, for the toriodal case, there was an "inversion point" at 3 K due to the winding number. Thereby, we saw a modification in the thermal properties due to the topological parameter α. Finally, we constructed a model to provide a description of *interacting* quantum gases; it was implemented for three different cases: a cubical box, a ring, and a torus. Such an interaction sector turned out to be more prominent since all results were derived analytically.

Another promising aspect to be investigated in condensed-matter physics, is the thermal properties of anisotropic systems (with or without considering Lorentz violation [534]). Such anisotropy may reveal new phenomena which can be confronted with experimental physics afterwards. In the case of phosphorene, one can assume electrons to have an anisotropic effective mass [494], which raises many possibilities: if we confine these electrons to a box, collisions with the walls will depend on the angle that the wall makes with the preferred direction that describes the anisotropy. More so, phonons behave likewise in such systems.

The chapter 5 aimed at studying the thermodynamic aspects of interacting quantum gases when Lorentz violation took place. We investigated the physical consequences of taking into account both fermion and boson sectors. In order to proceed further, we have utilized the grand canonical ensemble as the starting point. Next, we obtained the so-called grand canonical partition function to address analytically all calculations of interest, namely, the particle number, the mean total energy, the entropy and the pressure. Moreover, the first three ones turned out to behave as extensive quantities although the presence of Lorentz-violating terms.

For fermion modes, we considered a system provided by scalar, vector, pseudovector and tensor operators. Particularly, the latter two scenarios exhibited an absence of the spin degeneracy. In this way, the system turned out to acquire greater energy and particle number for spin-down particle modes in comparison with spin-down ones. Besides, pseudoscalar operator played no role at the leading order dispersion relation studied here. On the other hand, for boson particles at high temperature regime the system showed that the particle number for the vector case decreased, while increased for the tensor case. More so, we

analysed the magnitude of Lorentz-violating coefficients estimating the upper bounds for the bosonic case; we proposed some possible applications in order to corroborate our results in two different contexts: *phosphorene* and *spin precession*.

The physical consequences of such thermal analysis of relativistic interacting quantum gases involving fermion and boson particles might possibly reveal new fingerprints of a hidden physical experimental data which might be measured by future experiments in the existence of Lorentz violation. Thereby, this theoretical proposition can lead to a toy model for further promising studies to search for any trace of Lorentz violation. In addition, being expected to go beyond the current analysis presented in this chapter, our procedure of treating a modified relativistic energy for an arbitrary quantum state, as long as there exist only momenta involved, may lead to further different investigations and applications depending on the scenario worked out.

As future perspectives, an analogous study for the thermodynamic functions regarding rather the nonminimal SME appears to be worthy to examine. Additionally, analyzing how the phase transition occurs for the minimal and nonminimal SME as well as investigating the implications of a system having an ensemble of antiparticles seem to be interesting open questions to be studied. These and other ideas are now under development.

The chapter 7 focused on investigating the thermodynamic properties of the graviton and a modified photon gas, which came from a generalized electrodynamics including anisotropic Podolsky and Lee-Wick terms, in a thermal reservoir when Lorentz violation is taken into account. In this direction, we determined the number of accessible states of the system which played a crucial role in obtaining the partition function. It sufficed to supply all the main thermodynamic functions, namely, spectral radiance, mean energy, Helmholtz free energy, entropy and heat capacity. Again, it is important to be noticed that the entire study was performed dealing with a high temperature regime, i.e., $\beta = 10^{-13}\ \mathrm{GeV}^{-1}$. Additionally, we proposed a correction to the black body radiation spectra as well as to the *Stefan–Boltzmann* law in terms of ξ and η_2.

Next, in the context of graviton thermodynamics with Lorentz violation, the parameter $\tilde{\alpha}(\xi)$ expressed the particular feature of being a monotonically increasing function. The same property was also displayed when one regarded the entropy $S(\xi)$ and the heat capacity $C_V(\xi)$. In contrast, being the distinct one, the Helmholtz free energy $F(\xi)$ indicated a monotonically decreasing function when parameter ξ increased.

On the other hand, considering the generalized Podolsky with addition of Lee-Wick terms, the $\bar{\alpha}(\eta_2)$ possessed significant positive curvature for huge values of η_2. Notably, taking into account the entropy $\bar{S}(\eta_2)$ and the heat capacity $\bar{C}_V(\eta_2)$, one verified that such plots had a monotonically increasing function with an attenuated curvature. In a complementary way, the Helmholtz free energy $\bar{F}(\eta_2)$ showed a monotonically decreasing

curve.

Lastly, the physical implications of the thermodynamic properties presented by the graviton might address some new fingerprints of a hidden physics which might be confronted with observatory data in the existence of Lorentz violation. In such direction, these proposals can address a toy model for further studies involving gravitation and cosmology. Besides, with respect to the generalized theory of Podolsky with Lee-Wick terms, these properties might be advantageous in either forthcoming approaches regarding condensed matter physics or statistical thermodynamics. As a future perspective, examining the thermal features of very recent models, which appeared in the literature involving the Stückelberg electrodynamics modified by a Carroll-Field-Jackiw term [535], and the graviton-dark photons in cosmological scenarios [536], seem to be interesting open questions to be investigated.

The chapter 6, we studied the thermodynamic properties of a photon gas in a heat bath in the context of higher-derivative electrodynamics. We calculated the accessible states of the system in order to obtain the partition function that allowed us to investigate the behavior of the main thermodynamic functions, i.e., Helmholtz free energy, mean energy, entropy, and heat capacity. It is worth to be mentioned that all analyses were performed in the context of the primordial temperature of the universe, i.e., $\beta = 10^{-13}$ GeV^{-1}. Moreover, we proposed a correction to the black body radiation in terms of the parameters θ and η, which accounted for Podolsky and its generalization with Lorentz violation, respectively.

Besides, we suggested corrections to the *Stefan–Boltzmann* law for both theories. In the case of $\tilde{\alpha}(\theta)$, we saw that, depending on the considerations ascribed to the mean energy, we might find different behaviors of such curves. Likewise, Helmholtz $F(\theta)$, entropy $S(\theta)$, and heat capacity $C_V(\theta)$ could also have three different curves depending on the initial circumstances ascribed to them.

On the other hand, the parameter $\bar{\alpha}(\eta)$ showed that there existed an accentuated increase as far as positive values of η were taken into account. The Helmholtz free energy $\bar{F}(\eta)$ started to decrease when η increased. Both $\bar{S}(\eta)$ and $\bar{C}_V$ increased for positive changes of η, but the latter exhibited an increase with a constant angular coefficient though.

Finally, the physical consequences of the thermodynamic functions of such theories should be taken into account in order to possibly address some new fingerprints of a hidden experimental physics. Such analysis could be confronted by future experiments in the existence of Lorentz symmetry breaking. With this theoretical background, we can address a toy model for further investigations stepping towards to discover any trace of Lorentz violation. Furthermore, this thermal study might also be useful in future applications considering condensed matter physics for instance. Within the context of Lorentz violation, as future perspective, we could analyze the behavior of the thermodynamic properties for the generalized Podolsky with Lee-Wick terms. Additionally, knowing whether such theory is in

agreement with either Cosmic Microwave Background regime or the electroweak epoch of the Universe seem also to be interesting investigations.

In the chapter 8, we considered the thermodynamical aspects of two higher-derivative Lorentz-breaking theories, namely, CPT-even and CPT-odd ones. Within our study, we focused on the dispersion relations rather than the specific form of the Lagrangians. In this way, we expect that our results can be applied not only to scalar field models as we assumed, but also to specific gauge or spinor field theories.

We calculated the modification to the black body radiation spectra and to the *Stefan–Boltzmann* law due to the parameters σ and l. For these theories, we explicitly obtained the corresponding equation of states and the thermodynamic functions as well, i.e., the mean energy, the Helmholtz free energy, the entropy, and the heat capacity. Moreover, all the calculations presented in this chapter were performed taking into account three different scenarios of the Universe: cosmic microwave background, electroweak epoch, and inflationary era.

Furthermore, since the heat capacity rapidly increased with the Lorentz-breaking parameters at high temperatures, perhaps one might expect a phase transition in those scenarios. Nevertheless, a further investigation in this direction might be accomplished in order to provide a proper examination. Thereby, as a further perspective, we suggest the detailed study of the whole field of Horava-Lifshitz gravity model and the possible phase transitions in our models. Another feasible continuation of this study can consist in its application to other higher-derivative Lagrangians of certain known field theories, f.e. those ones discussed in [349].

In this chapter 9, we focused on examining the thermal behavior of a photon gas within the context of bouncing universe. To accomplish this, we started from a modified dispersion relation which accounted for modified Friedmann equations with a bounce solution. All of our results were derived *analytically*. Furthermore, we considered three different scenarios of temperature of the universe: inflationary epoch, electroweak era and cosmic microwave background. Initially, we calculated the accessible states of the system. With it, we performed an analysis of the impact of the parameters l_P and η on the modification of the thermodynamic properties of interest.

The spectral radiance $\chi(\nu)$ turned out to have an intriguing behavior, i.e., it had a fluctuation between positive and negative frequencies. Perhaps, it could be a consequence of either an disturbing issue due to the bouncing solution or for the periodic aspect of the trigonometric function which came from the dispersion relation.

More so, we calculated the mean energy, the entropy, the Helmholtz free energy, and the heat capacity as well. Nevertheless, one intriguing aspect also brought out: after applying the integration limits, the mean energy and the heat capacity turned out to have

no contribution in our calculations. On the other hand, the Helmholtz free energy and the entropy demonstrated to be consistent with previous studies, i.e., the second law of the thermodynamics was maintained. However, when we considered the low temperature regime, such thermal functions exhibited a fluctuation aspect as appeared in the spectral radiance. The critical temperature for both configurations of entropy and Helmholtz free energy were $T \leq 3.5 \times 10^{-5}$ GeV. In this regime, the system seemed to have instability since such quantities showed fluctuation between negative and positive values. Such a phenomenon might have happened due to proximity to the bouncing point. Nevertheless, further investigation might be accomplished in order answer properly this issue.

Bibliography

[1] Duane C Wallace. "Statistical mechanics of monatomic liquids". In: *Physical Review E* 56.4 (1997), p. 4179.

[2] John C Mauro and Morten M Smedskjaer. "Statistical mechanics of glass". In: *Journal of non-crystalline solids* 396 (2014), pp. 41–53.

[3] John G Kirkwood. "Statistical mechanics of fluid mixtures". In: *The Journal of chemical physics* 3.5 (1935), pp. 300–313.

[4] Denis J Evans and Gary P Morriss. *Statistical mechanics of nonequilbrium liquids*. ANU Press, 2007.

[5] Louis A Girifalco. *Statistical mechanics of solids*. Vol. 58. OUP USA, 2003.

[6] Y Imry. "On the statistical mechanics of coupled order parameters". In: *Journal of Physics C: Solid State Physics* 8.5 (1975), p. 567.

[7] Sergio Albeverio et al. "The statistical mechanics of quantum lattice systems". In: (2009).

[8] David Ruelle. "Statistical mechanics of a one-dimensional lattice gas". In: *Communications in Mathematical Physics* 9.4 (1968), pp. 267–278.

[9] Barry Simon. *The Statistical Mechanics of Lattice Gases, Volume I*. Princeton University Press, 2014.

[10] Elliott W Montroll and Joseph E Mayer. "Statistical mechanics of imperfect gases". In: *The Journal of Chemical Physics* 9.8 (1941), pp. 626–637.

[11] RP Ojha et al. "Statistical mechanics of a gas-fluidized particle". In: *Nature* 427.6974 (2004), pp. 521–523.

[12] FJ Rogers. "Statistical mechanics of Coulomb gases of arbitrary charge". In: *Physical Review A* 10.6 (1974), p. 2441.

[13] Alexander Leonidovich Kuzemsky. *Statistical mechanics and the physics of many-particle model systems*. World Scientific, 2017.

[14] AL Kuzemsky. "Statistical mechanics and the physics of many-particle model systems". In: *Physics of Particles and Nuclei* 40.7 (2009), pp. 949–997.

[15] Duane C Wallace. “Renormalization and statistical mechanics in many-particle systems. I. Hamiltonian perturbation method”. In: *Physical Review* 152.1 (1966), p. 247.

[16] Shuguang Li et al. “Particle robotics based on statistical mechanics of loosely coupled components”. In: *Nature* 567.7748 (2019), pp. 361–365.

[17] Antony Valentini. “Hidden variables, statistical mechanics and the early universe”. In: *Chance in physics*. Springer, 2001, pp. 165–181.

[18] B Harms and Y Leblanc. “Statistical mechanics of black holes”. In: *Physical Review D* 46.6 (1992), p. 2334.

[19] Haim Sompolinsky et al. “Statistical mechanics of neural networks”. In: *Physics Today* 41.21 (1988), pp. 70–80.

[20] HE Stanley et al. “Statistical mechanics in biology: how ubiquitous are long-range correlations?” In: *Physica A: Statistical Mechanics and its Applications* 205.1-3 (1994), pp. 214–253.

[21] Sarah Marzen, Hernan G Garcia, and Rob Phillips. “Statistical mechanics of Monod–Wyman–Changeux (MWC) models”. In: *Journal of molecular biology* 425.9 (2013), pp. 1433–1460.

[22] Thierry Mora and William Bialek. “Are biological systems poised at criticality?” In: *Journal of Statistical Physics* 144.2 (2011), pp. 268–302.

[23] Edward H Kerner. “A statistical mechanics of interacting biological species”. In: *The bulletin of mathematical biophysics* 19.2 (1957), pp. 121–146.

[24] Edward H Kerner. “Further considerations on the statistical mechanics of biological associations”. In: *The bulletin of mathematical biophysics* 21.2 (1959), pp. 217–255.

[25] T Chou, K Mallick, and RKP Zia. “Non-equilibrium statistical mechanics: from a paradigmatic model to biological transport”. In: *Reports on progress in physics* 74.11 (2011), p. 116601.

[26] Saul Fisher. “Pierre Gassendi”. In: (2005).

[27] Steven Shapin. “Who was Robert Hooke?” In: (1989).

[28] Daniel Bernoulli. “Hydrodynamica”. In: *Dulsecker. Consultable en ligne http://imgbase-scd-ulp. u-strasbg. fr/displayimage. php* (1738).

[29] William Bird Herapath. “XXVI. On the optical properties of a newly-discovered salt of quinine, which crystalline substance possesses the power of polarizing a ray of light, like tourmaline, and at certain angles of rotation of depolarizing it, like selenite”. In: *The London, Edinburgh, and Dublin Philosophical Magazine and Journal of Science* 3.17 (1852), pp. 161–173.

[30] ROBERT FOX. "James Prescott Joule:(1818–1889)". In: *Mid-nineteenth-century scientists*. Elsevier, 1969, pp. 72–103.

[31] James Jeans, James Hopwood Jeans, and James S Jeans. *An introduction to the kinetic theory of gases*. CUP Archive, 1940.

[32] Stefan L Wolff. "Rudolph Clausius–A pioneer of the modern theory of heat". In: *Vacuum* 90 (2013), pp. 102–108.

[33] Rudolf Clausius. "X. On the mean length of the paths described by the separate molecules of gaseous bodies on the occurrence of molecular motion: together with some other remarks upon the mechanical theory of heat". In: *The London, Edinburgh, and Dublin Philosophical Magazine and Journal of Science* 17.112 (1859), pp. 81–91.

[34] Paul Ehrenfest and Tatiana Ehrenfest. *The conceptual foundations of the statistical approach in mechanics*. Courier Corporation, 1990.

[35] Harvey R Brown and Wayne Myrvold. "Boltzmann's H-theorem, its limitations, and the birth of (fully) statistical mechanics". In: *arXiv preprint arXiv:0809.1304* (2008).

[36] John T Blackmore. *Ludwig Boltzmann: His Later Life and Philosophy, 1900-1906: Book Two: The Philosopher*. Vol. 174. Springer Science & Business Media, 1995.

[37] Lewis Campbell. *The Life of James Clerk Maxwell.*, 1884.

[38] James Clerk Maxwell. *The Scientific Papers of James Clerk Maxwell...* Vol. 2. University Press, 1890.

[39] James Clerk Maxwell. "Illustrations of the dynamical theory of gases". In: *The Kinetic Theory Of Gases: An Anthology of Classic Papers with Historical Commentary*. World Scientific, 2003, pp. 148–171.

[40] James Clerk Maxwell. "II. Illustrations of the dynamical theory of gases". In: *The London, Edinburgh, and Dublin Philosophical Magazine and Journal of Science* 20.130 (1860), pp. 21–37.

[41] James Clerk Maxwell. "IV. On the dynamical theory of gases". In: *Philosophical transactions of the Royal Society of London* 157 (1867), pp. 49–88.

[42] Sydney Chapman. "The kinetic theory of simple and composite monatomic gases: viscosity, thermal conduction, and diffusion". In: *Proceedings of the Royal Society of London. Series A, Containing Papers of a Mathematical and Physical Character* 93.646 (1916), pp. 1–20.

[43] Sydney Chapman. "VI. On the law of distribution of molecular velocities, and on the theory of viscosity and thermal conduction, in a non-uniform simple monatomic gas". In: *Philosophical Transactions of the Royal Society of London. Series A, Containing Papers of a Mathematical or Physical Character* 216.538-548 (1916), pp. 279–348.

[44] David Enskog. “Kinetische theorie der Vorgänge in mässig verdünnten Gasen. I. Allgemeiner Teil”. In: *Uppsala: Almquist & Wiksells Boktryckeri* (1917).

[45] J Loschmidt. “Wiener Ber. 73, 128. Loschmidt, J. 1877”. In: *Wiener Ber* 75 (1876), p. 67.

[46] Ernst Zermelo. “Über einen Satz der Dynamik und die mechanische Wärmetheorie”. In: *Annalen der Physik* 293.3 (1896), pp. 485–494.

[47] Robert S Cohen and Raymond J Seeger. *Ernst Mach: physicist and philosopher*. Vol. 6. Springer Science & Business Media, 2013.

[48] Wilhelm Ostwald. *Natural philosophy*. Williams and Norgate, 1911.

[49] Lord Kelvin. “I. Nineteenth century clouds over the dynamical theory of heat and light”. In: *The London, Edinburgh, and Dublin Philosophical Magazine and Journal of Science* 2.7 (1901), pp. 1–40.

[50] Ludwig Boltzmann. *Vorlesungen über Gastheorie: 2. Teil*. BoD–Books on Demand, 2017.

[51] Ludwig Boltzmann. *Vorlesungen über gastheorie*. Vol. 2. Barth, 1912.

[52] Raj Kumar Pathria. *Statistical mechanics*. Vol. 45. Pergamon, 1972.

[53] Walter Greiner, Ludwig Neise, and Horst Stöcker. *Thermodynamics and statistical mechanics*. Springer Science & Business Media, 2012.

[54] James Clerk Maxwell. “VII. On stresses in rarified gases arising from inequalities of temperature”. In: *Philosophical Transactions of the royal society of London* 170 (1879), pp. 231–256.

[55] GH Bryan. “Elementary principles in statistical mechanics”. In: *Nature* 66.1708 (1902), pp. 291–292.

[56] J Willard Gibbs. *Elementary principles in statistical mechanics*. Courier Corporation, 2014.

[57] Max Plank. “Verh. deutsch. phys”. In: *Ges* 2 (1900), pp. 202–237.

[58] Albert Einstein et al. “On the electrodynamics of moving bodies”. In: *Annalen der physik* 17.10 (1905), pp. 891–921.

[59] Arthur H Compton. “A quantum theory of the scattering of X-rays by light elements”. In: *Physical review* 21.5 (1923), p. 483.

[60] Arthur H Compton. “The spectrum of scattered X-rays”. In: *Physical Review* 22.5 (1923), p. 409.

[61] Satyendra Nath Bose. “Plancks gesetz und lichtquantenhypothese”. In: (1924).

[62] Albert Einstein. “Quantum theory of the monatomic ideal gas”. In: *Sitzungsberichte der Preussischen Akademie der Wissenschaften, Physikalisch-mathematische Klasse* (1924), pp. 261–267.

[63] Albert Einstein. “Unified field theory of gravitation and electricity”. In: *Session Report of Prussian Acad. Sci* (1925), pp. 414–419.

[64] Fritz London. “On the bose-einstein condensation”. In: *Physical Review* 54.11 (1938), p. 947.

[65] Fritz London. “The λ-phenomenon of liquid helium and the Bose-Einstein degeneracy”. In: *Nature* 141.3571 (1938), pp. 643–644.

[66] Wolfgang Pauli. “Über den Zusammenhang des Abschlusses der Elektronengruppen im Atom mit der Komplexstruktur der Spektren”. In: *Zeitschrift für Physik* 31.1 (1925), pp. 765–783.

[67] Ralph H Fowler. “On dense matter”. In: *Monthly Notices of the Royal Astronomical Society* 87 (1926), pp. 114–122.

[68] Wolfgang Pauli. “Über Gasentartung und Paramagnetismus”. In: *Zeitschrift für Physik A Hadrons and nuclei* 41.2-3 (1927), pp. 81–102.

[69] Arnold Sommerfeld. “Zur elektronentheorie der metalle auf grund der fermischen statistik”. In: *Zeitschrift für Physik* 47.1-2 (1928), pp. 1–32.

[70] Eduard Riecke. “Zur Theorie des Galvanismus und der Wärme”. In: *Annalen der Physik* 302.11 (1898), pp. 353–581.

[71] Max Planck. *Am 5. Juli dieses Jahres ist Paul Drude*. 1906.

[72] HA Lorentz. “The motion of electrons in metallic bodies II”. In: *Koninklijke Nederlandse Akademie van Wetenschappen Proceedings Series B Physical Sciences* 7 (1904), pp. 585–593.

[73] HA Lorentz. “The motion of electrons in metallic bodies I”. In: *KNAW, proceedings*. Vol. 7. 1905, pp. 438–453.

[74] Enrico Fermi. “Eine statistische Methode zur Bestimmung einiger Eigenschaften des Atoms und ihre Anwendung auf die Theorie des periodischen Systems der Elemente”. In: *Zeitschrift für Physik* 48.1-2 (1928), pp. 73–79.

[75] Llewellyn H Thomas. “The calculation of atomic fields”. In: *Mathematical proceedings of the Cambridge philosophical society*. Vol. 23. 5. Cambridge University Press. 1927, pp. 542–548.

[76] Llewellyn Hilleth Thomas. "I. The kinematics of an electron with an axis". In: *The London, Edinburgh, and Dublin Philosophical Magazine and Journal of Science* 3.13 (1927), pp. 1–22.

[77] Lev Landau. "Das dämpfungsproblem in der wellenmechanik". In: *Zeitschrift für Physik* 45.5-6 (1927), pp. 430–441.

[78] John Von Neumann. "Wahrscheinlichkeitstheoretischer aufbau der quantenmechanik". In: *Nachrichten von der Gesellschaft der Wissenschaften zu Göttingen, Mathematisch-Physikalische Klasse* 1927 (1927), pp. 245–272.

[79] Paul Adrien Maurice Dirac. "The quantum theory of the emission and absorption of radiation". In: *Proceedings of the Royal Society of London. Series A, Containing Papers of a Mathematical and Physical Character* 114.767 (1927), pp. 243–265.

[80] PAM Dirac. "The basis of statistical quantum mechanics". In: *Mathematical Proceedings of the Cambridge Philosophical Society*. Vol. 25. 1. Cambridge University Press. 1929, pp. 62–66.

[81] Paul Adrien Maurice Dirac. "Quantum mechanics of many-electron systems". In: *Proceedings of the Royal Society of London. Series A, Containing Papers of a Mathematical and Physical Character* 123.792 (1929), pp. 714–733.

[82] Paul AM Dirac. "Note on exchange phenomena in the Thomas atom". In: *Mathematical proceedings of the Cambridge philosophical society*. Vol. 26. 3. Cambridge University Press. 1930, pp. 376–385.

[83] PAM Dirac. "Note on the interpretation of the density matrix in the many-electron problem". In: *Mathematical Proceedings of the Cambridge Philosophical Society*. Vol. 27. 2. Cambridge University Press. 1931, pp. 240–243.

[84] W PAULI Jr. "On the quantum mechanics of magnetic electrons". In: *Nature* 119 (1927), p. 282.

[85] FJ Belinfante. "A New Form of the Baryteron Equation and Some Related Questions". In: *Nature* 143.3614 (1939), pp. 201–201.

[86] FJ Belinfante. "On the spin angular momentum of mesons". In: *Physica* 6.7-12 (1939), pp. 887–898.

[87] Frederik Jozef Belinfante. "Undor calculus and charge-conjugation". In: *Theory of Heavy Quanta*. Springer, 1939, pp. 1–21.

[88] Wolfgang Pauli. "The connection between spin and statistics". In: *Physical Review* 58.8 (1940), p. 716.

[89] W Pauli and FJ Belinfante. “On the statistical behaviour of known and unknown elementary particles”. In: *Physica* 7.3 (1940), pp. 177–192.

[90] Klaus von Klitzing and Roland Wiesendanger. “NanoScience and Technology”. In: ().

[91] A Fuhrer et al. “Energy spectra of quantum rings”. In: *Nature* 413.6858 (2001), pp. 822–825.

[92] S Viefers et al. “Quantum rings for beginners: energy spectra and persistent currents”. In: *Physica E: Low-dimensional Systems and Nanostructures* 21.1 (2004), pp. 1–35.

[93] Péter Földi et al. “Quantum rings as electron spin beam splitters”. In: *Physical Review B* 73.15 (2006), p. 155325.

[94] E Räsänen et al. “Optimal control of quantum rings by terahertz laser pulses”. In: *Physical review letters* 98.15 (2007), p. 157404.

[95] Vladimir M Fomin. *Physics of quantum rings*. Springer Science & Business Media, 2013.

[96] Tobias Nowozin. *Self-organized quantum dots for memories: Electronic properties and carrier dynamics*. Springer Science & Business Media, 2013.

[97] Peter Michler. *Single quantum dots: Fundamentals, applications and new concepts*. Vol. 90. Springer Science & Business Media, 2003.

[98] Artur Zrenner. “A close look on single quantum dots”. In: *The journal of chemical physics* 112.18 (2000), pp. 7790–7798.

[99] Antonio Badolato et al. “Deterministic coupling of single quantum dots to single nanocavity modes”. In: *Science* 308.5725 (2005), pp. 1158–1161.

[100] Peter Lodahl, Sahand Mahmoodian, and Søren Stobbe. “Interfacing single photons and single quantum dots with photonic nanostructures”. In: *Reviews of Modern Physics* 87.2 (2015), p. 347.

[101] A Fuhrer et al. “Energy spectra of quantum rings”. In: *Nature* 413.6858 (2001), pp. 822–825.

[102] Ho-Fai Cheung et al. “Persistent currents in small one-dimensional metal rings”. In: *Physical Review B* 37.11 (1988), p. 6050.

[103] FE Meijer, AF Morpurgo, and TM Klapwijk. “One-dimensional ring in the presence of Rashba spin-orbit interaction: Derivation of the correct Hamiltonian”. In: *Physical Review B* 66.3 (2002), p. 033107.

[104] Diego Frustaglia and Klaus Richter. “Spin interference effects in ring conductors subject to Rashba coupling”. In: *Physical Review B* 69.23 (2004), p. 235310.

[105] Axel Lorke et al. “Spectroscopy of nanoscopic semiconductor rings”. In: *Physical review letters* 84.10 (2000), p. 2223.

[106] Stefan Kettemann, Peter Fulde, and Peter Strehlow. “Correlated persistent tunneling currents in glasses”. In: *Physical review letters* 83.21 (1999), p. 4325.

[107] S Viefers et al. “Quantum rings for beginners: energy spectra and persistent currents”. In: *Physica E: Low-dimensional Systems and Nanostructures* 21.1 (2004), pp. 1–35.

[108] Janine Splettstoesser, Michele Governale, and Ulrich Zülicke. “Persistent current in ballistic mesoscopic rings with Rashba spin-orbit coupling”. In: *Physical Review B* 68.16 (2003), p. 165341.

[109] Satofumi Souma and Branislav K Nikolić. “Modulating unpolarized current in quantum spintronics: Visibility of spin-interference effects in multichannel Aharonov-Casher mesoscopic rings”. In: *Physical Review B* 70.19 (2004), p. 195346.

[110] AV Chaplik. “Magnetoexcitons in quantum rings and in antidots”. In: *Soviet Journal of Experimental and Theoretical Physics Letters* 62.11 (1995), pp. 900–904.

[111] W-C Tan and JC Inkson. “Magnetization, persistent currents, and their relation in quantum rings and dots”. In: *Physical Review B* 60.8 (1999), p. 5626.

[112] WC Tan and JC Inkson. “Electron states in a two-dimensional ring-an exactly soluble model”. In: *Semiconductor science and technology* 11.11 (1996), p. 1635.

[113] W-C Tan and JC Inkson. “Landau quantization and the Aharonov-Bohm effect in a two-dimensional ring”. In: *Physical Review B* 53.11 (1996), p. 6947.

[114] DV Bulaev, VA Geyler, and VA Margulis. “Effect of surface curvature on magnetic moment and persistent currents in two-dimensional quantum rings and dots”. In: *Physical Review B* 69.19 (2004), p. 195313.

[115] CM Duque et al. “Optical nonlinearities associated to applied electric fields in parabolic two-dimensional quantum rings”. In: *Journal of luminescence* 143 (2013), pp. 81–88.

[116] K Bakke and C Furtado. “On the confinement of a Dirac particle to a two-dimensional ring”. In: *Physics Letters A* 376.15 (2012), pp. 1269–1273.

[117] MP Nowak and B Szafran. “Spin-orbit coupling effects in two-dimensional circular quantum rings: Elliptical deformation of confined electron density”. In: *Physical Review B* 80.19 (2009), p. 195319.

[118] R Citro and F Romeo. “Pumping in a mesoscopic ring with Aharonov-Casher effect”. In: *Physical Review B* 73.23 (2006), p. 233304.

[119] R Citro, F Romeo, and M Marinaro. "Zero-conductance resonances and spin filtering effects in ring conductors subject to Rashba coupling". In: *Physical Review B* 74.11 (2006), p. 115329.

[120] H Belich et al. "Aharonov-Bohm-Casher problem with a nonminimal Lorentz-violating coupling". In: *Physical Review D* 83.12 (2011), p. 125025.

[121] Junsaku Nitta and Tobias Bergsten. "Time reversal Aharonov–Casher effect using Rashba spin–orbit interaction". In: *New Journal of Physics* 9.9 (2007), p. 341.

[122] Yakir Aharonov and Aharon Casher. "Topological quantum effects for neutral particles". In: *Physical Review Letters* 53.4 (1984), p. 319.

[123] AE Hansen et al. "Mesoscopic decoherence in Aharonov-Bohm rings". In: *Physical Review B* 64.4 (2001), p. 045327.

[124] Bertrand Reulet et al. "Dynamic response of isolated aharonov-bohm rings coupled to an electromagnetic resonator". In: *Physical review letters* 75.1 (1995), p. 124.

[125] Urs Aeberhard, Katsunori Wakabayashi, and Manfred Sigrist. "Effect of spin-orbit coupling on zero-conductance resonances in asymmetrically coupled one-dimensional rings". In: *Physical Review B* 72.7 (2005), p. 075328.

[126] IA Shelykh et al. "Interplay of h/ e and h/ 2 e oscillations in gate-controlled Aharonov-Bohm rings". In: *Physical Review B* 71.11 (2005), p. 113311.

[127] David R Gaskell and David E Laughlin. *Introduction to the Thermodynamics of Materials*. CRC press, 2017.

[128] Robert DeHoff. *Thermodynamics in materials science*. CRC Press, 2006.

[129] B Mühlschlegel, DJ Scalapino, and R Denton. "Thermodynamic properties of small superconducting particles". In: *Physical Review B* 6.5 (1972), p. 1767.

[130] Jefferson W Tester, Michael Modell, et al. *Thermodynamics and its Applications*. Prentice Hall PTR, 1997.

[131] Chengteh Lee, Weitao Yang, and Robert G Parr. "Development of the Colle-Salvetti correlation-energy formula into a functional of the electron density". In: *Physical Review B* 37.2 (1988), p. 785.

[132] Adailton A Araújo-Filho et al. "Structural, electronic and optical properties of monoclinic Na2Ti3O7 from density functional theory calculations: A comparison with XRD and optical absorption measurements". In: *Journal of Solid State Chemistry* 250 (2017), pp. 68–74.

[133] Mark E Casida et al. “Molecular excitation energies to high-lying bound states from time-dependent density-functional response theory: Characterization and correction of the time-dependent local density approximation ionization threshold”. In: *The Journal of Chemical Physics* 108.11 (1998), pp. 4439–4449.

[134] M D Segall et al. “First-principles simulation: ideas, illustrations and the CASTEP code”. In: *Journal of Physics: Condensed Matter* 14.11 (2002), p. 2717.

[135] David C Langreth and M J Mehl. “Beyond the local-density approximation in calculations of ground-state electronic properties”. In: *Physical Review B* 28.4 (1983), p. 1809.

[136] Fábio Lacerda Resende Silva et al. “Polarized Raman, FTIR, and DFT study of Na2Ti3O7 microcrystals”. In: *Journal of Raman Spectroscopy* 49.3 (2018), pp. 538–548.

[137] Anahita Imanian and Mohammad Modarres. “Thermodynamics as a fundamental science of reliability”. In: *Proceedings of the Institution of Mechanical Engineers, Part O: Journal of Risk and Reliability* 230.6 (2016), pp. 598–608.

[138] Frederick Reif. *Fundamentals of statistical and thermal physics*. Waveland Press, 2009.

[139] Alexander A Balandin. “Thermal properties of graphene and nanostructured carbon materials”. In: *Nature Materials* 10.8 (2011), pp. 569–581.

[140] Adrian Bejan. *Advanced engineering thermodynamics*. John Wiley & Sons, 2016.

[141] H Potempa and L Schweitzer. “Dependence of critical level statistics on the sample shape”. In: *Journal of Physics: Condensed Matter* 10.25 (1998), p. L431.

[142] Wu-Sheng Dai and Mi Xie. “Quantum statistics of ideal gases in confined space”. In: *Physics Letters A* 311.4-5 (2003), pp. 340–346.

[143] Wu-Sheng Dai and Mi Xie. “Geometry effects in confined space”. In: *Physical Review E* 70.1 (2004), p. 016103.

[144] Luca Angelani et al. “Topology and phase transitions: From an exactly solvable model to a relation between topology and thermodynamics”. In: *Physical Review E* 71.3 (2005), p. 036152.

[145] D Braun, G Montambaux, and M Pascaud. “Boundary conditions at the mobility edge”. In: *Physical Review Letters* 81.5 (1998), p. 1062.

[146] Vladimir E Kravtsov and Vladimir I Yudson. “Topological spectral correlations in 2D disordered systems”. In: *Physical Review Letters* 82.1 (1999), p. 157.

[147] Rubens RS Oliveira et al. “Thermodynamic properties of an Aharonov-Bohm quantum ring”. In: *The European Physical Journal Plus* 134.10 (2019), p. 495.

[148] R R S Oliveira et al. “The relativistic Aharonov–Bohm–Coulomb system with position-dependent mass”. In: *Journal of Physics A: Mathematical and Theoretical* 53.4 (2020), p. 045304.

[149] Lev D Landau and Evgeny M Lifshitz. *Statistical Physics: Volume 5*. Vol. 5. Elsevier, 2013.

[150] Nouredine Zettili. *Quantum mechanics: concepts and applications*. 2003.

[151] Hermann Weyl. *Gesammelte Abhandlungen: Band 1 bis 4*. Vol. 4. Springer-Verlag, 1968.

[152] David R Gaskell. *Introduction to the Thermodynamics of Materials*. CRC press, 2012.

[153] B Mühlschlegel, DJ Scalapino, and R Denton. “Thermodynamic properties of small superconducting particles”. In: *Physical Review B* 6.5 (1972), p. 1767.

[154] Robert DeHoff. *Thermodynamics in materials science*. CRC Press, 2006.

[155] RT Jones. “Thermodynamics and its applications–an overview”. In: (1974).

[156] Joseph Davidovits. “Geopolymers: inorganic polymeric new materials”. In: *Journal of Thermal Analysis and calorimetry* 37.8 (1991), pp. 1633–1656.

[157] Samuel Safran. *Statistical thermodynamics of surfaces, interfaces, and membranes*. CRC Press, 2018.

[158] Frank S Bates and Glenn H Fredrickson. “Block copolymer thermodynamics: theory and experiment”. In: *Annual review of physical chemistry* 41.1 (1990), pp. 525–557.

[159] Fábio Lacerda Resende e Silva et al. “Polarized Raman, FTIR, and DFT study of Na2Ti3O7 microcrystals”. In: *Journal of Raman Spectroscopy* 49.3 (2018), pp. 538–548.

[160] Mark E Casida et al. “Molecular excitation energies to high-lying bound states from time-dependent density-functional response theory: Characterization and correction of the time-dependent local density approximation ionization threshold”. In: *The Journal of chemical physics* 108.11 (1998), pp. 4439–4449.

[161] MD Segall et al. “First-principles simulation: ideas, illustrations and the CASTEP code”. In: *Journal of physics: condensed matter* 14.11 (2002), p. 2717.

[162] John P Perdew and Alex Zunger. “Self-interaction correction to density-functional approximations for many-electron systems”. In: *Physical Review B* 23.10 (1981), p. 5048.

[163] John P Perdew. “Density-functional approximation for the correlation energy of the inhomogeneous electron gas”. In: *Physical Review B* 33.12 (1986), p. 8822.

[164] John P Perdew and Yue Wang. “Accurate and simple analytic representation of the electron-gas correlation energy”. In: *Physical review B* 45.23 (1992), p. 13244.

[165] John P Perdew, Kieron Burke, and Matthias Ernzerhof. "Generalized gradient approximation made simple". In: *Physical review letters* 77.18 (1996), p. 3865.

[166] Wu-Sheng Dai and Mi Xie. "Quantum statistics of ideal gases in confined space". In: *Physics Letters A* 311.4-5 (2003), pp. 340–346.

[167] Wu-Sheng Dai and Mi Xie. "Geometry effects in confined space". In: *Physical Review E* 70.1 (2004), p. 016103.

[168] H Potempa and L Schweitzer. "Dependence of critical level statistics on the sample shape". In: *Journal of Physics: Condensed Matter* 10.25 (1998), p. L431.

[169] Luca Angelani et al. "Topology and phase transitions: From an exactly solvable model to a relation between topology and thermodynamics". In: *Physical Review E* 71.3 (2005), p. 036152.

[170] Martin Philip Bendsoe and Ole Sigmund. *Topology optimization: theory, methods, and applications*. Springer Science & Business Media, 2013.

[171] RRS Oliveira et al. "The relativistic Aharonov–Bohm–Coulomb system with position-dependent mass". In: *Journal of Physics A: Mathematical and Theoretical* 53.4 (2020), p. 045304.

[172] Prineha Narang, Christina AC Garcia, and Claudia Felser. "The topology of electronic band structures". In: *Nature Materials* 20.3 (2021), pp. 293–300.

[173] Lev Davidovich Landau and Evgenii Mikhailovich Lifshitz. *Course of theoretical physics*. Elsevier, 2013.

[174] Linda E Reichl. *A modern course in statistical physics*. 1999.

[175] Kerson Huang. *Introduction to statistical physics*. CRC press, 2009.

[176] Nouredine Zettili. *Quantum mechanics: concepts and applications*. 2003.

[177] Edward M Purcell et al. *Electricity and magnetism*. Vol. 2. McGraw-Hill New York, 1965.

[178] Paul A Tipler and Ralph Llewellyn. *Modern physics*. Macmillan, 2003.

[179] Hermann Weyl. *Gesammelte Abhandlungen: Band 1 bis 4*. Vol. 4. Springer-Verlag, 1968.

[180] VV Sreedhar. "The classical and quantum mechanics of a particle on a knot". In: *Annals of Physics* 359 (2015), pp. 20–30.

[181] Subir Ghosh. "Particle on a torus knot: Anholonomy and Hannay angle". In: *International Journal of Geometric Methods in Modern Physics* 15.06 (2018), p. 1850097.

[182] Praloy Das, Souvik Pramanik, and Subir Ghosh. "Particle on a torus knot: Constrained dynamics and semi-classical quantization in a magnetic field". In: *Annals of Physics* 374 (2016), pp. 67–83.

[183] Dripto Biswas and Subir Ghosh. "Quantum mechanics of a particle on a torus knot: Curvature and torsion effects". In: *EPL (Europhysics Letters)* 132.1 (2020), p. 10004.

[184] RCT Da Costa. "Quantum mechanics of a constrained particle". In: *Physical Review A* 23.4 (1981), p. 1982.

[185] Yong-Long Wang et al. "Geometric effects resulting from square and circular confinements for a particle constrained to a space curve". In: *Physical Review A* 97.4 (2018), p. 042108.

[186] Carmine Ortix. "Quantum mechanics of a spin-orbit coupled electron constrained to a space curve". In: *Physical Review B* 91.24 (2015), p. 245412.

[187] Luiz CB da Silva, Cristiano C Bastos, and Fábio G Ribeiro. "Quantum mechanics of a constrained particle and the problem of prescribed geometry-induced potential". In: *Annals of Physics* 379 (2017), pp. 13–33.

[188] Giulio Ferrari and Giampaolo Cuoghi. "Schrödinger equation for a particle on a curved surface in an electric and magnetic field". In: *Physical review letters* 100.23 (2008), p. 230403.

[189] Loring W Tu. "Manifolds". In: *An Introduction to Manifolds*. Springer, 2011, pp. 47–83.

[190] Loring W Tu. *Differential geometry: connections, curvature, and characteristic classes*. Vol. 275. Springer, 2017.

[191] Lei Liu, CS Jayanthi, and SY Wu. "Structural and electronic properties of a carbon nanotorus: Effects of delocalized and localized deformations". In: *Physical Review B* 64.3 (2001), p. 033412.

[192] Oxana V Kharissova, Mauricio Garza Castañón, and Boris I Kharisov. "Inorganic nanorings and nanotori: State of the art". In: *Journal of Materials Research* 34.24 (2019), pp. 3998–4010.

[193] Nan Chen et al. "Mechanical properties of connected carbon nanorings via molecular dynamics simulation". In: *Physical Review B* 72.8 (2005), p. 085416.

[194] S Madani and Ali Reza Ashrafi. "The energies of (3, 6)-fullerenes and nanotori". In: *Applied Mathematics Letters* 25.12 (2012), pp. 2365–2368.

[195] Zuzanna A Lewicka et al. "Nanorings and nanocrescents formed via shaped nanosphere lithography: a route toward large areas of infrared metamaterials". In: *Nanotechnology* 24.11 (2013), p. 115303.

[196] Hua Yu Feng et al. “Magnetoplasmonic Nanorings as Novel Architectures with Tunable Magneto-optical Activity in Wide Wavelength Ranges”. In: *Advanced Optical Materials* 2.7 (2014), pp. 612–617.

[197] Lei Liu et al. “Colossal paramagnetic moments in metallic carbon nanotori”. In: *Physical review letters* 88.21 (2002), p. 217206.

[198] Smiljan Vojkovic et al. “Magnetization ground state and reversal modes of magnetic nanotori”. In: *Journal of Applied Physics* 120.3 (2016), p. 033901.

[199] JA Rodrıguez-Manzo et al. “Magnetism in corrugated carbon nanotori: The importance of symmetry, defects, and negative curvature”. In: *Nano Letters* 4.11 (2004), pp. 2179–2183.

[200] Hongli Du, Wei Zhang, and Yan Li. “Silicon nitride nanorings: Synthesis and optical properties”. In: *Chemistry Letters* 43.8 (2014), pp. 1360–1362.

[201] Yue Chan, Barry J Cox, and James M Hill. “Carbon nanotori as traps for atoms and ions”. In: *Physica B: Condensed Matter* 407.17 (2012), pp. 3479–3483.

[202] Laura Peña-Parás et al. “Novel carbon nanotori additives for lubricants with superior anti-wear and extreme pressure properties”. In: *Tribology International* 131 (2019), pp. 488–495.

[203] Simon Judes and Matt Visser. “Conservation laws in “doubly special relativity””. In: *Phys. Rev. D* 68 (2003), p. 045001.

[204] H. P. Robertson. “Postulate versus Observation in the Special Theory of Relativity”. In: *Rev. Mod. Phys.* 21 (1949), pp. 378–382.

[205] Robert C. Myers and Maxim Pospelov. “Ultraviolet Modifications of Dispersion Relations in Effective Field Theory”. In: *Phys. Rev. Lett.* 90 (2003), p. 211601.

[206] O. Bertolami and J. G. Rosa. “Bounds on cubic Lorentz-violating terms in the fermionic dispersion relation”. In: *Phys. Rev. D* 71 (2005), p. 097901.

[207] C. M. Reyes, L. F. Urrutia, and J. D. Vergara. “Quantization of the Myers-Pospelov model: The photon sector interacting with standard fermions as a perturbation of QED”. In: *Phys. Rev. D* 78 (2008), p. 125011.

[208] David Mattingly. “Have we tested Lorentz invariance enough?” In: *arXiv preprint arXiv:0802.1561* (2008).

[209] G.I. Rubtsov, P.S. Satunin, and S.M. Sibiryakov. “THE INFLUENCE OF LORENTZ VIOLATION ON UHE PHOTON DETECTION”. In: *CPT and Lorentz Symmetry* (2014), pp. 192–195.

[210] Stefano Liberati. "Tests of Lorentz invariance: a 2013 update". In: *Classical and Quantum Gravity* 30.13 (2013), p. 133001.

[211] Jay D Tasson. "What do we know about Lorentz invariance?" In: *Reports on Progress in Physics* 77.6 (2014), p. 062901.

[212] Aurélien Hees et al. "Tests of Lorentz symmetry in the gravitational sector". In: *Universe* 2.4 (2016), p. 30.

[213] Carlo Rovelli. *Quantum gravity*. Cambridge university press, 2004.

[214] V. Alan Kostelecký and Stuart Samuel. "Spontaneous breaking of Lorentz symmetry in string theory". In: *Phys. Rev. D* 39 (1989), pp. 683–685.

[215] V. Alan Kostelecký and Stuart Samuel. "Phenomenological gravitational constraints on strings and higher-dimensional theories". In: *Phys. Rev. Lett.* 63 (3 1989), pp. 224–227.

[216] V. Alan Kostelecký and Stuart Samuel. "Gravitational phenomenology in higher-dimensional theories and strings". In: *Phys. Rev. D* 40 (1989), pp. 1886–1903.

[217] V. Alan Kostelecký and Robertus Potting. "CPT and strings". In: *Nuclear Physics B* 359.2 (1991), pp. 545–570. ISSN: 0550-3213.

[218] V. Alan Kostelecký and Robertus Potting. "CPT, strings, and meson factories". In: *Phys. Rev. D* 51 (), pp. 3923–3935.

[219] Rodolfo Gambini and Jorge Pullin. "Nonstandard optics from quantum space-time". In: *Phys. Rev. D* 59 (1999), p. 124021.

[220] Martin Bojowald, Hugo A. Morales-Técotl, and Hanno Sahlmann. "Loop quantum gravity phenomenology and the issue of Lorentz invariance". In: *Phys. Rev. D* 71 (2005), p. 084012.

[221] Giovanni Amelino-Camelia and Shahn Majid. "Waves on noncommutative space–time and gamma-ray bursts". In: *International Journal of Modern Physics A* 15.27 (2000), pp. 4301–4323.

[222] Sean M. Carroll et al. "Noncommutative Field Theory and Lorentz Violation". In: *Phys. Rev. Lett.* 87 (2001), p. 141601.

[223] Frans R. Klinkhamer and Christian Rupp. "Spacetime foam, CPT anomaly, and photon propagation". In: *Phys. Rev. D* 70 (2004), p. 045020.

[224] S. Bernadotte and F. R. Klinkhamer. "Bounds on length scales of classical spacetime foam models". In: *Phys. Rev. D* 75 (2007), p. 024028.

[225] F.R. Klinkhamer. "Z-string global gauge anomaly and Lorentz non-invariance". In: *Nuclear Physics B* 535.1 (1998), pp. 233–241. ISSN: 0550-3213.

[226] F.R. Klinkhamer. "A CPT anomaly". In: *Nuclear Physics B* 578.1 (2000), pp. 277–289. ISSN: 0550-3213.

[227] F.R. Klinkhamer and J. Schimmel. "CPT anomaly: a rigorous result in four dimensions". In: *Nuclear Physics B* 639.1 (2002), pp. 241–262. ISSN: 0550-3213.

[228] K.J.B. Ghosh and F.R. Klinkhamer. "Anomalous Lorentz and CPT violation from a local Chern–Simons-like term in the effective gauge-field action". In: *Nuclear Physics B* 926 (2018), pp. 335–369. ISSN: 0550-3213.

[229] Petr Ho řava. "Quantum gravity at a Lifshitz point". In: *Phys. Rev. D* 79 (8 2009), p. 084008.

[230] Guido Cognola et al. "Covariant Hořava-like and mimetic Horndeski gravity: cosmological solutions and perturbations". In: *Classical and quantum gravity* 33.22 (2016), p. 225014.

[231] Alessandro Casalino et al. "Alive and well: mimetic gravity and a higher-order extension in light of GW170817". In: *Classical and Quantum Gravity* 36.1 (2018), p. 017001.

[232] Don Colladay and V Alan Kosteleck. "Lorentz-violating extension of the standard model". In: *Physical Review D* 58.11 (1998), p. 116002.

[233] Don Colladay and V Alan Kosteleck. "Lorentz-violating extension of the standard model". In: *Physical Review D* 58.11 (1998), p. 116002.

[234] V Alan Kosteleck and Stuart Samuel. "Phenomenological gravitational constraints on strings and higher-dimensional theories". In: *Physical Review Letters* 63.3 (1989), p. 224.

[235] V Alan Kosteleck and Stuart Samuel. "Spontaneous breaking of Lorentz symmetry in string theory". In: *Physical Review D* 39.2 (1989), p. 683.

[236] V Alan Kosteleck and Rob Potting. "Expectation values, Lorentz invariance, and CPT in the open bosonic string". In: *Physics Letters B* 381.1-3 (1996), pp. 89–96.

[237] V Alan Kosteleck. "Gravity, Lorentz violation, and the standard model". In: *Physical Review D* 69.10 (2004), p. 105009.

[238] Matthew Mewes. "Signals for Lorentz violation in gravitational waves". In: *Physical Review D* 99.10 (2019), p. 104062.

[239] RV Maluf et al. "Antisymmetric tensor propagator with spontaneous Lorentz violation". In: *EPL (Europhysics Letters)* 124.6 (2019), p. 61001.

[240] V Alan Kosteleck and Ralf Lehnert. "Stability, causality, and Lorentz and CPT violation". In: *Physical Review D* 63.6 (2001), p. 065008.

[241] Graham M Shore. "Strong equivalence, Lorentz and CPT violation, anti-hydrogen spectroscopy and gamma-ray burst polarimetry". In: *Nuclear Physics B* 717.1-2 (2005), pp. 86–118.

[242] Don Colladay and V Alan Kosteleck. "Cross sections and Lorentz violation". In: *Physics Letters B* 511.2-4 (2001), pp. 209–217.

[243] OG Kharlanov and V Ch Zhukovsky. "CPT and Lorentz violation effects in hydrogenlike atoms". In: *Journal of mathematical physics* 48.9 (2007), p. 092302.

[244] Robert Bluhm, V Alan Kosteleck, and Charles D Lane. "CPT and Lorentz tests with muons". In: *Physical Review Letters* 84.6 (2000), p. 1098.

[245] SI Kruglov. "Modified Dirac equation with Lorentz invariance violation and its solutions for particles in an external magnetic field". In: *Physics Letters B* 718.1 (2012), pp. 228–231.

[246] J. A. A. S. Reis and M. Schreck. "Lorentz-violating modification of Dirac theory based on spin-nondegenerate operators". In: *Phys. Rev. D* 95 (2017), p. 075016.

[247] M. Schreck. "Vacuum Cherenkov radiation for Lorentz-violating fermions". In: *Phys. Rev. D* 96 (2017), p. 095026.

[248] C Adam and Frans R Klinkhamer. "Causality and CPT violation from an Abelian Chern–Simons-like term". In: *Nuclear Physics B* 607.1-2 (2001), pp. 247–267.

[249] Alexander A Andrianov and R Soldati. "Patterns of Lorentz symmetry breaking in QED by CPT-odd interaction". In: *Physics Letters B* 435.3-4 (1998), pp. 449–452.

[250] Alexander A Andrianov, R Soldati, and L Sorbo. "Dynamical Lorentz symmetry breaking from a (3+ 1)-dimensional axion-Wess-Zumino model". In: *Physical Review D* 59.2 (1998), p. 025002.

[251] H Belich et al. "The photino sector and a confining potential in a supersymmetric Lorentz-symmetry-violating model". In: *The European Physical Journal C* 73.11 (2013), p. 2632.

[252] AP Baeta Scarpelli et al. "Aspects of causality and unitarity and comments on vortex-like configurations in an Abelian model with a Lorentz-breaking term". In: *Physical Review D* 67.8 (2003), p. 085021.

[253] J Alfaro et al. "Bare and induced lorentz and cpt invariance violations in qed". In: *International Journal of Modern Physics A* 25.16 (2010), pp. 3271–3306.

[254] Rodolfo Casana et al. "Maxwell electrodynamics modified by CPT-even and Lorentz-violating dimension-6 higher-derivative terms". In: *Phys. Rev. D* 97 (2018), p. 115043.

[255] Manoel M. Ferreira et al. “Maxwell electrodynamics modified by a CPT-odd dimension-five higher-derivative term”. In: *Phys. Rev. D* 100 (5 2019), p. 055036.

[256] J. A. A. S. Reis, Manoel M. Ferreira, and Marco Schreck. “Dimensional reduction of the electromagnetic sector of the nonminimal standard model extension”. In: *Phys. Rev. D* 100 (9 2019), p. 095026.

[257] V Alan Kosteleck and Matthew Mewes. “Cosmological constraints on Lorentz violation in electrodynamics”. In: *Physical Review Letters* 87.25 (2001), p. 251304.

[258] FR Klinkhamer and M Risse. “Ultrahigh-energy cosmic-ray bounds on nonbirefringent modified Maxwell theory”. In: *Physical Review D* 77.1 (2008), p. 016002.

[259] Brett Altschul. “Vacuum Čerenkov Radiation in Lorentz-Violating Theories Without C P T Violation”. In: *Physical review letters* 98.4 (2007), p. 041603.

[260] Marco Schreck. “Analysis of the consistency of parity-odd nonbirefringent modified Maxwell theory”. In: *Physical Review D* 86.6 (2012), p. 065038.

[261] V Alan Kosteleck and Matthew Mewes. “Electrodynamics with Lorentz-violating operators of arbitrary dimension”. In: *Physical Review D* 80.1 (2009), p. 015020.

[262] V Alan Kosteleck and Matthew Mewes. “Neutrinos with Lorentz-violating operators of arbitrary dimension”. In: *Physical Review D* 85.9 (2012), p. 096005.

[263] V Alan Kosteleck and Matthew Mewes. “Fermions with Lorentz-violating operators of arbitrary dimension”. In: *Physical Review D* 88.9 (2013), p. 096006.

[264] Yunhua Ding and V. Alan Kostelecký. “Lorentz-violating spinor electrodynamics and Penning traps”. In: *Phys. Rev. D* 94 (2016), p. 056008.

[265] V. Alan Kostelecký and Zonghao Li. “Gauge field theories with Lorentz-violating operators of arbitrary dimension”. In: *Phys. Rev. D* 99 (2019), p. 056016.

[266] R Casana et al. “New C P T-even and Lorentz-violating nonminimal coupling in the Dirac equation”. In: *Physical Review D* 87.4 (2013), p. 047701.

[267] R Casana et al. “Radiative generation of the CPT-even gauge term of the SME from a dimension-five nonminimal coupling term”. In: *Physics Letters B* 726.4-5 (2013), pp. 815–819.

[268] H Belich et al. “Magnetic moment generation from non-minimal couplings in a scenario with Lorentz-symmetry violation”. In: *The European Physical Journal C* 62.2 (2009), pp. 425–432.

[269] M Schreck. “Quantum field theoretic properties of Lorentz-violating operators of non-renormalizable dimension in the fermion sector”. In: *Physical Review D* 90.8 (2014), p. 085025.

[270] RR Cuzinatto et al. “How can one probe Podolsky Electrodynamics?” In: *International Journal of Modern Physics A* 26.21 (2011), pp. 3641–3651.

[271] Rodolfo Casana et al. “Maxwell electrodynamics modified by C P T-even and Lorentz-violating dimension-6 higher-derivative terms”. In: *Physical Review D* 97.11 (2018), p. 115043.

[272] A.A. Araújo Filho and R.V Maluf. “Thermodynamic properties in higher-derivative electrodynamics”. In: *arXiv preprint arXiv:2003.02380* (2020).

[273] MA Anacleto et al. “Lorentz-violating dimension-five operator contribution to the black body radiation”. In: *Physics Letters B* 785 (2018), pp. 191–196.

[274] LHC Borges et al. “Higher order derivative operators as quantum corrections”. In: *Nuclear Physics B* 944 (2019), p. 114634.

[275] Don Colladay and Patrick McDonald. “Statistical mechanics and Lorentz violation”. In: *Physical Review D* 70.12 (2004), p. 125007.

[276] Don Colladay and Patrick McDonald. “Bose-Einstein condensates as a probe for Lorentz violation”. In: *Physical Review D* 73.10 (2006), p. 105006.

[277] Elıas Castellanos and Claus Lämmerzahl. “Ideal-Modified Bosonic Gas Trapped in AN Arbitrary Three-Dimensional Power-Law Potential”. In: *Modern Physics Letters A* 27.31 (2012), p. 1250181.

[278] Elias Castellanos and Abel Camacho. “Critical points in a relativistic bosonic gas induced by the quantum structure of spacetime”. In: *General Relativity and Gravitation* 41.11 (2009), pp. 2677–2685.

[279] M Gomes et al. “Free energy of Lorentz-violating QED at high temperature”. In: *Physical Review D* 81.4 (2010), p. 045013.

[280] Rodolfo Casana et al. “Finite temperature behavior of the C P T-even and parity-even electrodynamics of the standard model extension”. In: *Physical Review D* 80.8 (2009), p. 085026.

[281] G Kaniadakis. “Statistical mechanics in the context of special relativity. II.” In: *Physical Review E* 72.3 (2005), p. 036108.

[282] Rodolfo Casana and Kleber A. T. da Silva. “Lorentz-violating effects in the Bose–Einstein condensation of an ideal bosonic gas”. In: *Modern Physics Letters A* 30.07 (2015), p. 1550037.

[283] Don Colladay and Patrick McDonald. “Nonrelativisitic Ideal Gases and Lorentz Violations”. In: *CPT and Lorentz Symmetry*. World Scientific, 2005, pp. 264–269.

[284] Matthew D Schwartz. *Quantum field theory and the standard model*. Cambridge University Press, 2014.

[285] Robert M Wald. *General relativity*. University of Chicago press, 2010.

[286] Nikolaos E Mavromatos. "Lorentz invariance violation from string theory". In: *arXiv preprint arXiv:0708.2250* (2007).

[287] Maxim Pospelov and Yanwen Shang. "Lorentz violation in Hořava-Lifshitz-type theories". In: *Physical Review D* 85.10 (2012), p. 105001.

[288] Sean M Carroll et al. "Noncommutative field theory and Lorentz violation". In: *Physical Review Letters* 87.14 (2001), p. 141601.

[289] Jorge Alfaro, Hugo A Morales-Tecotl, and Luis F Urrutia. "Loop quantum gravity and light propagation". In: *Physical Review D* 65.10 (2002), p. 103509.

[290] C Adam and Frans R Klinkhamer. "Causality and CPT violation from an Abelian Chern–Simons-like term". In: *Nuclear Physics B* 607.1-2 (2001), pp. 247–267.

[291] Alexander A Andrianov and R Soldati. "Patterns of Lorentz symmetry breaking in QED by CPT-odd interaction". In: *Physics Letters B* 435.3-4 (1998), pp. 449–452.

[292] Alexander A Andrianov, R Soldati, and L Sorbo. "Dynamical Lorentz symmetry breaking from a (3+ 1)-dimensional axion-Wess-Zumino model". In: *Physical Review D* 59.2 (1998), p. 025002.

[293] H Belich et al. "The photino sector and a confining potential in a supersymmetric Lorentz-symmetry-violating model". In: *The European Physical Journal C* 73.11 (2013), p. 2632.

[294] AP Baeta Scarpelli et al. "Aspects of causality and unitarity and comments on vortex-like configurations in an Abelian model with a Lorentz-breaking term". In: *Physical Review D* 67.8 (2003), p. 085021.

[295] J Alfaro et al. "Bare and induced lorentz and cpt invariance violations in qed". In: *International Journal of Modern Physics A* 25.16 (2010), pp. 3271–3306.

[296] Boris Podolsky. "A generalized electrodynamics part I—non-quantum". In: *Physical Review* 62.1-2 (1942), p. 68.

[297] Antonio Accioly and Eslley Scatena. "Limits on the coupling constant of higher-derivative electromagnetism". In: *Modern Physics Letters A* 25.04 (2010), pp. 269–276.

[298] TD Lee and GC Wick. "Negative metric and the unitarity of the S-matrix". In: *Nuclear Physics B* 9.2 (1969), pp. 209–243.

[299] TD Lee and GC Wick. "Finite theory of quantum electrodynamics". In: *Physical Review D* 2.6 (1970), p. 1033.

[300] R Sekhar Chivukula et al. "Global symmetries and renormalizability of Lee-Wick theories". In: *Physical Review D* 82.3 (2010), p. 035015.

[301] Thomas EJ Underwood and Roman Zwicky. "Electroweak precision data and the Lee-Wick standard model". In: *Physical Review D* 79.3 (2009), p. 035016.

[302] Benjamin Grinstein and Donal O'Connell. "One-loop renormalization of Lee-Wick gauge theory". In: *Physical Review D* 78.10 (2008), p. 105005.

[303] Christopher D Carone and Richard F Lebed. "A higher-derivative Lee-Wick standard model". In: *Journal of High Energy Physics* 2009.01 (2009), p. 043.

[304] Ezequiel Alvarez et al. "Vertex displacements for acausal particles: testing the Lee-Wick standard model at the LHC". In: *Journal of High Energy Physics* 2009.10 (2009), p. 023.

[305] R Turcati and MJ Neves. "Probing features of the Lee-Wick quantum electrodynamics". In: *Advances in High Energy Physics* 2014 (2014).

[306] Antonio Accioly et al. "Straightforward prescription for computing the interparticle potential energy related to D-dimensional electromagnetic models". In: *Physical Review D* 90.10 (2014), p. 105029.

[307] FA Barone, G Flores-Hidalgo, and AA Nogueira. "Point-charge self-energy in Lee-Wick theories". In: *Physical Review D* 91.2 (2015), p. 027701.

[308] Enrico Barausse and Thomas P Sotiriou. "Black holes in Lorentz-violating gravity theories". In: *Classical and Quantum Gravity* 30.24 (2013), p. 244010.

[309] P James E Peebles and Bharat Ratra. "The cosmological constant and dark energy". In: *Reviews of modern physics* 75.2 (2003), p. 559.

[310] Nima Arkani-Hamed et al. "A theory of dark matter". In: *Physical Review D* 79.1 (2009), p. 015014.

[311] Stephen W Hawking and George Francis Rayner Ellis. *The large scale structure of space-time*. Vol. 1. Cambridge university press, 1973.

[312] AF Ferrari et al. "Lorentz violation in the linearized gravity". In: *Physics Letters B* 652.4 (2007), pp. 174–180.

[313] JL Boldo et al. "Graviton excitations and Lorentz–Violating gravity with cosmological constant". In: *Physics Letters B* 689.2-3 (2010), pp. 112–115.

[314] B Pereira-Dias, CA Hernaski, and JA Helayël-Neto. "Probing the effects of Lorentz-symmetry violating Chern-Simons and Ricci-Cotton terms in higher derivative gravity". In: *Physical Review D* 83.8 (2011), p. 084011.

[315] Peter W Higgs. "Broken symmetries and the masses of gauge bosons". In: *Physical Review Letters* 13.16 (1964), p. 508.

[316] Peter W Higgs. "Spontaneous symmetry breakdown without massless bosons". In: *Physical Review* 145.4 (1966), p. 1156.

[317] Lewis H Ryder. *Quantum field theory*. Cambridge university press, 1996.

[318] Ashok Das. *Lectures on quantum field theory*. World Scientific, 2008.

[319] Liang-Cheng Tu, Jun Luo, and George T Gillies. "The mass of the photon". In: *Reports on Progress in Physics* 68.1 (2004), p. 77.

[320] Boris Podolsky and Chihiro Kikuchi. "A generalized electrodynamics part II—quantum". In: *Physical Review* 65.7-8 (1944), p. 228.

[321] Boris Podolsky and Philip Schwed. "Review of a generalized electrodynamics". In: *Reviews of Modern Physics* 20.1 (1948), p. 40.

[322] Carlos AP Galvao and BM Pimentel. "The canonical structure of Podolsky generalized electrodynamics". In: *Canadian Journal of Physics* 66.5 (1988), pp. 460–466.

[323] R Bufalo, BM Pimentel, and GER Zambrano. "Renormalizability of generalized quantum electrodynamics". In: *Physical Review D* 86.12 (2012), p. 125023.

[324] Rodrigo Bufalo, Bruto Max Pimentel, and German Enrique Ramos Zambrano. "Path integral quantization of generalized quantum electrodynamics". In: *Physical Review D* 83.4 (2011), p. 045007.

[325] Patricio Gaete. "Some considerations about Podolsky-axionic electrodynamics". In: *International Journal of Modern Physics A* 27.11 (2012), p. 1250061.

[326] CA Bonin et al. "Podolsky electromagnetism at finite temperature: Implications on the Stefan-Boltzmann law". In: *Physical Review D* 81.2 (2010), p. 025003.

[327] CA Bonin, BM Pimentel, and PH Ortega. "Multipole expansion in generalized electrodynamics". In: *International Journal of Modern Physics A* 34.24 (2019), p. 1950134.

[328] RR Cuzinatto et al. "Bopp–Podolsky black holes and the no-hair theorem". In: *The European Physical Journal C* 78.1 (2018), pp. 1–9.

[329] RR Cuzinatto et al. "de Broglie-Proca and Bopp-Podolsky massive photon gases in cosmology". In: *EPL (Europhysics Letters)* 118.1 (2017), p. 19001.

[330] SI Kruglov. "Solutions of Podolsky's electrodynamics equation in the first-order formalism". In: *Journal of Physics A: Mathematical and Theoretical* 43.24 (2010), p. 245403.

[331] Alexei E Zayats. "Self-interaction in the Bopp–Podolsky electrodynamics: Can the observable mass of a charged particle depend on its acceleration?" In: *Annals of Physics* 342 (2014), pp. 11–20.

[332] DR Granado et al. "Podolsky electrodynamics from a condensation of topological defects". In: *EPL (Europhysics Letters)* 129.5 (2020), p. 51001.

[333] AA Nogueira, C Palechor, and AF Ferrari. "Reduction of order and Fadeev–Jackiw formalism in generalized electrodynamics". In: *Nuclear Physics B* 939 (2019), pp. 372–390.

[334] Luca Bonetti et al. "Effective photon mass by Super and Lorentz symmetry breaking". In: *Physics Letters B* 764 (2017), pp. 203–206.

[335] V Alan Kosteleck and Matthew Mewes. "Fermions with Lorentz-violating operators of arbitrary dimension". In: *Physical Review D* 88.9 (2013), p. 096006.

[336] Stefano Liberati and Luca Maccione. "Astrophysical constraints on Planck scale dissipative phenomena". In: *Physical Review Letters* 112.15 (2014), p. 151301.

[337] Jay D Tasson. "What do we know about Lorentz invariance?" In: *Reports on Progress in Physics* 77.6 (2014), p. 062901.

[338] Aurélien Hees et al. "Tests of Lorentz symmetry in the gravitational sector". In: *Universe* 2.4 (2016), p. 30.

[339] RV Maluf et al. "Antisymmetric tensor propagator with spontaneous Lorentz violation". In: *EPL (Europhysics Letters)* 124.6 (2019), p. 61001.

[340] Jorge Alfaro, Hugo A Morales-Tecotl, and Luis F Urrutia. "Loop quantum gravity and light propagation". In: *Physical Review D* 65.10 (2002), p. 103509.

[341] Maxim Pospelov and Yanwen Shang. "Lorentz violation in Hořava-Lifshitz-type theories". In: *Physical Review D* 85.10 (2012), p. 105001.

[342] Nikolaos E Mavromatos. "Lorentz invariance violation from string theory". In: *arXiv preprint arXiv:0708.2250* (2007).

[343] Sean M Carroll et al. "Noncommutative field theory and Lorentz violation". In: *Physical Review Letters* 87.14 (2001), p. 141601.

[344] V Alan Kosteleck and Neil Russell. "Data tables for Lorentz and C P T violation". In: *Reviews of Modern Physics* 83.1 (2011), p. 11.

[345] John Collins et al. "Lorentz invariance and quantum gravity: an additional fine-tuning problem?" In: *Physical Review Letters* 93.19 (2004), p. 191301.

[346] JR Nascimento, A Yu Petrov, and Carlos M Reyes. "Renormalization in a Lorentz-violating model and higher-order operators". In: *The European Physical Journal C* 78.7 (2018), pp. 7, 578.

[347] Robert C Myers and Maxim Pospelov. "Ultraviolet modifications of dispersion relations in effective field theory". In: *Physical Review Letters* 90.21 (2003), p. 211601.

[348] V Alan Kosteleck and Matthew Mewes. "Electrodynamics with Lorentz-violating operators of arbitrary dimension". In: *Physical Review D* 80.1 (2009), p. 015020.

[349] T Mariz et al. "Quantum aspects of the higher-derivative Lorentz-breaking extension of QED". In: *Physical Review D* 99.9 (2019), p. 096012.

[350] Don Colladay and Patrick McDonald. "Statistical mechanics and Lorentz violation". In: *Physical Review D* 70.12 (2004), p. 125007.

[351] Rodolfo Casana, Manoel M Ferreira Jr, and Josberg S Rodrigues. "Lorentz-violating contributions of the Carroll-Field-Jackiw model to the CMB anisotropy". In: *Physical Review D* 78.12 (2008), p. 125013.

[352] Rodolfo Casana et al. "Finite temperature behavior of the C P T-even and parity-even electrodynamics of the standard model extension". In: *Physical Review D* 80.8 (2009), p. 085026.

[353] M Gomes et al. "Free energy of Lorentz-violating QED at high temperature". In: *Physical Review D* 81.4 (2010), p. 045013.

[354] AA Araújo Filho. "Lorentz-violating scenarios in a thermal reservoir". In: *The European Physical Journal Plus* 136.4 (2021), pp. 1–14.

[355] AA Araújo Filho and RV Maluf. "Thermodynamic properties in higher-derivative electrodynamics". In: *Brazilian Journal of Physics* 51.3 (2021), pp. 820–830.

[356] AA Araújo Filho and JAAS Reis. "Thermal aspects of interacting quantum gases in Lorentz-violating scenarios". In: *The European Physical Journal Plus* 136.3 (2021), pp. 1–30.

[357] MA Anacleto et al. "Lorentz-violating dimension-five operator contribution to the black body radiation". In: *Physics Letters B* 785 (2018), pp. 191–196.

[358] Sudipta Das, Subir Ghosh, and Dibakar Roychowdhury. "Relativistic thermodynamics with an invariant energy scale". In: *Physical Review D* 80.12 (2009), p. 125036.

[359] A Yu Petrov et al. "Bouncing universe in a heat bath". In: *arXiv preprint arXiv:2105.05116* (2021).

[360] JAAS Reis, Subir Ghosh, et al. "Fermions on a torus knot". In: *arXiv preprint arXiv:2108.07336* (2021).

[361] Ted Jacobson. "Thermodynamics of spacetime: the Einstein equation of state". In: *Physical Review Letters* 75.7 (1995), p. 1260.

[362] Yi Ling, Wei-Jia Li, and Jian-Pin Wu. "Bouncing universe from a modified dispersion relation". In: *Journal of Cosmology and Astroparticle Physics* 2009.11 (2009), p. 016.

[363] Rong-Gen Cai and Sang Pyo Kim. "First law of thermodynamics and Friedmann equations of Friedmann-Robertson-Walker universe". In: *Journal of High Energy Physics* 2005.02 (2005), p. 050.

[364] Christopher Eling, Raf Guedens, and Ted Jacobson. "Nonequilibrium thermodynamics of spacetime". In: *Physical Review Letters* 96.12 (2006), p. 121301.

[365] T Padmanabhan. "Classical and quantum thermodynamics of horizons in spherically symmetric spacetimes". In: *Classical and Quantum Gravity* 19.21 (2002), p. 5387.

[366] M Akbar and Rong-Gen Cai. "Thermodynamic behavior of field equations for f (R) gravity". In: *Physics Letters B* 648.2-3 (2007), pp. 243–248.

[367] Ahmad Sheykhi, Bin Wang, and Rong-Gen Cai. "Deep connection between thermodynamics and gravity in Gauss-Bonnet braneworlds". In: *Physical Review D* 76.2 (2007), p. 023515.

[368] Xian-Hui Ge. "First law of thermodynamics and Friedmann-like equations in braneworld cosmology". In: *Physics Letters B* 651.1 (2007), pp. 49–53.

[369] Raf Guedens, Ted Jacobson, and Sudipta Sarkar. "Horizon entropy and higher curvature equations of state". In: *Physical Review D* 85.6 (2012), p. 064017.

[370] Rong-Gen Cai, Li-Ming Cao, and Ya-Peng Hu. "Corrected entropy-area relation and modified Friedmann equations". In: *Journal of High Energy Physics* 2008.08 (2008), p. 090.

[371] M Sharif and M Zubair. "Thermodynamics in f (R, T) theory of gravity". In: *Journal of Cosmology and Astroparticle Physics* 2012.03 (2012), p. 028.

[372] Martin Bojowald. "Quantum nature of cosmological bounces". In: *General Relativity and Gravitation* 40.12 (2008), pp. 2659–2683.

[373] Abhay Ashtekar, Tomasz Pawlowski, and Parampreet Singh. "Quantum nature of the big bang". In: *Physical review letters* 96.14 (2006), p. 141301.

[374] Abhay Ashtekar, Tomasz Pawlowski, and Parampreet Singh. "Quantum nature of the big bang: improved dynamics". In: *Physical Review D* 74.8 (2006), p. 084003.

[375] Abhay Ashtekar, Tomasz Pawlowski, and Parampreet Singh. "Quantum nature of the big bang: an analytical and numerical investigation". In: *Physical Review D* 73.12 (2006), p. 124038.

[376] Giovanni Amelino-Camelia et al. “Black-hole thermodynamics with modified dispersion relations and generalized uncertainty principles”. In: *Classical and Quantum Gravity* 23.7 (2006), p. 2585.

[377] Giovanni Amelino-Camelia. “Testable scenario for relativity with minimum length”. In: *Physics Letters B* 510.1-4 (2001), pp. 255–263.

[378] Alexander A Balandin. “Thermal properties of graphene and nanostructured carbon materials”. In: *Nature materials* 10.8 (2011), pp. 569–581.

[379] Eric Pop, Vikas Varshney, and Ajit K Roy. “Thermal properties of graphene: Fundamentals and applications”. In: *MRS bulletin* 37.12 (2012), pp. 1273–1281.

[380] A Alofi and GP Srivastava. “Thermal conductivity of graphene and graphite”. In: *Physical Review B* 87.11 (2013), p. 115421.

[381] Jianwei Che, Tahir Cagin, and William A Goddard III. “Thermal conductivity of carbon nanotubes”. In: *Nanotechnology* 11.2 (2000), p. 65.

[382] Rodney S Ruoff and Donald C Lorents. “Mechanical and thermal properties of carbon nanotubes”. In: *carbon* 33.7 (1995), pp. 925–930.

[383] AA Araújo Filho and JAAS Reis. “Thermal aspects of interacting quantum gases in Lorentz-violating scenarios”. In: *The European Physical Journal Plus* 136.3 (2021), pp. 1–30.

[384] JAAS Reis et al. “How does geometry affect quantum gases?” In: *arXiv preprint arXiv:2012.13613* (2020).

[385] Joao CR Magueijo. “Cosmic magnetic field imprints on cosmic radiation”. In: *Physical Review D* 49.2 (1994), p. 671.

[386] Analia N Cillis and Diego D Harari. “Photon-graviton conversion in a primordial magnetic field and the cosmic microwave background”. In: *Physical Review D* 54.8 (1996), p. 4757.

[387] Pisin Chen. “Resonant photon-graviton conversion and cosmic microwave background fluctuations”. In: *Physical review letters* 74.5 (1995), p. 634.

[388] Damian Ejlli. “Graviton production from the CMB in large scale magnetic fields”. In: *Physical Review D* 87.12 (2013), p. 124029.

[389] Pisin Chen and Teruaki Suyama. “Constraining primordial magnetic fields by CMB photon-graviton conversion”. In: *Physical Review D* 88.12 (2013), p. 123521.

[390] AA Araújo Filho and RV Maluf. “Thermodynamic Properties in Higher-Derivative Electrodynamics”. In: *Brazilian Journal of Physics* 51 (2021), pp. 820–830.

[391] AA Araújo Filho and A Yu Petrov. "Higher-derivative Lorentz-breaking dispersion relations: a thermal description". In: *The European Physical Journal C* 81.9 (2021), pp. 1–16.

[392] Walter Greiner et al. *Relativistic quantum mechanics*. Vol. 2. Springer, 2000.

[393] Yakir Aharonov and David Bohm. "Significance of electromagnetic potentials in the quantum theory". In: *Physical Review* 115.3 (1959), p. 485.

[394] David J Griffiths and Darrell F Schroeter. *Introduction to quantum mechanics*. Cambridge University Press, 2018.

[395] Richard W Robinett. "Quantum mechanics". In: *Classical Results, Modern Systems, and Visualized Examples (Oxford: Oxford University Press) ch* 11 (1997), p. 1974.

[396] Siegfried Flügge. *Practical quantum mechanics*. Springer Science & Business Media, 2012.

[397] Max Jammer et al. *The conceptual development of quantum mechanics*. McGraw-Hill New York, 1966.

[398] Jun John Sakurai and Eugene D Commins. *Modern quantum mechanics, revised edition*. 1995.

[399] Nouredine Zettili. *Quantum mechanics: concepts and applications*. 2003.

[400] Rodolfo P Martriaanez y Romero, Matriaaas Moreno, and Arturo Zentella. "Supersymmetric properties and stability of the Dirac sea". In: *Physical Review D* 43.6 (1991), p. 2036.

[401] RP Martinez-y-Romero, HN Núnez-Yépez, and AL Salas-Brito. "Relativistic quantum mechanics of a Dirac oscillator". In: *European Journal of Physics* 16.3 (1995), p. 135.

[402] MH Pacheco et al. "Three-dimensional Dirac oscillator in a thermal bath". In: *EPL (Europhysics Letters)* 108.1 (2014), p. 10005.

[403] Walter Greiner, Ludwig Neise, and Horst Stöcker. *Thermodynamics and statistical mechanics*. Springer Science & Business Media, 2012.

[404] David J Griffiths and Darrell F Schroeter. *Introduction to quantum mechanics*. Cambridge University Press, 2018.

[405] Tamaz Kereselidze et al. "Energy spectra of a particle confined in a finite ellipsoidal shaped potential well". In: *Physica E: Low-dimensional Systems and Nanostructures* 81 (2016), pp. 196–204.

[406] Paul Adrien Maurice Dirac. *Lectures on quantum mechanics*. Vol. 2. Courier Corporation, 2001.

[407] George E Andrews, Richard Askey, and Ranjan Roy. *Special functions*. Vol. 71. Cambridge university press, 1999.

[408] Richard A Silverman et al. *Special functions and their applications*. Courier Corporation, 1972.

[409] William Wallace Bell. *Special functions for scientists and engineers*. Courier Corporation, 2004.

[410] H Krivine. "Finite size effects on the momentum distribution of non-interacting fermions". In: *Nuclear Physics A* 457.1 (1986), pp. 125–145.

[411] Dripto Biswas and Subir Ghosh. "Quantum Mechanics of Particle on a torus knot: Curvature and Torsion Effects". In: *preprint arXiv:1908.06423* (2019).

[412] Andrey Chaves and David Neilson. *Two-dimensional semiconductors host high-temperature exotic state*. 2019.

[413] L V Butov et al. "Towards Bose–Einstein condensation of excitons in potential traps". In: *Nature* 417.6884 (2002), pp. 47–52.

[414] Zefang Wang et al. "Evidence of high-temperature exciton condensation in two-dimensional atomic double layers". In: *Nature* 574.7776 (2019), pp. 76–80.

[415] G William Burg et al. "Strongly enhanced tunneling at total charge neutrality in double-bilayer graphene-WSe 2 heterostructures". In: *Physical Review Letters* 120.17 (2018), p. 177702.

[416] SH Chen and P Tartaglia. "Light scattering from N non-interacting particles". In: *Optics Communications* 6.2 (1972), pp. 119–124.

[417] V V Romanov et al. "2D electron gas density of states at the Fermi level in silicon nanosandwich". In: *Journal of Physics: Conference Series*. Vol. 1236. 1. IOP Publishing. 2019, p. 012014.

[418] D A Baghdasaryan et al. "Thermal and magnetic properties of electron gas in toroidal quantum dot". In: *Physica E: Low-Dimensional Systems and Nanostructures* 101 (2018), pp. 1–4.

[419] Markus Däne and Antonios Gonis. "On the v-representabilty problem in density functional theory: application to non-interacting systems". In: *Computation* 4.3 (2016), p. 24.

[420] Swetlana Jungblut, Jan-Ole Joswig, and Alexander Eychmüller. "Diffusion-and reaction-limited cluster aggregation revisited". In: *Physical Chemistry Chemical Physics* 21.10 (2019), pp. 5723–5729.

[421] Ryszard Kutner. “Chemical diffusion in the lattice gas of non-interacting particles”. In: *Physics Letters A* 81.4 (1981), pp. 239–240.

[422] Martin Ligare. “Classical thermodynamics of particles in harmonic traps”. In: *American Journal of Physics* 78.8 (2010), pp. 815–819.

[423] Martin Wilkens and Christoph Weiss. “Particle number fluctuations in an ideal Bose gas”. In: *Journal of Modern Optics* 44.10 (1997), pp. 1801–1814.

[424] HR Pajkowski and RK Pathria. “Criteria for the onset of Bose-Einstein condensation in ideal systems confined to restricted geometries”. In: *Journal of Physics A: Mathematical and General* 10.4 (1977), p. 561.

[425] Peter Freyd et al. “A new polynomial invariant of knots and links”. In: *Bulletin of the American Mathematical Society* 12.2 (1985), pp. 239–246.

[426] Asim Gangopadhyaya et al. “Exactness of SWKB for Shape Invariant Potentials”. In: *preprint arXiv:2005.06683* (2020).

[427] J Benbourenane and H Eleuch. “Exactly solvable new classes of potentials with finite discrete energies”. In: *Results in Physics* (2020), p. 103034.

[428] Edward Anderson. “Triangleland: II. Quantum mechanics of pure shape”. In: *Classical and Quantum Gravity* 26.13 (2009), p. 135021.

[429] Kevin A Mitchell. “Gauge fields and extrapotentials in constrained quantum systems”. In: *Physical Review A* 63.4 (2001), p. 042112.

[430] Zongping Gong et al. “Error bounds for constrained dynamics in gapped quantum systems: Rigorous results and generalizations”. In: *Physical Review A* 101.5 (2020), p. 052122.

[431] Jakob Wachsmuth and Stefan Teufel. “Constrained quantum systems as an adiabatic problem”. In: *Physical Review A* 82.2 (2010), p. 022112.

[432] Hai-Feng Zhang, Chong-Min Wang, and Lai-Sheng Wang. “Helical crystalline SiC/SiO2 core- shell nanowires”. In: *Nano Letters* 2.9 (2002), pp. 941–944.

[433] Sheng Xu et al. “Assembly of micro/nanomaterials into complex, three-dimensional architectures by compressive buckling”. In: *Science* 347.6218 (2015), pp. 154–159.

[434] Peter Freyd et al. “A new polynomial invariant of knots and links”. In: *Bulletin of the American Mathematical Society* 12.2 (1985), pp. 239–246.

[435] Edward Witten. “Quantum field theory and the Jones polynomial”. In: *Communications in Mathematical Physics* 121.3 (1989), pp. 351–399.

[436] Edward Witten. “Topological quantum field theory”. In: *Communications in Mathematical Physics* 117.3 (1988), pp. 353–386.

[437] Harold NV Temperley and Elliott H Lieb. "Relations between the percolation and colouring problem and other graph-theoretical problems associated with regular planar lattices: some exact results for the percolation problem". In: *Proceedings of the Royal Society of London. A. Mathematical and Physical Sciences* 322.1549 (1971), pp. 251–280.

[438] DW Sumners. "Knot theory and DNA". In: *Proceedings of Symposia in Applied Mathematics*. Vol. 45. 1992, pp. 39–72.

[439] Mark Bodner, J Patera, and M Peterson. "Affine reflection groups for tiling applications: Knot theory and DNA". In: *Journal of Mathematical Physics* 53.1 (2012), p. 013516.

[440] Wen-yuan Qiu and Hou-wen Xin. "Topological chirality and achirality of DNA knots". In: *Journal of Molecular Structure: THEOCHEM* 429 (1998), pp. 81–86.

[441] Jenny Tompkins. "Modeling DNA with Knot Theory: An Introduction". In: *Rose-hulman. edu* (2005).

[442] Wen-yuan Qiu and Hou-wen Xin. "Topological chirality and achirality of DNA knots". In: *Journal of Molecular Structure: THEOCHEM* 429 (1998), pp. 81–86.

[443] James R Munkres. *Elements of algebraic topology*. CRC Press, 2018.

[444] Srećko Kilić, Eckhard Krotscheck, and Robert Zillich. "Binding of two helium atoms in confined geometries". In: *Journal of Low Temperature Physics* 116.3-4 (1999), pp. 245–260.

[445] Srećko Kilić, Eckhardt Krotscheck, and Leandra Vranješ. "Binding of two helium atoms in confined geometries. II. Dimerization on flat attractive substrates". In: *Journal of Low Temperature Physics* 119.5-6 (2000), pp. 715–722.

[446] Willard M Gersbacher and Frederick J Milford. "The significance of many-body interactions in physical adsorption". In: *Journal of Low Temperature Physics* 9.3-4 (1972), pp. 189–201.

[447] E Zaremba and Walter Kohn. "Theory of helium adsorption on simple and noble-metal surfaces". In: *Physical Review B* 15.4 (1977), p. 1769.

[448] Michael Bretz and J G Dash. "Quasiclassical and Quantum Degenerate Helium Monolayers". In: *Physical Review Letters* 26.16 (1971), p. 963.

[449] Michael Bretz and J G Dash. "Ordering transitions in helium monolayers". In: *Physical Review Letters* 27.10 (1971), p. 647.

[450] Mildred S Dresselhaus et al. "Carbon nanotubes". In: *The physics of fullerene-based and fullerene-related materials*. Springer, 2000, pp. 331–379.

[451] Ado Jorio, Gene Dresselhaus, and Mildred S Dresselhaus. *Carbon nanotubes: advanced topics in the synthesis, structure, properties and applications*. Vol. 111. Springer Science & Business Media, 2007.

[452] M Saarela et al. "Phase transitions in the growth of 4 He films". In: *Journal of Low Temperature Physics* 93.5-6 (1993), pp. 971–985.

[453] M Saarela and F V Kusmartsev. "Many-body structure of quantum vortices in thin 4He films". In: *Physics Letters A* 202.4 (1995), pp. 317–323.

[454] RL Humphries, PG James, and GR Luckhurst. "Molecular field treatment of nematic liquid crystals". In: *Journal of the Chemical Society, Faraday Transactions 2: Molecular and Chemical Physics* 68 (1972), pp. 1031–1044.

[455] Michael W Klein. "Molecular-Field Theory of a Random Ising System in the Presence of an External Magnetic Field". In: *Physical Review* 188.2 (1969), p. 933.

[456] Peter J Wojtowicz and Martin Rayl. "Phase Transitions of an Isotropic Ferromagnet in an External Magnetic Field". In: *Physical Review Letters* 20.26 (1968), p. 1489.

[457] Dirk Ter Haar and ME Lines. "A molecular-field theory of anisotropic ferromagnetica". In: *Philosophical Transactions of the Royal Society of London. Series A, Mathematical and Physical Sciences* 254.1046 (1962), pp. 521–555.

[458] Adailton A Araújo-Filho et al. "Structural, electronic and optical properties of monoclinic Na2Ti3O7 from density functional theory calculations: A comparison with XRD and optical absorption measurements". In: *Journal of Solid State Chemistry* 250 (2017), pp. 68–74.

[459] Fábio Lacerda Resende e Silva et al. "Polarized Raman, FTIR, and DFT study of Na2Ti3O7 microcrystals". In: *Journal of Raman Spectroscopy* 49.3 (2018), pp. 538–548.

[460] A. A Araújo Filho and A Yu Petrov. "Higher-derivative Lorentz-breaking dispersion relations: a thermal description". In: *The European Physical Journal C* 81.9 (2021), pp. 1–16.

[461] A. A Araújo Filho and JAAS Reis. "Thermal aspects of interacting quantum gases in Lorentz-violating scenarios". In: *The European Physical Journal Plus* 136.3 (2021), pp. 1–30.

[462] A. A Araújo Filho. "Lorentz-violating scenarios in a thermal reservoir". In: *The European Physical Journal Plus* 136.4 (2021), pp. 1–14.

[463] A. A Araújo Filho and RV Maluf. "Thermodynamic Properties in Higher-Derivative Electrodynamics". In: *Brazilian Journal of Physics* (2021), pp. 1–11.

[464] A. A Araújo Filho and A. Yu. Petrov. "Bouncing universe in a heat bath". In: *International Journal of Modern Physics A* 36.34n35 (2021), p. 2150242.

[465] A. A Araújo Filho. "Thermodynamics of massless particles in curved spacetime". In: *arXiv preprint arXiv:2201.00066* (2021).

[466] A. A Araújo Filho. "Particles in Loop Quantum Gravity formalism: a thermodynamical description". In: *arXiv preprint arXiv:2202.13907* (2022).

[467] RRS Oliveira and A. A Araújo Filho. "Thermodynamic properties of neutral Dirac particles in the presence of an electromagnetic field". In: *The European Physical Journal Plus* 135.1 (2020), p. 99.

[468] A. A Araújo Filho, J A A S Reis, and Subir Ghosh. "Fermions on a torus knot". In: *arXiv preprint arXiv:2108.07336* (2021).

[469] Rubens RS Oliveira et al. "Thermodynamic properties of an Aharonov-Bohm quantum ring". In: *The European Physical Journal Plus* 134.10 (2019), p. 495.

[470] RRS Oliveira and AA Araújo Filho. "Thermodynamic properties of neutral Dirac particles in the presence of an electromagnetic field". In: *The European Physical Journal Plus* 135.1 (2020), p. 99.

[471] AA Araújo Filho. "Lorentz-violating scenarios in a thermal reservoir". In: *The European Physical Journal Plus* 136.4 (2021), pp. 1–14.

[472] A. A Araújo Filho. "Thermodynamics of massless particles in curved spacetime". In: *arXiv preprint arXiv:2201.00066* (2021).

[473] V Alan Kosteleck and Matthew Mewes. "Lorentz-violating electrodynamics and the cosmic microwave background". In: *Physical review letters* 99.1 (2007), p. 011601.

[474] V Alan Kosteleck and Matthew Mewes. "Electrodynamics with Lorentz-violating operators of arbitrary dimension". In: *Physical Review D* 80.1 (2009), p. 015020.

[475] Mauro Cambiaso, Ralf Lehnert, and Robertus Potting. "Massive photons and Lorentz violation". In: *Physical Review D* 85.8 (2012), p. 085023.

[476] Matthew Mewes. "Optical-cavity tests of higher-order Lorentz violation". In: *Physical Review D* 85.11 (2012), p. 116012.

[477] Benjamin R Edwards and V Alan Kosteleck. "Riemann–Finsler geometry and Lorentz-violating scalar fields". In: *Physics Letters B* 786 (2018), pp. 319–326.

[478] E Passos and A Yu Petrov. "Two-dimensional Lorentz-violating Chern–Simons-like action". In: *Physics Letters B* 662.5 (2008), pp. 441–444.

[479] M Gomes and JR Nascimento. "AYu. Petrov, AJ da Silva". In: *Phys. Rev. D* 81 (2010), p. 045018.

[480] Dao T Khoa, GR Satchler, and W Von Oertzen. "Nuclear incompressibility and density dependent NN interactions in the folding model for nucleus-nucleus potentials". In: *Physical Review C* 56.2 (1997), p. 954.

[481] R Michael Barnett et al. "Review of particle physics". In: *Physical Review D* 54.1 (1996), p. 1.

[482] Simon Eidelman et al. "Review of particle physics". In: *Physics letters B* 592.1-4 (2004), pp. 1–5.

[483] GA Lalazissis et al. "New relativistic mean-field interaction with density-dependent meson-nucleon couplings". In: *Physical Review C* 71.2 (2005), p. 024312.

[484] Walter Greiner, Ludwig Neise, and Horst Stöcker. *Thermodynamics and statistical mechanics*. Springer Science & Business Media, 2012.

[485] Sılvio RA Salinas. *Introdução a fısica estatıstica vol. 09*. Edusp, 1997.

[486] RK Pathria and Paul D Beale. "Statistical mechanics, 1996". In: *Butter worth* 32 ().

[487] Araújo AA Filho. "Lorentz-violating scenarios in a thermal reservoir". In: *arXiv preprint arXiv:2004.07799* (2020).

[488] RRS Oliveira and AA Araújo Filho. "Thermodynamic properties of neutral Dirac particles in the presence of an electromagnetic field". In: *The European Physical Journal Plus* 135.1 (2020), p. 99.

[489] Rubens RS Oliveira et al. "Thermodynamic properties of an Aharonov-Bohm quantum ring". In: *The European Physical Journal Plus* 134.10 (2019), p. 495.

[490] MH Pacheco et al. "Three-dimensional Dirac oscillator in a thermal bath". In: *EPL (Europhysics Letters)* 108.1 (2014), p. 10005.

[491] Rodolfo Casana, Manoel M Ferreira Jr, and Josberg S Rodrigues. "Lorentz-violating contributions of the Carroll-Field-Jackiw model to the CMB anisotropy". In: *Physical Review D* 78.12 (2008), p. 125013.

[492] Andrew G Cohen and Sheldon L Glashow. "Very special relativity". In: *Physical review letters* 97.2 (2006), p. 021601.

[493] EE Kolomeitsev and DN Voskresensky. "Fluctuations in non-ideal pion gas with dynamically fixed particle number". In: *Nuclear Physics A* 973 (2018), pp. 89–103.

[494] S M Cunha et al. "Electronic and transport properties of anisotropic semiconductor quantum wires". In: *Physical Review B* 102.4 (2020), p. 045427.

[495] V Alan Kosteleck and Matthew Mewes. "Testing local Lorentz invariance with gravitational waves". In: *Physics Letters B* 757 (2016), pp. 510–514.

[496] V Alan Kosteleck and Matthew Mewes. “Constraints on relativity violations from gamma-ray bursts”. In: *Physical review letters* 110.20 (2013), p. 201601.

[497] Frederick Reif. *Fundamentals of statistical and thermal physics*. Waveland Press, 2009.

[498] Abel Camacho and Alfredo Macıas. “Thermodynamics of a photon gas and deformed dispersion relations”. In: *General Relativity and Gravitation* 39.8 (2007), pp. 1175–1183.

[499] Hassan Hassanabadi and Mansoureh Hosseinpour. “Thermodynamic properties of neutral particle in the presence of topological defects in magnetic cosmic string background”. In: *The European Physical Journal C* 76.10 (2016), p. 553.

[500] Weiping Yao, Chaohui Yang, and Jiliang Jing. “Holographic insulator/superconductor transition with exponential nonlinear electrodynamics probed by entanglement entropy”. In: *The European Physical Journal C* 78.5 (2018), p. 353.

[501] R.V Maluf et al. “Antisymmetric tensor propagator with spontaneous Lorentz violation”. In: *EPL (Europhysics Letters)* 124.6 (2019), p. 61001.

[502] AP Baeta Scarpelli et al. “Aspects of causality and unitarity and comments on vortex-like configurations in an Abelian model with a Lorentz-breaking term”. In: *Physical Review D* 67.8 (2003), p. 085021.

[503] RV Maluf et al. “Einstein-Hilbert graviton modes modified by the Lorentz-violating bumblebee field”. In: *Physical Review D* 90.2 (2014), p. 025007.

[504] RV Maluf et al. “Matter-gravity scattering in the presence of spontaneous Lorentz violation”. In: *Physical Review D* 88.2 (2013), p. 025005.

[505] Frederick Reif. *Fundamentals of statistical and thermal physics*. Waveland Press, 2009.

[506] Lee Smolin. “On the intrinsic entropy of the gravitational field”. In: *General relativity and gravitation* 17.5 (1985), pp. 417–437.

[507] Lee Smolin. “The thermodynamics of gravitational radiation”. In: *General relativity and gravitation* 16.3 (1984), pp. 205–210.

[508] M Gomes et al. “Free energy of Lorentz-violating QED at high temperature”. In: *Physical Review D* 81.4 (2010), p. 045013.

[509] Stefano Bianco, Victor Nicolai Friedhoff, and Edward Wilson-Ewing. “Modified dispersion relations, inflation, and scale invariance”. In: *Physical Review D* 97.4 (2018), p. 046006.

[510] M Gomes et al. “One-loop corrections in the z= 3 Lifshitz extension of QED”. In: *Physical Review D* 98.10 (2018), p. 105016.

[511] Petr Horava. "Quantum Gravity at a Lifshitz Point". In: *Phys. Rev. D* 79 (2009), p. 084008. DOI: 10.1103/PhysRevD.79.084008. arXiv: 0901.3775 [hep-th].

[512] KEL de Farias et al. "Lifshitz-scaling in CPT-even Lorentz-violating electrodynamics and GRB time delay". In: *Eur. Phys. J. Plus* 136.2 (2021), p. 257. DOI: 10.1140/epjp/s13360-021-01228-y. arXiv: 2004.07661 [hep-th].

[513] Frederick Reif. *Fundamentals of Statistical and Thermal Physics*. 1998.

[514] Herbert B Callen. *Thermodynamics and an Introduction to Thermostatistics*. 1998.

[515] RV Maluf, DM Dantas, and CAS Almeida. "The Casimir effect for the scalar and Elko fields in a Lifshitz-like field theory". In: *The European Physical Journal C* 80 (2020), pp. 1–10.

[516] IP Lobo et al. "Effects of Planck-scale-modified dispersion relations on the thermodynamics of charged black holes". In: *Physical Review D* 101.8 (2020), p. 084004.

[517] IP Lobo and GB Santos. "Thermal dimensional reduction and black hole evaporation". In: *arXiv preprint arXiv:2009.08556* (2020).

[518] Giovanni Amelino-Camelia et al. "Thermal dimension of quantum spacetime". In: *Physics Letters B* 767 (2017), pp. 48–52.

[519] Giacomo Rosati et al. "Planck-scale-modified dispersion relations in FRW spacetime". In: *Physical Review D* 92.12 (2015), p. 124042.

[520] Giovanni Amelino-Camelia et al. "IceCube and GRB neutrinos propagating in quantum spacetime". In: *Physics Letters B* 761 (2016), pp. 318–325.

[521] Giovanni Amelino-Camelia et al. "In vacuo dispersion features for gamma-ray-burst neutrinos and photons". In: *Nature Astronomy* 1.7 (2017), pp. 1–6.

[522] Giovanni Amelino-Camelia. "Relativity in spacetimes with short-distance structure governed by an observer-independent (Planckian) length scale". In: *International Journal of Modern Physics D* 11.01 (2002), pp. 35–59.

[523] Joao Magueijo and Lee Smolin. "Gravity's rainbow". In: *Classical and Quantum Gravity* 21.7 (2004), p. 1725.

[524] Wen-Jian Pan and Yong-Chang Huang. "Bouncing universe with modified dispersion relation". In: *General Relativity and Gravitation* 48.11 (2016), pp. 1–15.

[525] Zhong-Wen Feng et al. "The thermodynamics and phase transition of a rainbow black hole". In: *Modern Physics Letters A* 35.05 (2020), p. 2050010.

[526] Yi Ling, Bo Hu, and Xiang Li. "Modified dispersion relations and black hole physics". In: *Physical Review D* 73.8 (2006), p. 087702.

[527] Xin Han, Huarun Li, and Yi Ling. "Modified dispersion relations and (A) dS Schwarzschild black holes". In: *Physics Letters B* 666.2 (2008), pp. 121–124.

[528] Yi Ling. "Rainbow universe". In: *Journal of Cosmology and Astroparticle Physics* 2007.08 (2007), p. 017.

[529] Wei Zhang and Xiao-Mei Kuang. "The quantum effect on Friedmann equation in FRW universe". In: *Advances in High Energy Physics* 2018 (2018).

[530] Giovanni Amelino-Camelia, Michele Arzano, and Andrea Procaccini. "Severe constraints on the loop-quantum-gravity energy-momentum dispersion relation from the black-hole area-entropy law". In: *Physical Review D* 70.10 (2004), p. 107501.

[531] Yi Ling, Xiang Li, and Hongbao Zhang. "Thermodynamics of modified black holes from gravity's rainbow". In: *Modern Physics Letters A* 22.36 (2007), pp. 2749–2756.

[532] AN Ikot et al. "Klein–Gordon Equation and Nonrelativistic Thermodynamic Properties with Improved Screened Kratzer Potential". In: *Journal of Low Temperature Physics* 202.3 (2021), pp. 269–289.

[533] AN Ikot et al. "Approximate energy spectra and statistical mechanical functions of some diatomic molecular hydrides". In: *Canadian Journal of Physics* 99.999 (2021), pp. 1–6.

[534] Don Colladay and V Alan Kosteleck. "Lorentz-violating extension of the standard model". In: *Physical Review D* 58.11 (1998), p. 116002.

[535] Manoel M Ferreira Jr et al. "Unitarity in Stückelberg electrodynamics modified by a Carroll-Field-Jackiw term". In: *Physics Letters B* (2020), p. 135379.

[536] Emi Masaki and Jiro Soda. "Conversion of gravitons into dark photons in cosmological dark magnetic fields". In: *Physical Review D* 98.2 (2018), p. 023540.

APPENDIX – LIST OF PUBLICATIONS

For a better understanding of my scientific journey, here we present the list of publications during my Ph.D with approximately **219 citations** yielding **h-index** 9 as follows:

1. Maluf, R. V., **Araújo Filho, A. A.**, Cruz, W. T., and Almeida, C. A. S. "Antisymmetric tensor propagator with spontaneous Lorentz violation." *EPL (Europhysics Letters)*, 124(6), 61001 (2018). (doi.org/10.1209/0295-5075/124/61001) – IF(2021): 1.958;

2. Oliveira, R. R., **Araújo Filho, A. A.**, Lima, F. C. E., Maluf, R. V., and Almeida, C. A. S. (2018). "Thermodynamic properties of an Aharonov-Bohm quantum ring." *The European Physical Journal Plus* 134.10 (2019): 495. (doi.org/10.1140/epjp/i2019-12880-x) – IF(2021): 3.911;

3. Oliveira, R. R. S., **Araújo Filho, A. A**, Maluf, R. V., and C. A. S. Almeida. "The relativistic Aharonov-Bohm-Coulomb system with position-dependent mass." *Journal of Physics A: Mathematical and Theoretical*, 53(4), 045304 (2019). (doi.org/10.1088/1751-8121/ab5cfb) – IF(2021): 2.331;

4. Oliveira, R. R and **Araújo Filho, A. A.** "Thermodynamic properties of neutral Dirac particles in the presence of an electromagnetic field." *The European Physical Journal Plus*, 135(1), 99 (2019). (doi.org/10.1140/epjp/s13360-020-00146-9) – IF(2021): 3.911;

5. Oliveira, R. R. S., **Araújo Filho, A. A.**, Maluf, R. V., and Almeida, C. A. S. (2020). Reply to comment on 'The relativistic Aharonov–Bohm–Coulomb system with position-dependent mass'. *Journal of Physics A: Mathematical and Theoretical*, 54(2), 028002. (doi.org/10.1088/1751-8121/abd154) – IF(2021): 2.331;

6. **Araújo Filho, A. A.**, and Maluf, R. V. "Thermodynamic properties in higher-derivative electrodynamics." *Brazilian Journal of Physics*, 51, 820–830 (2021). (doi.org/10.1007/s13538-021-00880-0) – IF(2021): 1.364;

7. **Araújo Filho, A. A.** "Lorentz-violating scenarios in a thermal reservoir." The European Physical Journal Plus 136, 417 (2021). (doi.org/10.1140/epjp/s13360-021-01434-8) – IF(2021): 3.911;

8. **Araújo Filho, A. A.**, and Reis, J. A. A. S. "Thermal aspects of interacting quantum gases in Lorentz-violating scenarios." *The European Physical Journal Plus*, 136, 310 (2021). (doi.org/10.1140/epjp/s13360-021-01289-z) – IF(2021): 3.911;

9. **Araújo Filho, A. A.**, and Reis, J. A. A. S. "How does geometry affect quantum gases?" *International Journal of Modern Physics A*, 37, 11n12 2250071 (2022). (doi.org/10.1142/S0217751X22500713) – IF(2021): 1.475;

10. **Araújo Filho, A. A.**, and A. Yu. Petrov. "Higher-derivative Lorentz-breaking dispersion relations: a thermal description." *The European Physical Journal C*, 81, 843 (2021). (doi.org/10.1140/epjc/s10052-021-09639-y) – IF(2021): 4.991;

11. **Araújo Filho, A. A.**, and A. Yu. Petrov. "Bouncing universe in a heat bath." *International Journal of Modern Physics A*, 36, 34n35 2150242 (2021). (doi.org/10.1142/S0217751X21502420)– IF(2021): 1.475;

12. **Araújo Filho, A. A.**, Reis, J. A. A. S, and Subir Ghosh "Fermions on a torus knot." *The European Physical Journal Plus*, 137, 614 (2022). (doi.org/10.1140/epjp/s13360-022-02828-y) – IF(2021): 3.911;

13. **Araújo Filho, A. A.** "Thermodynamics of massless modes in curved spacetime" arXiv preprint arXiv: 2201.00066;

14. **Araújo Filho, A. A.** "Particles in Loop Quantum Gravity formalism: a thermodynamical description" arXiv preprint arXiv: 2202.13907;

15. **Araújo Filho, A. A.**, Gonzalo J. Olmo "Mapping General Relativity into modified gravity: a perturbative approach" arXiv preprint arXiv:;

16. **Araújo Filho, A. A.**, J. R. Nascimento, A. Yu. Petrov, P. J. Porfírio "Lorentz-violating coefficients in metric-affine formalism" arXiv preprint arXiv:;

17. **Araújo Filho, A. A.**, J. A. A. S. Reis, Subir Ghosh "Dressing a torus knot with quantum gases" arXiv preprint arXiv:;

18. **Araújo Filho, A. A.** "Como partículas interagem na eletrodinâmica de Kalb-Ramond?" Editora Dialética – **book chapter** (doi.org/10.48021/978-65-252-4048-0-c4);

19. **Araújo Filho, A. A.** "Graviton and Kalb-Ramond field with Lorentz violation" – **book author** – (ISBN nº 978-65-00-44382-0) – Amazon.com;

20. **Araújo Filho, A. A.**, Rocha, D. M.; Mendes, F. A. S.; Milograna, J.; Carrano, R. C.; Ferreira, R. A "A sociedade do conhecimento e suas tecnologias: estudos em Ciências Exatas e Engenharias: Volume 2. Editora Dialética" – **book author** – (ISBN nº 978-652524048-0);

21. **Araújo Filho, A. A.**, "Thermal aspects of field theories" – **book author** – (ISBN nº 978-65-00-46365-1) – Amazon.com;

22. **Araújo Filho, A. A.**, "A sociedade do conhecimento e suas tecnologias: estudos em Ciências Exatas e Engenharias: Volume 2. Editora Dialética." – **book organizer** – (ISBN nº 978-652524048-0);

23. **Araújo Filho, A. A.** "A sociedade do conhecimento e suas tecnologias: estudos em Ciências Exatas e Engenharias: Volume 3. Editora Dialética." – **book organizer** – (ISBN nº 978-65-252-4742-7);

24. **Araújo Filho, A. A.**; B. A. Aguiar "The Genesis of Statistical Mechanics." Editora Dialética – **book chapter** (doi.org/10.48021/978-65-252-4448-8-c4);

25. **Araújo Filho, A. A.**, B. A. Aguiar "A sociedade do conhecimento e suas tecnologias: estudos em Ciências Exatas e Engenharias: Volume 4" – **book author** – (ISBN nº 978-65-252-4448-8);

26. **Araújo Filho, A. A.** "A sociedade do conhecimento e suas tecnologias: estudos em Ciências Exatas e Engenharias: Volume 4. Editora Dialética" – **book organizer** – (ISBN nº 978-65-252-4448-8);

27. **Araújo Filho, A. A.**; "A sociedade do conhecimento e suas tecnologias: estudos em Ciências Exatas e Engenharias: Volume 5. Editora Dialética" – **book organizer** – **book organizer** – (ISBN nº 978-65-252-5172-1);.

28. **Araújo Filho, A. A.**; B. A. Aguiar "Aplicação de nanotecnologia em doenças neurodegenerativas" – **book chapter**;

29. **Araújo Filho, A. A.**; B. A. Aguiar "A sociedade do conhecimento e suas tecnologias: estudos em Ciências Exatas e Engenharias: Volume 6. Editora Dialética" – **book author**.

30. **Araújo Filho, A. A.**; B. A. Aguiar "A sociedade do conhecimento e suas tecnologias: estudos em Ciências Exatas e Engenharias: Volume 6. Editora Dialética" – **book organizer**.